2005

Vanadium phosphinimide complexes for ethylene polymerization and the chemistry of phosphinimines and phosphine oxides with borane reagents

Sarah Bess Hawkeswood
University of Windsor

INFORMATION TO USERS

This manuscript has been reproduced from the microfilm master. UMI films the text directly from the original or copy submitted. Thus, some thesis and dissertation copies are in typewriter face, while others may be from any type of computer printer.

The quality of this reproduction is dependent upon the quality of the copy submitted. Broken or indistinct print, colored or poor quality illustrations and photographs, print bleedthrough, substandard margins, and improper alignment can adversely affect reproduction.

In the unlikely event that the author did not send UMI a complete manuscript and there are missing pages, these will be noted. Also, if unauthorized copyright material had to be removed, a note will indicate the deletion.

Oversize materials (e.g., maps, drawings, charts) are reproduced by sectioning the original, beginning at the upper left-hand corner and continuing from left to right in equal sections with small overlaps.

ProQuest Information and Learning
300 North Zeeb Road, Ann Arbor, MI 48106-1346 USA
800-521-0600

Vanadium Phosphinimide Complexes for Ethylene Polymerization and The Chemistry of Phosphinimines and Phosphine Oxides with Borane Reagents

By

Sarah Bess Hawkeswood

A Dissertation

Submitted to the Faculty of Graduate Studies and Research

Through the Department of Chemistry and Biochemistry

In Partial Fulfillment of the Requirements for

The Degree of Doctor of Philosophy

At the University of Windsor

Windsor, Ontario, Canada

2005

Abstract

A reproducible and high yielding synthesis of the vanadium imide phosphinimide complexes of the general formula $V(NAr)(NPR_3)Cl_2$ (Ar = Ph, C_6H_3-2,6-*i*-Pr_2; R = *i*-Pr, *t*-Bu, Ph) has been developed. These complexes upon activation by methylaluminoxane demonstrated low to moderate ethylene polymerization activities comparable to published vanadium imide complexes. The dichloride derivatives react readily with a variety of alkali metal salts and Grignard reagents to produce vanadium imide phosphinimide thiolate, alkyl, aryl, amide and alkoxide complexes. In the presence of Zn, reduction of $V(NPh)(NP$*t*-$Bu_3)Cl_2$ occurred to afford what is proposed to be a vanadium(IV) imide bridged dimeric species $(V(\mu\text{-}NPh)(NP$*t*-$Bu_3)Cl)_2$.

The reaction of pinacolborane with phosphinimines ($HNPR_3$) proceeds via two observable reaction pathways: a metathesis reaction, in which hydrogen gas is evolved, or the reduction of phosphorus, in which the corresponding borylamine and tertiary phosphine are formed. Experimental results and a DFT study showed that the preferred mechanism is dictated by the steric bulk of the R groups. The analogous reductions of phosphine oxides with pinacolborane gave tertiary phosphines and $O(Bpin)_2$. Alternative synthetic procedures and subsequent reactions of $O(Bpin)_2$ with both metal and main group complexes were investigated. These reactions led to the synthesis of $Zr(C_5H_5)_2(OBpin)_2$, [*t*-Bu_3PNH_2][pinB$(OBpin)_2$], and degradation products.

N-borylphosphinimines of the general formula $(R_3P\mu\text{-}NBcat)_x$ (cat = $O_2C_6H_4$; R = Et, *n*-Bu, *i*-Pr, Ph, *t*-Bu; R_3 = *n*-Bu(*t*-Bu)$_2$; x = 1,2) were synthesized. The dimeric or monomeric nature of the above compounds were probed by X-ray and NMR methods, revealing that the steric bulk of the R groups affected the preferred bonding mode of the complexes in solution and in solid state.

Therefore, metathesis reactions have led to the synthesis of both vanadium phosphinimide complexes and *N*-borylphosphinimine complexes. It has been determined that the steric bulk of the substituents of the phosphinimine affect the bonding mode of the *N*-borylphosphinimine complexes and their reactivity with boranes.

Dedication

This work is dedicated to my family, for your unwavering love, encouragement and support that continued to fill me up on this rollercoaster ride called graduate school.

Acknowledgements

There are numerous folks I need to acknowledge with thanks for their help and support in completing this work. I would like to thank the Stephan group members both past and present for creating a work environment that was welcoming and productive, especially: Dr. Chad Beddie, Ms. Lourisa Cabrera, Mr. Steve Clemens, Dr. Silke Courtenay, Dr. Todd Graham, Ms. Sharonna Greenberg, Dr. Emily Hollink, Dr. Aaron Hoskin, Ms. Rodica Leu, Mr. Jason Masuda, Ms. Jenny McCahill, Ms. Edyta Urbanska, Dr. Denise Walsh and Ms. Nancy Yue. I would like to thank Dr. Emily Hollink for constantly helping me in the lab and for being my kindred spirit through grad school. I would like to thank Dr. Aaron Hoskin for watching out for me and encouraging me to stick with this. I would like to thank Mr. Jason Masuda for patiently helping me with the X-ray diffractometer and in the lab. I would like to thank Dr. James Gauld and Dr. Chad Beddie for their advice with the computational study in this thesis. I would like to thank Mr. Mike Fuerth for all of his help with the NMR spectrometers and listening to me chatter on in the NMR room. I would like to acknowledge NOVA Chemicals Corporation for performing the GPC analyses of the polyethylene generated from the work in Chapter 2. I would like to thank Dr. Emily Hollink, Mr. Jason Masuda, Ms. Sharonna Greenberg and Dr. James Gauld for their help in editing this thesis. Thank you.

I would like to thank my husband for loving me, marrying me, listening to me and making me smile everyday. I would like to thank my mom for being my crutch in life and teaching me how to be an incredible, independent woman. I would like to thank my dad for believing in me, teaching me to think outside the box and pushing me to persevere. Thank you.

Finally, I would like to thank Dr. Douglas Stephan for being an amazing supervisor, who has instilled much confidence in me as a scientist and has supported my dream of teaching. Thank you.

Table of Contents

List of Tables

List of Figures

List of Equations and Schemes

Compound Numbering Scheme

Chapter 2

2.1 $V(NPh)Cl_3$

2.2 $V(NC_6H_3\text{-}2,6\text{-}i\text{-}Pr_2)Cl_3$

2.3 $[V(NPPh_3)_3Cl]Cl$

2.4 $V(NPh)(NPi\text{-}Pr_3)Cl_2$

2.5 $V(NPh)(NPt\text{-}Bu_3)Cl_2$

2.6 $V(NPh)(NPPh_3)Cl_2$

2.7 $V(NC_6H_3\text{-}2,6\text{-}i\text{-}Pr_2)(NPi\text{-}Pr_3)Cl_2$

2.8 $V(NC_6H_3\text{-}2,6\text{-}i\text{-}Pr_2)(NPt\text{-}Bu_3)Cl_2$

2.9 $V(NC_6H_3\text{-}2,6\text{-}i\text{-}Pr_2)(NPPh_3)Cl_2$

2.10 $V(NC_6H_3\text{-}2,6\text{-}i\text{-}Pr_2)(NPt\text{-}Bu_3)Me_2$

2.11 $(V(\mu\text{-}NPh)(NPt\text{-}Bu_3)Cl)_2$

2.12 $V(NC_6H_3\text{-}2,6\text{-}i\text{-}Pr_2)(NPt\text{-}Bu_3)Ph_2$

2.13 $V(NPh)(NPt\text{-}Bu_3)Ph_2$

2.14 $V(NC_6H_3\text{-}2,6\text{-}i\text{-}Pr_2)(NPi\text{-}Pr_3)Ph_2$

2.15 $V(NPh)(NPi\text{-}Pr_3)Bn_2$

2.16 $V(NPh)(NPt\text{-}Bu_3)Bn_2$

2.17 $V(NC_6H_3\text{-}2,6\text{-}i\text{-}Pr_2)(NPPh_3)Bn_2$

2.18 $V(NPh)(NPt\text{-}Bu_3)(SEt)_2$

2.19 $V(NC_6H_3\text{-}2,6\text{-}i\text{-}Pr_2)(NPt\text{-}Bu_3)(SEt)_2$

2.20 $V(NC_6H_3\text{-}2,6\text{-}i\text{-}Pr_2)(NPt\text{-}Bu_3)(SBn)_2$

2.21 $V(NPh)(NPt\text{-}Bu_3)(SBn)Cl$

2.22 $V(NPh)(NPt\text{-}Bu_3)(SBn)_2$

2.23 $V(NPh)(NPi\text{-}Pr_3)(SBn)_2$

2.24 $V(NPh)(NPt\text{-}Bu_3)(N(SiMe_3)_2)Cl$

2.25 $\mu\text{-}O(V(NPh)(NPt\text{-}Bu_3)(N(SiMe_3)_2))_2$

2.26 $V(NPh)(NPt\text{-}Bu_3)(Ot\text{-}Bu)_2$

2.27 $V(NC_6H_3\text{-}2,6\text{-}i\text{-}Pr_2)(NPi\text{-}Pr_3)(Ot\text{-}Bu)_2$

Chapter 3

Chapter 4

Chapter 5

List of Abbreviations and Symbols

Å	Angstrom
Abs coeff	Absorption coefficient
Ad	adamantyl
Ar	aryl
atm	atmosphere
Bn	benzyl
br	broad
calcd	calculated
CCD	Charge Coupled Device
CD	Compact Disc
CGC	Constrained Geometry Catalyst
Cp	Cyclopentadienyl
Cy	cyclohexyl
°C	degrees Celsius
D_{calc}	calculated density
d	doublet
dd	doublet of doublets
DFT	Density Functional Theory
dt	doublet of triplets
dq	doublet of quartets
dseptet	doublet of septets
eq	equivalents
Et	ethyl
FT-IR	Fourier Transform - Infrared
g	grams
GoF	Goodness of Fit
GPC	Gel Permeation Chromatography
HBcat	catecholborane
HBpin	pinacolborane

h	hour
Hz	Hertz
I	nuclear spin
i-Pr	*iso*-propyl
J	coupling constant
k	overall rate constant
k_{obs}	observed rate constant
kcal	kilocalories
L	liter
m	multiplet
M	mol L^{-1}
MAO	methylaluminoxane
m	meta
Me	methyl
mg	milligram
MHz	Megahertz
min	minute
mL	milliliter
MMA	methyl methacrylate
mmol	millimole
M_n	number average molecular weight (g mol^{-})
M_w	weight average molecular weight (g mol^{-})
NBO	Natural Bond Order
n-Bu	*neo*-butyl
NMR	Nuclear Magnetic Resonance
o	ortho
ORTEP	Oak Ridge Thermal Ellipsoid Plot
p	para
PDI	Polydispersity Index
Ph	Phenyl
ppm	parts per million

R	residual
R_w	weighted residual
RT	room temperature
s	singlet, seconds
t	triplet
t-Bu	*tert*-butyl
THF	tetrahydrofuran
TMA	tetramethylaluminum
wt%	weight percent
α	alpha
β	beta
δ	chemical shift
η	eta (haptacity)
γ	gamma
$\Delta\nu_{1/2}$	line width at half height
λ	lambda (wavelength)
μ	mu (bridging)
π	pi
σ	sigma
θ	theta

1 Introduction

1.1 Overture

The work described herein was performed with the intention of bringing further insight into the reactivity and therefore the utility of the phosphinimine fragment (NPR_3). The initial discovery that titanium phosphinimide complexes act as highly efficient catalysts in olefin polymerization on an industrial level has provoked much interest in these ligands, including the work described herein. This thesis includes a description of the synthesis of vanadium phosphinimide complexes and their catalytic behaviour. These complexes were synthesized with the intention of mimicking the titanium (IV) phosphinimide complexes to determine if these Group V complexes could also be successful polymerization catalysts (Chapter 2). Secondly, the reactions of phosphinimines with borane reagents are described. The impact of the steric size of the substituents of the phosphinimine on the reactivity of these derivatives was established (Chapter 3 and 4). Furthermore, it was observed that pinacolborane ($HBO_2C_2(CH_3)_4$) can act as a reducing agent when treated with sterically unhindered phosphinimines and phosphine oxides.(Chapter 3 and 5) The content of this introduction is meant to brief the reader on topics of relevance within the proceeding chapters.

1.2 Synthesis of Phosphinimine/Phosphinimide Ligand Precursors

The phosphinimine or phosphinimide ligand precursors (Me_3SiNPR_3, where R = alkyl, aryl, amido) can be synthesized using the procedure outlined by Staudinger,[1, 2] in which azidotrimethylsilane reacts with tertiary phosphines to produce an equivalent of nitrogen gas and the corresponding phosphinimine molecules (Figure 1.1).

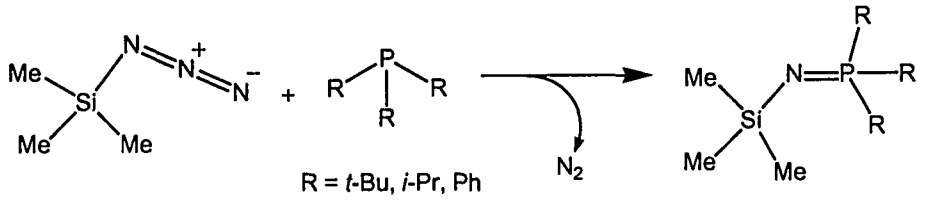

Figure 1.1: Synthesis of phosphinimine derivatives via the Staudinger reaction.[1, 2]

The conditions to effect completion of the Staudinger reaction depend on the size and basicity of the substituents that are bonded to the phosphorus atom and the azide functional group.[1-3] Phosphines with smaller substituents, such as PEt_3, react cleanly with azidotrimethylsilane at ambient temperatures to yield the corresponding phosphinimines.[3] The oxidation of phosphines that contain bulkier substituents, such as P*i*-Pr_3 or P*t*-Bu_3, or substituents that are not as basic, such as PPh_3, require elevated temperatures to drive the reaction to completion.[4] The steric encumbrance or electron withdrawing groups provided by the substituents on the phosphorus atom can prevent the oxidation of the phosphorus centre. Examples of phosphines that may not be oxidized using this methodology to the corresponding phosphinimines include $P(C_3H_{13}B_{10})_3$,[5] P(*N*-3-methylindolyl)$_3$[6] and $P(C_6H_2\text{-}2,4,6\text{-}Me_3)_3$[6], which are depicted in Figure 1.2.

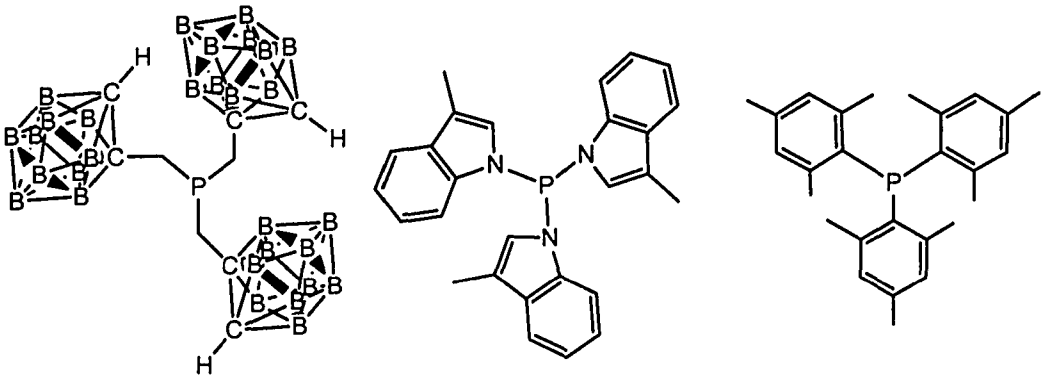

Figure 1.2: The phosphines $P(C_3H_{13}B_{10})_3$,[5] P(*N*-3-methylindolyl)$_3$,[6] and $P(C_6H_2$-2,4,6-$Me_3)_3$, which may not be oxidized by the Staudinger reaction.

When substituents on the phosphorus atom of the phosphine become too sterically crowded and/or too electron withdrawing, the oxidation of the tertiary phosphine with azide reagents does not occur, therefore, there is a need for alternative methodologies to synthesize phosphinimine complexes. Recently, Manners and coworkers reported a high-yielding synthesis of $Me_3SiNPCl_3$. This methodology involves the reaction of PCl_3 with $Li[N(SiMe_3)_2]$ to yield $PCl_2(N(SiMe_3)_2)$, followed by chlorination using SO_2Cl_2 to yield the desired phosphinimine product.[7]

1.3 Comparison of Phosphinimide (NPR_3^-), Cyclopentadienyl (Cp^-) and Imide (NR^{2-}) Ancillary Ligands

Isolobal relationships between the cyclopentadienyl (η^5-$C_5H_5^-$ or Cp^-), imide (NR^{2-}) and phosphinimide (NPR_3^-) ancillary ligands have been postulated with respect to the symmetry of the frontier orbitals as depicted in Figure 1.3.[8-10] All three of these ligand types have been described as "σ and 2π" donor ligands, indicating a maximum of six electrons available for bonding to the metal centre. This isolobal analogy allows for the comparison of cyclopentadienyl-, imide- and phosphinimide-transition metal complexes.

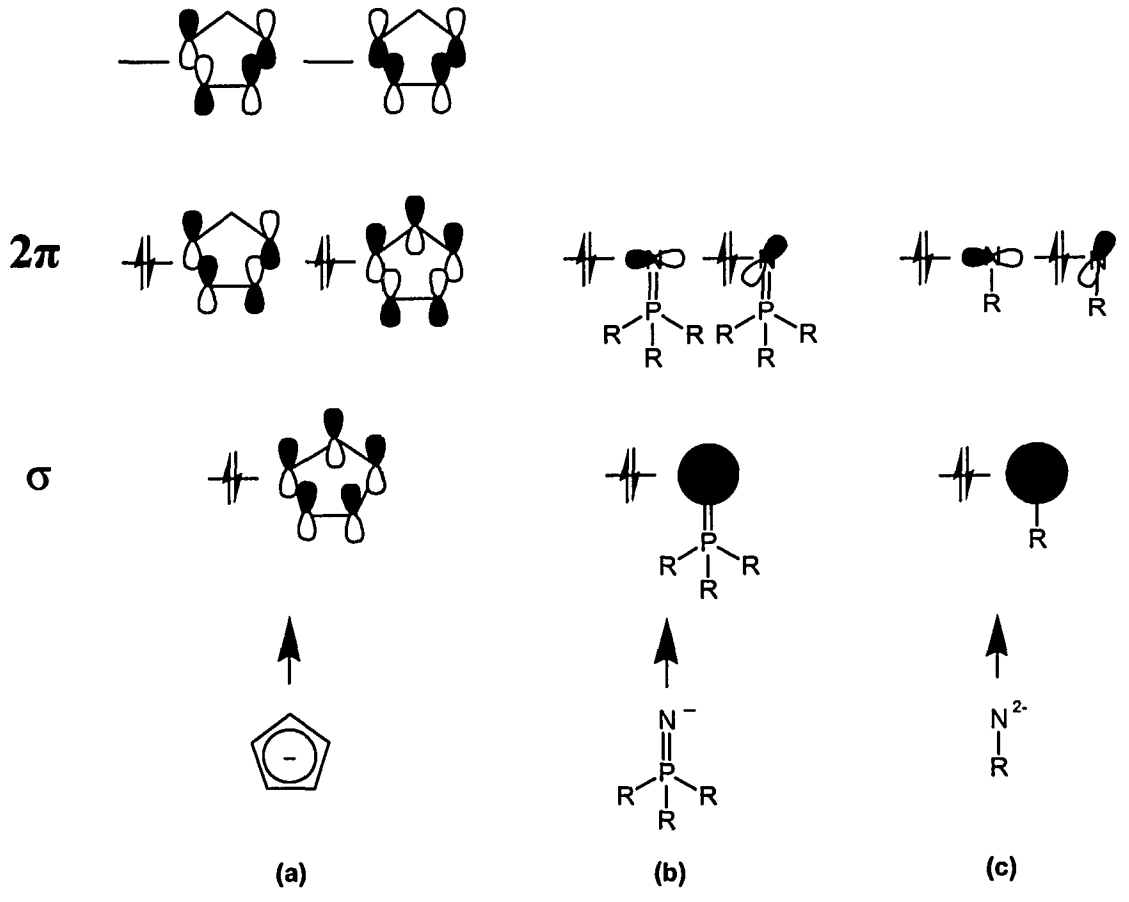

Figure 1.3: Isolobal relationship of the frontier orbitals of the (a) Cp^-, (b) NPR_3^- and (c) NR^{2-} ligands.

The different bonding modes of the phosphinimide ligand to metal centers have been reviewed by Dehnicke and coworkers.[8] The bonding mode depicted in Figure 1.4 represents a metal-nitrogen triple bond, consisting of one σ and two π bonds between the metal and ligand. This bonding mode is thought to predominate when the phosphinimide ligand is bound to metal centres in high oxidation states and therefore has empty d-orbitals, such as Ti^{4+} and V^{5+}.[8] The analogous bonding mode for the imide ligand to a metal atom with empty d-orbitals is also depicted in Figure 1.4.

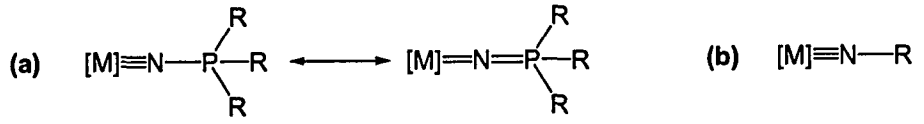

Figure 1.4: Potential bonding mode(s) of (a) the phosphinimide ligand and (b) the imide ligand to metal atoms in high oxidation states.

Both the phosphinimide and cyclopentadienyl ligands have a formal charge of 1⁻. Therefore, given the isolobal relationship described above, the bonding and reactivity of metal-Cp and metal-NPR_3 complexes, with the same kind of metal atoms in identical oxidation states, can be compared and any differences in reactivity of the metal complexes would provide interesting information about the subtle differences that govern the chemistry. Alternatively, the imido ligand has a formal charge of 2-. Hence, the bonding and reactivity of metal-NR complexes can be compared to metal-Cp or metal-NPR_3 compounds which have metal centres with one less d-electron or metal centres in a lower oxidation state.

Given the vast amount of literature encompassing the chemistry of metallocene derivatives,[11-14] and the isolobal relationship between Cp, NR and NPR_3 ligands, there is purpose in investigating the chemistry of imide and phosphinimide metal analogues. For example, zirconocene derivatives such as $ZrCp_2Cl_2$ upon activation are considered to be good homogeneous olefin polymerization catalysts.[15] Therefore, synthesizing vanadium(V) imide complexes or vanadium(IV) phosphinimide complexes is warranted in order to compare the polymerization activities.

1.4 An Overview of the Chemistry of Metal-Phosphinimide Complexes

The chemistry of transition metal-phosphinimide complexes has been reviewed by Dehnicke and coworkers.[8, 16] Since the publication of these reviews, there has been continued interest in phosphinimine chemistry. In the past 5 years within our research group much emphasis has been placed on the synthesis of metal-phosphinimide

complexes and their utility in polymerization catalysis.[17-41]. Group IV metal-phosphinimide complexes are currently being used as homogeneous olefin polymerization pre-catalysts as part of an industrial process to provide various polyolefins.[42] Titanium complexes of the form $TiCp^*(NPt\text{-}Bu_3)Cl_2$ ($Cp^* = C_5Me_5$, C_5H_4-*n*-Bu)[36] and $Ti(NPt\text{-}Bu_3)_2Me_2$[17] upon activation with a cocatalyst have extremely high ethylene polymerization activities that surpass the activities observed for metallocenes such as $ZrCp_2Me_2$ and half-sandwich complexes[43] such as the CGC catalyst $Ti(Cp\text{-}Si(Me)_2Nt\text{-}Bu)Me_2$[44] (Figure 1.5). These high activities have been attributed to the steric and electronic properties of the -$NPt\text{-}Bu_3$ ligand; similar to those of the cyclopentadienyl ligand (*vide supra*).

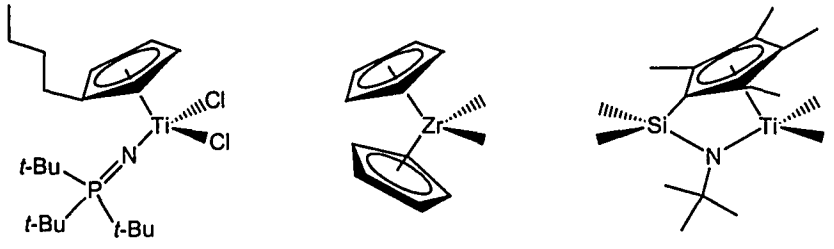

Figure 1.5: Examples of successful ethylene polymerization pre-catalysts.

Recently, titanium phosphinimide polymerization catalysts of the form $TiCp^*(NP(NR^1R^2)_3)Me_2$ have been tested for the polymerization of ethylene. From this study, a direct relationship between the steric bulk of the phosphinimide ligand and the polymerization activity has been determined.[6] It was found that upon increasing the steric bulk of the electron-donating phosphinimide ligands the polymerization activity increases.

Polymerizations catalyzed by Ti-phosphinimide complexes result in activities that are dependent on the type of metal precursor and cocatalyst employed. The activities are much higher upon activation with $B(C_6F_5)_3$ or $[CPh_3][B(C_6F_5)_4]$ than with MAO.[17] Given these results, reactions of Group IV metal-phosphinimide complexes with a variety of Lewis acids and hydrogen gas have been completed to try to rationalize the chemistry that occurs upon treatment with an activating agent.[17, 18, 20, 22-25, 30, 36, 39, 45, 46] The reactions of $Ti(NPt\text{-}Bu_3)_2Me_2$ with trimethylaluminum (TMA) are noteworthy because

they describe competitive reactions of ligand metathesis and C-H activation.[30] These are thought to be possible deactivation pathways for olefin polymerization reactions in which $Ti(NPt\text{-}Bu_3)_2Me_2$ and similar derivatives are activated with Al-based activators such as MAO which contain small amounts of TMA.

In general, metal-phosphinimide complexes show great promise in the catalysis world. Given the enhanced polymerization activities observed for Group IV metal-phosphinimide complexes, the synthesis of similar complexes with other early metal, late metal and main group elements and the investigation of the subsequent chemistry which evolves from these derivatives are certainly warranted.

1.5 Vanadium Phosphinimide Complexes

Relatively few vanadium(V)-phosphinimide complexes can be found in the literature. This is most likely a consequence of the scarcity of vanadium(V) starting materials, and commercially available reagents are limited to vanadium oxy trihalide compounds and other vanadium-oxo complexes. The majority of vanadium(V)-phosphinimide complexes have been synthesized via metathesis reactions of VOX_3 with the appropriate phosphinimide reagent. Using this metathetical route, Choukroun and coworkers [47] synthesized the first vanadium(V) phosphinimide complexes: $VOCl_2(NPPh_3)$, $VOCl(NPPh_3)_2$ and $VCl_3(NPPh_3)_2$. Other compounds produced via this method include: $VOF_2(NPPh_3)$, $VOCl_2(NPPh_2NS(O)Me_2)$ and $VCl_2(N(NPPh_2)_2)$.[48-50] (Figure 1.6)

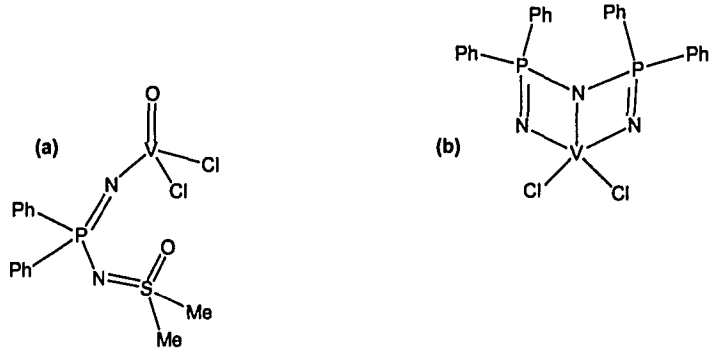

Figure 1.6: Chemical drawings of (a) $VOCl_2(NPPh_2NS(O)Me_2$ and (b) $VCl_2(N(NPPh_2)_2)$.[48-50]

An alternative approach taken to synthesize vanadium(V)-phosphinimide complexes involves the initial formation of the vanadium-imide complex, $V(NSiMe_3)Cl_3$, followed by the addition of a phosphorus(V) compound with the general formula PR_3Cl_2 to yield $V(NPR_3)Cl_4$ and Me_3SiCl.[51, 52] Subsequent stoichiometric additions of trimethylsilyl derivatives yielded the corresponding *bis*-, *tris*- and *tetrakis*-substituted vanadium(V)-phosphinimide complexes.[53] Moreover, an elegant synthetic strategy was reported by Roesky and coworkers in which a number of complexes were prepared.[49, 52] For example the dinuclear complex, $(VCl_2(NP(C_2F_5)_2N))_2$ was synthesized by reacting $V(NSiMe_3)Cl_3$ with one molar equivalent of $Me_3SiNP(Cl)(C_2F_5)_2$ as shown in Figure 1.7. This method incorporates dual metathesis reactions, one at the metal centre and the other at nitrogen atom of the imido group.

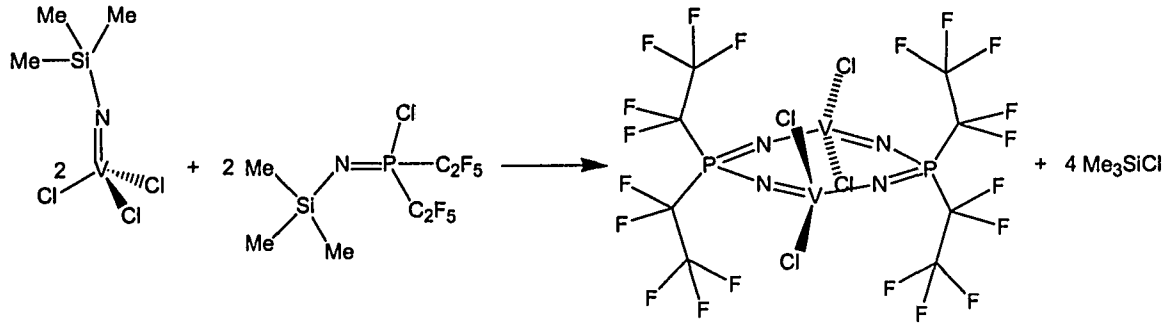

Figure 1.7: Synthetic route involving metathesis at the metal centre and the nitrogen atom of the imido functional group to produce the vanadium(V)-phosphinimide complex $(VCl_2(NP(C_2F_5)_2N))_2$.[52]

In addition to the compounds mentioned above, several groups have synthesized a variety of vanadium(III)- and vanadium(IV)-phosphinimide complexes.[54-58] On a whole, the synthesis and subsequent chemistry of vanadium-phosphinimide complexes has not been exploited and therefore a need for the exploration of this chemistry remains.

1.6 Vanadium Imide Complexes

Given that vanadium(V) oxide complexes are the only commercially available vanadium(V) reagents, the obvious extension in vanadium(V) chemistry is the syntheses of vanadium-imide complexes. Both oxide and imide ligands provide enhanced stability to high oxidation state transition metal complexes[59-62] by readily participating in ligand to metal π-donation of electron density. However, unlike the oxide ligand, the electronic and steric properties of the imide ligand are modular. This is a consequence of the organic group attached to the nitrogen atom of the imide ligand. In turn, this has made the synthesis of vanadium imide complexes extremely appealing. Therefore, the chemistry of vanadium-imide complexes has received much attention in the last 20 years. This frontier has been led mainly by Preuss and coworkers.[63-84] and Maatta and coworkers[85-88]

The stability provided by the imido group has been utilized to synthesize a number of vanadium(V) derivatives including alkyl derivatives,[84, 89, 90] cations,[91] and the first stable V(V) phosphido complex[80] (Figure 1.8).

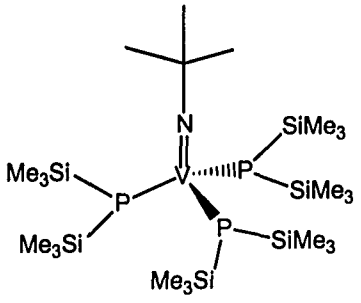

Figure 1.8: The first stable vanadium(V) phosphido complex V(N*t*-Bu)(P(SiMe$_3$)$_2$)$_3$.[80]

The imido group can function solely as an ancillary ligand in vanadium-imide complexes that effect the polymerization of ethylene or other monomers to produce copolymers or elastomers.[92-95] and in hydroamination catalysis.[96] Moreover, it has been shown that for select vanadium-imide complexes, the imide ligand can act as a reactive centre, as demonstrated by the reaction of V(N*t*-Bu)Cl$_3$ with phosphaalkynes (Figure 1.9),[97, 98]and the C-H activation of hydrocarbons.[99, 100].

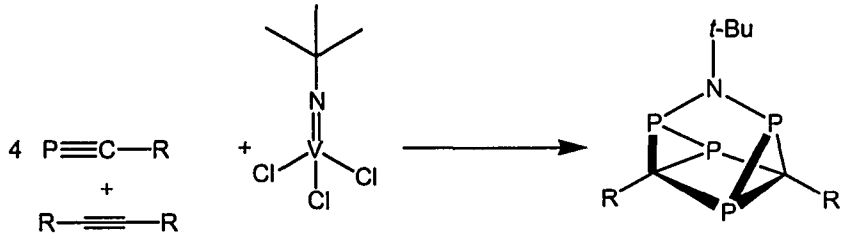

Figure 1.9: The synthesis of azatetraphosphaquaddricyclanes by reaction of phosphaalkynes and alkynes with V(N*t*-Bu)Cl$_3$.[97]

1.7 Vanadium Catalysts for Homogeneous Olefin Polymerization

The topic of homogeneous olefin polymerization employing vanadium catalysts has been reviewed recently.[101-103] In general, activated vanadium complexes tend to polymerize olefins with grossly inferior activities relative to their Group IV sister complexes. Since the initial discovery of Ziegler-Natta polymerization, Natta has shown that some tri-valent and tetra-valent vanadium complexes with aluminum trialkyl compounds catalyze random copolymerization reactions of ethylene and propylene.[104, 105] Low activities especially relative to their Group IV counterparts, have been attributed to the deactivation of the metal complex via reduction of the active metal centre.[106-109] On a more positive note, some of the advantages in using vanadium-based catalysts include: the production of high molecular weight polymer with narrow polydispersity indexes,[110] increased α-olefin incorporation into ethylene/α-olefin copolymers, and the production of syndiotactic polypropylene.[111-117] In addition, vanadium catalysts are important entities for the production of elastomers such as EPDM (ethlyene propylene diene monomer).[94, 101, 118-122]

A handful of vanadium complexes in the +V oxidation state have been tested as olefin polymerization catalysts.[93, 94, 109, 118, 121, 123-125] There are a few key features of vanadium(V) complexes that dictate the usefulness of this class of precursor as valuable homogeneous catalysts for olefin polymerization catalysts. First, alkylating agents were shown to reduce the metal centre of vanadium dichloride derivatives.[109] Therefore most polymerization reactions were performed using the dichloride derivatives and methylaluminoxane (MAO) as an activator. Secondly, the polymerization activities derived from vanadium(V) catalysts are considered to be generally low to moderate.[10] Lastly, the vanadium(V) complexes that have been tested as olefin polymerization catalysts have been limited to those containing imido, *tris*(pyrazoyl)borate, silsesquioxanes, and cyclopentadienyl-linked-amide ligands (see two examples in Figure 1.10).[92-94, 118, 124, 126, 127]

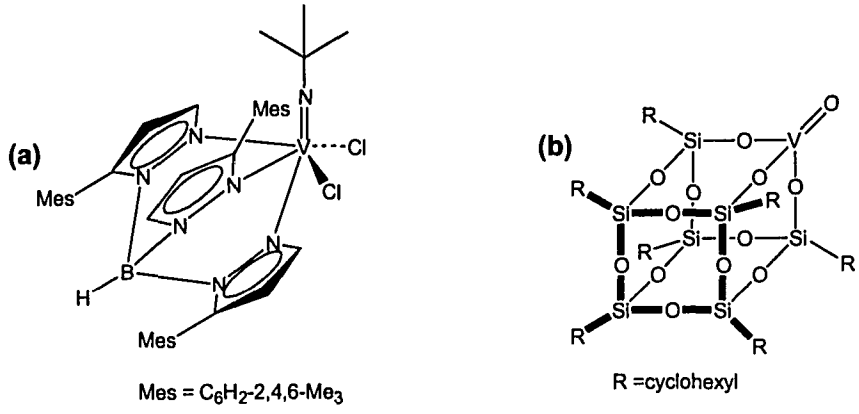

Figure 1.10: (a) Vanadium-*tris*(pyrazolyl)borate imide pre-catalyst,[126] and (b) vanadium-silsesquioxane pre-catalyst for olefin polymerization.[118]

Therefore, the synthesis of vanadium-phosphinimide complexes should be completed to examine their catalytic ability to effect the polymerization. We propose that due to the similarities that the phosphinimide ligand possesses compared to the cyclopentadienyl and imide ligands and the roaring success of the Group IV metal-phosphinimide complexes as catalysts in ethylene polymerization, that we might be able to extend this chemistry to vanadium derivatives.

1.8 Cocatalysts/Activators in Olefin Polymerization

Traditional Ziegler-Natta olefin polymerization is catalyzed by a two-component system containing a pre-catalyst component (transition metal) and a cocatalyst component (activator, usually a main group compound). The major role of the cocatalyst is to activate the pre-catalyst into a form in which olefin will bind and perform insertion chemistry in an iterative fashion. It has been shown that the resultant ion pair can also influence polymerization and the polymer product. The cocatalyst has the ability to affect many aspects of the polymerization such as catalytic activity, stability and the molecular weight of the polymer.[128] In many cases the cocatalyst can be more expensive to synthesize than the pre-catalyst itself. Therefore inexpensive syntheses of novel cocatalysts are greatly desired from an industrial perspective. Most cocatalysts in the

literature are based on the Group 13 elements aluminum and boron. Active cocatalysts include complexes such as aluminum alkyls, alkylaluminoxane, perfluorinated boranes and alanes, and borate and aluminate salts. The activator that is used most frequently in early metal olefin polymerization is methylaluminoxane (MAO), with the general formula $(AlO(Me))_n$. The synthesis of MAO involves the controlled hydrolysis of trimethylaluminum.[129, 130] There have been many studies conducted to unveil the composition of MAO,[131-135] however, the exact composition of the active species in MAO is to this day ambiguous. MAO has a few different roles in the olefin polymerization reaction: first it can serve as an alkylating agent to a metal halide precursor, secondly it can abstract a methyl or halide group from the metal centre and lastly it serves to purify the solvent/ethylene feed. The pre-catalyst/cocatalyst ratio required (500-10000 equivalents MAO: 1 equivalent of pre-catalyst) and the varying amounts of impurities such as TMA are two drawbacks in utilizing MAO as a cocatalyst.

Cocatalysts that are used frequently in the academic world are perfluorinated boranes. Unlike MAO, *tris*(pentafluorophenyl)borane ($B(C_6F_5)_3$) activates metal-alkyl pre-catalysts in a stoichiometric fashion (1 boron centre for every metal centre) which lends itself to mechanistic studies. A variety of other complexes in which the electron-withdrawing perfluorinated aryl rings have been incorporated have also been tested as cocatalysts. A couple examples of perfluorinated cocatalysts are depicted in Figure 1.11.[136-138]

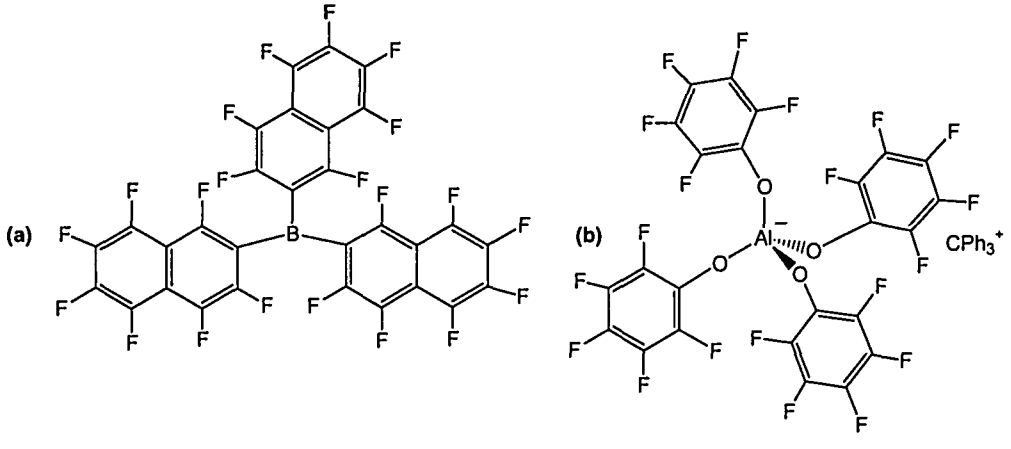

Figure 1.11: Examples of a neutral activator (a) *tris*(*β*-perfluoronapthyl)borane[136] and an ionic activator (b)trityl *tetra*(perfluorophenoxy)aluminate.[138]

The synthesis of boraluminoxanes, compounds in which aluminum and boron atoms are bridged by an oxygen atom, have been an interest to the research groups of Hessen,[139] Gibson[140] and Serwatowski.[141, 142] It is noteworthy that when the boraluminoxane Al(*t*-Bu_2Al)(*t*-BuAl)$_2$(O_2BAr)$_4$ (Ar = 2,6-*i*-$Pr_2C_6H_3$) (Figure 1.12) is combined with $ZrCpMe_2$, ethylene is polymerized with an activity of 2.59 kg mol^{-1} h^{-1} bar^{-1} in toluene at 5 bar of ethylene and 23°C over a period of 30 minutes.[139] It is proposed that this complex is active due to the presence of edge-sharing four-membered Al-O-Al-O rings, which mimics the proposed four-membered rings in MAO that Barron and coworkers believe may account for the "latent" Lewis acidic behaviour of MAO.[143-146] Investigations of boraluminoxanes and similar Al/O/B complexes are of significant interest to further our understanding of the nature of MAO and to potentially find new cocatalysts that perform as well or better than MAO.

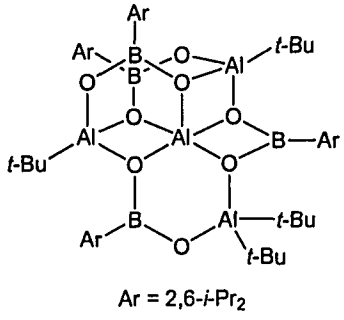

Figure 1.12: Illustration of the boraluminoxane Al(*t*-Bu_2Al)(*t*-BuAl)$_2$(O_2BAr)$_4$ (Ar = 2,6-*i*-$Pr_2C_6H_3$).[139]

1.9 Group 13 Phosphinimide Complexes

While the chemistry of transition metal-phosphinimide complexes has become well developed, the chemistry of phosphinimine complexes containing main group elements is relatively undeveloped. Complexes of this sort have been reviewed by Dehnicke and Weller.[147] The reactions of borane reagents with phosphinimines have led to a variety of both borane-phosphinimine coordination compounds[148-151] and

borylphosphinimide derivatives which contain a boron-nitrogen covalent bond.[148, 152-163] Examples of known *N*-borylphosphinimide complexes include the boratophosphazenes ($N(PCl_2NMe)BF_2$) [163] and dimeric complexes such as $(BCl_2(NPEt_3))_2$[164] and $[Fe_2(\eta\text{-}C_5H_5)_2(\eta\text{-}C_5H_4B(Br)(\mu\text{-}NPEt_3)_2]Br$.[155]

Given our interest in olefin polymerization, not only in catalyst synthesis but in cocatalyst development, investigations of Group 13 phosphinimine complexes were desirable. Aluminum-phosphinimide complexes such as $(Al(\mu\text{-}NP\textit{t}\text{-}Bu_3)X_2)_2$ (Figure 1.13) were synthesized via the reaction of alanes (TMA or $AlH_3{\cdot}NEt_2Me$) with $HNP\textit{t}\text{-}Bu_3$, however these complexes did not effect olefin polymerization solely or in conjunction with $ZrCp_2Me_2$.[21, 165] Treatment of two or more equivalents of this phosphinimine with the above alane reagents resulted solely in the synthesis of a monosubstituted aluminum phosphinimide compound. This could be attributed to the steric bulk of the *t*-Bu groups on phosphorus and the stability of the four-membered Al-N-Al-N core. The steric bulk provided by the $-NP\textit{t}\text{-}Bu_3$ ligand is apparent in complexes such as the borinium salt $[B(NP\textit{t}\text{-}Bu_3)_2]Cl$ in which the N-B-N and P-N-B bond angles are linear (Figure 1.13).[166] This monomeric form differs from most other boron derivatives of smaller phosphinimine substituents that adopt either dimeric and trimeric structures as demonstrated in the complexes $[(B(\mu\text{-}NPEt_3)_2)_2]Br_2$ [153] and $[(HB(\mu\text{-}NPEt_3)_3)_3]I_3$[162]. The addition of a third equivalent of $LiNP\textit{t}\text{-}Bu_3$ invoked no change and therefore did not result in the trisubstituted borane. It has been possible to get three appropriate phosphinimine substituents around the boron centre, however, as illustrated by the synthesis of the triphenylphosphiniminine derivative $B(NPPh_3)_3$.[154]

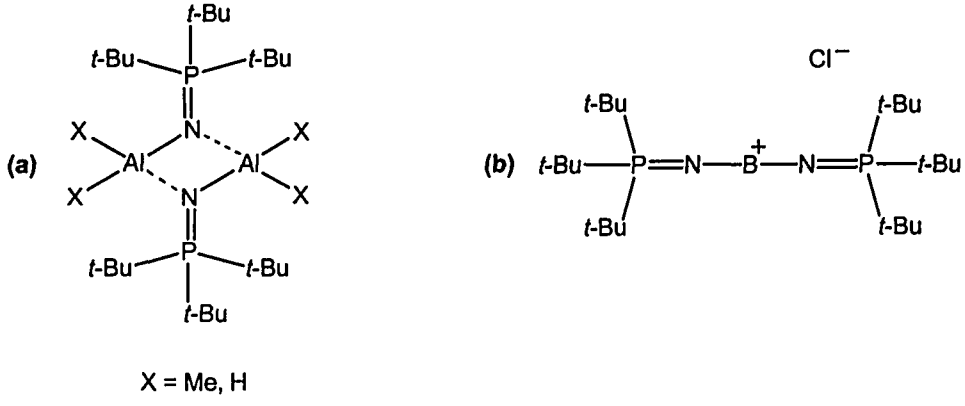

Figure 1.13: (a) The dimeric aluminum-phosphinimide complexes of the form (Al(μ-NP*t*-Bu$_3$)X$_2$)$_2$ (X = Me, H)[21, 165] and (b) the monomeric borinium salt [B(NP*t*-Bu$_3$)$_2$]Cl with a linear geometry of the five PNBNP atoms.[166]

The *t*-Bu groups of the disubstituted borylphosphinimine derivatives[166] provide enough protection to make complexes of this sort extremely inert. For this reason, they do not act as activators for the polymerization of ethylene.

1.10 Reactivity of the Phosphinimine Fragment

The utility of the phosphinimine fragment extends beyond that of an ancillary ligand to metal or main group elements. Within the last 20 years phosphinimines have become useful reagents in organic synthesis, in particular, aza-Wittig reactions. Phosphinimines can react with a series of small molecules such as carbonyl compounds to form imine complexes,[167, 168] and carbon dioxide, isocyanates, isothiocyanates and carbon disulfides to form heterocumulenes (Figure 1.14).[169, 170] The recent increase in the availability of functionalized-*N*-phosphinimines has made this class of compounds a versatile tool in the synthesis of various *N*-heterocycles via intra-[171, 172] or intermolecular[173, 174] aza-Wittig reactions.

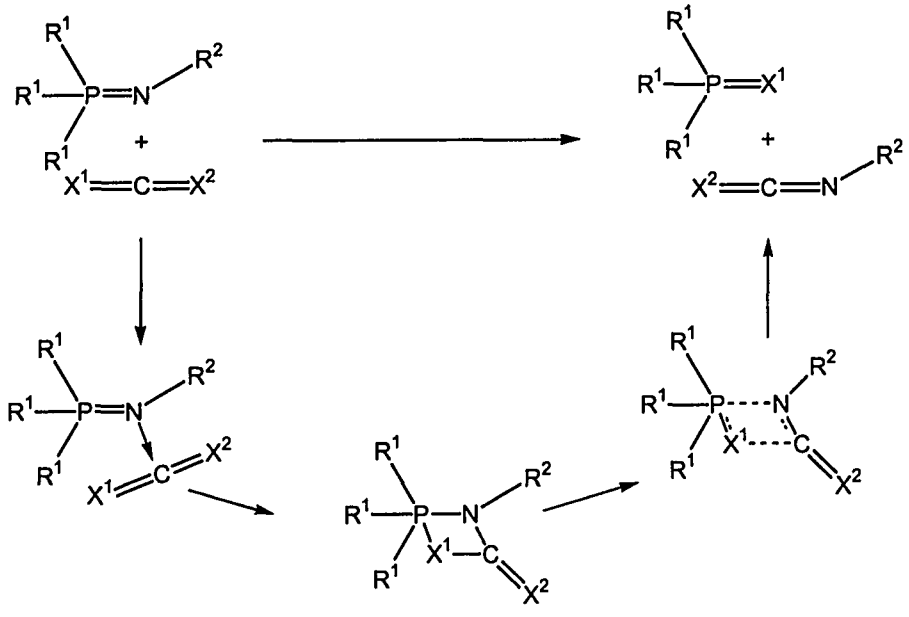

Figure 1.14: A general reaction scheme for aza-Wittig reactions of phosphinimines with small molecules such as CO_2, OCNR, SCNR, and CS_2.

Aza-Wittig reactions occur as a consequence of the polarity of the nitrogen-phosphorus bond, with a partial positive charge on phosphorus and a partial negative charge on nitrogen. It is the polarity of this bond that helps to dictate the reactivity. Many theoretical investigations have looked at the bonding in phosphinimines[175-180] and the mechanism of the aza-Wittig reaction.[181-184] Sundermann and Schoeller used an NBO partitioning scheme to indicate which Lewis structure (a) or (b) in Figure 1.15, best describes the phosphinimide ion $[NPH_3]^-$.[180] It was determined that the Lewis structure (a) best describes the free phosphinimide anion whereas a ligand coordinated to a metal centre is best described by Lewis structure (b).[180]

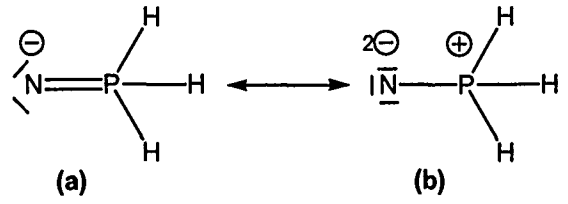

Figure 1.15: Possible Lewis structures of the phosphinimide anion $[NPH_3]^-$.

From calculated NH group charges of $HNPX_3$, Lu and coworkers determined the polarity of the P-N bond on a relative scale for a variety of substituents on phosphorus.[177] These calculations predict that the polarity of the P-N bond increases in the order Cl < Br < F < H < CH_3 < C_6H_5 < CH_2CH_3 < $C(CH_3)_3$, therefore suggesting that the ionic structure (HN^--P^+X_3) would be favoured for the phosphinimines with alkyl and aryl substituents on phosphorus.

Meyer and coworkers have reported that main group complexes, specifically phosphinimines of the formula $RNPX_3$ where X=Cl, pyrroyl; and R = alkyl, aryl, can act as transition metal catalyst alternatives for imine metathesis reactions.[185-188] The driving force behind these investigations on the catalytic properties of phosphinimines was the apparent similarities between the Wittig reaction (and the aza-Wittig reaction) and transition metal catalyzed alkene metathesis reactions.[187] The imine catalyzed metathesis reactions occur via a formal [2+2] addition of carbodiimides to the P-N multiple bond to form a diazaphosphetidine intermediate (Figure 1.16).

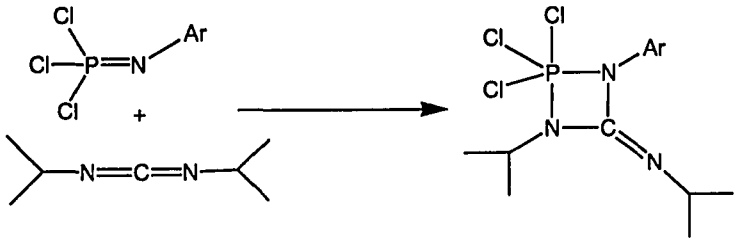

Figure 1.16: Synthesis of a diazaphosphetidine intermediate by reaction of phosphinimine with a carbodiimide.[186]

Studies on such phosphetidine intermediates have shown that phosphinimines containing electron-withdrawing groups can catalytically induce metathesis of imine substituents of carbodiimides to afford the asymmetric product (Figure 1.17).[186]

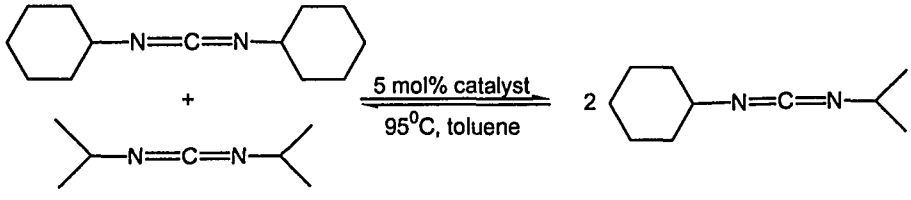

Figure 1.17: The scrambling of the carbodiimides ($(CyN)_2C$ and $(i\text{-}PrN)_2C$) as catalyzed by the phosphinimines (Cl_3PNR, where R = *p*-tolyl, Ph, *t*-Bu, *n*-Pr, *i*-Pr, 2-fluorophenyl).[186]

Recently, Manners and coworkers have reported that the reaction of $Me_3SiNPCl_3$ with PR_3 (R = Ph or *n*-Bu) resulted in the formation of Cl_2PNPR_3.[189] They propose that this reaction proceeds via imine transfer, loss of PCl_3 and subsequent loss of Me_3SiCl. The above examples suggest that there may be more potential applications for phosphinimines in organic transformations and in catalysis, thus rendering them worthy of investigation.

1.11 Reduction of Main Group Complexes Using Borane Reagents

A variety of complexes containing Group 15 and Group 16 elements in high oxidation states undergo reduction when reacted with borane reagents (Figure 1.18).[190-195]

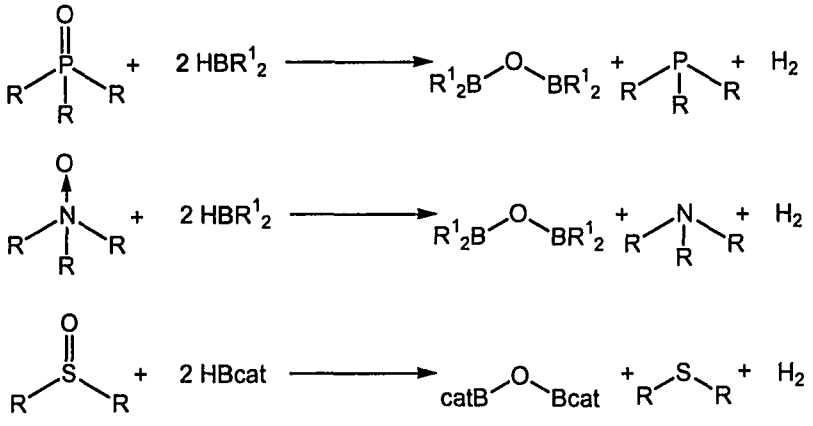

Figure 1.18: The reduction of complexes containing Group 15 and Group 16 elements in high oxidation states by borane reagents.[190-196]

The deoxygenation of sulfoxides (R_2SO) using HBcat has been reported by Westcott, Baker and coworkers.[190] In these reactions the diboron complex $O(Bcat)_2$ is formed in addition to the desired sulfide. At lower temperatures the boron-containing product forms an adduct with any remaining sulfoxide, therefore three equivalents of HBcat are required to achieve complete conversion.[190] However, in the presence of a Rh(I) catalyst, these reactions occur with stoichiometric amounts of catecholborane at room temperature within an hour.[190]

Köster and Morita showed that triphenylphosphine oxide could be reduced by tetrapropyldiborane, tripropylborane, diethylborane and trialkylamineboranes.[191] In these reactions, multiple boron-containing products were produced. More recently, Wolczanski and coworkers showed that deoxygenation of R_3PO could be achieved by using metal-silox complexes ($M(silox)_3$ where M = V, NbL (L = PMe_3, 4-picoline), Ta; silox = $OSi\textit{t}\text{-}Bu_3$) that are illustrated in Figure 1.19.[196] Reduction of phosphine oxides

occurs in the presence of $BH_3{\cdot}SMe_2$, producing phosphine-borane adducts.[193, 195] Also, BH_3 is added to diphosphines in the synthesis of *bis*(phosphine)monoxide ligands, which have been subsequently used to synthesize α-chiral amines.[197] The coordination of phosphinamide ligands to borane has been used to facilitate asymmetric catalysis of the reduction of ketones by boranes.[198]

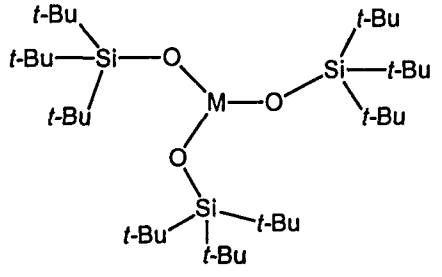

M= V, NbL (L = PMe_3, 4-picoline), Ta

Figure 1.19: Metal complexes capable of reducing phosphine oxides.[196]

Little chemistry has been reported on the reactivity of boryloxide complexes such as those formed as by-products during the deoxygenation of phosphine oxides or sulfoxides by borane reagents.[141] Published syntheses of boryloxide derivatives include the cautious hydrolysis of (dialkylamino)dihaloboranes (R_2NBCl_2 (R = *i*-Pr, *s*-Bu, *i*-Bu)) in the presence of a non-nucleophilic base.[199-201] Alternatively, the reaction of $(Me_2N)_2BC_2H_5$ with $(C_2H_5BO)_3$ yielded the boryloxide complex $(Me_2N)(C_2H_5)BOB(C_2H_5)(NMe_2)$.[202] Another route utilizes the reaction of a 3-cyano-1,2,4,3-triazaborole with Ag_2O to yield the *bis*(1,2,4,3-triazaboroyl)oxane (Figure 5.3).[203]

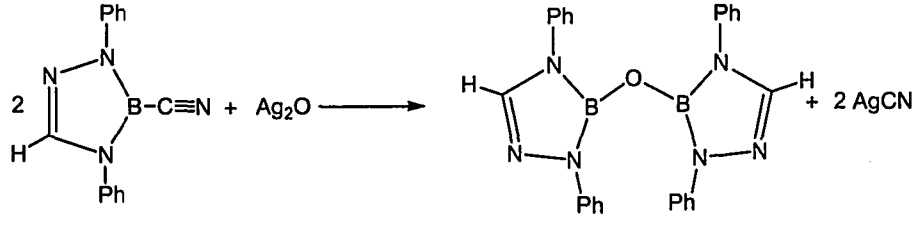

Figure 1.20: The synthesis of *bis*(1,2,4,3-triazaboroyl)oxane.

The groups of Power, Chisholm, Gibson and Serwatowski have utilized boryl reagents of the types $HOBAr_2$ and $LiOBAr_2$ to prepare metal diboryloxide complexes.[140, 142, 204-208] There are two examples of zirconium complexes containing boron-oxygen ligands found within the literature. The reaction of $ZrCp_2Me_2$ with $(PhBO)_3$ resulted in the formation of $(ZrCp_2(\mu\text{-}O_2BAr))_2$ (Ar = C_6H_5, C_6H_2-2,4,6-Me_3, C_6F_5)[209] and the reaction of $HOB(OSi(Ot\text{-}Bu)_3)_2$ with $ZrCp_2Me_2$ produced $ZrCp_2(Me)(OB(OSi(Ot\text{-}Bu)_3)_2)$.[210] These zirconium complexes are depicted in Figure 1.21 below.

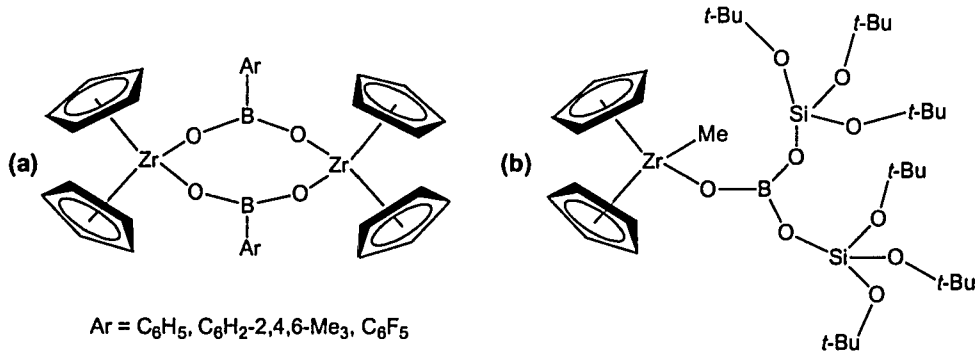

Figure 1.21: Chemical drawings of $(ZrCp_2(\mu\text{-}O_2BAr))_2$ (Ar = C_6H_5, C_6H_2-2,4,6-Me_3, C_6F_5) [209] and $ZrCp_2(Me)(OB(OSi(Ot\text{-}Bu)_3)_2)$ [210].

1.12 Scope of this Thesis

There is a desire, both industrially and academically, for the discovery of new organometallic catalysts. The industrial success of titanium phosphinimide complexes as catalysts for the polymerization of olefins was the driving force for our study of the synthesis of vanadium phosphinimide complexes and investigation into their potential utility as olefin polymerization catalysts. The high activities observed for the titanium phosphinimide catalysts were attributed to great steric bulk provided by the tri(*t*-butyl)phosphinimide ligand. This thesis will show that the steric influence of the phosphinimine ligand also governs the chemistry of main group derivatives. For

example, a detailed study of reactions of phosphinimines with pinacolborane reveal two divergent pathways, in which preference is dictated by the steric bulk of the substituents on the phosphorus atom of the phosphinimine. The steric effects are also realized in the bonding mode adopted by *N*-catecholborylphosphinimine derivatives, the reactivity of phosphinimines in the presence of alcohols and the reactivity of phosphine oxides with pinacolborane. Therefore, phosphinimines have been investigated with respect to their utility as an ancillary ligand in the synthesis of novel organometallic and main group compounds and as an organic reagent when reacted with pinacolborane in the synthesis of borylamines and tertiary phosphines.

2 Vanadium Imide Phosphinimide Complexes

2.1 Introduction

Since 1999, the majority of the scientific explorations conducted within the Stephan research group have involved the use of the phosphinimide fragment as an ancillary ligand complexed to an array of elements.[20-25, 27-32, 45, 149, 166, 211] The greatest industrial impact from this research remains the utility of select Group IV phosphinimide complexes as high activity olefin polymerization catalysts.[17-19, 36, 42] This discovery planted the seed for many other fruitful projects, including the work contained within this chapter.

The initial rationale given for the high activities observed for such compounds stemmed from a comparison of the phosphinimide ligand to the cyclopentadienyl ligand (Cp^-). As discussed in Chapter 1, the phosphinimide ligand may be considered to be isoelectronic with the Cp^- ligand.[212] Similarly, the imide functional group (NR^{2-}) and the Cp^- ligand have also been regarded as isoelectronic ligands in numerous reports.[9, 10, 213-218] All three molecular fragments (Cp^-, NPR_3^- and NR^{2-}) have frontier orbitals that bind to the metal atom through a combination of one σ and two π orbitals.

As high activities are observed for Group IV metallocene and phosphinimide catalysts during the polymerization of ethylene,[12, 18, 36] the synthesis of analogous Group V d^0 and d^1 complexes, specifically vanadium phosphinimide derivatives, was of particular interest. Given the analogies that have been drawn between the cyclopentadienyl, phosphinimide and imide ligands, the synthesis of vanadium complexes containing a phosphinimide and an imide ligand, or a phosphinimide and a cyclopentadienyl ligand were envisioned (Figure 2.1).

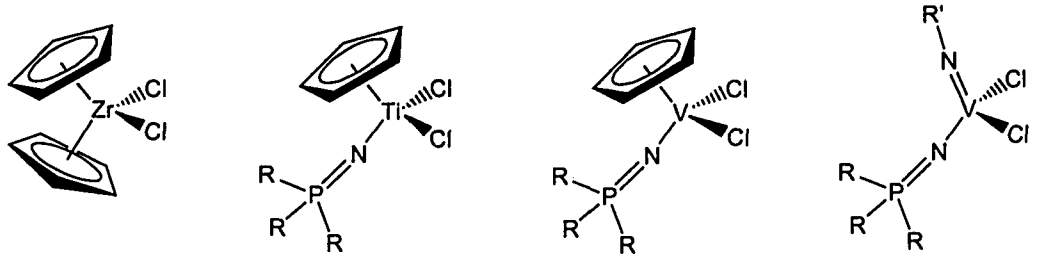

Figure 2.1: Given the isoelectronic nature of the phosphinimide, cyclopentadienyl and imide ligands, the above Group IV and Group V metal complexes could be considered analogous.[10, 18, 36, 58, 219, 220]

Therefore, to determine whether vanadium phosphinimide complexes have comparable activities to those observed for the Group IV phosphinimide-based catalysts, a series of complexes of the general formula, $V(NAr)(NPR_3)X_2$ (Ar = C_6H_5, C_6H_3-2,6-*i*-Pr_2; R = *t*-Bu, *i*-Pr, Ph; X = halide, alkyl, aryl, amide, oxide, thiolate and alkoxide ligands), were synthesized. The dichloride derivatives were evaluated as pre-catalysts for ethylene polymerization. The results are discussed herein.

2.2 Experimental

2.2.1 General Considerations

All preparations were performed under an atmosphere of dry O_2-free N_2 either employing Schlenk-line techniques or working in a Vacuum Atmospheres inert atmosphere glovebox. ^1H, $^{13}C\{^1H\}$, and $^{31}P\{^1H\}$ NMR spectra were recorded on a Bruker Avance 300 or 500 spectrometer operating at 300 and 500 MHz respectively. Line widths at half height ($\Delta\nu_{1/2}$) are given in Hertz. For ^1H and $^{13}C\{^1H\}$ NMR spectra, trace amounts of protonated solvents were used as references, and the chemical shifts are reported in parts per million relative to tetramethylsilane. $^{31}P\{^1H\}$ NMR spectra are referenced to an external standard consisting of an 85% aqueous solution of phosphoric acid. All coupling constants are reported as absolute values. DEPT and 2-D $^1H/^{13}C$ correlation experiments were completed for assignment of the carbon atoms.

Combustion analyses were performed at the University of Windsor Chemical Laboratories employing a Perkin Elmer CHN Series 2400 Analyzer and at Galbraith Laboratories in Knoxville, Tennessee. Some of the following complexes do not have combustion analyses reported. This data was not obtained either due to the sensitive nature of the compound or the isolated form of the complex.

2.2.2 Solvents

Anhydrous toluene, hexanes, *n*-pentane, tetrahydrofuran, diethylether, benzene and dichloromethane were purchased from Aldrich Chemical Company and were purified employing Grubbs-type column systems manufactured by Innovative Technologies or in-house by the University of Windsor Physics Machine Shop. Subsequently, toluene, hexanes, benzene, *n*-pentane and tetrahydrofuran were distilled from sodium and benzophenone under a nitrogen atmosphere. Dichloromethane was dried over calcium hydride and distilled. Deuterated benzene and toluene were purchased from Cambridge Isotopes Laboratories and purified by stirring over sodium and benzophenone for 16 h, followed by three freeze/pump/thaw degas cycles, and finally collected by vacuum distillation.

2.2.3 Materials

Hyflo Super Cel®, which will be referred to as Celite throughout the text, was purchased from Aldrich Chemical Company and dried in a vacuum oven for 16 h before storing in the glovebox. 4 Å Molecular sieves were purchased from Aldrich Chemical Company, dried at 100°C under vacuum prior to use and stored in the glovebox.

2.2.4 Reagents

Vanadium oxytrichloride, vanadium tetrachloride, phenylisocyanate, 2,6-di-*i*-propylphenylisocyanate, triphenylphosphine, azidotrimethylsilane, methyllithium, butyllithium, methylmagnesium bromide, phenylmagnesium bromide, benzylmagnesium bromide, benzylmercaptan, potassium *t*-butoxide and lithium hexamethylsilylamide were

used as purchased from Aldrich Chemical Company. Tri-*i*-propylphosphine and tri-*t*-butylphosphine were used as received from Strem Chemicals. *N*-trimethylsilyl-tri-*t*-butylphosphinimine in a 50 wt% solution in toluene was generously donated by Nova Chemicals Corporation. The toluene solution of phosphinimine was stored at *ca.* -30°C from which white crystalline solid was collected via filtration and dried *in vacuo*. *N*-trimethylsilyl-triphenylphosphinimine,[2] and *N*-trimethylsilyl-tri-*i*-propylphosphinimine[2] were prepared via literature methods.

2.2.5 Synthesis of Starting Materials

$V(NPh)Cl_3$ (2.1): This compound was synthesized using a modified literature procedure.[55, 85] A red solution of $VOCl_3$ (11.2 mL, 20.38 g, 117.62 mmol) in 50 mL of toluene was cooled in an ice bath and added via cannula to a colourless solution of PhNCO (10 mL, 10.96 g, 92.00 mmol) in 50 mL of toluene, also cooled in an ice bath. The mixture was slowly warmed up to room temperature and then heated at reflux for 36 h. Removal of the volatile products afforded a dark purple solid. Drying *in vacuo* for 10 h provided 19.4 g (85%) of this compound. ^1H NMR (300 MHz, C_6D_6) δ: 6.82 (d, 2H, $C_6\mathbf{H}_5$ (*o*-H), $^3J_{H\text{-}H}$ = 8 Hz), 6.48 (m, 3H, $C_6\mathbf{H}_5$ (*m*-H, *p*-H)). $^{13}C\{^1H\}$ NMR (partial) (75.5 MHz, C_6D_6) δ: 132.0 ($\mathbf{C}_6H_5$, (*o*-C)), 128.7 ($\mathbf{C}_6H_5$ (*p*-C)), 126.6 ($\mathbf{C}_6H_5$ (*m*-C)).

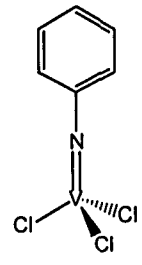

$V(NC_6H_3\text{-}2,6\text{-}i\text{-}Pr_2)Cl_3$ (2.2): This compound was prepared via a modified literature procedure.[90, 221] A red solution of $VOCl_3$ (4.7 mL, 8.56 g, 49.41 mmol) in 50 mL of toluene was cooled in an ice bath and slowly added via cannula to a cold, colourless solution of C_6H_3-2,6-*i*-Pr_2NCO (13.73 mL, 13.06 g, 64.23 mmol) in 50 mL of toluene. The mixture was slowly warmed up to room temperature and then heated at reflux for 24 h. Removal of the volatile products afforded a dark green solid. Drying *in vacuo* for 10 h provided 13.4 g (82%) of this compound. ^1H NMR (500 MHz, C_6D_6) δ: 6.67 (d, 2H, $C_6\mathbf{H}_3$ (*m*-H), $^3J_{H\text{-}H}$ = 7 Hz), 6.61 (t, 1H, $C_6\mathbf{H}_3$ (*p*-H), $^3J_{H\text{-}H}$ = 7 Hz), 4.31

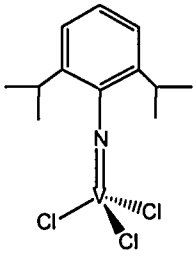

(septet, 2H, C**H**$(CH_3)_2$, $^3J_{H-H}$ = 7 Hz), 1.17 (d, 12H, CH(C**H**$_3)_2$, $^3J_{H-H}$ = 7 Hz). $^{13}C\{^1H\}$ NMR (partial) (75.5 MHz, C_6D_6) δ: 132.2 (**C**$_6H_3$ (*m*-C)), 123.0 (**C**$_6H_3$ (*p*-C)), 29.5 (**C**H$(CH_3)_2$), 24.2 (CH(**C**$H_3)_2$).

2.2.6 Synthesis of Vanadium Phosphinimide Complexes

[V(NPPh$_3$)$_3$Cl]Cl (2.3): A few crystals of the known compound [V(NPPh$_3$)$_3$Cl]Cl[53] were obtained in low yield from the reaction of $Me_3SiNPPh_3$ and $VOCl_3$. The crystals were grown from a toluene solution at 25°C. X-ray crystallographic data was obtained for these crystals. However, no NMR data was collected from this small amount of material.

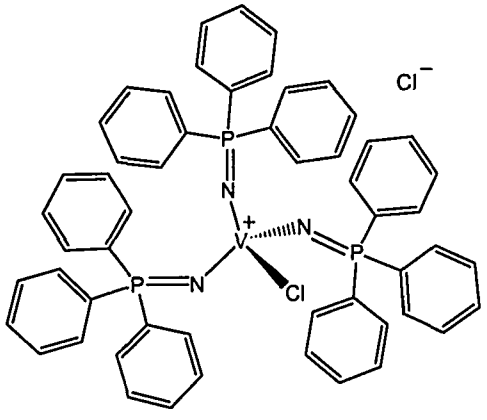

V(NPh)(NP*i*-Pr$_3$)Cl$_2$ (2.4): A colourless solution of Me_3SiNP*i*-Pr_3 (2.00 g, 8.08 mmol) in 20 mL of toluene was added at RT to a burgundy solution of V(NPh)Cl_3 **2.1**) (2.00 g, 8.05 mmol) in 50 mL of toluene. The resulting green solution was heated at reflux for 48 h. The solvent was removed *in vacuo* and the product was washed with hexanes (3 x 10 mL). Drying *in vacuo* for 8 h afforded a dark green solid (2.43 g, 78%). ^1H NMR (300 MHz, C_6D_6) δ: 7.11 (d, 2H, C_6**H**$_5$ (*o*-H) $^3J_{H-H}$ = 8 Hz), 6.94 (t, 2H, C_6**H**$_5$ (*m*-H), $^3J_{H-H}$ = 8 Hz), 6.72 (t, 1H, C_6**H**$_5$ (*p*-H), $^3J_{H-H}$ = 7 Hz), 1.73 (dseptet, 2H, C**H**$(CH_3)_2$, $^3J_{H-H}$ = 7 Hz, $^2J_{P-H}$ = 11 Hz), 0.78 (dd, 18H, CH(C**H**$_3)_2$, $^3J_{H-H}$ = 7 Hz, $^3J_{P-H}$ = 17 Hz). $^{31}P\{^1H\}$ NMR δ: (121.5 MHz, C_6D_6) δ: 56.9 ($\Delta\nu_{1/2}$ = 702 Hz). $^{13}C\{^1H\}$ NMR (partial) (75.5 MHz, C_6D_6) δ: 128.7 (**C**$_6H_5$ (*m*-C)), 125.6 (**C**$_6H_5$ (*p*-C)), 123.5 (**C**$_6H_5$ (*o*-C)), 25.4 (d, **C**H$(CH_3)_2$, $^1J_{P-C}$ = 53 Hz), 16.7 (CH(**C**$H_3)_2$). Calculated: H: 6.77%, C: 46.53%, N: 7.23%. Found: 6.78%, C: 46.63%, N: 6.76%.

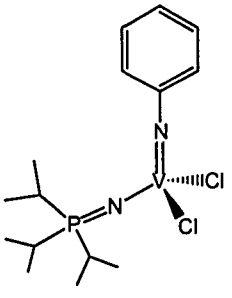

V(NPh)(NP*t*-Bu$_3$)Cl$_2$ (2.5): A colourless solution of Me$_3$SiNP*t*-Bu$_3$ (1.17 g, 4.03 mmol) in 10 mL of toluene was added at RT to a burgundy solution of V(NPh)Cl$_3$ (**2.1**) (1.00 g, 4.03 mmol) in 50 mL of toluene. The resulting green solution was heated at reflux for 36 h. The solvent was removed *in vacuo* and the product was washed with hexanes (3 x 10 mL). Drying *in vacuo* for 8 h afforded a dark green solid (1.41g, 75%). ^{1}H NMR (300 MHz, C_6D_6) δ: 7.07 (d, 2H, $C_6\mathbf{H}_5$ (*o*-H) $^3J_{H-H}$ = 8 Hz), 6.96 (t, 2H, $C_6\mathbf{H}_5$ (*m*-H) $^3J_{H-H}$ = 8 Hz), 6.71 (t, 1H, $C_6\mathbf{H}_5$ (*p*-H), $^3J_{H-H}$ = 7 Hz), 1.05 (d, 27H, C(C**H**$_3$)$_3$, $^3J_{P-H}$ = 14 Hz). ^{31}P{^{1}H} NMR (121.5 MHz, C_6D_6) δ: 64.4 ($\Delta\nu_{1/2}$ = 625 Hz). ^{13}C{^{1}H} NMR (partial) (75.5 MHz, C_6D_6) δ: 128.7 ($\mathbf{C}_6H_5$ (*m*-C)), 125.2 ($\mathbf{C}_6H_5$ (*p*-C)), 123.1 ($\mathbf{C}_6H_5$ (*o*-C)), 42.1 (d, **C**(CH$_3$)$_3$, $^1J_{P-C}$ = 40.0 Hz), 29.7 (C(**C**H$_3$)$_3$). Calculated: H: 7.51%, C: 50.36%, N: 6.53%. Found: H: 7.86%, C: 50.51%, N: 6.10%.

V(NPh)(NPPh$_3$)Cl$_2$ (2.6): A colourless solution of Me$_3$SiNPPh$_3$ (1.41 g, 4.03 mmol) in 25 mL of toluene was added at RT to a burgundy solution of V(NPh)Cl$_3$ (**2.1**) (1.00 g, 4.03 mmol) in 40 mL of toluene. The resulting burgundy solution was heated at reflux for 24 h. The solvent was removed *in vacuo* and the product was washed with hexanes (4 x 15 mL). Drying *in vacuo* for 5 h afforded a brown solid (1.41 g, 72%). ^{1}H NMR (300 MHz, C_6D_6) δ: 7.49 (dd, 6H, $PC_6\mathbf{H}_5$ (*o*-H) $^3J_{H-H}$ = 8 Hz, $^3J_{P-H}$ = 13 Hz), 6.94 (t, 3H, $PC_6\mathbf{H}_5$ (*p*-H) $^3J_{H-H}$ = 7 Hz), 6.83 (d of t, 6H, $PC_6\mathbf{H}_5$ (*m*-H), $^3J_{H-H}$ = 7 Hz, $^4J_{P-H}$ = 3 Hz), 6.63 (m, 4H, $NC_6\mathbf{H}_5$ (*o*-H, *m*-H), 6.56 (t, 1H, $NC_6\mathbf{H}_5$ (*p*-H) $^3J_{H-H}$ = 5 Hz). ^{31}P{^{1}H} NMR: (121.5 MHz, C_6D_6) δ: 22.6 ($\Delta\nu_{1/2}$ = 605 Hz). ^{13}C{^{1}H} NMR (partial): (75.5 MHz, C_6D_6) δ: 133.0 ($N\mathbf{C}_6H_5$ (*m*-C)), 132.9 (d, $NP\mathbf{C}_6H_5$ (*o*-C), $^2J_{P-C}$ = 11 Hz), 129.2 (d, $NP\mathbf{C}_6H_5$ (*m*-C), $^3J_{P-C}$ = 13 Hz), 128.0 ($NP\mathbf{C}_6H_5$ (*p*-C)), 125.4 ($N\mathbf{C}_6H_5$ (*p*-C)), 124.2 ($N\mathbf{C}_6H_5$ (*o*-C)), Calculated: H: 4.12%, C: 58.92%, N: 5.73%. Found: H: 4.31%, C: 58.27%, N: 5.35%.

V(NC$_6$H$_3$-2,6-*i*-Pr$_2$)(NP*i*-Pr$_3$)Cl$_2$ (2.7) A colourless solution of Me$_3$SiNP*i*-Pr$_3$ (1.48 g, 5.98 mmol) in 10 mL of toluene was added at RT to a green solution of V(NC$_6$H$_3$-2,6-*i*-Pr$_2$)Cl$_3$ (**2.2**) (1.99 g, 5.98 mmol) in 50 mL of toluene. The resulting green solution was heated at reflux for 18 h. The solvent was removed *in vacuo* and the product was washed with hexanes (3 x 10 mL). Drying *in vacuo* for 4 h afforded a green solid (2.06 g, 73%). ^{1}H NMR (300 MHz, C_6D_6) δ: 7.01 (d, 2H, NC$_6$**H**$_3$ (*m*-H), $^3J_{H\text{-}H}$ = 8 Hz), 6.88 (t, 1H, NC$_6$**H**$_3$ (*p*-H) $^3J_{H\text{-}H}$ = 7 Hz), 4.17 (septet, 2H, C**H**(CH$_3$)$_2$, $^3J_{H\text{-}H}$ = 7 Hz) 1.68 (dseptet, 3H, PC**H**(CH$_3$)$_2$, $^3J_{H\text{-}H}$ = 7 Hz, $^2J_{P\text{-}H}$ = 11 Hz), 1.39 (d, 12H, CH(C**H**$_3$)$_2$, $^3J_{H\text{-}H}$ = 9 Hz), 0.77 (dd, 18H, PCH(C**H**$_3$)$_2$, $^3J_{H\text{-}H}$ = 7 Hz, $^3J_{P\text{-}H}$ = 16 Hz). ^{31}P{^{1}H} NMR: (121.5 MHz, C_6D_6) δ: 56.3 (Δν$_{½}$ = 609 Hz). ^{13}C{^{1}H} NMR (partial) (75.5 MHz, C_6D_6) δ: 144.4 (N**C**$_6$H$_3$ (*o*-C)), 126.2 (N**C**$_6$H$_3$ (*p*-C)), 122.8 (N**C**$_6$H$_3$ (*m*-C), 29.2 (**C**H(CH$_3$)$_2$), 26.2 (d, P**C**H(CH$_3$)$_2$), $^1J_{P\text{-}C}$ = 53 Hz), 24.5 (CH(**C**H$_3$)$_2$), 16.7 (PCH(**C**H$_3$)$_2$). Calculated: H: 8.13%, C: 53.51%, N: 5.94%. Found: H: 7.84%, C: 52.87%, N: 6.63%.

V(NC$_6$H$_3$-2,6-*i*-Pr$_2$)(NP*t*-Bu$_3$)Cl$_2$ (2.8): A colourless solution of Me$_3$SiNP*t*-Bu$_3$ (1.25 g, 4.32 mmol) in 10 mL of toluene was added at RT to a green solution of V(NC$_6$H$_3$-2,6-*i*-Pr$_2$)Cl$_3$ (**2.2**) (1.44 g, 4.32 mmol) in 50 mL of toluene. The resulting green solution was heated at reflux for 16 h. The solvent was removed *in vacuo* and the product was washed with hexanes (3 x 10 mL). Drying *in vacuo* for 4 h afforded a green solid (2.02 g, 84 %). ^{1}H NMR (300 MHz, C_6D_6) δ: 7.03 (d, 2H, NC$_6$**H**$_5$ (*m*-H), $^3J_{H\text{-}H}$ = 8 Hz), 6.89 (t, 1H, NC$_6$**H**$_5$ (*p*-H), $^3J_{H\text{-}H}$ = 7 Hz), 4.10 (septet, 2H, C**H**(CH$_3$)$_2$, $^3J_{H\text{-}H}$ = 7 Hz) 1.41 (d, 12H, CH(C**H**$_3$)$_2$, $^3J_{H\text{-}H}$ = 7 Hz), 1.04 (d, 27H, C(C**H**$_3$)$_3$, $^3J_{P\text{-}H}$ = 14 Hz). ^{31}P{^{1}H} NMR: (121.5 MHz, C_6D_6) δ: 62.4 (Δν$_{½}$ = 732 Hz). ^{13}C{^{1}H} NMR (partial) (75.5 MHz, C_6D_6) δ: 143.7 (N**C**$_6$H$_5$ (*o*-C)), 126.0 (N**C**$_6$H$_5$ (*p*-C)), 122.7 (N**C**$_6$H$_5$ (*m*-C)), 45.6 (d, **C**(CH$_3$)$_3$, $^1J_{P\text{-}C}$ = 41 Hz), 29.6 (C(**C**H$_3$)$_3$), 29.3 (**C**H(CH$_3$)$_2$), 24.5 (CH(**C**H$_3$)$_2$). Calculated: H: 8.64%, C: 56.14%, N: 5.46%. Found: H: 8.40%, C: 56.64%, N: 5.53%.

V(NC$_6$H$_3$-2,6-*i*-Pr$_2$)(NPPh$_3$)Cl$_2$ (2.9): A solution of Me$_3$SiNPPh$_3$ (1.05 g, 3.01 mmol) in 10 mL of toluene was added at RT to a green solution of V(NC$_6$H$_3$-2,6-*i*-Pr$_2$)Cl$_3$ (**2.2**) (1.00 g, 3.01 mmol) in 50 mL of toluene. The resulting green solution was heated at reflux for 18 h. The solvent was removed *in vacuo* and the product was washed with hexanes (5 x 10 mL). Drying *in vacuo* for 6 h afforded a greenish-brown solid (1.37 g, 75%). ^{1}H NMR (300 MHz, C$_6$D$_6$) δ: 7.54 (dd, 6H, PC$_6$**H**$_5$ (*o*-H), $^3J_{H\text{-}H}$ = 8 Hz, $^3J_{P\text{-}H}$ = 13 Hz), 6.91 (t, 3H, PC$_6$**H**$_5$ (*p*-H), $^3J_{H\text{-}H}$ = 8 Hz), 6.80 (m, 9H, PC$_6$**H**$_5$ (*m*-H), NC$_6$**H**$_3$ (*p*-H, *m*-H)), 3.99 (septet, 2H, C**H**(CH$_3$)$_2$, $^3J_{H\text{-}H}$ = 7 Hz), 1.14 (d, 12H, CH(C**H**$_3$)$_2$, $^3J_{H\text{-}H}$ = 7 Hz). ^{31}P{^{1}H} NMR: (121.5 MHz, C$_6$D$_6$) δ: 20.4 ($\Delta\nu_{1/2}$ = 532 Hz). ^{13}C{^{1}H} NMR (partial) (75.5 MHz, C$_6$D$_6$) δ: 145.8 (P**C**$_6$H$_5$ (*ipso*-C)), 133.4 (N**C**$_6$H$_3$ (*o*-C)), 133.2 (d, P**C**$_6$H$_5$ (*o*-C), $^2J_{P\text{-}C}$ =11 Hz), 129.6 (d, (P**C**$_6$H$_5$ (*m*-C), $^3J_{P\text{-}C}$ = 13 Hz) 126.5 (N**C**$_6$H$_3$ (*p*-C)), 122.7 (N**C**$_6$H$_3$ (*m*-C)), 29.3 (**C**H(CH$_3$)$_2$), 24.4 (CH(**C**H$_3$)$_2$). Calculated: H: 5.62%, C: 62.84%, N: 4.89%; Found: H: 6.10%, C: 62.39%, N: 4.96%.

V(NC$_6$H$_3$-2,6-*i*-Pr$_2$)(NPt-Bu$_3$)Me$_2$ (2.10): A solution of MeLi (0.46 mmol) in Et$_2$O was added at RT to a green solution of V(NC$_6$H$_3$-2,6-*i*-Pr$_2$)(NPt-Bu$_3$)Cl$_2$ (**2.8**) (0.10 g, 0.18 mmol) in 30 mL of benzene. The resulting red solution was stirred for 1 h, then the solvent was removed *in vacuo*. The product was extracted with hexanes and filtered through Celite. Removal of the hexanes *in vacuo* afforded a red-brown solid. (0.070 g, 76%). ^{1}H NMR (300 MHz, C$_6$D$_6$) δ: 7.19 (d, 2H, C$_6$**H**$_5$ (*m*-H), $^3J_{H\text{-}H}$ = 8 Hz), 6.99 (t, 1H, C$_6$**H**$_5$ (*p*-H), $^3J_{H\text{-}H}$ = 8 Hz), 4.22 (septet, 2H, C**H**(CH$_3$)$_2$, $^3J_{H\text{-}H}$ = 7 Hz), 1.46 (d, 12H, CH(C**H**$_3$)$_2$, $^3J_{H\text{-}H}$ = 7 Hz), 1.39 (s, 6H, C**H**$_3$), 1.08 (d, 27H, C(C**H**$_3$)$_3$, $^3J_{P\text{-}H}$ = 13 Hz). ^{31}P{^{1}H} NMR: (121.5 MHz, C$_6$D$_6$) δ: 46.4 ($\Delta\nu_{1/2}$ = 931 Hz). ^{13}C{^{1}H} NMR (75.5 MHz, C$_6$D$_6$) δ: 142.8 (N**C**$_6$H$_3$ (*ipso*-C)), 128.3 (**C**$_6$H$_5$ (*m*-H)), 122.9 (**C**$_6$H$_5$ (*p*-H)), 122.5 (**C**$_6$H$_5$ (*o*-H)), 41.3 (d, **C**(CH$_3$)$_3$, $^1J_{P\text{-}C}$ = 45 Hz), 29.6 (C(**C**H$_3$)$_3$), 29.2 (**C**H(CH$_3$)$_2$), 24.4 (CH(**C**H$_3$)$_2$).

(V(μ-NPh)(NP*t*-Bu$_3$)Cl)$_2$ (2.11): Solid Zn metal (0.010 g, 0.153 mmol) was added to a green solution of V(NPh)(NP*t*-Bu$_3$)Cl$_2$ (**2.5**) (0.025 g, 0.0538 mmol) in 10 mL of toluene. This green solution was stirred for 16 h resulting in a red solution. The solution was filtered through Celite, the solvent was removed *in vacuo* and the product was dried for 4 hrs. (0.016 g, 76%). ^{1}H NMR (300 MHz, C_6D_6) δ: 7.87 (d, 2H, $C_6\mathbf{H}_5$ (*o*-H), $^3J_{H\text{-}H}$ = 7 Hz), 7.34 (t, 2H, $C_6\mathbf{H}_5$ (*m*-H), $^3J_{H\text{-}H}$ = 8 Hz), 6.96 (t, 1H, $C_6\mathbf{H}_5$ (*p*-H), $^3J_{H\text{-}H}$ = 7 Hz), 1.08 (d, 27H, C(C$\mathbf{H}_3$)$_3$, $^3J_{P\text{-}H}$ = 14 Hz). ^{31}P{^{1}H} NMR: (121.5 MHz, C_6D_6) δ: 53.1 ($\Delta\nu_{1/2}$ = 558 Hz). ^{13}C{^{1}H} NMR (75.5 MHz, C_6D_6) δ: 162.8 ($\mathbf{C}_6H_5$ (*ipso*-C)), 128.5 ($\mathbf{C}_6H_5$ (*m*-C)), 123.1 ($\mathbf{C}_6H_5$ (*p*-C)), 122.4 ($\mathbf{C}_6H_5$ (*o*-C)), 41.0 (d, $\mathbf{C}(CH_3)_3$, $^1J_{P\text{-}C}$ = 45 Hz), 29.5 (C($\mathbf{C}H_3$)$_3$). Calculated: H: 8.18%, C: 54.90%, N: 7.11% Found: H: 7.70% , C: 52.87%, N: 6.63%.

V(NC$_6$H$_3$-2,6-*i*-Pr$_2$)(NP*t*-Bu$_3$)Ph$_2$ (2.12) A solution of PhMgBr (0.304 mmol) in Et$_2$O was added at RT to a green solution of V(NC$_6$H$_3$-2,6-*i*-Pr$_2$)(NP*t*-Bu$_3$)Cl$_2$ (**2.8**) (0.05 g, 0.0911 mmol) in benzene/Et$_2$O. The resulting purple-red solution was stirred for 4 h. The solvent was removed *in vacuo* and the product extracted with hexanes. The solution was filtered through Celite and removal of the hexanes afforded a red-purple solid. (0.025 g, 44%). X-ray quality crystals were grown from hexanes at -30°C. ^{1}H NMR (300 MHz, C_6D_6) δ: 8.32 (d, 4H, VC$_6\mathbf{H}_5$ (*o*-H), $^3J_{H\text{-}H}$ = 7 Hz), 7.22 (t, 4H, VC$_6\mathbf{H}_5$ (*m*-H), $^3J_{H\text{-}H}$ = 7 Hz), 7.20 (t, 2H, VC$_6\mathbf{H}_5$ (*p*-H), $^3J_{H\text{-}H}$ = 5 Hz), 7.10 (d, 2H, $C_6\mathbf{H}_3$ (*m*-H), $^3J_{H\text{-}H}$ = 6 Hz), 6.98 (t, 1H, $C_6\mathbf{H}_3$ (*p*-H), $^3J_{H\text{-}H}$ = 8 Hz), 4.24 (septet, 2H, C$\mathbf{H}$(CH$_3$)$_2$, $^3J_{H\text{-}H}$ = 7 Hz), 1.29 (d, 12H, CH(C$\mathbf{H}_3$)$_2$, $^3J_{H\text{-}H}$ = 7 Hz), 1.13 (d, 27H, C(C$\mathbf{H}_3$)$_3$, $^3J_{P\text{-}H}$ = 13 Hz). ^{31}P{^{1}H} NMR (121.5 MHz, C_6D_6) δ: 51.6 ($\Delta\nu_{1/2}$ = 777 Hz). ^{13}C{^{1}H} NMR (partial) (75.5 MHz, C_6D_6) δ: 143.7 (N$\mathbf{C}_6$H$_3$ (*o*-C), 135.4 (V$\mathbf{C}_6$H$_5$ (*o*-C)), 126.9 (V$\mathbf{C}_6$H$_5$ (*p*-C)), 123.4 (N$\mathbf{C}_6$H$_3$ (*p*-C)), 122.5 (V$\mathbf{C}_6$H$_5$ (*m*-C), N$\mathbf{C}_6$H$_3$ (*m*-C)), 29.4 (s, PC($\mathbf{C}$H$_3$)$_3$), 28.2 (C$\mathbf{H}$(CH$_3$)$_2$), 24.8 (CH(C$\mathbf{H}_3$)$_2$).

V(NPh)(NP*t*-Bu$_3$)Ph$_2$ (2.13): A solution of PhMgBr (0.356 mmol) in Et_2O was added at RT to a green solution of V(NPh)(NP*t*-Bu$_3$)Cl$_2$ (**2.5**) (0.05 g, 0.108 mmol) in benzene/Et_2O. The resulting red solution was stirred for 4 h. The solvent was removed *in vacuo* and the product was extracted with hexanes. Filtering through Celite and subsequent removal of hexanes afforded a red solid. (0.028 g, 48%). ^{1}H NMR (300 MHz, C_6D_6) δ: 8.57 (d, 4H, VC_6**H**$_5$ (*o*-H), $^3J_{H\text{-}H}$ = 7 Hz), 7.44 (d, 2H, NC_6**H**$_5$ (*o*-H) $^3J_{H\text{-}H}$ = 8 Hz), 7.18 (m, 8H, VC_6**H**$_5$ (*m*-H, *p*-H), NC_6**H**$_5$ (*m*-H)), 6.87 (t, 1H, NC_6**H**$_5$ (*p*-H), $^3J_{H\text{-}H}$ = 7 Hz), 1.09 (d, 27H, C(C**H**$_3$)$_3$, $^3J_{P\text{-}H}$ = 13 Hz). ^{31}P{^{1}H} NMR (121.5 MHz, C_6D_6) δ: 52.7 ($\Delta\nu_{1/2}$ = 1192 Hz). ^{13}C{^{1}H} NMR (partial) (75.5 MHz, C_6D_6) δ: 136.1 (V**C**$_6$H$_5$ (*o*-C)), 129.0 (N**C**$_6$H$_5$ (*m*-C)), 127.4 (V**C**$_6$H$_5$ (*p*-C)),127.0 (V**C**$_6$H$_5$ (*m*-C)), 124.0 (N**C**$_6$H$_5$ (*p*-C)), 122.4 (N**C**$_6$H$_5$ (*o*-C)), 40.3 (d, **C**(CH$_3$)$_3$, $^1J_{P\text{-}C}$ = 44 Hz), 29.3 (PC(**C**H$_3$)$_3$).

V(NC$_6$H$_3$-2,6-*i*-Pr$_2$)(NP*i*-Pr$_3$)Ph$_2$ (2.14): A solution of PhMgBr (0.318 mmol) in Et_20 was added at RT to a green solution of V(NC$_6$H$_3$-2,6-*i*-Pr$_2$)(NP*i*-Pr$_3$)Cl$_2$ (**2.7**) (0.050 g, 0.106 mmol) in benzene. The resulting red solution was stirred for 2 h. The solvent was removed *in vacuo* and the product was extracted with hexanes and filtered through Celite. Removal of hexanes *in vacuo* afforded a burgundy solid (0.021 g, 36%). ^{1}H NMR (300 MHz, C_6D_6) δ: 8.34 (d, 4H, VC_6**H**$_5$ (*o*-H), $^3J_{H\text{-}H}$ = 7 Hz), 7.45 (d, 2H, C_6**H**$_3$ (*m*-H), $^3J_{H\text{-}H}$ = 7 Hz), 7.16 (m, 6H, VC_6**H**$_5$ (*m*-H, *p*-H)), 6.98 (t, 1H, C_6**H**$_3$ (*p*-H), $^3J_{H\text{-}H}$ = 7 Hz), 4.46 (septet, 2H, C**H**(CH$_3$)$_2$, $^3J_{H\text{-}H}$ = 6 Hz) 1.73 (dseptet, 3H, PC**H**(CH$_3$)$_2$, $^3J_{H\text{-}H}$ = 7 Hz, $^2J_{P\text{-}H}$ = 11 Hz), 1.28 (d, 12H, CH(C**H**$_3$)$_2$, $^3J_{H\text{-}H}$ = 7 Hz), 0.86 (dd, 18H, CH(C**H**$_3$)$_2$, $^3J_{H\text{-}H}$ = 7 Hz, $^3J_{P\text{-}H}$ = 15 Hz). ^{31}P{^{1}H} NMR: (121.5 MHz, C_6D_6) δ: 40.5 ($\Delta\nu_{1/2}$ = 668 Hz). ^{13}C{^{1}H} NMR (partial) (75.5 MHz, C_6D_6) δ: 143.7 (N**C**$_6$H$_3$ (*o*-C), 135.9 (V**C**$_6$H$_5$ (*o*-C)), 127.0 (V**C**$_6$H$_5$ (*p*-C)), 123.7 (N**C**$_6$H$_3$ (*p*-C), 122.7 (V**C**$_6$H$_5$ (*m*-C), N**C**$_6$H$_3$ (*m*-C)), 28.3 (**C**H(CH$_3$)$_2$), 25.8 (d, P**C**H(CH$_3$)$_2$, $^1J_{P\text{-}C}$ = 57 Hz), 24.7 (CH(**C**H$_3$)$_2$), 16.8 (PCH(**C**H$_3$)$_2$).

V(NPh)(NP*i*-Pr$_3$)Bn$_2$ (2.15): A solution of BnMgBr (0.773 mmol) in Et_2O was added at RT to a green mixture of V(NPh)(NP*i*-Pr$_3$)Cl$_2$ (**2.4**) (0.15 g, 0.387 mmol) in Et_2O. The resulting red solution was stirred for 3 h, and subsequently the solvent was removed *in vacuo*. The product was extracted with *n*-pentane and filtered through Celite. Removal of the solvent afforded a burgundy solid. (0.116 g, 62%). ^{1}H NMR (500 MHz, C_6D_6) δ: 7.30 (d, 4H, $VCH_2C_6\mathbf{H}_5$ (*o*-H), $^3J_{H-H}$ = 7 Hz), 7.18 (m, 8H, $VCH_2C_6\mathbf{H}_5$ (*m*-H), $NC_6\mathbf{H}_5$ (*m*-H, *o*-H), 6.93 (t, 2H, $VCH_2C_6\mathbf{H}_5$ (*p*-H), $^3J_{H-H}$ = 7 Hz), 6.83 (t, 1H, $NC_6\mathbf{H}_5$ (*p*-H), $^3J_{H-H}$ = 7 Hz), 3.15 (d, 2H, $VC\mathbf{H}_2C_6H_5$, $^2J_{H-H}$ = 8 Hz), 2.84 (d, 2H, $VC\mathbf{H}_2C_6H_5$, $^2J_{H-H}$ = 8 Hz), 1.55 (dseptet, 3H, $C\mathbf{H}(CH_3)_2$, $^3J_{P-H}$ = 7 Hz, $^2J_{H-H}$ = 11 Hz), 0.72 (dd, 18H, $CH(C\mathbf{H}_3)_2$, $^3J_{P-H}$ = 15 Hz, $^3J_{H-H}$ = 7 Hz). $^{31}P\{^1H\}$ NMR: (121.5 MHz, C_6D_6) δ: 43.6 ($\Delta\nu_{1/2}$ = 729 Hz). $^{13}C\{^1H\}$ NMR (partial) (125.8 MHz, C_6D_6) δ: 147.2 ($N\mathbf{C}_6H_5$ (*ipso*-C)), 130.2 ($VCH_2\mathbf{C}_6H_5$ (*o*-C)), 128.9 ($VCH_2\mathbf{C}_6H_5$ (*m*-C)), 128.8 ($N\mathbf{C}_6H_5$ (*o*-C)), 124.0 ($N\mathbf{C}_6H_5$ (*m*-C)), 123.2 ($VCH_2\mathbf{C}_6H_5$ (*p*-C)), 122.6 ($N\mathbf{C}_6H_5$ (*p*-C)), 38.6 ($V\mathbf{C}H_2C_6H_5$), 25.5 (d, $P\mathbf{C}H(CH_3)_2$, $^1J_{P-C}$ = 55 Hz), 16.9 ($PCH(\mathbf{C}H_3)_2$). Calculated: H: 8.09%, C: 69.86%, N: 5.62%, Found: H: 7.35% C: 68.61%, N: 5.46%.

V(NPh)(NP*t*-Bu$_3$)(Bn)$_2$ (2.16): A 1.0 M solution of BnMgCl (0.43 mL, 0.43 mmol) in Et_2O was added to a green slurry of V(NPh)(NP*t*-Bu$_3$)Cl$_2$ (**2.5**) (0.100 g, 0.215 mmol) in Et_2O. The resulting bright cherry red solution was stirred for 3 h. The Et_2O was removed *in vacuo*. The red oil was dissolved in toluene and filtered through Celite. The toluene was removed *in vacuo* and the product was washed with *n*-pentane (3 x 5 mL). The product was isolated as a red oil in 55% yield (0.068 g). ^{1}H NMR (500 MHz, C_6D_6) δ: 7.31 (d, 4H, $VCH_2C_6\mathbf{H}_5$ (*o*-H), $^3J_{H-H}$ = 8 Hz), 7.18 (m, 8H, $VCH_2C_6\mathbf{H}_5$ (*m*-H), $NC_6\mathbf{H}_5$ (*m*-H), $NC_6\mathbf{H}_5$ (*o*-H)), 6.93 (t, 2H, $VCH_2C_6\mathbf{H}_5$ (*p*-H), $^3J_{H-H}$ = 7 Hz), 6.83 (m, 1H, $NC_6\mathbf{H}_5$ (*p*-H), $^3J_{H-H}$ = 7 Hz), 3.12 (d, 2H, $VC\mathbf{H}_2C_6H_5$, $^2J_{H-H}$ = 9 Hz), 2.99 (d, 2H, $VC\mathbf{H}_2C_6H_5$, $^2J_{H-H}$ = 9 Hz), 0.98 (d, 27H, $PC(C\mathbf{H}_3)_3$, $^3J_{P-H}$ = 13 Hz). $^{31}P\{^1H\}$ NMR (202.46 MHz, C_6D_6) δ: 51.0. $^{13}C\{^1H\}$ NMR (partial) (125.76 MHz, C_6D_6) δ: 129.7

($VCH_2C_6H_5$ (*o*-C)), 128.8 ($VCH_2C_6H_5$ (*m*-C)), 128.7 (NC_6H_5 (*o*-C)), 124.0 (NC_6H_5 (*m*-C), 123.0 ($VCH_2C_6H_5$ (*p*-C)), 122.5 (NC_6H_5 (*p*-C)), 40.5 (d, $PC(CH_3)_3$, $^1J_{P-C}$ = 44 Hz), 38.6 ($VCH_2C_6H_5$), 29.6 ($PC(CH_3)_3$).

$V(NC_6H_3$-2,6-*i*-$Pr_2)(NPPh_3)Bn_2$ (2.17): A solution of BnMgBr (0.205 mmol) in Et_2O was added at RT to green solution of $V(NC_6H_3$-2,6-*i*-$Pr_2)(NPPh_3)Cl_2$ (**2.9**) (0.05 g, 0.082 mmol) in toluene. The purple solution was stirred for 30 min. The solvent was removed, the product was extracted with hexanes and filtered through Celite. Removal of the solvent afforded a purple solid (0.021 g, 36 %). ^{1}H NMR (500 MHz, C_6D_6) δ: 7.40 (dd, 6H, $PC_6\mathbf{H}_5$ (*o*-H), $^3J_{P-H}$ = 13 Hz, $^3J_{H-H}$ = 8 Hz), 7.13 (m, 10 H, $VCH_2C_6\mathbf{H}_5$ (*o*-H, *m*-H, *p*-H)), 6.94 (m, 12H, $NC_6\mathbf{H}_3$ (*m*-H, *p*-H) $PC_6\mathbf{H}_5$ (*m*-H, *p*-H)), 4.23 (septet, 2H, $NC_6H_3(C\mathbf{H}(CH_3)_2)$, $^3J_{H-H}$ = 7 Hz), 3.47 (d, 2H, $VC\mathbf{H}_2C_6H_5$, $^2J_{H-H}$ = 10 Hz), 2.99 (d, 2H, $VC\mathbf{H}_2C_6H_5$, $^2J_{H-H}$ = 10 Hz), 1.16 (d, 12H, $CH(C\mathbf{H}_3)_2$), $^3J_{H-H}$ = 7 Hz). $^{31}P\{^1H\}$ NMR: (121.5 MHz, C_6D_6) δ: 7.9. $^{13}C\{^1H\}$ NMR (partial) (75.5 MHz, C_6D_6) δ: 148.8 ($VCH_2C_6H_5$ (*ipso*-C)), 145.0 (PC_6H_5 (*ipso*-C)), 133.3 (d, PC_6H_5 (*o*-C), $^2J_{P-C}$ = 10 Hz), 132.5 ($VCH_2C_6H_5$ (*o*-C)), 131.8 (NC_6H_3 (*o*-C)), 130.4 ($VCH_2C_6H_5$ (*m*-C)), 129.4 (d, PC_6H_5 (*m*-C), $^3J_{P-C}$ = 12 Hz), 124.4 (NC_6H_3 (*p*-C)), 123.6 (NC_6H_3 (*m*-C)), 123.2 ($VCH_2C_6H_5$ (*p*-C)), 29.3 ($C\mathbf{H}(CH_3)_2$), 24.7 ($CH(C\mathbf{H}_3)_2$).

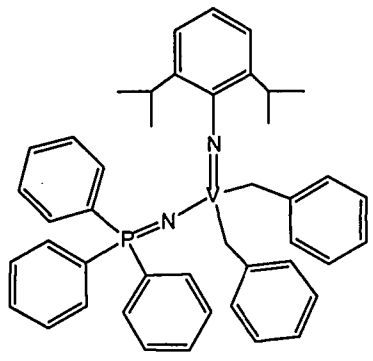

V(NPh)(NP*t*-Bu_3)$(SEt)_2$ (2.18): Solid NaSEt (0.018 g, 0.215 mmol) was added to a green solution of V(NPh)(NP*t*-Bu_3)Cl_2 (**2.5**) (0.050 g, 0.108 mmol) in 10 mL of toluene. After approximately 2 h the solution turned bright red. The resulting red solution was filtered through Celite, and the solvent was removed *in vacuo*. The product was dissolved in hexane and filtered through Celite. Hexane was removed *in vacuo* and a red powder was isolated. The product precipitated as a crystalline solid from a saturated benzene solution in 36% yield. ^{1}H NMR (300 MHz, C_6D_6) δ: 7.34 (d, 2H, $C_6\mathbf{H}_5$ (*o*-H) $^3J_{H-H}$ = 8 Hz), 7.08 (t, 2H, $C_6\mathbf{H}_5$ (*m*-H) $^3J_{H-H}$ =8 Hz), 6.80 (t, 1H, $C_6\mathbf{H}_5$ (*p*-H) $^3J_{H-H}$

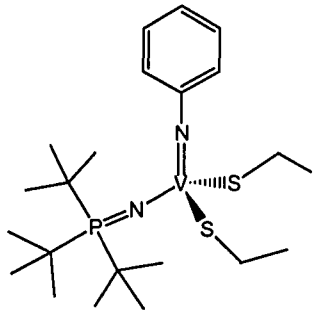

= 7 Hz), 3.96 (dq, 2H, SCH_2CH_3, $^3J_{H-H}$ = 7 Hz, $^2J_{H-H}$ = 11 Hz), 3.89 (dq, 2H, SCH_2CH_3, $^3J_{H-H}$ = 7 Hz, $^2J_{H-H}$ = 12 Hz), 1.67 (t, 6H, SCH_2CH_3, $^3J_{H-H}$ = 8 Hz), 1.12 (d, 27H, $C(CH_3)_3$, $^3J_{P-H}$ = 14 Hz). $^{31}P\{^1H\}$ NMR: (202.5 MHz, C_6D_6) δ: 52.6 (Δν½ = 980 Hz). $^{13}C\{^1H\}$ NMR (partial) (75.5 MHz, C_6D_6) δ: 129.0 (NC_6H_5 (*m*-C)), 123.9 (NC_6H_5 (*p*-C)), 123.6 (NC_6H_5 (*o*-C)), 41.2 (d, $C(CH_3)_3$, $^1J_{P-H}$ = 45 Hz), 32.0 (SCH_2CH_3), 30.6 ($C(CH_3)_3$), 20.4 (SCH_2CH_3). Calculated: H: 8.81%, C: 54.98%, N: 5.88%; Found: H: 9.51%, C: 54.93%, N: 5.20%.

V(NC$_6$H$_3$-2,6-*i*-Pr$_2$)(NP*t*-Bu$_3$)(SEt)$_2$ (2.19): A 5 mL THF solution of V(NC$_6$H$_3$-2,6-*i*-Pr$_2$)(NP*t*-Bu$_3$)Cl$_2$ (**2.8**) (0.05 g, 0.091 mmol) was added to a 5 mL THF solution of NaSEt (0.017 g, 0.200 mmol). After stirring for 5 min the green solution turned a reddish brown colour. The solution was stirred for 1 h, and the solvent was removed *in vacuo*. The product was dissolved in toluene and filtered through Celite and stored in the glovebox for crystallization. Over time the solvent evaporated leaving a red solid (0.012 g, 25%). ^1H NMR (500 MHz, C_6D_6) δ: 7.13 (d, 2H, NC_6H_3 (*m*-H), $^3J_{H-H}$ = 8 Hz), 6.97 (t, 1H, NC_6H_3 (*p*-H), $^3J_{H-H}$ = 8 Hz), 4.45 (septet, 2H, $CH(CH_3)_2$), $^3J_{H-H}$ = 7 Hz), 3.90 (m, 4H, SCH_2CH_3), 1.58 (t, 6H, SCH_2CH_3, $^3J_{H-H}$ = 7 Hz), 1.48 (d, 12H, $CH(CH_3)_2$, $^3J_{H-H}$ = 7 Hz), 1.10 (d, 27H, $PC(CH_3)_3$, $^3J_{P-H}$ = 13 Hz). $^{31}P\{^1H\}$ NMR: (202.5 MHz, C_6D_6) δ: 52.5 (Δν½ = 825 Hz). $^{13}C\{^1H\}$ NMR (partial) (75.5 MHz, C_6D_6) δ: 124.3 (NC_6H_3 (*p*-C), 122.8 (NC_6H_3 (*m*-C)), 31.8 (SCH_2CH_3), 29.7 ($PC(CH_3)_3$, 28.9 ($CH(CH_3)_2$), 25.0 ($CH(CH_3)_2$), 19.8 (SCH_2CH_3). Calculated: H: 9.64%, C: 59.54%, N: 4.96%; Found: H: 9.11%, C: 59.19%, N: 4.86%.

V(NC$_6$H$_3$-2,6-*i*-Pr$_2$)(NP*t*-Bu$_3$)(SBn)$_2$ (2.20): A 5 mL toluene solution of V(NC$_6$H$_3$-2,6-*i*-Pr$_2$)(NP*t*-Bu$_3$)Cl$_2$ (**2.8**) (0.05 g, 0.091 mmol) was added to a 5 mL toluene solution of LiSBn (0.027 g, 0.207 mmol). The solution was stirred for 30 min and filtered through Celite. The solvent was removed *in vacuo* and the resulting red oil was washed with hexanes (3 x 5 mL) to remove residual grease and other hexane-soluble impurities. The product was dried *in vacuo*, affording a dark reddish brown solid. (0.026 g, 40%). ^{1}H NMR (300 MHz, C_6D_6) δ: 7.53 (d, 4H, SCH$_2$C$_6$**H**$_5$ (*o*-H), $^3J_{H\text{-}H}$ = 7 Hz), 7.15 (m, 6H, SCH$_2$C$_6$**H**$_5$ (*m*-H, *p*-H)), 7.05 (d, 2H, NC$_6$**H**$_3$ (*m*-H), $^3J_{H\text{-}H}$ = 6 Hz), 6.97 (t, 1H, NC$_6$**H**$_3$ (*p*-H), $^3J_{H\text{-}H}$ = 7 Hz), 5.17 (d, 2H, SC**H**$_2$C$_6$H$_5$, $^2J_{H\text{-}H}$ = 13 Hz), 5.05 (d, 2H, SC**H**$_2$C$_6$H$_5$, $^2J_{H\text{-}H}$ = 13 Hz), 4.43 (septet, 2H, C**H**(CH$_3$)$_2$, $^3J_{H\text{-}H}$ = 7 Hz), 1.46 (d, 12H, CH(C**H**$_3$)$_2$, $^3J_{H\text{-}H}$ = 7 Hz), 1.09 (d, 27H, PC(C**H**$_3$)$_3$, $^3J_{P\text{-}H}$ = 14 Hz), ^{31}P{^{1}H} NMR: (121.5 MHz, C_6D_6) δ: 54.27 ($\Delta\nu_{1/2}$ = 510.83 Hz). ^{13}C{^{1}H} NMR (partial) (75.5 MHz, C_6D_6) δ: 143.9 (SCH$_2$**C**$_6$H$_5$ (*ipso*-C)), 143.1 (N**C**$_6$H$_3$ (*o*-C), 129.5 (SCH$_2$**C**$_6$H$_5$ (*o*-C)), 128.9 (SCH$_2$**C**$_6$H$_5$ (*m*-C)), 128.1 (SCH$_2$**C**$_6$H$_5$ (*p*-C)), 124.6 (N**C**$_6$H$_3$ (*p*-C), 122.8 (N**C**$_6$H$_3$ (*m*-C)), 41.8 (S**C**H$_2$C$_6$H$_5$), 41.5 (d, P**C**(CH$_3$)$_3$, $^1J_{P\text{-}C}$ = 31.5 Hz) 29.7 (PC(**C**H$_3$)$_3$), 29.0 (**C**H(CH$_3$)$_2$), 25.0 (CH(**C**H$_3$)$_2$).

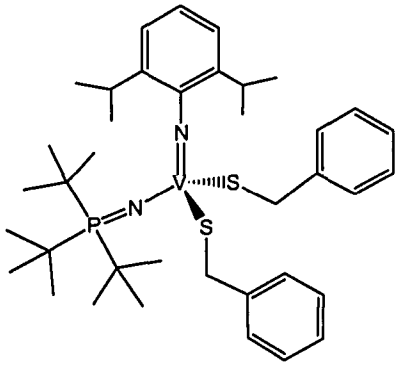

V(NPh)(NP*t*-Bu$_3$)(SBn)Cl (2.21): Solid NaSBn (0.026 g, 0.172 mmol) was added to slurry of V(NPh)(NP*t*-Bu$_3$)Cl$_2$ (**2.5**) (0.080 g, 0.172 mmol) in 10 mL of *n*-pentane. The greenish slurry was stirred for 2 h, during which time the colour changed to brown. The mixture was filtered through Celite, resulting in a fire engine red solution. *n*-Pentane was removed from the supernatant *in vacuo* resulting in a bright red oil (0.043 g). By NMR analyses, the oil contained a 1:1 mixture of the mono-substituted complex and the *bis*-substituted complex. The mono-substituted thiolate complex could not be isolated. However, upon addition of another equivalent of NaSBn, this compound was completely converted to the *bis*-substituted thiolate complex. The spectral data corresponding to V(NPh)(NP*t*-Bu$_3$)(SBn)Cl is included below. ^{1}H

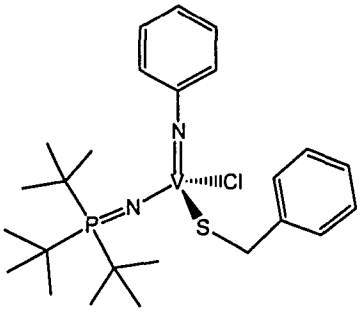

NMR (500 MHz, C_6D_6) δ: 7.49 (d, 2H, $SCH_2C_6\mathbf{H}_5$ (*o*-H), $^3J_{H-H}$ = 7 Hz), 7.20 (d, 2H, $NC_6\mathbf{H}_5$ (*o*-H), $^3J_{H-H}$ = 8 Hz) 7.09 (m, 5H, $SCH_2C_6\mathbf{H}_5$ (*m*-H, *p*-H), $NC_6\mathbf{H}_5$ (*m*-H)), 6.75 (t, 1H, $NC_6\mathbf{H}_5$ (*p*-H), $^3J_{H-H}$ = 7 Hz) 5.40 (d, 1H, $SC\mathbf{H}_2C_6H_5$, $^2J_{H-H}$ = 13 Hz), 5.27 (d, 1H, $SC\mathbf{H}_2C_6H_5$, $^2J_{H-H}$ = 13 Hz), 1.06 (d, 27H, $PC(C\mathbf{H}_3)_3$, $^3J_{P-H}$ = 12 Hz). $^{31}P\{^1H\}$ NMR: (121.5 MHz, C_6D_6) δ: 44.0. $^{13}C\{^1H\}$ NMR (partial) (125.76 MHz, C_6D_6) δ: 129.8, 129.5, 129.1, 127.1, 124.5, 123.8 (aryl peaks, unassigned), 42.8 ($S\mathbf{C}H_2Ph$), 41.1 (d, $P\mathbf{C}(CH_3)_3$ $^1J_{P-C}$ = 43 Hz), 29.7 ($PC(\mathbf{C}H_3)_3$).

V(NPh)(NP*t*-Bu$_3$)(SBn)$_2$ (2.22): Solid NaSBn (0.049 g, 0.335 mmol) was added to a green solution of V(NPh)(NP*t*-Bu$_3$)Cl$_2$ (**2.5**) (0.073 g, 0.157 mmol) in 20 mL of THF. The resulting red solution was stirred for 5 min and filtered through Celite. Removal of the solvent afforded a red oil. (0.030 g, 35%). ^{1}H NMR (300 MHz, C_6D_6) δ: 7.54 (d, 4H, $SCH_2C_6\mathbf{H}_5$ (*o*-H), $^3J_{H-H}$ = 8 Hz), 7.26 (d, 2H, $NC_6\mathbf{H}_5$ (*o*-H), $^3J_{H-H}$ = 8 Hz) 7.06 (m, 8H, $SCH_2C_6\mathbf{H}_5$ (*m*-H, *p*-H), $NC_6\mathbf{H}_5$ (*m*-H)), 6.80 (t, 1H, $NC_6\mathbf{H}_5$ (*p*-H), $^3J_{H-H}$ = 7 Hz) 5.19 (d, 2H, $SC\mathbf{H}_2C_6H_5$, $^2J_{H-H}$ = 13 Hz), 5.08 (d, 2H, $SC\mathbf{H}_2C_6H_5$, $^2J_{H-H}$ = 14 Hz), 1.09 (d, 27H, $PC(C\mathbf{H}_3)_3$, $^3J_{P-H}$ = 14 Hz). $^{31}P\{^1H\}$ NMR: (202.5 MHz, C_6D_6) δ: 54.7 ($\Delta\nu_{1/2}$ = 560 Hz). $^{13}C\{^1H\}$ NMR (partial) (125.76 MHz, C_6D_6) δ: 144.2, 129.5, 128.9, 128.7, 126.8, 123.9, 123.8 (aryl peaks unassigned), 41.8 ($S\mathbf{C}H_2C_6H_5$), 41.1 (d, $P\mathbf{C}(CH_3)_3$, $^1J_{P-C}$ = 42.1 Hz) 29.7 ($PC(\mathbf{C}H_3)_3$). Calculated: H: 7.67%, C: 63.55%, N: 4.63%; Found: H: 6.67%, C:64.30%, N: 4.25%.

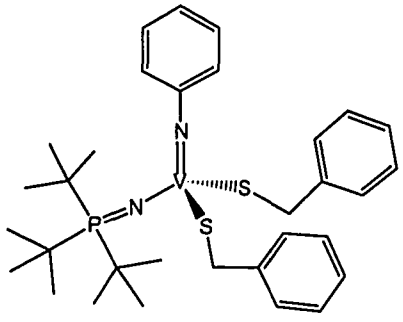

V(NPh)(NP*i*-Pr$_3$)(SBn)$_2$ (2.23): A 5 mL green solution of V(NPh)(NP*i*-Pr$_3$)Cl$_2$ (**2.4**) (0.050 g, 0.129 mmol) in toluene was added to a 5 mL solution of LiSBn (0.056 g, 0.52 mmol) in toluene. The solution turned bright red upon addition of the vanadium compound. The solution was stirred for 30 min and subsequently filtered through Celite. The toluene was removed *in vacuo* resulting in a red oily

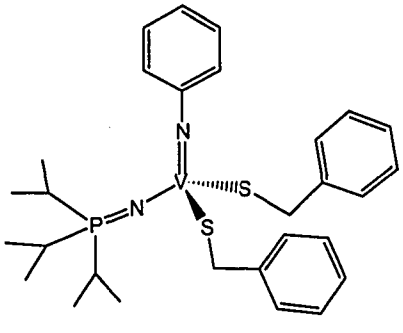

product. (0.048 g, 63%). ^{1}H NMR (500 MHz, C_6D_6) δ: 7.56 (d, 4H, $SCH_2C_6\mathbf{H}_5$ (*o*-H), $^{3}J_{H\text{-}H}$ = 7 Hz), 7.26 (d, 2H, $NC_6\mathbf{H}_5$ (*o*-H), $^{3}J_{H\text{-}H}$ = 7 Hz), 7.05 (m, 8H, $SCH_2C_6\mathbf{H}_5$ (*m*-H, *p*-H), $NC_6\mathbf{H}_5$ (*m*-H)), 6.34 (t, 1H, $NC_6\mathbf{H}_5$ (*p*-H), $^{3}J_{H\text{-}H}$ = 7 Hz), 5.13 (d, 2H, $SC\mathbf{H}_2C_6H_5$, $^{2}J_{H\text{-}H}$ = 13 Hz), 5.08 (d, 2H, $SC\mathbf{H}_2C_6H_5$, $^{2}J_{H\text{-}H}$ = 13 Hz) 1.62 (m, 3H, $C\mathbf{H}(CH_3)_2$), 0.81 (dd, 18H, $CH(C\mathbf{H}_3)_2$, $^{3}J_{H\text{-}H}$ = 8 Hz , $^{3}J_{P\text{-}H}$ = 14 Hz). ^{31}P{^{1}H} NMR (121.5 MHz, C_6D_6) δ: 48.2.

V(NPh)(NP*t*-Bu$_3$)(N(SiMe$_3$)$_2$)Cl (2.24): A solution of LiN(SiMe$_3$)$_2$ (0.018 g, 0.11 mmol) in THF was added to a green toluene solution of V(NPh)(NP*t*-Bu$_3$)Cl$_2$ (**2.5**) (0.035 g, 0.075 mmol) at -30°C. The resulting red solution was stirred for 5 min. The solvent was removed *in vacuo* and the product was redissolved in benzene and filtered through Celite. The removal of benzene afforded a red-brown oil. (0.020 g, 49%) ^{1}H NMR: (500 MHz, C_6D_6) δ: 7.40 (d, 2H, $NC_6\mathbf{H}_5$ (*o*-H), $^{3}J_{H\text{-}H}$ = 8 Hz), 7.04 (t, 2H, $NC_6\mathbf{H}_5$ (*m*-H), $^{3}J_{H\text{-}H}$ = 8 Hz), 6.76 (t, 1H, $NC_6\mathbf{H}_5$ (*p*-H), $^{3}J_{H\text{-}H}$ = 8 Hz), 1.16 (d, 27H, $C(C\mathbf{H}_3)_3$, $^{3}J_{P\text{-}H}$ = 13 Hz), 0.66 (s, 18H, $Si(C\mathbf{H}_3)_3$). ^{31}P{^{1}H} NMR (121.5 MHz, C_6D_6) δ: 52.3 ($\Delta\nu_{1/2}$ = 727 Hz). ^{13}C{^{1}H} NMR (partial) (75.5 MHz, C_6D_6) δ: 128.3 ($N\mathbf{C}_6H_5$ (*m*-C)), 123.9 ($N\mathbf{C}_6H_5$ (*o*-C)), 123.7 ($N\mathbf{C}_6H_5$ (*p*-C)), 41.3 (d, $P\mathbf{C}(CH_3)_3$, $^{1}J_{P\text{-}C}$ = 90 Hz), 29.7 ($PC(\mathbf{C}H_3)_3$), 6.1 ($Si(\mathbf{C}H_3)_3$).

μ-O(V(NPh)(NP*t*-Bu$_3$)(N(SiMe$_3$)$_2$))$_2$ (2.25): A red solution of V(NPh)(NP*t*-Bu$_3$)(N(SiMe$_3$)$_2$)Cl (**2.24**) (0.033 g, 0.06 mmol) in *n*-pentane was stored in the glovebox at room temperature for three months during which time oxidation occurred from an unknown oxidizing agent. Red X-ray quality crystals formed in the vial in very low yield (0.003 g, 5%). ^{1}H NMR (300 MHz, C_6D_6) δ: 7.47 (d, 4H, $NC_6\mathbf{H}_5$ (*o*-H), $^{3}J_{H\text{-}H}$ = 8 Hz), 7.13 (t, 4H, $NC_6\mathbf{H}_5$ (*m*-H), $^{3}J_{H\text{-}H}$ = 8 Hz), 6.77 (t, 2H, $NC_6\mathbf{H}_5$ (*p*-H), $^{3}J_{H\text{-}H}$ = 8 Hz), 1.31 (d, 54H, $C(C\mathbf{H}_3)_3$, $^{3}J_{P\text{-}H}$ = 13 Hz), 0.76 (s, 36H, $Si(C\mathbf{H}_3)_3$). ^{31}P{^{1}H} NMR (121.5 MHz, C_6D_6) δ: 45.0 ($\Delta\nu_{1/2}$ = 1164 Hz). ^{13}C{^{1}H} NMR

(partial) (75.5 MHz, C_6D_6) δ: 126.4 (NC_6H_5), 123.1 (NC_6H_5), 41.8 (d, $PC(CH_3)_3$, $^1J_{P-C}$ = 45.4 Hz), 30.8 ($PC(CH_3)_3$), 8.2 ($Si(CH_3)_3$)) 7.2 ($Si(CH_3)_3$)).

V(NPh)(NP*t*-Bu$_3$)(O*t*-Bu)$_2$ (2.26): Solid KO*t*-Bu (0.012 g, 0.107 mmol) was added to a green solution of V(NPh)(NP*t*-Bu$_3$)Cl$_2$ (**2.5**) (0.025 g, 0.053 mmol) in 5 mL of toluene. The resulting solution was stirred for 5 min during which time the colourless solution turned bright cherry red. Toluene was removed *in vacuo* and the red solid was dissolved in 5 mL of *n*-pentane, filtered through Celite and reduced to a 2 mL solution. This solution was stored at -30°C from which bright red X-ray quality crystals were obtained. ^{1}H NMR (500 MHz, C_6D_6) δ: 7.34 (d, 2H, NC_6H_5 (*o*-H), $^3J_{H-H}$ = 8 Hz), 7.13 (t, 2H, NC_6H_5 (*m*-H), $^3J_{H-H}$ = 8 Hz), 6.78 (t, 1H, NC_6H_5 (*p*-H), $^3J_{H-H}$ = 7 Hz), 1.65 (s, 18H, $OC(CH_3)_3$), 1.22 (d, 27H, $PC(CH_3)_3$, $^3J_{P-H}$ = 13 Hz). $^{31}P\{^1H\}$ NMR: (202.5 MHz, C_6D_6) δ: 45.0 ($\Delta\nu_{1/2}$ = 656 Hz). $^{13}C\{^1H\}$ NMR (partial) (125.76 MHz, C_6D_6) δ: 128.8 (NC_6H_5 (*o*-C)), 124.0 (NC_6H_5 (*p*-C)), 122.5 (NC_6H_5 (*m*-C)), 42.0 (d, $PC(CH_3)_3$, $^1J_{P-C}$ = 46 Hz), 33.8 ($OC(CH_3)_3$), 30.0 ($PC(CH_3)_3$).

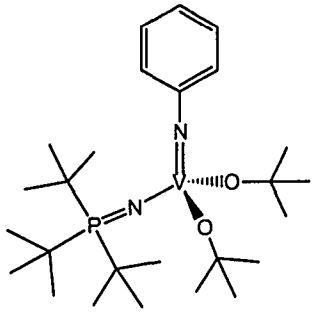

V(NC$_6$H$_3$-2,6-*i*-Pr$_2$)(NP*i*-Pr$_3$)(O*t*-Bu)$_2$ (2.27): Solid KO*t*-Bu (0.024 g, 0.212 mmol) was added to a greenish purple solution of V(NC$_6$H$_3$-2,6-*i*-Pr$_2$)(NP*i*-Pr$_3$)Cl$_2$ (**2.7**) (0.050 g, 0.106 mmol) in 5 mL of toluene. The resulting fire engine red solution was stirred for 1 h. The toluene was removed *in vacuo* and the remaining red solid was dissolved in *n*-pentane and filtered through Celite. The *n*-pentane solution was reduced to 2.5 mL and stored at -30°C. From this cold solution X-ray quality crystals were obtained. ^{1}H NMR (500 MHz, C_6D_6) δ: 7.10 (d, 2H, NC_6H_3 (*m*-H), $^3J_{H-H}$ = 8 Hz), 6.92 (t, 1H, NC_6H_3 (*p*-H), $^3J_{H-H}$ = 8 Hz), 4.69 (septet, 2H, $CH(CH_3)_2$, $^3J_{H-H}$ = 7 Hz), 1.87 (dseptet, 3H, $PCH(CH_3)$, $^3J_{H-H}$ = 7 Hz, $^2J_{P-H}$ = 11 Hz), 1.59 (s, 18H, $OC(CH_3)_3$), 1.43 (d, 12H, $(CH(CH_3)_2)$, $^3J_{H-H}$ = 7 Hz), 0.99 (dd, 18H, $PCH(CH_3)_2$), $^3J_{H-H}$ = 7 Hz, $^3J_{P-H}$ = 15 Hz). $^{31}P\{^1H\}$ NMR: (202.5 MHz, C_6D_6) δ: 35.8 ($\Delta\nu_{1/2}$ = 814 Hz). $^{13}C\{^1H\}$ NMR (partial)

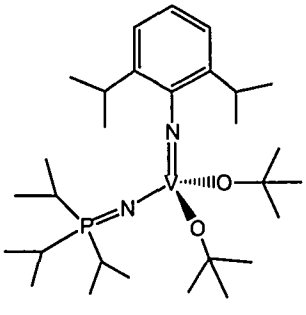

(75.5 MHz, $C_6D_5CD_3$) δ: 137.1 (NC_6H_3 (*o*-C)), 123.0 (NC_6H_3 (*p*-C)), 122.3 (NC_6H_3 (*m*-C)), 32.6 ($CH(CH_3)_2$), 26.7 (d, $PCH(CH_3)_2$, $^1J_{P-C}$ = 44 Hz), 24.6 ($OC(CH_3)_3$), 16.7 ($PCH(CH_3)_2$), 13.9 ($CH(CH_3)_2$).

2.2.7 Experimental for X-ray Crystallography

2.2.7.1 X-ray Data Collection and Reduction:

In order to maintain the integrity of the crystals' composition they were manipulated and mounted into glass capillaries bought from Charles Supper Company with diameters of 0.7 mm or 0.5 mm, in a dry, O_2-free, N_2 atmosphere. The diffraction experiments were performed on a Siemens SMART System CCD diffractometer at 20°C with Mo Kα radiation (λ = 0.71069 Å). The observed extinctions were consistent with the space groups determined for each sample. Measures of decay were obtained by re-collecting the first 50 frames of each data set. The intensities of the reflections within these frames showed no statistically significant change over the duration of the respective data collections. Empirical absorption corrections based on redundant data were applied to each set. Subsequent solution and refinements were performed using the SHELXTL solution package.

2.2.7.2 Structure Solutions and Refinements

Non-hydrogen atomic scattering factors were taken from literature tabulations.[222] The heavy atom positions were determined using the direct methods or Patterson techniques. The remaining non-hydrogen atoms were located from successive difference Fourier map calculations. The refinements were carried out by using full-matrix least squares techniques on F, minimizing the function $w(|F_o| - |F_c|)^2$ where the weight, w, is defined as $4F_o^2/2\sigma(F_o^2)$ and F_o and F_c are the observed and calculated structure factor amplitudes. In the final cycle of each refinement, all non-hydrogen atoms were assigned anisotropic temperature factors, except where noted otherwise. Carbon-bound hydrogen atom positions were calculated and allowed to ride on the carbon to which they are bonded. Hydrogen atom temperature factors were fixed at 1.5 times the isotropic

temperature factor of the carbon atom to which they are bonded. The hydrogen atom parameters were calculated, but not refined.

X-ray structural solutions of $[V(NPPh_3)_3Cl]Cl$ (**2.3**), $V(NC_6H_3\text{-}2,6\text{-}i\text{-}Pr_2)(NPt\text{-}Bu_3)Ph_2$ (**2.12**), $\mu\text{-}O(V(NPh)(NPt\text{-}Bu_3)(N(SiMe_3)_2))_2$ (**2.25**) and $V(NPh)(NPt\text{-}Bu_3)(Ot\text{-}Bu)_2$ (**2.26**) were performed as described above. Compound **2.26** was solved as a twinned crystal with the twin rotated from the first domain by 85.3° about the reciprocal axis -0.044, 1.00, -0.049 and the real axis -0.217, 1.00, -0.214. In addition, a preliminary solution was obtained for $V(NPh)(NPi\text{-}Pr_3)Cl_2$ (**2.4**) although a detailed discussion is precluded due to unusual disorder of the molecule in the solid state. In the same vein, a solution was obtained for $V(NPh)(NPi\text{-}Pr_3)Bn_2$ (**2.15**) however the data was of poor quality and is used only to confirm connectivity. Cell parameters, R, R_w and goodness of fit values are located in Table 2.1 and Table 2.2, while detailed structural parameters have been included as appendix on CD (Appendix A). For the better data, no residual electron density remained in any of the solutions that were of any chemical significance. ORTEP drawings of **2.3**, **2.4**, **2.12**, **2.18**, **2.25** and **2.26** are depicted in Figure 2.2, Figure 2.6, Figure 2.9, Figure 2.13 and Figure 2.15. Selected bond distances and bond angles are provided in the text.

Table 2.1: X-ray crystallographic data obtained from crystals of $[V(NPPh_3)_3Cl]Cl$ **(2.3)**, $V(NPh)(NP\textit{i}\text{-}Pr_3)Cl_2$ **(2.4)**, and $V(NC_6H_3\text{-}2,6\text{-}\textit{i}\text{-}Pr_2)(NP\textit{t}\text{-}Bu_3)Ph_2$ **(2.12)**.

Crystal	2.3	2.4	2.12
Molecular Formula	$C_{54}H_{45}Cl_2N_3P_3V$	$C_{15}H_{26}Cl_2N_2PV$	$C_{36}H_{54}N_2PV$
Formula Weight	980.72	387.20	596.72
a (Å)	13.646(6)	28.8766(2)	12.220(3)
b (Å)	13.646(6)	8.7410(2)	13.049(6)
c (Å)	47.73(3)	15.4261(2)	13.109(5)
α°	90	90	88.73(3)
β°	90	93.99	73.30(3)
γ°	120	90	63.48(3)
Crystal System	Trigonal	Monoclinic	Triclinic
Space Group	R-3	Cc	P-1
Volume ($Å^3$)	7697(7)	3884.3(1)	1778(1)
D_{calc} (gcm^{-3})	1.269	1.324	1.115
Z	6	4	2
Abs coeff, μ, mm^{-1}	0.430	0.864	0.348
θ range (°)	1.92 - 23.28	2.75 – 24.00	2.25 – 25.00
Reflections Collected	11110	8739	2935
Data $F_o^2 > 3\sigma(F_o^2)$	2438	5396	2935
Parameters	200	415	361
R^a	0.0359	0.0553	0.0793
$R_w{}^b$	0.0811	0.1067	0.1396
Goodness of Fit	0.881	0.980	1.204

This data was collected at 20°C with Mo Kα radiation (λ = 0.71069 Å).

[a] $R = \Sigma(F_o\text{-}F_c)/\Sigma F_o$

[b] $R_w = (\Sigma[w(F_o^2\text{-}F_c^2)^2] / \Sigma[w(F_o)^2])^{½}$

Table 2.2: X-ray crystallographic data obtained from crystals of V(NPh)(NP*i*-Pr$_3$)Bn$_2$ **(2.15)**, μ-O(V(NPh)(NP*t*-Bu$_3$)(N(SiMe$_3$)$_2$))$_2$ **(2.25)**, and V(NPh)(NP*t*-Bu$_3$)(O*t*-Bu)$_2$ **(2.26)**.

Crystal	2.15	2.25	2.26
Molecular Formula	$C_{29}H_{40}N_2PV$	$C_{48}H_{100}N_6OP_2Si_4V_2$	$C_{26}H_{56}N_2O_2PV$
Formula Weight	498.54	1053.52	504.59
a (Å)	9.9897(2)	12.471(6)	9.980(2)
b (Å)	10.3492(3)	20.06(1)	16.282(3)
c (Å)	14.5740(4)	25.45(1)	10.385(2)
α°	88.473(2)	90	90
β°	74.175(1)	90	116.22(3)
γ°	84.576(1)	90	90
Crystal System	Triclinic	Orthorhombic	Monoclinic
Space Group	P-1	$P2_12_12_1$	$P2_1/m$
Volume (Å^3)	1443.14(6)	6369(6)	1531.8(5)
D_{calc} (gcm^{-3})	1.147	2.197	1.107
Z	2	8	2
Abs coeff, μ, mm^{-1}	0.417	0.907	0.402
θ range (°)	2.13 – 24.69	1.29 – 23.23	2.19 – 25.00
Reflections Collected	4788	27500	2990
Data $F_o^2 > 3\sigma(F_o^2)$	3004	9079	2990
Parameters	288	568	158
R[a]	0.1702	0.0371	0.0663
R_w[b]	0.3640	0.0741	0.1854
Goodness of Fit	1.071	1.087	1.013

This data was collected at 20°C with Mo Kα radiation (λ = 0.71069 Å).

[a] $R=\Sigma(F_o-F_c)/\Sigma F_o$

[b] $R_w=(\Sigma[w(F_o^2-F_c^2)^2]/\Sigma[w(F_o)^2])^{1/2}$

2.2.8 Protocol for Ethylene Polymerization Testing

2.2.8.1 General Considerations

Polymerization testing was conducted at the University of Windsor using Schlenk-line techniques or a Büchi polymerization reactor that was built by Dr. Chad Beddie.[6] The latter polymerization experiments were performed by a summer undergraduate student, Mr. Thahn Nguyen. GPC analyses of the polymer samples were performed by NOVA Chemicals Corporation employing a Waters 150C GPC instrument using 1,2,4-trichlorobenzene as the mobile phase at 150°C. Sample preparation involved the dissolution of the polymer sample in 1,2,4-trichlorobenzene and subsequent filtration of the mixture.

2.2.8.2 Solvents, Reagents and Materials

All polymerization reactions were performed in toluene that was purchased from Aldrich Chemical Corporation. The solvent was dried using a Grubbs-type column system made by Innovative Technologies. Concentrated hydrochloric acid was purchased and used as received from EM Science. ACS grade methanol and ACS grade acetone were purchased and used as received from Aldrich Chemical Corporation. Ethylene was purchased from Matheson Gas Corporation. For reactions carried out in the Büchi reactor vessel, the ethylene was dried over alumina and 4Å molecular sieves. Methylaluminoxane (MAO) was donated by NOVA Chemical Corporation, and used as received. All reagents and solutions were handled in an inert atmosphere with the exception of the workup of the polymer product, which was washed with acidic methanol.

2.2.8.3 Atmospheric Pressure Polymerization Procedure

To a 100 mL Schlenk flask was added 50 mL of toluene and 500 equivalents of MAO. The flask was purged with ethylene for 10 min. Under a positive pressure of ethylene, a toluene solution containing the precatalyst in known concentration (Table 2.3)

was syringed in to the cocatalyst solution. The reaction mixture was stirred for 2 min, after which the ethylene flow was removed and a 1M HCl/MeOH solution was added. The resulting mixture was filtered and washed with water and acetone. The resulting polyethylene precipitate was dried for 16 h in an oven at 130°C and weighed. A polymerization reaction using the known precatalyst, $ZrCp_2Cl_2$, and the same cocatalyst (MAO) was performed to ensure a meaningful comparison with the newly synthesized catalyst systems.

2.2.8.4 Higher Pressure Polymerization Procedure (Büchi autoclave)

The autoclave was dried for 1 h under vacuum. 500 mL of toluene was added to the autoclave and the solvent and autoclave were heated to 30°C (± 2°C). 500 equivalents of the MAO cocatalyst were added to the Büchi reactor vessel. Subsequently the cocatalyst/toluene solution was stirred for 5 min. A toluene solution of catalyst precursor of known concentration (Table 2.4) was injected into the reactor vessel and was stirred for 3 min. Ethylene was added to a pressure of 30 psi. The reaction mixture was stirred at this pressure for 60 min. The reaction mixture was then quenched with acidified methanol, the resulting mixture was filtered and washed with water and acetone. The polyethylene precipitate was dried for 16 h in an oven at 130°C and weighed.

2.3 Results and Discussion

2.3.1 Initial Attempts to Synthesize Vanadium Phosphinimide Complexes

Due to the success of the titanium phosphinimide complexes of the general formulae $TiCp(NPR_3)Cl_2$ and $Ti(NPR_3)_2Cl_2$ as pre-catalysts for the polymerization of ethylene,[17, 18, 36] syntheses of the analogous vanadium complexes were attempted. Preparation of the titanium phosphinimide complexes is straightforward and generates the products in high yield,[23, 26] however this is not the case for vanadium complexes. The general method of preparation of the titanium phosphinimide complexes stem from reactions involving $TiCl_4$, however all reactions of VCl_4 with trimethylsilylphosphinimines or alkali metal phosphinimide salts resulted in intractable mixtures of compounds.

Since paramagnetic vanadium (IV) phosphinimide complexes may not be readily characterized using conventional NMR spectroscopy, a variety of diamagnetic vanadium (V) phosphinimide derivatives were envisioned. Unlike tantalum pentachloride and niobium pentachloride, vanadium pentachloride is unavailable, leaving vanadium oxo complexes as the lone vanadium (V) starting materials. Initial trials to obtain vanadium (V) phosphinimide complexes from reactions of $VOCl_3$ and Me_3SiNPR_3 or $Li[NPR_3]$ were unsuccessful. When the known reaction of $VOCl_3$ with $Me_3SiNPPh_3$[223] was repeated, several crystals of the known species formulated as $VCl_2(NPPh_3)_3$ (**2.3**)[53] were isolated. Compound **2.3** was originally synthesized via the reaction of $V(NSiMe_3)Cl_3$ [224] with PPh_3Cl_2 to give $V(NPPh_3)Cl_4$, followed by three subsequent reactions with $Me_3SiNPPh_3$.[53] Multiple attempts to synthesize the vanadium imide complex $V(NSiMe_3)Cl_3$ via the reaction of VCl_4 and Me_3SiN_3 resulted in poor yields of 2-5% of a red crystalline product isolated by sublimation, which readily decomposed in one hour.

Compound **2.3** was previously proposed to be neutral with a trigonal bipyramidal geometry about the vanadium metal centre.[53] However, X-ray crystallographic data revealed that compound **2.3** is best formulated as the salt $[V(NPPh_3)_3Cl]Cl$, adopting a pseudo tetrahedral geometry about the vanadium metal centre with averaged N-V-Cl and N-V-N angles of 108.3(1)° and 110.6(1)°, respectively (Figure 2.4). The average V-N bond distance was determined to be 1.740(3) Å; this is slightly shorter than the average

bond distance (1.769(9) Å) observed for the *tetrakis* substituted complex, $[V(NPPh_3)_4]Cl$.[53] In addition, this bond distance is an intermediate distance between the distances observed for vanadium-imido bonds and vanadium-amido bonds.[85, 91, 94, 99, 221, 225, 226] The average N-P bond distance for compound **2.3** was determined to be 1.606(3) Å, which is slightly longer than the average bond distance observed for $[V(NPPh_3)_4]Cl$ (1.573(9) Å).[53] The shorter V-N and longer N-P bond distances in $[V(NPPh_3)_3Cl]Cl$, in comparison to $[V(NPPh_3)_4]Cl$, is consistent with the less electron donating chloride atom covalently bound to the metal centre in the case of the former complex. The average V-N-P angle in compound **2.3** is 147.6(2)°, which is larger than three of the V-N-P angles in $[V(NPPh_3)_4]Cl$ (141.0(3)°, 146.2(3)° and 145.8(3)°).[53] The fourth V-N-P angle in $[V(NPPh_3)_4]Cl$ (177.0(3)°) is almost linear, which is attributed to crystal packing forces.[53] The chloride anion is well removed from the vanadium centre at a distance of 8.476 Å. The crystal structure of $[V(NPPh_3)_3Cl]Cl$ (**2.3**) in depicted in Figure 2.2.

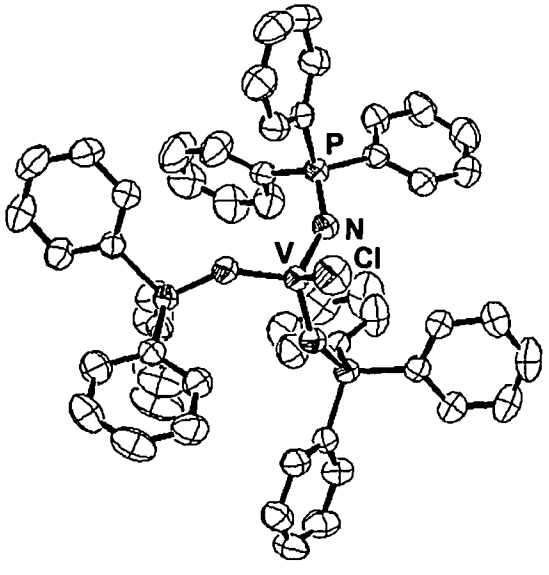

Figure 2.2: ORTEP diagram (50% probability thermal ellipsoids) of $[V(NPPh_3)_3Cl]Cl$ **(2.3).** Hydrogen atoms and the chloride anion have been omitted for clarity.

2.3.2 Synthesis of Vanadium Imide Complexes

One approach implemented in the design of Group V catalysts has been to make use of the relationship between the monoanionic Cp^- ligand and the isolobal dianionic imide fragment.[10, 214, 215, 219, 220, 227] The reactions of vanadium oxytrichloride ($VOCl_3$) and arylisocyanates (ArNCO) were reported for the preparation of vanadium(V) arylimide complexes ($V(NAr)Cl_3$).[85, 87] These reactions are high yielding and convenient[55, 90, 228] unlike other synthetic protocols published for vanadium(V) imide complexes.[224, 229-233] A modified procedure from the reported literature preparation[85] was employed to synthesize the vanadium arylimide complexes, $VCl_3(NPh)$ (**2.1**) and $VCl_3(NC_6H_3\text{-}2,6\text{-}i\text{-}Pr_2)$ (**2.2**) and is depicted in Figure 2.3.

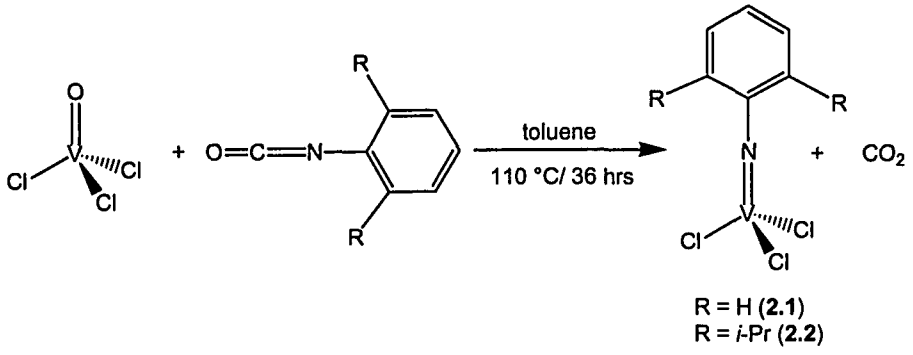

Figure 2.3: The syntheses of vanadium arylimide trichloride complexes, $V(NPh)Cl_3$ and $VCl_3(NC_6H_3\text{-}2,6\text{-}i\text{-}Pr_2)$, from ArNCO (Ar = Ph, $C_6H_3\text{-}i\text{-}Pr_2$) and $VOCl_3$.

Compound **2.1** was first published by Preuss and coworkers,[78] however the products were insoluble in most organic solvents, unlike the compounds made by Hills and coworkers, Devore and coworkers and our research group. The use of toluene instead of *n*-octane did not hinder the reaction. Following the removal of toluene and the excess $VOCl_3$ *in vacuo*, the resulting vanadium arylimide trichloride solids were used without further purification.

2.3.3 Synthesis of Vanadium Imide Phosphinimide Complexes

The vanadium imide phosphinimide dichloride complexes $V(NC_6H_3\text{-}2,6\text{-}(R^1)_2)(NP(R^2)_3))Cl_2$ (R^1 = H, R^2 = *i*-Pr (**2.4**), (R^1 = H, R^2 = *t*-Bu (**2.5**), (R^1 = H, R^2 = Ph (**2.6**), (R^1 = *i*-Pr, R^2 = *i*-Pr (**2.7**), (R^1 = *i*-Pr, R^2 = *t*-Bu (**2.8**), (R^1 = *i*-Pr, R^2 = Ph (**2.9**)) were synthesized via the reaction of $V(NAr)Cl_3$ (Ar = Ph (**2.1**), $C_6H_3\text{-}2,6\text{-}i\text{-}Pr_2$ (**2.2**)) and the phosphinimide ligand precursors, $R_3PNSiMe_3$ (R = *i*-Pr, *t*-Bu, Ph), heated in refluxing toluene for 16 – 48 hours, as depicted in Figure 2.4.

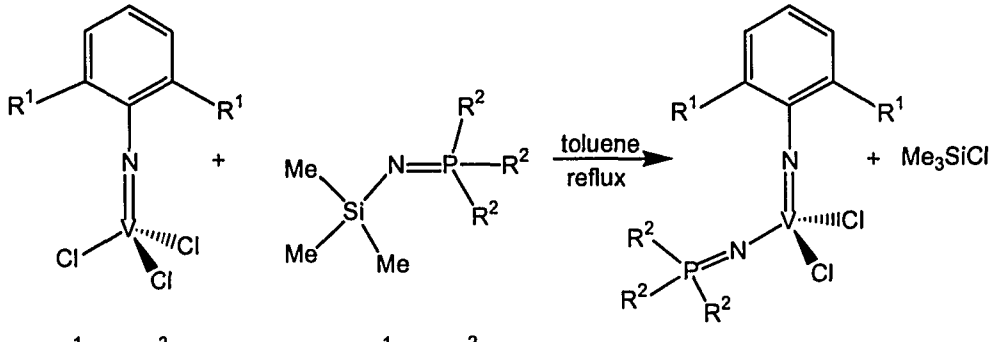

Figure 2.4: Synthesis of vanadium imide phosphinimide dichloride derivatives of general formula $V(NC_6H_3\text{-}2,6\text{-}(R^1)_2)(NP(R^2)_3))Cl_2$.

$^{31}P\{^1H\}$ NMR spectroscopy was used to monitor the formation of compounds **2.4**, **2.5**, **2.6**, **2.7**, **2.8** and **2.9**. The peaks observed in the proton decoupled $^{31}P\{^1H\}$ NMR spectra for all of the phosphinimide ligand precursors were sharp singlets. However, a very broad peak, with peak widths at half height ranging from 532 - 702 Hz was observed for each vanadium imide phosphinimide complex, indicating that the phosphinimide ligand was covalently bound to the vanadium atom. The broadness of the peaks is a consequence of the coupling of the ^{31}P atom (I = ½) with the ^{51}V atom (I = $^7/_2$). A well-resolved spectrum, like that observed for the complex $[V(NPPh_3)_4]Cl$ (see Figure 2.5),[53] would have a spectrum with a multiplicity of 8 due to the $^{31}P/^{51}V$ two-bond coupling of approximately 120 Hz.[53, 234] Examples of a peak with unresolved $^{31}P/^{51}V$ two-bond

coupling and a peak with resolved $^{31}P/^{51}V$ two-bond coupling are illustrated in Figure 2.5.

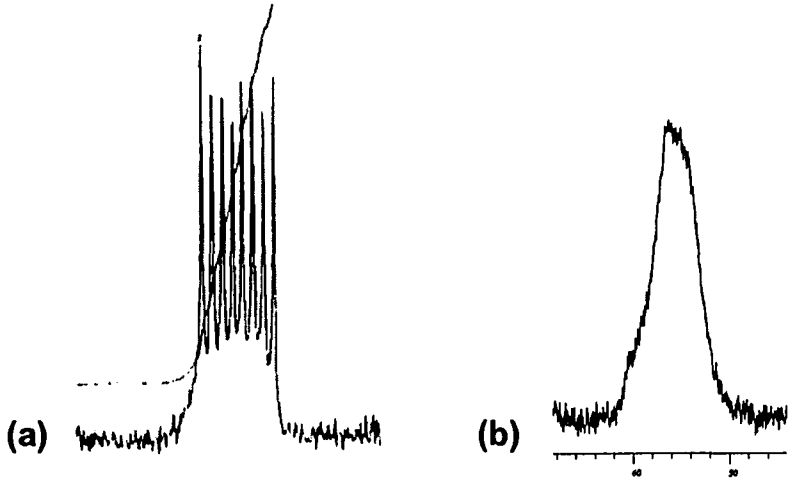

Figure 2.5: $^{31}P\{^{1}H\}$ NMR spectra: (a) peak of $[V(NPPh_3)_4]Cl$ with resolved $^{31}P/^{51}V$ two-bond coupling.[53] and (b) peak of $V(NPh)(NPPh_3)Cl_2$ (**2.6**) illustrating unresolved $^{31}P/^{51}V$ two-bond coupling

The absence of resolved coupling for complexes **2.4** - **2.9** is not unusual. For longitudinal relaxation not to be affected and therefore permit observed coupling, the quadrupolar interaction must be small due to the environment of the quadrupolar nucleus having spherical symmetry, like the vanadium centre in $[V(NPPh_3)_4]Cl$, or the quadrupolar nucleus must have a small quadrupole moment.[235] The vanadium atoms in vanadium imide phosphinimide complexes do not sit in an environment of spherical symmetry, unlike $[V(NPPh_3)_4]Cl$, and therefore the $^{31}P/^{51}V$ two-bond coupling is not observed.

Crystals of $V(NPh)(NP\textit{i}\text{-}Pr_3)Cl_2$ (**2.4**) were analyzed by X-ray crystallography, and an unusual disordering of the molecule in the solid state was revealed. The data indicated the presence of two molecules per asymmetric unit, containing two phosphinimide ligands, two chloride ligands, and two aryl rings of the imide group with ordered positions, and N(imide) atoms and vanadium atoms with disordered positions on either side (*para*) of one of the aryl rings and in the *meta* positions of the second aryl ring.[34] This is depicted in the ORTEP drawing in Figure 2.6. This is a satisfactory

crystallographic model that confirms the connectivity of the atoms within the molecules; however, a detailed discussion of bond distances and bond angles is not appropriate.

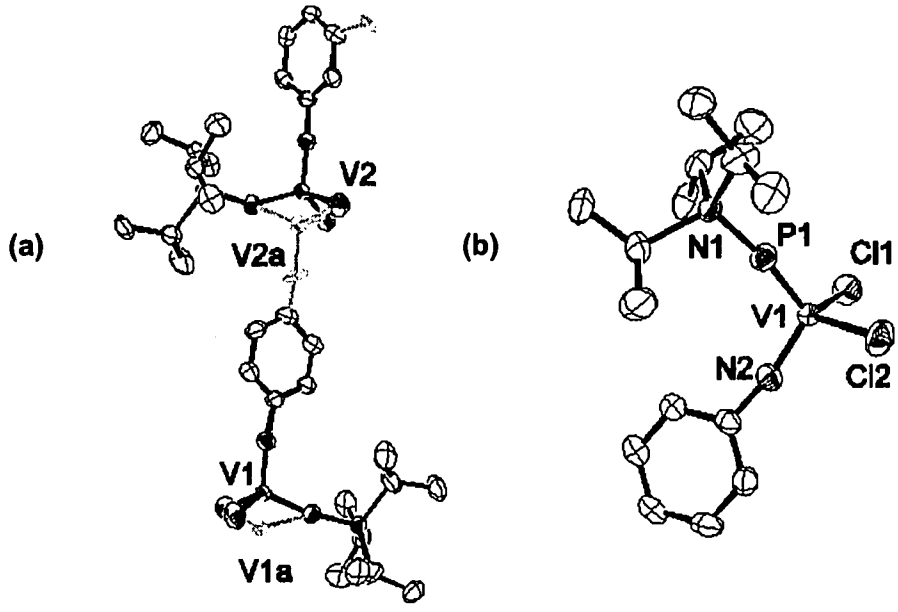

Figure 2.6: ORTEP diagrams (30% probability thermal ellipsoids) of compound **2.4** revealing (a) the disorder of the VN atoms; one of the two disordered VN positions is shown in grey and (b) one of the molecules of $V(NPh)(NP\textit{i}\text{-}Pr_3)Cl_2$ (**2.4**) in the asymmetric unit. Hydrogen atoms have been omitted for clarity.

2.3.4 Polymerization Testing of the Vanadium Imide Phosphinimide Complexes

The complexes $V(NC_6H_3\text{-}2,6\text{-}(R^1)_2)(NP(R^2)_3)Cl_2$ (R^1 = H, R^2 = *i*-Pr (**2.4**), R^1 = H, R^2 = *t*-Bu (**2.5**), R^1 = H, R^2 = Ph (**2.6**), R^1 = *i*-Pr, R^2 = *i*-Pr (**2.7**), R^1 = *i*-Pr, R^2 = *t*-Bu (**2.8**), R^1 = *i*-Pr, R^2 = Ph (**2.9**)) were activated with methylaluminoxane (MAO) and tested as olefin polymerization catalysts. Preliminary experiments using compound **2.9** and Schlenk-line techniques (Section 2.2.8.3) prematurely identified it as a high activity catalyst[10] comparable to zirconocene dichloride (Table 2.3). Activity values are dependent on a number of variables including pressure, temperature, rate of stirring, ethylene flow, type of cocatalyst used, concentration of catalyst and reaction time.[103] It is

probable that the short period of time in which these polymerization reactions were conducted is responsible for the high activities observed.[93, 236]

Table 2.3: Results from Schlenk-line polymerization reactions using $V(NC_6H_3\text{-}2,6\text{-}i\text{-}Pr_2)(NPPh_3)Cl_2$ (**2.9**) as the pre-catalyst with 500 eq of MAO at 25°C and 1 atm.

[Catalyst] (mmol L^{-1})	Rxn Time (min)	Activity (g $mmol^{-1}$ hr^{-1})	Activity of $ZrCp_2Cl_2$ (g $mmol^{-1}$ hr^{-1})
3.45	2	527	536
7.58	3	636	828
4.93	2	984	830
4.93	4	837	841

Moreover, upon performing polymerization tests on compounds **2.4**, **2.5**, **2.6**, **2.7**, **2.8** and **2.9** in the Büchi reactor (Section 2.2.8.4) for a duration of 60 minutes, moderate to low polymerization acitivities were observed[10](Table 2.4). If the results from Table 2.3 and Table 2.4 are compared, it may be postulated that these complexes have high initial polymerization activities, but are deactivated in short order. Vanadium catalysts that produce initial high activities that dwindle after the first few minutes of polymerization are certainly not unprecedented.[106-108, 237] The reduction of the vanadium metal centre and abstraction of the ligands when combined with an excess of MAO may contribute to the loss in activity.

Table 2.4: Results from polymerization reactions performed in the Büchi autoclave for a duration of 60 minutes using 500 equivalents of MAO.

Precatalyst	[Catalyst] (mmol L^{-1})	Polymer Yield (g)	Average Activity (g $mmol^{-1}$ hr^{-1})
$V(NC_6H_3\text{-}2,6\text{-}i\text{-}Pr_2)(NPPh_3)Cl_2$ **2.9**	0.035	0.50	35
	0.035	0.72	
$V(NC_6H_3\text{-}2,6\text{-}i\text{-}Pr_2)(NPt\text{-}Bu_3)Cl_2$ **2.8**	0.008	0.09	23
	0.008	0.09	
$V(NC_6H_3\text{-}2,6\text{-}i\text{-}Pr_2)(NPi\text{-}Pr_3)Cl_2$ **2.7**	0.016	0.23	31
	0.016	0.29	
$V(NPh)(NPPh_3)Cl_2$ **2.6**	0.060	0.06	2
	0.060	0.09	
$V(NPh)(NPt\text{-}Bu_3)Cl_2$ **2.5**	0.045	0.25	11
	0.045	0.27	
$V(NPh)(NPi\text{-}Pr_3)Cl_2$ **2.4**	0.020	0.12	7
	0.020	0.03	
$V(Ntol)CpCl_2$[93]	3.5 mmol	0.19	27
$Ti(NPt\text{-}Bu_3)CpMe_2$[36]	0.020	53.5	830
$ZrCp_2Me_2$	0.02	24.2	1210

Compounds **2.7**, **2.8** and **2.9** each contain a *bis-ortho*-substituted phenyl ring. When activated by MAO, these complexes produced slightly higher polymerization activities than the corresponding complexes **2.4**, **2.5** and **2.6** which contain unsubstituted phenyl rings. This could be attributed to the extra steric bulk provided by the *i*-propyl groups in the *ortho* positions of the phenyl ring, which may inhibit attack of the basic nitrogen of the imido fragment by MAO.[90, 238] The polymerization activities observed for the vanadium imide phosphinimide complexes are similar to the activity observed for the vanadium imide cyclopentadienyl complex, $V(Ntol)CpCl_2$.[93] However, all of the vanadium imide complexes generated much lower polymerization activities relative to the activities observed for zirconocene dimethyl or the titanium phosphinimide cyclopentadienyl complex, $TiCp(NPt\text{-}Bu_3)Me_2$.

The polymer samples isolated from the polymerization reactions employing complexes **2.7**, **2.8** and **2.9** were analyzed by gel permeation chromatography (GPC). The output revealed the number-average molecular weight (M_n), the weight-average

molecular weight (M_w), and the polydispersity index (PDI) of each polymer sample (Table 2.5). When activated by MAO, compounds **2.7**, **2.8** and **2.9** all generated high molecular weight polyethylene with number-average molecular weights ranging from 44 800 – 201 200 g mol^{-1}. The PDIs for compounds **2.7** and **2.9** were similar at 3.07 and 3.66, however the PDI for compound **2.8** was much larger at 14.21. These broad molecular weight distributions of polymer suggest that single-site catalysts are not responsible for the formation of the polymer product. This is not unusual given the tendency for vanadium catalyst decomposition via reduction of the vanadium centre or ligand abstraction.[92, 109, 227]

Table 2.5: GPC data of polyethylene samples produced using complexes **2.7, 2.8** and **2.9.**

Pre-catalyst	Avg. Activity (g $mmol^{-1}$ hr^{-1})	M_n[a]	PDI[b]
$VCl_2(NC_6H_3$-2,6-*i*-$Pr_2)(NP$*i*-$Pr_3)$ (**2.7**)	31	166 700	3.07
$VCl_2(NC_6H_3$-2,6-*i*-$Pr_2)(NP$*t*-$Bu_3)$ (**2.8**)	23	44 800	14.21
$VCl_2(NC_6H_3$-2,6-*i* -Pr_2)$(NPPh_3)$ (**2.9**)	35	201 200	3.66

[a] M_n = number-average molecular weight, [b] PDI = polydispersity index

Even though complexes **2.4**, **2.5**, **2.6**, **2.7**, **2.8** and **2.9** do polymerize ethylene upon activation by MAO, the rate of polyethylene production and the polymer properties are not exceptional. Recently Bayer patented vanadium imide phosphinimide complexes and vanadium oxide phosphinimide complexes for the copolymerization of ethylene and propylene, and the polymerization of ethylene propylene diene monomer (EPDM).[95] Therefore a useful industrial application has been uncovered for this class of compounds.

Having postulated that these catalysts deactivate in the first few minutes of the polymerization reaction, the synthesis of the methylated complexes could provide access to alkyl cationic species and perhaps insight into the deactivation process. Multiple attempts to synthesize the methylated vanadium imide phosphinimide complexes were unsuccessful. The reactions employing methylmagnesium bromide or dimethylzinc with complexes **2.4**, **2.5**, **2.6**, **2.7**, **2.8** and **2.9** produced multiple products with indiscernible

identities. Attempted methylation by Gibson and coworkers of the related vanadium imide cyclopentadienyl complex $V(NC_6H_3\text{-}2,6\text{-}i\text{-}Pr_2)CpCl_2$ with MeMgBr led to reductive dimerization of the vanadium centre, producing different products depending on the conditions employed.[109] The reactions of the vanadium imide phosphinimide dichloride complexes with MeLi proceeded more directly; however, the products formed were not reproducible, with the exception of the reaction of $V(NC_6H_3\text{-}2,6\text{-}i\text{-}Pr_2)(NPt\text{-}Bu_3)Cl_2$ **(2.8)** with MeLi, in which the dimethyl complex $V(NC_6H_3\text{-}2,6\text{-}i\text{-}Pr_2)(NPt\text{-}Bu_3)Me_2$ **(2.10)** was produced. It has been observed that vanadium imide cyclopentadienyl complexes with less steric congestion about the metal centre are more likely to undergo reductive dimerization upon addition of an alkylating agent.[65, 85] Compound **2.10** contains the bulkiest imido group and the most sterically encumbered phosphinimide ligand, which could prevent dimerization, and may account for its reproducible isolation.

Compound **2.10** was characterized by $^{31}P\{^1H\}$, ^1H and $^{13}C\{^1H\}$ NMR spectroscopy. An indicative upfield shift of the signal in the $^{31}P\{^1H\}$ NMR and a peak at 1.39 ppm in the ^1H NMR spectrum, representing the six methyl protons were observed. The carbon atom of the methyl groups was not observed in the $^{13}C\{^1H\}$ NMR spectrum. This is most likely due to broadening caused by $^{51}V\text{-}^{13}C$ one-bond coupling. Attempts to synthesize the corresponding cationic vanadium complex by addition of *tris*pentafluorophenylborane were unsuccessful.

Vanadium complexes readily undergo reduction via ligand leaching by the cocatalyst or via reaction with zinc.[239, 240] Thus, the generation of reduced vanadium imido phosphinimido complexes was surveyed. The reactions of the vanadium dichloride derivatives with magnesium or sodium led to mixtures of products. However, the addition of an excess of Zn to a green toluene solution of $V(NPh)(NPt\text{-}Bu_3)Cl_2$ **(2.5)** yielded a single product in the form of a deep red solid. Compound **2.11** was characterized by $^{31}P\{^1H\}$, ^1H and $^{13}C\{^1H\}$ NMR spectroscopy and elemental analysis, however, attempts at crystallizing compound **2.11** were unsuccessful. The $^{31}P\{^1H\}$ NMR spectrum revealed an upfield shift of the broad peak from 64.4 ppm for the starting material to 53.1 ppm for the product. In the ^1H NMR spectrum, the signal representing the *tert*-butyl groups of the phosphinimide ligand showed no significant shift whereas the

signals for the aryl protons on the imido group were shifted significantly, as shown in Table 2.6.

Table 2.6: Comparison of the ^{1}H NMR spectra of V(NPh)(NP*t*-Bu$_3$)Cl$_2$ (**2.5**) to the product obtained from the addition of zinc (**2.11**).

Protons	Chemical shifts (δ) for 2.5 (ppm)	Chemical shifts (δ) for 2.11 (ppm)
P(C(CH$_3$)$_3$)$_3$	1.05	1.08
C$_6$H$_5$ (*o*-H)	7.07	7.87
C$_6$H$_5$ (*m*-H)	6.96	7.34
C$_6$H$_5$ (*p*-H)	6.71	6.96

The shifts of the aryl protons of the imido group suggest that a reduced dinuclear vanadium(IV) species bridged through the imido nitrogen atoms is produced (Figure 2.7). Several complexes that contain this cyclodivanadazene (V_2N_2) core have been reported in the literature.[73, 79, 96, 228, 241]

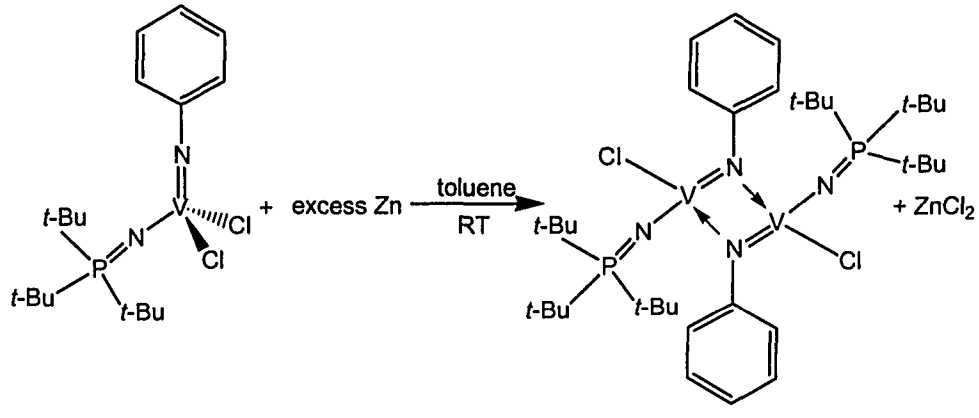

Figure 2.7: Reaction of V(NPh)NP*t*-Bu$_3$)Cl$_2$ (**2.5**) with Zn yielding the proposed product (V(μ-NPh)(NP*t*-Bu$_3$)Cl)$_2$ (**2.11**).

The reaction of VCl_3 in tetrahydrofuran with zinc was originally thought to produce $VCl_2(THF)_2$ and $ZnCl_2 \cdot x$THF,[242, 243] however it has been shown by X-ray crystallography that this reaction yields the compound $[V_2(\mu\text{-}Cl)_3(THF)_6]_2Zn_2Cl_6$ (91%).[240, 244] Examples of more complicated reactions of vanadium halides with Zn

reagents have also been reported.[245] All of these reduced species were paramagnetic. Compound **2.11** however, acts as a diamagnetic complex in solution as evidenced by the sharp resolved peaks observed in the ^{1}H NMR spectrum. The proposed structure for compound **2.11** contains two vanadium centres, each with an oxidation state of +4, and therefore each with one unpaired electron. Since compound **2.11** is observed as a diamagnetic entity, there is most likely a strong electronic coupling between the two vanadium centres. This coupling could occur through the bridging nitrogen atoms of the imido ligands or directly through the vanadium atoms if the V-V distance is sufficiently short.[228] This is consistent with the proposed formula of **2.11**. Efforts in generating X-ray quality crystals of **2.11** to verify this formulation were unsuccessful. Attempts to methylate **2.11** were fruitless.

2.3.5 Syntheses of Vanadium Imide Phosphinimide Phenyl and Benzyl Complexes

By implementing the general reaction of a vanadium imide phosphinimide dichloride complex with two equivalents of a Grignard reagent, the diphenyl derivatives $V(NC_6H_3\text{-}2,6\text{-}R^1_2)(NPR^2_3)Ph_2$ (R^1 = *i*-Pr, R^2 = *t*-Bu (**2.12**), R^1 = H, R^2 = *t*-Bu (**2.13**), R^1 = *i*-Pr, R^2 = *i*-Pr (**2.14**)) and the dibenzyl derivatives $V(NC_6H_3\text{-}2,6\text{-}R^1_2)(NPR^2_3)Bn_2$ (R^1 = H, R^2 = *i*-Pr (**2.15**), R^1 = H, R^2 = *t*-Bu (**2.16**), R^1 = *i*-Pr, R^2 = Ph (**2.17**)) were synthesized (Figure 2.8).

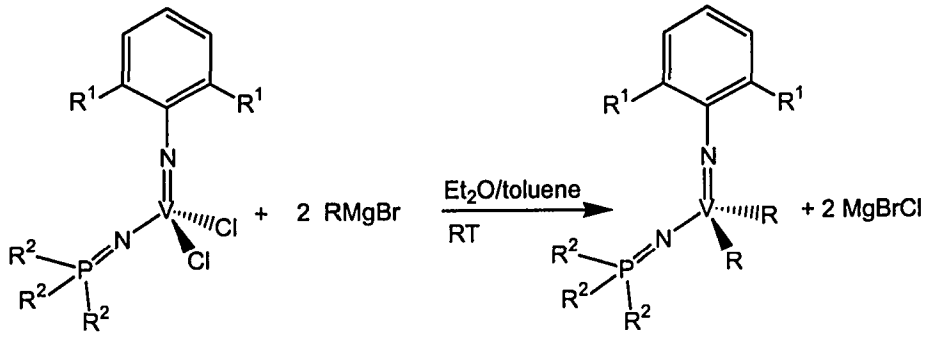

2.12 R^1 = *i*-Pr, R^2 = *t*-Bu, R = Ph **2.13** R^1 = H, R^2 = *t*-Bu, R = Ph
2.14 R^1 = *i*-Pr, R^2 = *i*-Pr, R = Ph **2.15** R^1 = H, R^2 = *i*-Pr, R = Bn
2.16 R^1 = H, R^2 = *t*-Bu, R = Bn **2.17** R^1 = *i*-Pr, R^2 =Ph, R = Bn

Figure 2.8: General reaction of vanadium imide phosphinimide dichloride complexes with phenyl and benzyl Grignard reagents.

Complexes **2.12, 2.13, 2.14, 2.15, 2.16** and **2.17** were isolated in moderate yields ranging from 36% - 48% as bright red oils or solids. These complexes were characterized by ^1H, $^{31}P\{^1H\}$ and $^{13}C\{^1H\}$ NMR spectroscopy. Broad peaks with peak widths at half-height ranging from 670 – 1190 Hz, similar to the dichloride derivatives, were observed in the $^{31}P\{^1H\}$ NMR spectra. This indicates the formation of a new product that still contains a V-phosphinimide bond, due to the presence of ^{31}P-^{51}V two-bond coupling. Upon arylation or alkylation of the vanadium dichloride complexes, the $^{31}P\{^1H\}$ NMR resonance signals show a clear upfield shift (10 - 15 ppm) which is consistent with the increased donating ability of the ligand.

In the ^1H NMR spectra, geminal coupling is observed for the methylene protons of the benzyl groups for complexes **2.15, 2.16** and **2.17**. This is due to the magnetic inequivalence of the protons, and therefore diagnostic doublets are observed. The magnitude of geminal coupling has been shown to depend on the H-C-H angle.[246] Since the $^2J_{H\text{-}H}$ = 8 Hz, a H-C-H angle of 116° is expected.[246]

Complexes **2.12, 2.13, 2.14, 2.16** and **2.17** were not stable in solution and decomposed over a time period of 1-12 hours in solution. The isolated oils and solids were more stable and could be stored for long periods of time if kept at -30°C, but readily changed colour if exposed to a humid atmosphere. Unexpectedly, crystals of $V(NC_6H_3$-

2,6-*i*-Pr_2)(NP*t*-Bu_3)Ph_2 (**2.12**) and V(NPh)(NP*i*-Pr_3)Bn_2 (**2.15**) formed in cold, concentrated toluene solutions. Both crystal structures revealed pseudo-tetrahedral geometries about vanadium, as depicted in Figure 2.9.

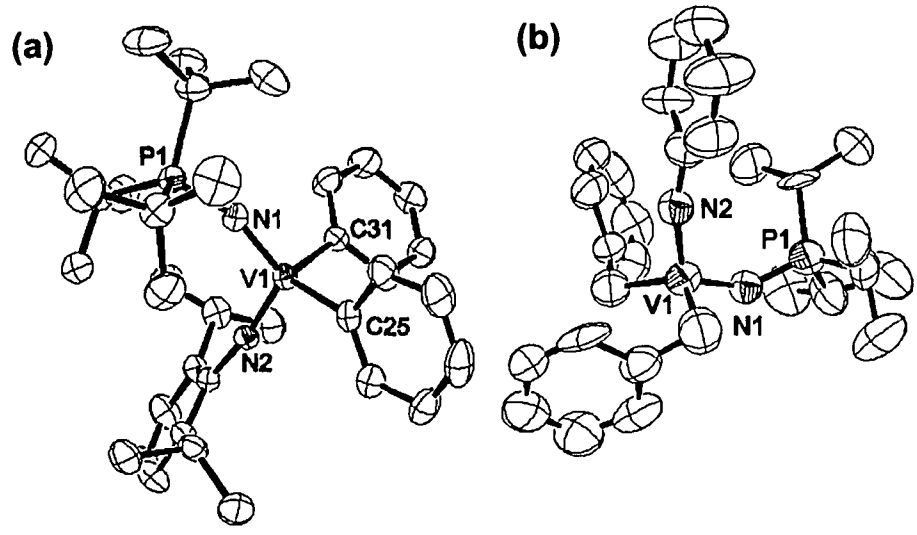

Figure 2.9: (a) ORTEP diagram (50% probability thermal ellipsoids) of V(NC_6H_3-2,6-*i*-Pr_2)(NP*t*-Bu_3)Ph_2 (**2.12**) and (b) ORTEP diagram (50% probability thermal ellipsoids) of V(NPh)(NP*i*-Pr_3)Bn_2 (**2.15**). Hydrogen atoms have been omitted for clarity.

The X-ray crystallographic data collected for V(NPh)(NP*i*-Pr_3)Bn_2 (**2.15**) were of poor quality and may only be used to support the proposed connectivity of the molecule. However, better crystallographic data for compound **2.12** revealed an average V-C bond distance of 2.06(1) Å and a C-V-C angle of 109.5(4)°. The V-N(imide) bond length of 1.674(7) Å is significantly shorter than the V-N(phosphinimide) bond distance of 1.741(7) Å. However, both bond lengths are consistent with multiple bond character, since the average V-N(amide) bond distance is 1.93(1) Å.[247-251] The V-N(imide) and V-N(phosphinimide) bond distances are typical for non-bridging vanadium-imide bond lengths (1.67(3) Å)[94, 100, 123, 221, 241, 252-256] and vanadium-phosphinimide bond lengths (1.73(2) Å),[48, 50, 51, 53, 55, 257] respectively. Comparison with published vanadium phosphinimide complexes indicates a correlation between the V-N(phosphinimide) and the N-P distance. As the V-N bond lengthens the corresponding N-P bond shortens and *vice versa*, as tabulated in Table 2.7. The lengthening of the V-N bond and subsequent

shortening of the corresponding N-P distance, coincides with the presence of strong π-donor ligands, such as phosphinimide, phosphine, imide and oxo ligands. The enhanced electron donation to the vanadium centre by other ligands increases the electron density at vanadium and therefore decreases the electron donation of the N(phosphinimide) to the vanadium atom. Alternatively, the presence of electron withdrawing ligands bound to vanadium will increase the electropositive nature of vanadium and strengthen the V-N(phosphinimide) interaction, in turn weakening the N-P interaction.

Table 2.7: A correlation of V-N(phosphinimide) and N-P bond distances for published vanadium-phosphinimide crystal structures.[34, 48, 50, 51, 53, 55, 257]

Vanadium-phosphinimide complex	V-N bond distance (Å)	N-P bond distance (Å)
μ-O(V(NPh)(NP*t*-Bu$_3$)(N(SiMe$_3$)$_2$))$_2$ **(2.25)**	1.804(4)	1.594(4)
-	1.787(4)	1.594(4)
[V(NPPh$_3$)$_4$]Cl	1.771(5)	1.578(4)
-	1.776(6)	1.557(6)
-	1.768(4)	1.578(4)
-	1.760(4)	1.58(5)
V(NPMe$_2$Ph)Cl$_3$(PMe$_2$Ph)$_2$	1.754(5)	1.604(5)
V(NPh)(NP*t*-Bu$_3$)(O*t*-Bu)$_2$ **(2.26)**	1.751(4)	1.569(4)
V(NC$_6$H$_3$-2,6-*i*-Pr$_3$)(NP*t*-Bu$_3$)Ph$_2$ **(2.12)**	1.741(7)	1.589(7)
[V(NPPh$_3$)$_3$Cl]Cl **(2.3)**	1.740(3)	1.606(3)
-	1.740(3)	1.606(3)
-	1.740(3)	1.606(3)
VO(NPPh$_3$)F$_2$	1.727(4)	1.616(5)
VO(NPPh$_2$(NS(O)Me$_2$))Cl$_2$	1.716(3)	1.633(3)
V(NC$_6$H$_3$-2,4,6-Cl$_3$)(NP*t*-Bu$_3$)Cl$_2$	1.695(3)	1.626(3)
V(NPMe$_2$Ph)Cl$_3$(PMe$_2$Ph)$_2$(H$_2$O)	1.68(2)	1.64(2)
V(NPMe$_2$Ph)Cl$_4$(NCMe)[a]	1.656(3)	1.667(3)
-	1.653(3)	1.660(3)

[a]Two different molecules in the unit cell.

2.3.6 Synthesis of Vanadium Imide Phosphinimide Thiolate Complexes

The vanadium imide phosphinimide thiolate complexes $V(NC_6H_3\text{-}2,6\text{-}R^1_2)(NPR^2_3)(SR^3)_{2-x}Cl_x$ (R^1 = H, R^2 = *t*-Bu, R^3 = Et, x = 0 (**2.18**); R^1 = *i*-Pr, R^2 = *t*-Bu, R^3 = Et, x = 0 (**2.19**); R^1 = *i*-Pr, R^2 = *t*-Bu, R^3 = Bn, x = 0 (**2.20**); R^1 = H, R^2 = *t*-Bu, R^3 = Bn, x = 1 (**2.21**); R^1 = H, R^2 = *t*-Bu, R^3 = Bn, x = 0 (**2.22**); R^1 = H, R^2 = *i*-Pr, R^3 = Bn, x = 0 (**2.23**)) were synthesized from the vanadium imide phosphinimide dichloride complexes with alkali thiolate salts as depicted in Figure 2.10.

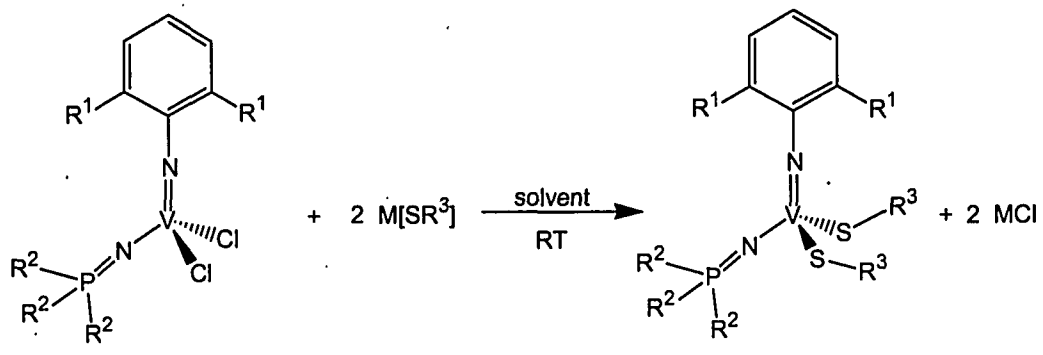

2.18 R^1 = H, R^2 = *t*-Bu, R^3 = Et, M = Na, solvent = toluene
2.19 R^1 = *i*-Pr, R^2 = *t*-Bu, R^3 = Et, M = Na, solvent = THF
2.20 R^1 = *i*-Pr, R^2 = *t*-Bu, R^3 = Bn, M = Li, solvent = toluene
2.21 R^1 = H, R^2 = *t*-Bu, R^3 = Bn & Cl M = Na, solvent = pentane
2.22 R^1 = H, R^2 = *t*-Bu, R^3 = Bn, M = Na, solvent = pentane
2.23 R^1 = H, R^2 = *i*-Pr, R^3 = Bn, M = Li, solvent = toluene

Figure 2.10: Synthetic protocol for vanadium imide phosphinimide thiolate complexes **2.18**, **2.19**, **2.20**, **2.21**, **2.22** and **2.23**.

Monitoring the reaction of V(NPh)(NP*t*-Bu$_3$)Cl$_2$ (**2.5**) with one molar equivalent of NaSBn by ^{1}H NMR spectroscopy revealed resonances consistent with the formation of both the mono-substituted thiolate complex, V(NPh)(NP*t*-Bu$_3$)(SBn)Cl (**2.21**) and the *bis*-substituted thiolate derivative V(NPh)(NP*t*-Bu$_3$)(SBn)$_2$ (**2.22**). Diagnostic doublets of the methylene protons of the benzyl groups were observed. The peaks corresponding to the methylene protons of the mono-substituted complex are observed downfield relative to those for the *bis*-substituted complex. Reactions employing a stoichiometric ratio of

2:1 or higher of the thiolate salt to the vanadium precursor proceeded to form **2.22** exclusively.

Erker and coworkers reported the reaction of $ZrCp_2(SCH_2Ph)_2$ with one equivalent of the zirconocenemethyl complex $[ZrCp_2Me]^+[CH_3B(C_6F_5)_3]^-$ in which methane evolution occurred upon concomitant formation of the cationic thio-bridged *bis*-zirconocene dimer, $[ZrCp_2(\mu\text{-}S\text{-}(\mu\text{-}CH)Ph)(\mu\text{-}SCH_2Ph)Cp_2Zr]^+[CH_3B(C_6F_5)_3]^-$.[152] The analogous reactions attempted with compounds **2.20**, **2.22** and **2.23** resulted in multiple sharp signals in the $^{31}P\{^1H\}$ NMR spectrum. Sharp signals suggest that abstraction of the phosphinimide ligand from the vanadium centre has occurred due to the lack of V-P coupling which causes the broad signals.

2.3.7 Synthesis of Amide and Alkoxide Derivatives of Vanadium Imide Phosphinimide Complexes

The vanadium imide phosphinimide amide complex, V(NPh)(NP*t*-Bu_3)($N(SiMe_3)_2$)Cl (**2.24**) was prepared via the addition of one molar equivalent of $Li[N(SiMe_3)_2]$ to V(NPh)(NP*t*-Bu_3)Cl_2 (**2.5**). The analogous reaction with excess amide gave only the same mono-substituted complex **2.24**. This is attributed to the considerable steric bulk of the disilylamide ($N(SiMe_3)_2$). Bright red crystals grew in 9% yield from a toluene solution which initially contained the mono-substituted amide complex **2.24**. However, X-ray crystallography identified the crystalline solid as the oxo-bridged complex, μ-O(V(NPh)(NP*t*-Bu_3)($N(SiMe_3)_2$))$_2$ (**2.25**) (Figure 2.11) of which the oxygen source is unknown. Interestingly, the solid state structure reveals three different nitrogen environments present in the molecule: an imide, a phosphinimide, and an amide. The corresponding V-N bond distances were averaged to be 1.669(6) Å, 1.796(6) Å and 1.947(6) Å, respectively. These bond distances are consistent with the donating ability of the ligands: N(imide) > N(phosphinimide) > N(amide). The bond distances also indicate multiple bond character for the V-N(imide) and V-N(phosphinimide) bonds relative to that of the V-N(amide) bond. The averaged V-(μ-O) bond distance in **2.25** is 1.809(4) Å which is in the middle of the range for typical V-(μ-O) bond distances (1.76-1.85 Å).[258-

[263] The average N-P distance 1.594(6) Å is typical for complexes in which other strong π-donors are present (see Table 2.7).

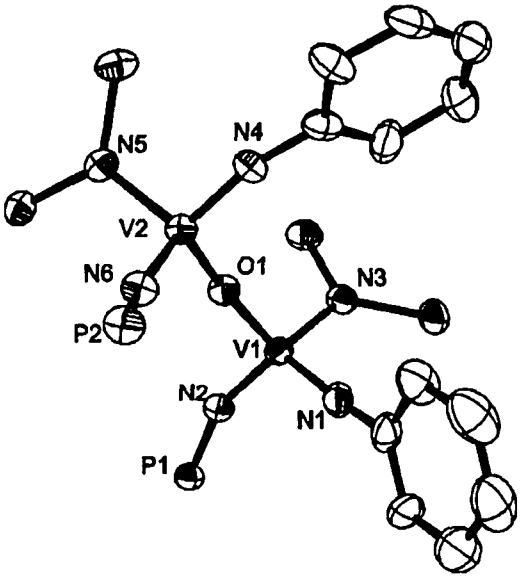

Figure 2.11: ORTEP drawing (30% probability thermal ellipsoids) of μ-O(V(NPh)(NP*t*-Bu$_3$)(N(SiMe$_3$)$_2$))$_2$ (**2.25**). The hydrogen atoms, *t*-Bu and Me groups have been omitted for clarity.

Compound **2.25** was also characterized by ^{1}H, ^{31}P{^{1}H} and ^{13}C{^{1}H} NMR spectroscopy. The ^{31}P{^{1}H} NMR signal retained a broad shape ($\Delta\nu_{1/2}$ = 1164 Hz), indicating the phosphinimide was still bound to vanadium. The upfield shift from 52 ppm for **2.24** to 45 ppm for **2.25** is consistent with the greater donating ability of the bridged oxygen atom versus that of the chloride ligand. Moreover, in the ^{1}H NMR spectrum, the resonances for all of the protons of **2.25** experienced a downfield shift compared to the resonances of **2.24**.

The vanadium imide phosphinimide alkoxide complexes, V(NPh)(NP*t*-Bu$_3$)(O*t*-Bu)$_2$ (**2.26**) and V(NPh)(NP*i*-Pr$_3$)(O*t*-Bu)$_2$ (**2.27**) were synthesized via the simple metathesis reaction of the vanadium dichloride precursor with two molar equivalents of K[O*t*-Bu] (Figure 2.12).

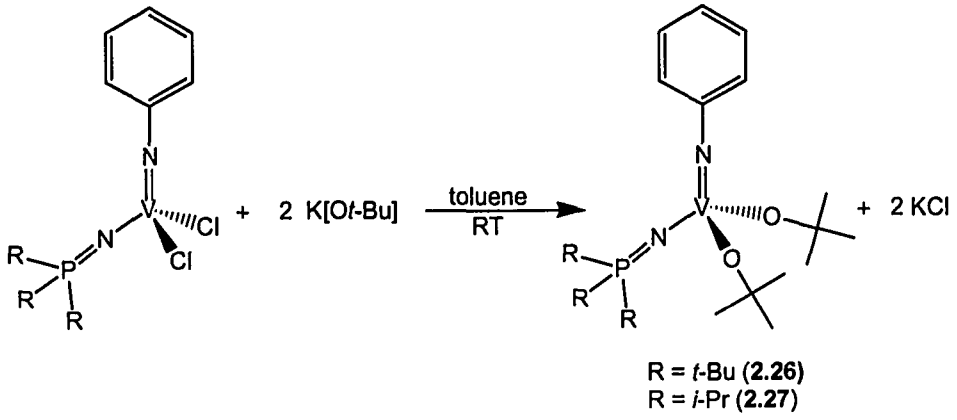

Figure 2.12: Synthesis of V(NPh)(NP*t*-Bu$_3$)(O*t*-Bu)$_2$ (**2.26**) and V(NC$_6$H$_3$-2,6-*i*-Pr$_2$)(NP*t*-Bu$_3$)(O*t*-Bu)$_2$ (**2.27**).

Compounds **2.26** and **2.27** were characterized by ^{1}H, ^{31}P{^{1}H} and ^{13}C{^{1}H} NMR spectroscopy. In the ^{31}P{^{1}H} NMR spectra, broad peaks were observed, confirming retention of the phosphinimide-vanadium bond. These resonances were shifted upfield by approximately 15 ppm from the dichloride precursors and approximately 5 ppm upfield from the analogous *bis*(phenyl) derivatives. This is likely a result of the *t*-butoxide ligand acting as a stronger donor than both the chloride and phenyl ligands.

V(NPh)(NP*t*-Bu$_3$)(O*t*-Bu)$_2$ (**2.26**) was also characterized by X-ray crystallography. Compound **2.26** has essentially tetrahedral coordination at the vanadium centre with V-N(imide) and V-N(phosphinimide) bond distances of 1.668(4) Å and 1.751(4) Å, respectively. These values fall within the ranges observed for vanadium imide and vanadium phosphinimide complexes.(Section 2.3.6) The V-N-C and V-N-P angles were determined to be 167.7(4)° and 172.8(3)°, respectively. Therefore both the imide and phosphinimide ligands are approaching linearity with respect to the vanadium centre. The V-O(alkoxide) bond distance of 1.787(2) Å is typical for non-bridging alkoxide-vanadium bonds (1.65 to 1.89 Å).[65, 73, 123, 264-270]

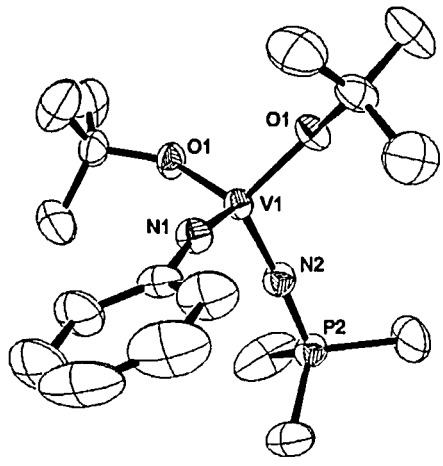

Figure 2.13: ORTEP diagram (30% probability thermal ellipsoids) for V(NPh)(NP*t*-Bu$_3$)(O*t*-Bu)$_2$ (**2.26**). Hydrogen atoms and methyl groups on the *t*-Bu groups of the phosphinimide ligand have been omitted for clarity.

2.4 Summary and Conclusions

A new class of vanadium imide phosphinimide complexes of the general formula V(NAr)(NPR$_3$)Cl$_2$ has been synthesized. The synthetic method is reproducible and the products are formed in high yields and readily handled in inert atmosphere. These compounds have proved to be reliable precursors that react cleanly with alkali metal salts or Grignard reagents to yield a variety of alkyl, aryl, thiolate, amide, and alkoxide derivatives. The reduction of V(NPh)(NP*t*-Bu$_3$)Cl$_2$ with zinc led to the proposed vanadium(IV) imide bridged dimeric species (V(μ-NPh)(NP*t*-Bu$_3$)Cl)$_2$.

Under the conditions stated in the text, the vanadium imide phosphinimide dichloride derivatives have been shown to polymerize ethylene upon activation by MAO. The polymerization activities determined for these catalysts are considered to be low to moderate and are comparable to those observed for other vanadium imide catalysts. However, these activities are significantly lower than the activities observed for the Group IV metallocene and Group IV phosphinimide catalysts. Therefore the substitution of cyclopentadienyl groups for an imide group or phosphinimide group, and replacement of Group IV metals with Group V metals, altered the active site enough to significantly

compromise the activity. Even with compromised activities, researchers at Bayer have demonstrated that complexes of this class are industrially relevant as catalysts for ethylene/propylene copolymerization and EPDM polymerization catalysts. Thus, the utility of organometallic complexes containing the phosphinimide fragment as an ancillary ligand continues to flourish.

3 Reactions of Pinacolborane with Phosphinimine Complexes

3.1 Introduction

The reaction of phosphinimines with various borane reagents has led to a range of borane-phosphinimine coordination compounds[148, 150, 151, 160, 164] and covalent borylphosphinimine complexes.[153-157, 159-162, 164, 166, 271] However, there has been no reported reactivity in which the N-P interaction has been cleaved with the exception of the reaction of $Me_3SiNPCl_3$ and PR_3 that yields R_3PNPCl_2, reported recently by Manners and coworkers.[189]

Herein, the reactions of metal-phosphinimide and -imide complexes with pinacolborane are discussed. Investigations we have performed on simple reactions of phosphinimines with specific boranes are described. In addition, the synthesis and characterization of various *N*-borylphosphinimine complexes and borylamines are discussed. Contrary to expectation, two distinct reaction pathways are observed for the reaction of pinacolborane with sterically encumbered phosphinimines or with phosphinimines that have small substituents on phosphorus. One pathway involves the formation of the expected *N*-borylphosphinimine complexes, while the other pathway results in an unexpected reduction of the phosphorus atom of the phosphinimine to free trialkylphosphine and the subsequent formation of a borylamine derivative. Experimental kinetic studies and density functional theory calculations provide insight into this structure-reactivity relationship: in particular, the electronic and steric attributes of the intermediate phosphinimine-borane adducts and the relative energies of the competing pathways.

3.2 Experimental

3.2.1 General Considerations

All preparations were performed under an atmosphere of dry O_2-free N_2 either employing Schlenk-line techniques or working in a Vacuum Atmospheres glovebox. ^1H,

$^{13}C\{^1H\}$, $^{31}P\{^1H\}$, $^{11}B\{^1H\}$ and ^{15}N NMR spectra were recorded on either a Bruker Avance 300 or 500 spectrometer. For broad peaks in the $^{11}B\{^1H\}$ or $^{31}P\{^1H\}$ NMR spectra, the line widths at half height ($\Delta\nu_{1/2}$) are given in Hertz. Trace amounts of protonated solvent were used as internal references for ^1H NMR spectra. The solvent was used as an internal reference for $^{13}C\{^1H\}$ NMR spectra. The chemical shifts for both ^1H and $^{13}C\{^1H\}$ are reported in ppm relative to tetramethylsilane. $^{31}P\{^1H\}$ NMR spectra are referenced to an external standard consisting of 85% aqueous solution of H_3PO_4. $^{11}B\{^1H\}$ NMR spectra are referenced externally to $BF_3{\cdot}Et_2O$. $^{15}N\{^1H\}$NMR spectra are referenced externally to neat CH_3NO_2. All coupling constants are reported as absolute values. Combustion analyses were performed at the University of Windsor Chemical Laboratories employing a Perkin Elmer CHN Series 2400 Analyzer. Infrared spectra were collected on a Bruker Vector 22 FT-IR spectrometer as Nujol mulls. Thick walled glass vessels equipped with Teflon screw caps will be referred to as "bombs" within this experimental section.

3.2.2 Solvents

Anhydrous toluene, benzene, hexanes, *n*-pentane, tetrahydrofuran and dichloromethane were purchased from Aldrich Chemical Company and were purified employing Grubbs-type column systems manufactured either by Innovative Technologies or in-house by the University of Windsor Physics Machine Shop. Subsequently, the solvents were dried over the appropriate drying agents[272] under an N_2 atmosphere and distilled. Methanol was purchased from BDH and was dried over activated magnesium and distilled. Deuterated benzene, toluene and tetrahydrofuran were purchased from Cambridge Isotopes Laboratories and purified by stirring over sodium and benzophenone for 16 h, followed by three freeze/pump/thaw degas cycles, and finally collected by vacuum distillation. Deuterated dichloromethane was purified by stirring over calcium hydride for 16 h, followed by three freeze/pump/thaw cycles, and finally collected by vacuum distillation.

3.2.3 Materials

Hyflo Super Cel®, hereafter referred to as Celite, was purchased from Aldrich Chemical Company and dried in a vacuum oven at 130°C for 16 h before storage in a glovebox. 4 Å molecular sieves were purchased from Aldrich Chemical Company and dried at 100°C under vacuum for 16 h. Reactions completed at -30°C were cooled in a CH_3NO_2/liquid N_2 bath, whereas crystals that were grown at -30°C, were stored in a freezer within a glovebox.

3.2.4 Reagents

Pinacolborane, dichlorophenylborane, 1-azidoadamantane, borane-dimethylsulfide adduct, triphenylphosphine, triphenylphosphine oxide, azidotrimethylsilane, and vanadiumoxytri-*i*-propoxide were used as received from Aldrich Chemical Company. Tri-*i*-propylphosphine, tri-*n*-butylphosphine, and triethylphosphine were used as received from Strem Chemicals. *N*-trimethylsilyl-*t*-butylphosphinimine in a 50 wt% solution in toluene, *N*-trimethylsilyl-di-*t*-butyl-*n*-butylphosphinimine, and titanium cyclopentadienyl tri-*t*-butylphosphinimide dichloride were generously donated by NOVA Chemicals Corporation. Phenylazide[273] was prepared with the aid of Ms. Jenny McCahill. Titanium cyclopentadienyl tri-*t*-butylphosphinimide dimethyl was prepared using a literature method.[18, 36] Vanadium phenyl imide *t*-butyl phosphinimide *bis*-*t*-butoxide (**2.29**) was prepared as outlined in Chapter 2, Section 2.2.6. *N*-H-tri-*i*-propylphosphinimine, *N*-H-tri-*t*-butylphosphinimine *N*-trimethylsilyl-tri-*n*-butylphosphinimine, *N*-H-triethylphosphinimine, and *N*-H-tri-*n*-butylphosphinimine, were prepared via literature methods.[2-4, 274] The modified literature methods are included in Section 3.2.5 below. $V(NPh)(O\textit{t}\text{-}Bu)_3$ (**3.5**) was previously synthesized via a different method.[77]

3.2.5 Syntheses of Phosphinimines

HNP*n*-Bu(*t*-Bu)$_2$ (3.1): An excess of methanol (10 mL, 180 mmol) was added to Me_3SiNPn-Bu(t-Bu)$_2$ (2.0 g, 6.91 mmol) via a cannula. The resulting solution was heated at reflux for 24 h. The removal of excess methanol and methoxytrimethylsilane *in vacuo* over an 8 h time period yielded the desired product as a colourless liquid in 98 % yield. ^{1}H NMR (300 MHz, C_6D_6) δ: 1.59 (m, 2H, PC**H**$_2$CH$_2$CH$_2$CH$_3$), 1.38 (m, 2H, PCH$_2$C**H**$_2$CH$_2$CH$_3$), 1.27 (sextet, 2H, PCH$_2$CH$_2$C**H**$_2$CH$_3$, $^3J_{H\text{-}H}$ = 7 Hz), 1.07 (d, 18H, PC(C**H**$_3$)$_3$, $^3J_{P\text{-}H}$ = 13 Hz), 0.86 (t, 3H, PCH$_2$CH$_2$CH$_2$C**H**$_3$, $^3J_{H\text{-}H}$ = 7 Hz); ^{31}P{^{1}H} NMR (121.5 MHz, C_6D_6) δ: 48.3; ^{13}C{^{1}H} NMR (75.5 MHz, C_6D_6) δ: 36.6 (d, P**C**(CH$_3$)$_3$, $^1J_{P\text{-}C}$ = 55 Hz) 27.6 (PC(**C**H$_3$)$_3$), 26.8 (d, PCH$_2$CH$_2$**C**H$_2$CH$_3$, $^3J_{P\text{-}C}$ = 4 Hz), 25.6 (d, PCH$_2$**C**H$_2$CH$_2$CH$_3$, $^2J_{P\text{-}C}$ = 11 Hz), 21.9 (d, P**C**H$_2$CH$_2$CH$_2$CH$_3$, $^1J_{P\text{-}C}$ = 49 Hz), 14.4 (PCH$_2$CH$_2$CH$_2$**C**H$_3$). Calculated: H: 12.98%, C: 66.32%, N: 6.44%; Found H: 9.43%, C: 64.10%, N: 6.20%.

PhNP*n*-Bu$_3$ (3.2) : A solution of PhN_3 (0.294 g, 2.47 mmol) in 25 mL of toluene was added over a 30 min period to a solution of P(n-Bu)$_3$ (0.616 mL, 2.47 mmol) in 5 mL of toluene. The evolution of gas was observed. The resulting solution was stirred for 16 h at ambient temperatures under static vacuum. Toluene was removed *in vacuo* resulting in the isolation of an orange oil. The oil was filtered through Celite and collected in 70% yield. ^{1}H NMR (300 MHz, C_6D_6) δ: 7.28 (t, 2H, m-Ph, $^3J_{H\text{-}H}$ = 7 Hz), 7.05 (d, 2H, o-Ph, $^3J_{H\text{-}H}$ = 8 Hz), 6.83 (t, 1H, p-Ph, $^3J_{H\text{-}H}$ = 7 Hz), 1.43 (m, 12H, PC**H**$_2$C**H**$_2$CH$_2$CH$_3$), 1.16 (sextet, 6H, PCH$_2$CH$_2$C**H**$_2$CH$_3$), 0.75 (t, 9H, PCH$_2$CH$_2$CH$_2$C**H**$_3$, $^3J_{H\text{-}H}$ = 7 Hz); ^{31}P{^{1}H} NMR (121.5 MHz, C_6D_6) δ: 15.1; ^{13}C{^{1}H} NMR (partial) (75.5 MHz, C_6D_6) δ: 129.6 (m-Ph), 123.5 (d, o-Ph, $^3J_{P\text{-}C}$ = 18 Hz), 117.1 (p-Ph), 26.3 (d, P**C**H$_2$CH$_2$CH$_2$CH$_3$, $^1J_{P\text{-}C}$ = 217 Hz), 25.9 (d, PCH$_2$**C**H$_2$CH$_2$CH$_3$, $^2J_{P\text{-}C}$ = 163 Hz), 24.9 (PCH$_2$CH$_2$**C**H$_2$CH$_3$), 14.1 (P(CH$_2$CH$_2$CH$_2$**C**H$_3$).

$PhNPEt_3$ (3.3): A solution of PEt_3 (1.0 mL, 6.77 mmol) in 25 mL of toluene was added over a 30 min period to a solution of PhN_3 (0.767 g, 6.43 mmol) in 10 mL of toluene. Gas evolution was observed. The resulting solution was stirred at room temperature for 16 h under static vacuum. Removal of the solvent and residual PEt_3 *in vacuo* resulted in the isolation of an orange oil in 96% yield. ^{1}H NMR (500 MHz, C_6D_6) δ: 7.20 (t, 2H, *m*-Ph, $^3J_{H-H}$ = 8 Hz), 6.92 (d, 2H, *o*-Ph, $^3J_{H-H}$ = 8 Hz), 6.76 (t, 1H, *p*-Ph, $^3J_{H-H}$ = 7 Hz), 1.32 (dq, 6H, PCH_2CH_3, $^2J_{P-H}$ = 12 Hz, $^3J_{H-H}$ = 8 Hz), 0.81 (dt, 9H, PCH_2CH_3, $^3J_{P-H}$ = 16 Hz, $^3J_{H-H}$ = 8 Hz); $^{31}P\{^1H\}$ NMR (202.5 MHz, C_6D_6) δ: 20.1; $^{13}C\{^1H\}$ NMR (125.8 MHz, C_6D_6) δ: 154.3 (*ipso*-Ph), 129.4 (*m*-Ph), 123.6 (d, *o*-Ph, $^3J_{P-C}$ = 9 Hz), 116.8 (*p*-Ph), 19.4 (d, PCH_2CH_3, $^1J_{P-C}$ = 64 Hz), 6.7 (d, PCH_2CH_3, $^2J_{P-C}$ = 7 Hz).

$AdNPEt_3$ (3.4): A solution of PEt_3 (1.0 mL, 6.77 mmol) in 40 mL of toluene was added to a solution of AdN_3 (1.023 g, 5.77 mmol) in 10 mL of toluene over a 30 min time period. This solution was stirred for 16 h at room temperature. Both the solvent and excess PEt_3 were removed *in vacuo* and the resulting pale yellow oil was collected in 96% yield. ^{1}H NMR (500 MHz, C_6D_6) δ: 2.08 (s, 3H, Ad-C**H**), 1.83 (d, 6H, Ad-C**H**$_2$, $^3J_{H-H}$ = 2.5), 1.68 (m, 6H, Ad-C**H**$_2$), 1.26 (dq, 6H, PCH_2CH_3, $^2J_{P-H}$ = 11 Hz, $^3J_{H-H}$ = 8 Hz), 0.91 (dt, 9H, PCH_2CH_3, $^3J_{P-H}$ = 16 Hz, $^3J_{H-H}$ = 8 Hz); $^{31}P\{^1H\}$ NMR (202.5 MHz, C_6D_6) δ: 5.2; $^{13}C\{^1H\}$ NMR (125.8 MHz, C_6D_6) δ: 51.1 (Ad-CH_2), 37.8 (Ad-CH_2), 31.6 (Ad-CH), 22.6 (d, PCH_2CH_3, $^1J_{P-C}$ = 63 Hz), 7.24 (d, PCH_2CH_3, $^2J_{P-C}$ = 2 Hz).

3.2.6 Synthesis of Metal-Phosphinimide/Alkoxide and Borylphosphinimine Complexes

V(NPh)(O*t*-Bu)$_3$ (3.5): Solid KO*t*-Bu (0.339 g, 3.02 mmol) was added to a 5 mL solution of V(NPh)Cl$_3$ (**2.4**) (0.250 g, 1.00 mmol) in toluene. Within the first few minutes after addition, the initially red solution turned yellow. The resulting solution was stirred for 5 h, followed by removal of toluene *in vacuo*. The product was dissolved in 5 mL of *n*-pentane. This solution was filtered through Celite, then reduced to 2 mL and stored at -30°C. The product was collected as a yellow solid in 83% yield (0.280 g). ^{1}H NMR (500 MHz, C_6D_6) δ: 7.36 (d, 2H, *o*-Ph, $^3J_{H-H}$ = 8 Hz), 6.98 (t, 2H, *m*-Ph, $^3J_{H-H}$ = 8 Hz), 6.74 (t, *p*-Ph, $^3J_{H-H}$ = 7 Hz), 1.46 (s, 27H, *t*-Bu); ^{13}C{^{1}H} NMR (75.5 MHz, partial, C_6D_6) δ: 129.1, 128.6, 125.6, 33.2; Calculated: H: 8.92%, C: 59.82%, N: 3.88%; Found: H: 8.21%, C: 59.17%, N: 3.53%.

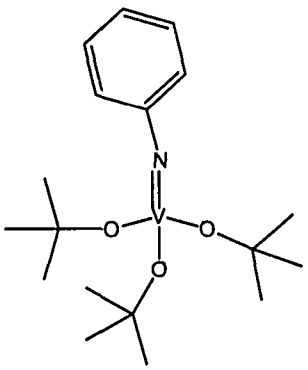

TiCp(NP*n*-Bu$_3$)Cl$_2$ (3.6): TiCpCl$_3$ (0.518 g, 2.36 mmol) was dissolved in 50 mL of toluene. To this solution, *n*-Bu$_3$PNSiMe$_3$ (0.684 g, 2.36 mmol) was added and the resulting solution was stirred for 16 h at room temperature. The solvent and trimethylsilylchloride were removed *in vacuo* and the resulting red oil was washed twice with *n*-pentane, dried *in vacuo* and collected in 96% yield. ^{1}H NMR (300 MHz, C_6D_6) δ: 6.44 (s, 5H, $C_5\mathbf{H}_5$), 1.27 (m, 18H, P**CH$_2$**C**H$_2$**C**H$_2$**CH$_3$, 0.83 (t, 9H, PCH$_2$CH$_2$CH$_2$**CH$_3$**, $^3J_{H-H}$ = 7 Hz); ^{31}P{^{1}H} NMR (121.5 MHz, C_6D_6) δ: 23.0; ^{13}C{^{1}H} NMR (75.5 MHz, C_6D_6) δ: 115.3 (**C$_5$H$_5$**); 27.0 (d, P**C**H$_2$CH$_2$CH$_2$CH$_3$, $^1J_{P-C}$ = 61 Hz); 24.5 (d, PCH$_2$**C**H$_2$CH$_2$CH$_3$, $^2J_{P-C}$ = 24 Hz), 24.4 (d, PCH$_2$CH$_2$**C**H$_2$CH$_3$, $^3J_{P-C}$ = 13 Hz), 14.2 (PCH$_2$CH$_2$CH$_2$**C**H$_3$); Calculated: H: 8.06%, C: 51.02%, N: 3.50%; Found: H: 7.65%, C: 50.58%, N: 4.05%. Compound **3.6** was synthesized via an alternate method in the patent literature.{Ijpeij, 2005 #863}

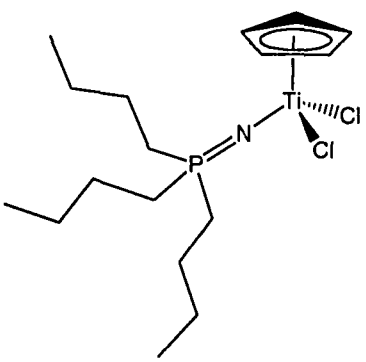

[$Me_3PN(H)Bpin$][$TiCpCl_3$] (3.7): Neat HBpin (0.027 mL, 0.185 mmol) was syringed into a 5 mL solution of $TiCp(NPMe_3)Cl_2$ (0.050 g, 0.185 mmol) in *n*-pentane. Within the first 30 min of stirring at room temperature, the solution turned from yellow to green. It was then stirred for an additional 12 h at room temperature, during which time it continued to change colour to dark blue. The solution was then filtered through Celite and stored at -33°C from which bright blue X-ray quality crystals were collected in 20% yield. After being sealed in the capillaries, the crystals changed colour from blue to yellow. During the second attempt to seal the capillary the blue crystals did not change colour. Both the yellow and blue crystals were solved as the salts above. ^1H NMR (500 MHz, C_6D_6): A spectrum made up of extremely broad signals from which no definitive peaks could be assigned; $^{31}P\{^1H\}$ NMR (202.5 MHz, C_6D_6) 38.8; $^{13}C\{^1H\}$ NMR: this spectrum was not collected, given the ^1H NMR spectrum. $^{11}B\{^1H\}$ NMR (160.5 MHz, C_6D_6) 21.7; Calculated: H: 6.22%, C: 38.44%, N: 3.20%; Found: H: 6.14%, C: 40.59%, N: 3.60%. The poor quality of the NMR data is most likely due to the sensitive nature of the Ti(III) salt.

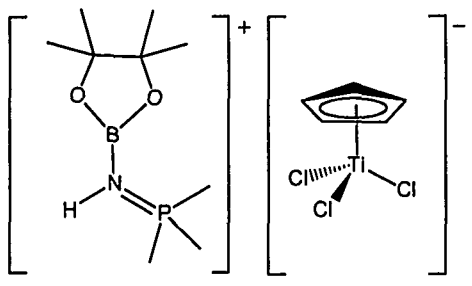

***t*-$Bu_3PNBpin$ (3.8)** : A solution of $HNPt\text{-}Bu_3$ (0.65 g, 3.29 mmol) in 3 mL of *n*-pentane was added to HBpin (0.48 mL, 3.29 mmol). Gas evolution was observed. The solution was stirred for 16 h, and then dried *in vacuo*. A colourless oil was isolated in 94% yield. ^1H NMR (300 MHz, C_6D_6) δ: 1.27 (d, 27H, $PC(CH_3)_3$, $^3J_{P\text{-}H}$ = 13 Hz), 1.24 (s, 12H, $BO_2C_2(CH_3)_4$); $^{31}P\{^1H\}$ NMR (121.5 MHz, C_6D_6) δ: 40.2; $^{13}C\{^1H\}$ NMR (75.5 MHz, C_6D_6) δ: 80.1 ($BO_2C_2(CH_3)_4$), 40.5 (d, $PC(CH_3)_3$, $^1J_{P\text{-}C}$ = 52 Hz), 30.0 ($PC(CH_3)_3$), 25.6 ($BO_2C_2(CH_3)_4$); $^{11}B\{^1H\}$ NMR (96.3 MHz, C_6D_6) δ: 23.4 (br, $\upsilon_{1/2}$ = 486 Hz); $^{15}N\{^1H\}$ NMR (30.4 MHz) δ: -348.02; IR υ(N-P): 1154 cm^{-1}; Calculated: H: 11.45%, C: 62.98%, N: 4.08%; Found: H: 11.43%, C: 62.85%, N: 4.07%.

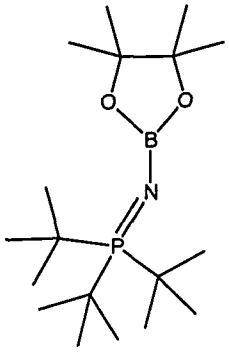

***n*-Bu(*t*-Bu)$_2$PNBpin (3.9):** A solution of HNP*n*-Bu(*t*-Bu)$_2$ (0.050 g, 0.23 mmol) in 3 mL of *n*-pentane was added to HBpin (0.067 mL, 0.46 mmol). Gas evolution was observed upon addition of the phosphinimine. The resulting solution was stirred at room temperature for 8 h during which time a white solid precipitated. The solvent and excess HBpin were decanted. The product was dried *in vacuo* and collected in 61% yield. ^{1}H NMR (300 MHz, C_6D_6) δ: 1.72 (m, 4H, PC**H**$_2$CH$_2$CH$_2$CH$_3$), 1.50 (m, 4H, PCH$_2$C**H**$_2$CH$_2$CH$_3$), 1.30 (sextet, 4H, PCH$_2$CH$_2$C**H**$_2$CH$_3$, $^3J_{H\text{-}H}$ = 7 Hz), 1.19 (s, 24H, BO$_2$C$_2$(C**H**$_3$)$_4$), 1.11 (d, 36H, PC(C**H**$_3$)$_3$, $^3J_{P\text{-}H}$ = 13 Hz), 0.89 (t, 6H, PCH$_2$CH$_2$CH$_2$C**H**$_3$, $^3J_{H\text{-}H}$ = 8 Hz); ^{31}P{^{1}H} NMR (121.5 MHz, C_6D_6) δ: 36.2; ^{13}C{^{1}H} NMR (75.5 MHz, C_6D_6) δ: 80.1 (BO$_2$**C**$_2$(CH$_3$)$_4$), 36.7 (d, P**C**(CH$_3$)$_3$, $^1J_{P\text{-}C}$ = 61 Hz) 27.7 (P(C(**C**H$_3$)$_3$), 26.6 (d, PCH$_2$CH$_2$**C**H$_2$CH$_3$, $^3J_{P\text{-}C}$ = 26 Hz), 25.6 (PCH$_2$**C**H$_2$CH$_2$CH$_3$), 25.1 (BO$_2$C$_2$(**C**H$_3$)$_4$), 22.5 (d, P**C**H$_2$CH$_2$CH$_2$CH$_3$, $^1J_{P\text{-}C}$ = 56 Hz), 14.4 (PCH$_2$CH$_2$CH$_2$**C**H$_3$); ^{11}B{^{1}H} NMR (96.3 MHz, C_6D_6) δ: 21.6; Calculated: H: 11.45%, C: 62.98%, N: 4.08%; Found: H: 9.80%, C: 61.97%, N: 3.64%.

***i*-Pr$_3$PNBpin (3.10)**: HBpin (0.414 mL, 2.85 mmol) was added slowly to a solution of HNP*i*-Pr$_3$ (0.250 g, 1.43 mmol) in 25 mL of toluene. Gas evolution was observed. The solution was stirred for 16 h under static vacuum. Removal of the solvent and excess borane yielded the product in 87% yield. The minor products produced were P(*i*-Pr)$_3$ and HN(Bpin)$_2$. The NMR spectral data included the three products formed. The NMR data for *i*-Pr$_3$PNBpin is as follows: ^{1}H NMR (300 MHz, C_6D_6) δ: 1.86 (dseptet, 3H, PC**H**(CH$_3$)$_2$, $^3J_{P\text{-}H}$ = 11 Hz, $^3J_{H\text{-}H}$ = 7 Hz), 1.22 (s, 12H, BO$_2$C$_2$(C**H**$_3$)$_4$), 1.03 (dd, 18H, PCH(C**H**$_3$)$_2$, $^3J_{P\text{-}H}$ = 15 Hz, $^3J_{H\text{-}H}$ = 7 Hz); ^{31}P{^{1}H} NMR (121.5 MHz, C_6D_6) δ: 36.0; ^{13}C{^{1}H} NMR (125.8 MHz, C_6D_6) δ: 80.1 (BO$_2$**C**$_2$(CH$_3$)$_4$), 25.7 (d, P**C**(CH$_3$)$_3$, $^1J_{P\text{-}C}$ = 61 Hz), 25.5 (BO$_2$C$_2$(**C**H$_3$)$_4$) 17.5 (PC(**C**H$_3$)$_3$); ^{11}B{^{1}H} NMR (96.3 MHz, C_6D_6) δ: 23.9.

HN(Bpin)$_2$ (3.11): *1*: HBpin (0.10 mL, 0.68 mmol) was added to a 3 mL solution of HNP*n*-Bu$_3$ (0.074 g, 0.34 mmol) in *n*-pentane. Immediate gas evolution was observed. The solution was stirred at 25°C for 2 h. A $^{31}P\{^1H\}$ NMR spectrum of the crude reaction mixture showed quantitative conversion of HNP*n*-Bu$_3$ to P*n*-Bu$_3$. The solution was concentrated to 1 mL and the white precipitate was collected and dried *in vacuo*. X-ray quality crystals of HN(Bpin)$_2$ were isolated from a concentrated *n*-pentane solution in 25% yield.

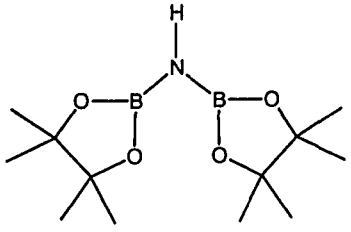

2: HBpin (0.81 mL, 5.60 mmol) was added to a 5 mL solution of HNPEt$_3$ (0.355 g, 2.67 mmol) in *n*-pentane. Immediate gas evolution was observed. The solution was stirred at 25°C for 2 h. The solvent, PEt$_3$ and excess HBpin were removed *in vacuo*. The resulting white solid was washed (3 x 1 mL) with cold *n*-pentane, dried *in vacuo* and isolated in 92% yield.

3: HBpin (0.71 mL, 4.88 mmol) was added to neat Me$_3$SiNPEt$_3$ (0.500 g, 2.44 mmol). The resulting solution was heated at 50°C for 5 h. The liquid was then cooled and the SiMe$_3$H and PEt$_3$ were removed *in vacuo*. A white solid was collected in 92% yield.

4: HBpin (0.247 mL, 1.702 mmol) was added to neat Me$_3$SiNP*n*-Bu$_3$ (0.224 g, 0.774 mmol) and stirred at room temperature for 16 h. The resulting mixture was dissolved in 5 mL of *n*-pentane and filtered through Celite. The solution was reduced to 2 mL from which X-ray quality crystals were grown in 50% yield.

^1H NMR (300 MHz, C_6D_6) δ: 1.04 (s, 24H); $^{13}C\{^1H\}$ NMR (75.5 MHz, C_6D_6) δ: 82.8 ($BO_2C_2(CH_3)_4$), 25.1 ($BO_2C_2(CH_3)_4$); $^{11}B\{^1H\}$ NMR (96.3 MHz, C_6D_6) δ: 25.2; IR υ(N-H): 3334 cm^{-1}; Calculated: H: 9.37%, C: 53.59%, N: 5.21%; Found: H: 9.58%, C: 54.09%, N: 5.22%.

PhNH(Bpin) (3.12): *1*: HBpin (0.3 mL, 2.06 mmol) was added slowly to a solution of PhNP*n*-Bu$_3$ (0.576 g, 1.96 mmol) in 5 mL of *n*-pentane. The resulting yellow solution was stirred for 6 h, after which time a colourless solution remained. At -33°C the product precipitated as a white crystalline solid in 48% yield.

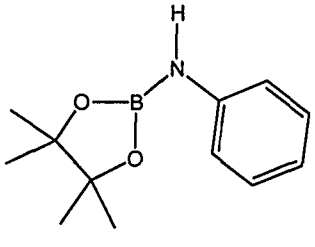

2: HBpin (0.348 mL, 2.40 mmol) was added slowly to a 5 mL

solution of $PhNPEt_3$ (0.500 g, 2.39 mmol) in *n*-pentane resulting in a bright yellow solution. After 16 h of stirring, a white precipitate had formed and a colourless solution remained. The precipitate was collected, dried *in vacuo* and the supernatant was stored at -33°C from which more product precipitated as a white crystalline solid, in a total yield of 81%. ^1H NMR (300 MHz, C_6D_6) δ: 7.09 (m, 4H, *m*-Ph, *o*-Ph), 6.77 (t, 1H, *p*-Ph, $^3J_{H-H}$ = 7 Hz), 1.07 (s, 12H, Me); $^{13}C\{^1H\}$ NMR (75.5 MHz, C_6D_6) δ: 144.3 (*ipso*-Ph), 129.6 (*m*-Ph), 120.8 (*o*-Ph), 118.4 (*p*-Ph), 83.0 ($BO_2\mathbf{C}_2(CH_3)_4$), 25.0 ($BO_2C_2(\mathbf{C}H_3)_4$); $^{11}B\{^1H\}$ NMR (96.3 MHz, C_6D_6) δ: 24.1; IR: υ(N-H): 3357 cm^{-1}; Calculated: H: 8.28%, C: 65.79%, N: 6.39%; Found: H: 8.21%, C: 65.56%, N: 6.62%.

AdN(H)(Bpin) (3.13): HBpin (0.8 mL, 5.5 mmol) was added slowly to a 15 mL toluene solution of $AdNPEt_3$ (0.72 g, 2.7 mmol). The resulting yellow solution was stirred for 6 h, during which time the solution turned colourless. The solution was reduced in volume to 3 mL and was stored at -33°C, from which the product was collected as a white crystalline solid in 83% yield. ^1H NMR (500 MHz, C_6D_6) δ: 2.37 (s, 1H, N**H**) 1.93 (s, 3H, Ad-C**H**), 1.81 (s, 6H, Ad-C$\mathbf{H}_2$), 1.52 (m, 6H, Ad-C$\mathbf{H}_2$), 1.14 (s, 12H, $BO_2C_2(C\mathbf{H}_3)_4$); $^{13}C\{^1H\}$ NMR (125.8 MHz, partial, C_6D_6) δ: 46.0 (Ad-$\mathbf{C}H_2$), 37.0 (Ad-$\mathbf{C}H_2$), 30.7 (Ad-**C**H), 25.1 ($BO_2C_2(\mathbf{C}H_3)_4$); $^{11}B\{^1H\}$ NMR (160.5 MHz, C_6D_6) δ: 24.1; Calculated: H: 10.18%, C: 69.33%, N: 5.05%; Found: H: 9.59%, C: 69.77%, N: 4.66%.

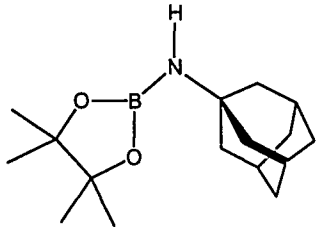

This is a modification of the procedure described in the literature.[166]

HB(NP*t*-Bu$_3$)$_2$ (3.14): A solution of HNP*t*-Bu_3 (0.150 g, 0.69 mmol) in 15 mL of toluene was added to a "bomb". $BH_3{\cdot}SMe_2$ (2M in Et_2O, 0.175 mL, 0.35mmol) was added to the "bomb" via syringe in the glovebox. On the Schlenk line, the solution was freeze-pump-thaw-degassed two times, and subsequently heated at 95°C for 6 h. Once cooled to room temperature and dried *in vacuo*. The white solid was dissolved in minimal amounts of toluene and kept at -33°C. Crystalline solid formed, which was collected by

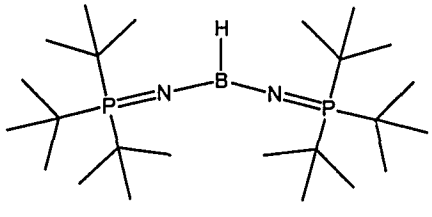

decanting the remaining solution and washing the precipitate with cold *n*-pentane, and drying *in vacuo*. ^{1}H NMR (300 MHz, C_6D_6) δ: 1.38 (d, 54H, PC(C**H**$_3$)$_3$, $^{3}J_{P\text{-}H}$ = 12.3 Hz); ^{31}P{^{1}H} NMR (121.5 MHz, C_6D_6) δ: 31.6; ^{13}C{^{1}H} NMR (75.5 MHz, C_6D_6) δ: 40.7 (d, P**C**(CH$_3$)$_3$, $^{1}J_{P\text{-}C}$ = 50 Hz), 30.5 (C(**C**H$_3$)$_3$); ^{11}B{^{1}H} NMR (96.3 MHz, C_6D_6) δ: 24.6. This data agreed with the literature reports.[166]

***n*-Bu(*t*-Bu)$_2$PN(H)·BH$_3$ (3.15)**: To a solution of HNP*n*-Bu(*t*-Bu)$_2$ (0.150 g, 0.690 mmol) in 10 mL of hexane was added BH_3·SMe_2 in diethylether (2 M, 0.173 mL, 0.345 mmol). The solution was stirred for 4 h and filtered. X-ray quality crystals were collected from the hexanes supernatant kept at -30°C. Yield: 87% : ^{1}H NMR (300 MHz, C_6D_6) δ: 1.76 (m, 2H, PC**H**$_2$CH$_2$CH$_2$CH$_3$), 1.60 (m, 2H, PCH$_2$C**H**$_2$CH$_2$CH$_3$), 1.26 (sextet, 2H, PCH$_2$CH$_2$C**H**$_2$CH$_3$, $^{3}J_{H\text{-}H}$ = 7 Hz), 0.89 (d, 18H, PC(C**H**$_3$)$_3$, $^{3}J_{P\text{-}H}$ = 14 Hz), 0.84 (t, 3H, PCH$_2$CH$_2$CH$_2$C**H**$_3$, $^{3}J_{H\text{-}H}$ = 8 Hz); ^{31}P{^{1}H} NMR (121.5 MHz, C_6D_6) δ: 61.6; ^{13}C{^{1}H} NMR (75.5 MHz, C_6D_6) δ: 27.7 (PC(**C**H$_3$)$_3$), 25.8 (d, PCH$_2$CH$_2$**C**H$_2$CH$_3$, $^{3}J_{P\text{-}C}$ = 19 Hz), 25.5 (d, PCH$_2$**C**H$_2$CH$_2$CH$_3$, $^{2}J_{P\text{-}C}$ = 26 Hz); 19.0 (d, P**C**H$_2$CH$_2$CH$_2$CH$_3$, $^{1}J_{P\text{-}C}$ = 30 Hz), 14.1 (PCH$_2$CH$_2$CH$_2$**C**H$_3$); ^{11}B{^{1}H} NMR (96.3 MHz, C_6D_6) δ: -21.0.

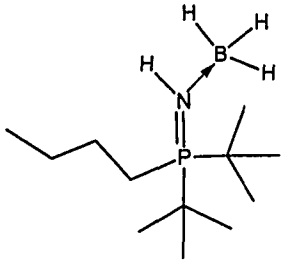

BCl(Ph)(NP*n*-Bu$_3$) (3.16): A solution of BCl_2Ph (0.2 mL, 1.542 mmol) in 5 mL of toluene was slowly added via syringe to a solution of Me_3SiNPn-Bu_3 (0.446 g, 1.541 mmol) in 35 mL of toluene. The Schlenk flask was put under static vacuum and stirred for 72 h. The solvent was removed *in vacuo* and the remaining white solid was washed with *n*-pentane. Yield: 52%. ^{1}H NMR (300 MHz, C_6D_6) δ: 8.72 (d, 2H, *o*-Ph, $^{3}J_{H\text{-}H}$ = 7 Hz), 7.47 (t, 2H, *m*-Ph, $^{3}J_{H\text{-}H}$ = 7 Hz), 7.28 (t, *p*-Ph, $^{3}J_{H\text{-}H}$ = 7 Hz), 1.60 (m, 6H, PC**H**$_2$CH$_2$CH$_2$CH$_3$), 1.22 (m, 6H, PCH$_2$C**H**$_2$CH$_2$CH$_3$), 1.02 (tq, 6H, PCH$_2$CH$_2$C**H**$_2$CH$_3$, $^{3}J_{H\text{-}H}$ = 7 Hz, $^{3}J_{H\text{-}H}$ = 7 Hz), 0.73 (t, 9H, PCH$_2$CH$_2$CH$_2$C**H**$_3$), $^{3}J_{H\text{-}H}$ = 7 Hz); ^{31}P{^{1}H} NMR (121.5 MHz, C_6D_6) δ: 39.8; ^{13}C{^{1}H} NMR (75.5MHz, C_6D_6) δ: 135.0 (*o*-Ph), 127.6 (*m*-Ph), 127.1 (*p*-Ph), 24.7 (PCH$_2$CH$_2$CH$_2$CH$_3$), 24.1

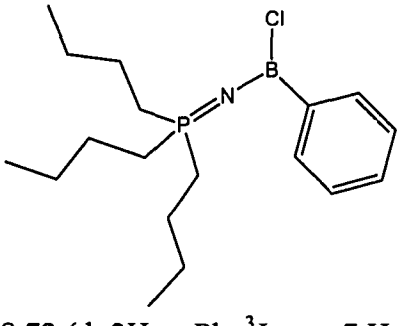

($P(CH_2CH_2CH_2CH_3)$, 23.8 ($PCH_2CH_2CH_2CH_3$) 14.0 ($PCH_2CH_2CH_2CH_3$); $^{11}B\{^1H\}$ NMR (96.3 MHz, C_6D_6) δ: 11.0; Calculated: H: 9.50%, C: 63.64%, N: 4.12%; Found: H: 9.73%, C: 63.39%, N: 4.08%.

3.2.7 Experimental for X-ray Crystallographic Data

3.2.7.1 X-ray Data Collection and Reduction

Refer to Section 2.2.7.1.

3.2.7.2 Structure Solutions and Refinements:

Refer to Section 2.2.7.2.

X-ray structural solutions of $[Me_3PN(H)Bpin][TiCpCl_3]$ (**3.7**), $HN(Bpin)_2$ (**3.11**), PhNH(Bpin) (**3.12**) and *n*-Bu(*t*-Bu)$_2$PNH·BH_3 (**3.15**) were performed as described above. Cell parameters, R, R_w and GoF values are located in Table 3.1 and Table 3.2 while detailed structural parameters have been included as an appendix on CD (Appendix A). No residual electron density of any chemical significance remained in any of the solutions that were. ORTEP drawings of are depicted in Figure 3.2, Figure 3.6, and Figure 3.21, respectively. Select bond distances and bond angles are provided in the text.

Table 3.1: X-ray crystallographic data obtained from crystals of compounds $[Me_3PN(H)Bpin][TiCpCl_3]$ **(3.7)**, $HN(Bpin)_2$ **(3.11)** and PhNH(Bpin) **(3.12)**.

Crystal	3.7	3.11	3.12
Molecular Formula	$TiH_{27}BC_{14}NPO_2$	$H_{25}B_2C_{12}NO_4$	$H_{18}BC_{12}NO_2$
Formula Weight	331.02	268.95	219.09
a (Å)	14.840(2)	12.400(6)	9.928(6)
b (Å)	12.287(1)	10.446(5)	11.970(7)
c (Å)	12.540(1)	12.336(6)	12.500(7)
α°	90	90	111.68(1)
β°	106.469(3)	90.24(1)	92.85(1)
γ°	90	90	112.435(9)
Crystal System	Monoclinic	Monoclinic	Triclinic
Space Group	$P2_1/c$	$P2_1/c$	P-1
Volume ($Å^3$)	2192.6(4)	1597(1)	1244(1)
D_{calc} (gcm^{-3})	1.322	1.118	1.170
Z	4	2	2
Abs coeff, μ, mm^{-1}	0.834	0.079	0.077
θ range (°)	1.43 – 23.29	2.55 – 23.27	2.07 – 23.30
Reflections Collected	10733	6628	5307
Data $F_o^2 > 3\sigma(F_o^2)$	3146	2287	3508
Parameters	208	175	290
R^a	0.0654	0.0552	0.0687
$R_w{}^b$	0.1085	0.0863	0.1695
Goodness of Fit	0.997	1.026	1.003

Data was collected at 20°C with Mo Kα radiation (λ = 0.71069 Å).

[a] $R=\Sigma(F_o-F_c)/\Sigma F_o$

[b] $R_w=(\Sigma[w(F_o^2-F_c^2)^2] /\Sigma[w(F_o)^2])^{½}$

Table 3.2: X-ray crystallographic data obtained from crystal of *n*-Bu(*t*-Bu)$_2$PNH·BH$_3$ **(3.15).**

Crystal	3.15
Molecular Formula	$H_{31}BC_{12}NP$
Formula Weight	231.17
a (Å)	8.212(5)
b (Å)	8.397(5)
c (Å)	11.678(6)
α°	84.13(1)
β°	85.68(1)
γ°	85.34(1)
Crystal System	Triclinic
Space Group	P-1
Volume (Å^3)	796.7(8)
D_{calc} (gcm^{-3})	0.964
Z	2
Abs coeff, μ, mm^{-1}	0.149
θ range (°)	2.87 – 23.27
Reflections Collected	3401
Data $F_o^2 > 3\sigma(F_o^2)$	2262
Parameters	152
R[a]	0.0551
R_w[b]	0.0733
Goodness of Fit	1.013

Data was collected at 20°C with Mo Kα radiation (λ = 0.71069 Å).

[a] $R=\Sigma(F_o-F_c)/\Sigma F_o$

[b] $R_w=(\Sigma[w(F_o^2-F_c^2)^2] /\Sigma[w(F_o)^2])^{1/2}$

3.2.8 Method for Kinetic Experiments

The kinetic study of the reaction of $Me_3SiNPEt_3$ with an excess amount of HBpin was conducted using the following procedure. A 1.5 M stock solution of $Me_3SiNPEt_3$ in toluene was prepared by adding 0.616 g of $Me_3SiNPEt_3$ to a 2 mL volumetric flask and diluting it with toluene to a give a total volume of 2 mL. To five 2 mL volumetric flasks was added 1 mL of HBpin and 0.25 mL of a 0.3 M PPh_3 solution in toluene. A different aliquot (0.05 mL, 0.1 mL, 0.2 mL, 0.4 mL or 0.6 mL) of the $Me_3SiNPEt_3$ stock solution was added to each of the five volumetric flasks. The contents of the flasks were then diluted to a total volume of 2 mL each. The final concentrations of HBpin, $Me_3SiNPEt_3$ and PPh_3 are shown in Table 3.1. An aliquot of each solution was put into a resealable NMR tube equipped with a Teflon screw cap. The NMR tubes were heated in an oil bath at 55°C for the duration of the experiment, except when the NMR data was being collected.

The kinetic study of the reaction HBpin with an excess of $Me_3SiNPEt_3$ was conducted using the following procedure: A 0.69 M stock solution of HBpin was made by adding 0.5 mL of HBpin to a 5 mL volumetric flask and diluting to a total volume of 5 mL with toluene. To four 2 mL volumetric flasks was added 0.5 g of $Me_3SiNPEt_3$ and 0.2 mL of a 0.038 mol/L stock solution of PPh_3 in toluene. A different aliquot (0.57 mL, 0.45 mL, 0.34 mL or 0.227 mL) of the HBpin stock solution was added to each of the five volumetric flasks. The contents of the flasks were then diluted to a total volume of 2 mL each. The final concentrations of HBpin, $Me_3SiNPEt_3$ and PPh_3 are shown in Table 3.3.

All of the above reactions were monitored using $^{31}P\{^1H\}$ NMR spectroscopy.[275-277] Each data set was collected at varying time intervals over a period of 7 days. Each spectrum was produced based on 32 consecutive 30° pulses. A delay time of 1 second between pulses was used. This is shorter than the relaxation times of the three ^{31}P nuclei in the reaction. It was determined, based on experiments conducted with varying delay times between pulses (1s, 5s, 10s, 25s and 60s), that the concentrations of reactants and products, based on ratios of integrals, did not vary with delay time. (Appendix B).

Table 3.3: Summary of the initial concentrations of HBpin, $Me_3SiNPEt_3$ and PPh_3 for reactions 1-9.

Reaction #	[HBpin] mol L^{-1}	[$Me_3SiNPEt_3$] mol L^{-1}	[PPh_3] mol L^{-1}
1	3.45	0.0375	0.0375
2	3.45	0.0750	0.0375
3	3.45	0.150	0.0375
4	3.45	0.300	0.0375
5	3.45	0.450	0.0375
6	0.078	1.22	0.0381
7	0.117	1.22	0.0381
8	0.155	1.22	0.0381
9	0.196	1.22	0.0381

3.2.9 Description of Computational Methods

All calculations were performed using the Gaussian 98[278] and Gaussian 03[279] suite of programs. The B3 exchange functional,[280, 281] as implemented in Gaussian 98 and 03,[282] was used in combination with the correlation functional of Lee, Yang and Parr (LYP).[283] Optimized geometries were obtained at the B3LYP/6-31G(d) level of theory, in the gas-phase. Relative energies were calculated by performing single point calculations at the B3LYP/6-311+G(2df,p) level of theory on the above optimized geometries, i.e. B3LYP/6-311+G(2df,p)//B3LYP-6-31G(d).(Appendix C) Unless otherwise noted, all relative energies are reported in kcal mol^{-1}, bond distances in Angstroms (Å) and angles in degrees (°).

3.3 Results and Discussion

3.3.1 Reaction of Vanadium and Titanium Complexes with Pinacolborane

The reactions of pinacolborane with V(NPh)(O*t*-Bu)$_3$ (**3.5**), V(NPh)(NP*t*-Bu$_3$)(O*t*-Bu)$_2$ (**2.29**), TiCp(NP*t*-Bu$_3$)Me$_2$, TiCp(NP*t*-Bu$_3$)Cl$_2$, and TiCp(NPMe$_3$)Cl$_2$, were monitored using NMR spectroscopy. The reaction of V(NPh)(O*t*-Bu)$_3$ (**3.5**) with three equivalents of HBpin resulted in the formation a single new peak at 21.7 ppm in the $^{11}B\{^1H\}$ NMR spectrum. The disappearance of the peaks due to the *t*-Bu (1.46 ppm) of V(NPh)(O*t*-Bu)$_3$ and the Me (0.99 ppm) of HBpin, with concomitant growth of new *t*-Bu (1.36 ppm) and methyl (1.04 ppm) peaks in the ^1H NMR spectrum, along with the growth of multiple new peaks in the phenyl region. These data suggest that the alkoxide ligands have been extracted to produce three equivalents of *t*-BuOBpin and indiscernible vanadium-containing products. Similarly, based on spectroscopic evidence, the reaction of V(NPh)(NP*t*-Bu$_3$)(O*t*-Bu)$_2$ (**2.29**) with HBpin resulted in extraction of both the phosphinimide and alkoxide ligands by HBpin, forming one equivalent of *t*-Bu$_3$PNBpin (**3.8**) and two equivalents of *t*-BuOBpin, as shown in Figure 3.1. The ^1H and $^{11}B\{^1H\}$ NMR spectra revealed identical peaks to those observed in the reaction of **3.5** with three equivalents of HBpin and those observed in the reaction of HNP*t*-Bu$_3$ and HBpin (*vide infra*). While the vanadium products were neither identified nor characterized, it is proposed that a vanadium-hydride species may be formed.[284, 285]

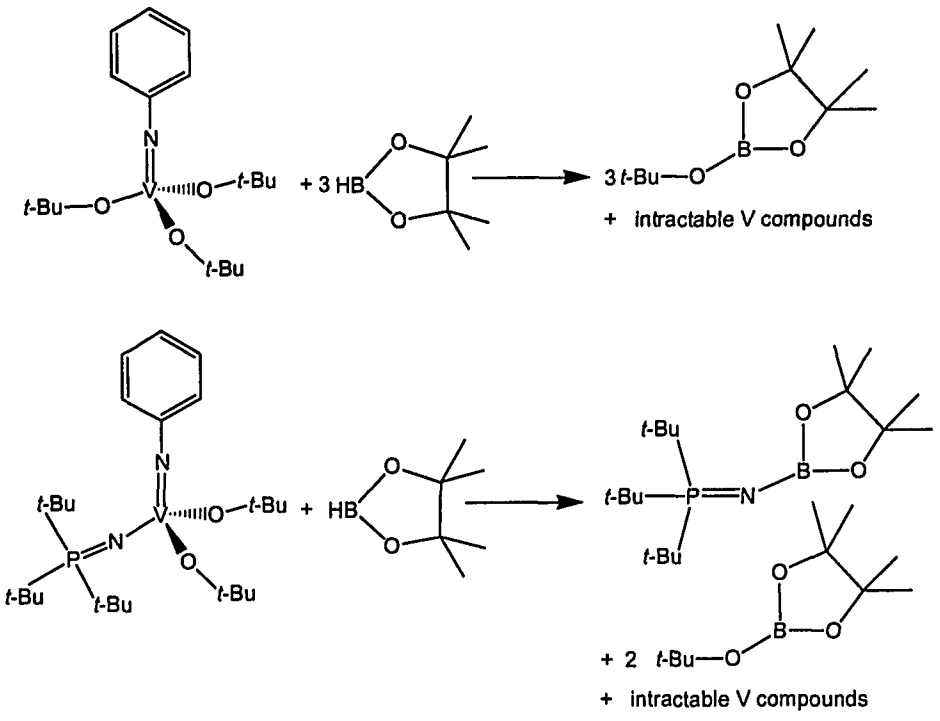

Figure 3.1: The reactions of V(NPh)(O*t*-Bu)$_3$ (**3.5**) and V(NPh)(NP*t*-Bu$_3$)(O*t*-Bu)$_2$ (**2.29**) with HBpin.

Similarly, the reaction of TiCp(NP*t*-Bu$_3$)Me$_2$ with pinacolborane at room temperature led to the formation of the borylphosphinimide complex *t*-Bu$_3$PNBpin (**3.8**). In contrast, under similar conditions, TiCp(NP*t*-Bu$_3$)Cl$_2$ did not react with HBpin. This may be a consequence of the stronger Ti-N interaction in TiCp(NP*t*-Bu$_3$)Cl$_2$ due to the now more electropositive metal centre when bound to the more electronegative chloride ligands. Moreover, the reaction of TiCp(NPMe$_3$)Cl$_2$ with HBpin at room temperature resulted in extraction of the phosphinimide ligand. This suggests that the alkyl or aryl groups attached to the phosphorus atom may also play a key role in the accessibility and reactivity of the nitrogen atom of the phosphinimide ligand. From the reaction mixture of TiCp(NPMe$_3$)Cl$_2$ and HBpin, large blue crystals[286] formed and these were determined by X-ray crystallography to be the salt [Me$_3$PN(H)Bpin][TiCpCl$_3$] (**3.7**), shown in Figure 3.2.

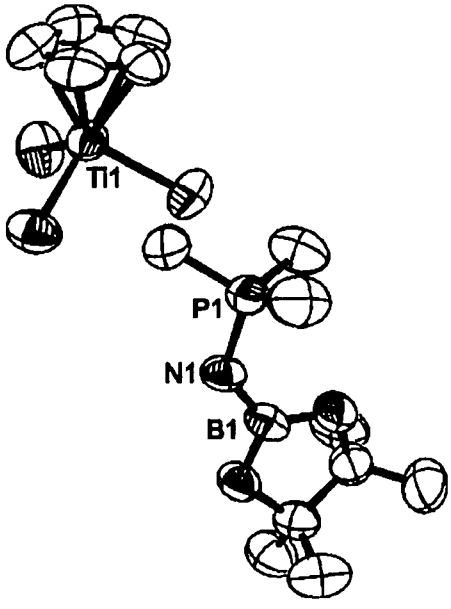

Figure 3.2: ORTEP diagram (50% probability thermal ellipsoids) of $[Me_3PN(H)Bpin][TiCpCl_3]$ (**3.7**). Hydrogen atoms have been omitted for clarity.

The initial crystallographic data was ambiguous, as one could not distinguish between two neutral molecules, $TiCpCl_3$ and $Me_3PNBpin$ and a salt formulation. To address this issue the bond angles were examined. The angle between P(1)-N(1)-B(1) was determined to be 127.2(5)°. This B-N-P angle is relatively small for a two-coordinate nitrogen centre of a phosphinimine,[154, 159] but is very similar to angles observed in phosphinimine-borane coordination compounds containing a three-coordinate nitrogen centre.[149-151, 160] Furthermore, due to the lack of steric crowding about the nitrogen atom if it were neutral, dimerization at the nitrogen and boron centres would be expected (see Chapter 4).[153, 155, 164] The average Ti-Cl bond distance in compound **3.7** was determined to be 2.343(3) Å. This value resembles the Ti-Cl bond distances of $TiCpCl_3$ anions rather than the neutral molecule.{Hughes, 1989 #864; Engelhardt, 1984 #865} In addition, the ^1H NMR for compound **3.7** is broad and unresolved indicating the possible presence of a paramagnetic species. It is proposed that the titanium centre has been reduced from Ti(IV) to Ti(III) in the presence of HBpin to give the ion pair

$[Me_3PN(H)Bpin][TiCpCl_3]$. Similarly, reduction of the Ti(IV) metal centre by catecholborane has been reported by Hartwig and coworkers.[287]

3.3.2 Reactions of Phosphinimines with Pinacolborane

Reactions of pinacolborane with phosphinimine compounds were investigated. Addition of pinacolborane to tri(*t*-butyl)phosphinimine led to vigorous evolution of gas, presumed to be H_2, and the formation of the pinacolboryl-tri(*t*-butyl)phosphinimine compound *t*-Bu_3PNBpin (**3.8**), which was isolated as a colourless oil (Figure 3.3). When this reaction was carried out neat or diluted in a toluene or pentane solution, it proceeded to completion within minutes. Compound **3.8** was characterized by ^1H, $^{31}P\{^1H\}$, $^{13}C\{^1H\}$, and $^{11}B\{^1H\}$ NMR spectroscopy and elemental analysis.

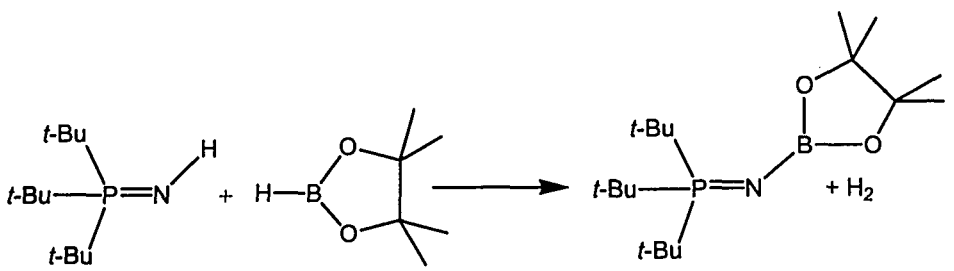

Figure 3.3: Synthesis of *t*-Bu_3PNBpin (**3.8**).

Compound **3.8** is proposed to be monomeric due to the large *t*-butyl groups about the phosphorus atom which shield the nitrogen atom from coordinating to an adjacent molecule (see Chapter 4). The catechol version of this compound was determined to be monomeric both in solution and in the solid state. Since pinacolborane is more bulky than catecholborane, *t*-Bu_3PNBpin is presumed to be monomeric as well.

Reaction of stoichiometric amounts of the phosphinimine derivative HNP*n*-Bu(*t*-$Bu)_2$, (**3.1**), which is slightly less sterically hindered, with HBpin in toluene at ambient temperature resulted in the formation of the borylphosphinimine complex *n*-Bu(*t*-$Bu)_2$PNBpin (**3.9**). This compound was isolated as a white solid. Attempts to obtain crystals of **3.9** that were suitable for an X-ray diffraction study were unsuccessful. Compound **3.9** is expected to be monomeric based on the chemical shift (21.6 ppm)

observed in the $^{11}B\{^1H\}$ NMR spectrum. In a similar vein, the reaction of one equivalent of HNP*i*-Pr$_3$ with one equivalent of HBpin in toluene at ambient temperatures produced the borylphosphinimine complex, *i*-Pr$_3$PNBpin (**3.10**) as the major product in 87% yield. The tertiary phosphine, P*i*-Pr$_3$, and diborylamine, HN(Bpin)$_2$ were identified using NMR spectroscopy to be the minor products, along with unreacted phosphinimine (Figure 3.4). When this reaction mixture was heated in the presence of excess pinacolborane, no reduction of the phosphorus atom of *i*-Pr$_3$PNBpin was observed. This is evidence that two distinct reaction pathways occur when pinacolborane is treated with tri-*i*-propylphosphinimine.

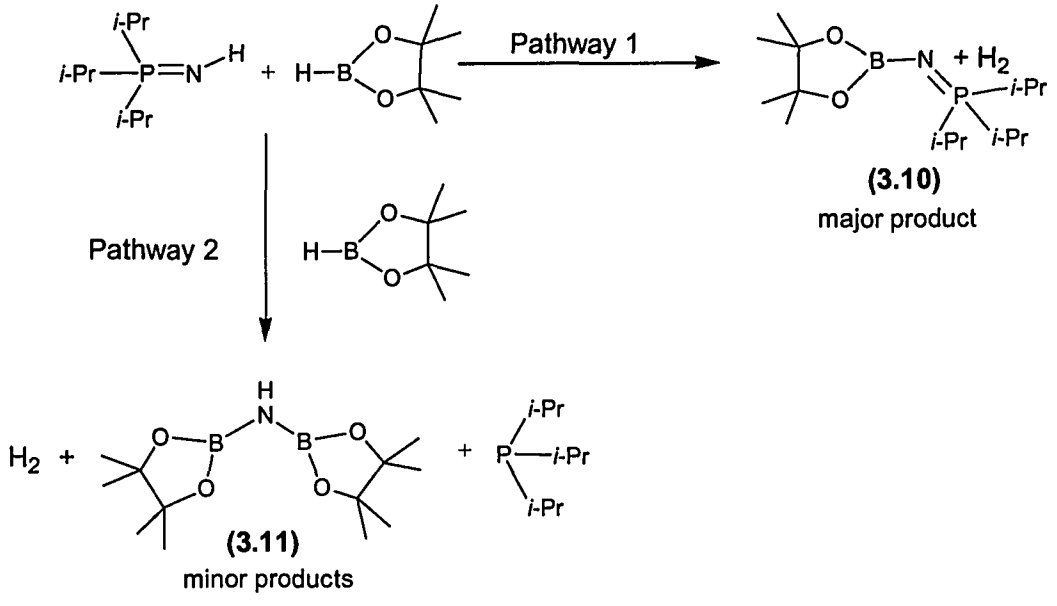

Figure 3.4: Divergent pathways observed for the reaction of pinacolborane with tri-*i*-propylphosphinimine.

Phosphinimines with smaller alkyl groups on phosphorus (HNP*n*-Bu$_3$ and HNPEt$_3$) were also treated with pinacolborane. In these reactions, formation of the borylphosphinimine complex was not observed. The reaction of one equivalent of tri-*n*-butylphosphinimine or triethylphosphinimine with two equivalents of pinacolborane

resulted in the complete reduction of the phosphorus centre of the phosphinimine to form the respective tertiary phosphine, and formation of the diborylamine, $HN(Bpin)_2$ (**3.11**), as depicted in Figure 3.5. The evolution of gas was observed and is consistent with hydrogen gas being liberated. Monitoring these reactions by $^{31}P\{^1H\}$ NMR spectroscopy revealed the generation of the free trialkylphosphine. IR spectral data revealed an absorption at 3334 cm^{-1}, consistent with the presence of an N-H functional group.

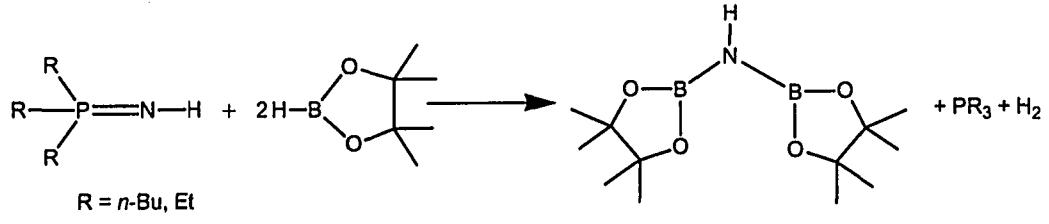

Figure 3.5: Formation of $HN(Bpin)_2$ (**3.11**) upon reaction of $HNPR_3$ (R = *n*-Bu and Et) with pinacolborane.

X-ray quality crystals of compound **3.11** were grown from a concentrated *n*-pentane solution and the X-ray data obtained confirmed the formulation as the diborylamine ($HN(Bpin)_2$). The B-N bond distances in compound **3.11** average 1.419(6) Å; which is a typical B-N bond distance for diborylamines.[288-291] Refinement of the proton on nitrogen revealed that the geometry at nitrogen is planar. The B(1)-N-B(2) angle was determined to be 132.9(3)° which compares with the corresponding angle of 135.4(2)° observed for the diborylamine $HN(BPh_2)_2$.[290]

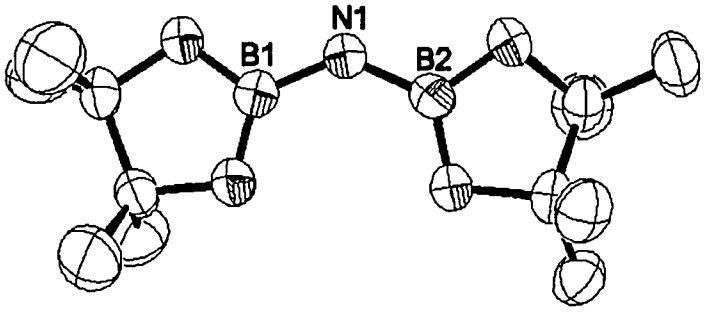

Figure 3.6 : ORTEP diagram (50% probability thermal ellipsoids) of $HN(Bpin)_2$ (**3.11**). Hydrogen atoms have been omitted for clarity.

The isolation of the different products $R_3PNBpin$ or $HN(Bpin)_2$ and PR_3 from the above reactions of phosphinimines with boranes clearly demonstrates that this type of reaction has at least two plausible reaction pathways. It seems reasonable that the pathway in which the borylphosphinimine is produced relies on the interaction of one molecule of pinacolborane with one molecule of phosphinimine. However, the order of reaction with respect to the second pathway was not as intuitive. The phosphinimines used provide much less shielding of the nitrogen atom and therefore, provided doubt with respect to the order of reaction in pinacolborane or phosphinimine. The reactions of the protonated phosphinimines with pinacolborane occur rapidly at room temperature, in turn making the progress during the reaction difficult to monitor. The reaction of *N*-trimethylsilyl-triethylphosphinimine with pinacolborane occurs at a much slower rate. Experimentally, it was determined that the reaction of HBpin with $Me_3SiNPEt_3$ proceeds in 2:1 stoichiometric ratio, respectively. The products of the reaction have been identified spectroscopically to be $HN(Bpin)_2$, PEt_3 and $SiMe_3H$. Therefore, the net chemical equation for the reaction of pinacolborane with *N*-trimethylsilyl-triethylphosphinimine is shown in Scheme 3.1.

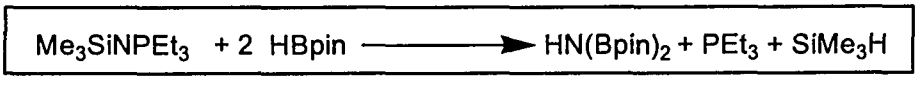

Scheme 3.1: The net equation for the reaction of pinacolborane and *N*-trimethylsilyl-triethylphosphinimine.

It is assumed that the trimethylsilylphosphinimine reacts with pinacolborane via the same mechanism as the reaction involving the protonated phosphinimine and pinacolborane. The reaction in Scheme 3.1 occurs slowly at room temperature, and therefore was determined to be suitable for a kinetic study. In general terms, the kinetics of the reaction of *N*-trimethylsilyl-triethylphosphinimine with pinacolborane follow the rate law shown in Equation 3.1.

$$\text{Rate} = k[\text{HBpin}]^x[\text{Me}_3\text{SiNPEt}_3]^y$$

where: k = the overall rate constant

x = the order of reaction with respect to HBpin

y = the order of reaction with respect to $Me_3SiNPEt_3$

Equation 3.1: The rate law for the reaction of pinacolborane and *N*-trimethylsilyl-triethylphosphinimine.

3.3.3 A Kinetic Study of the Reaction of *N*-trimethylsilyl-triethylphosphinimine with Pinacolborane

To determine the order of reaction (x and y, Equation 3.1) with respect to each reactant, two sets of NMR experiments were conducted. The first set of experiments involved multiple reactions of an excess of pinacolborane (HBpin) (3.45 M) and *N*-trimethylsilyl-triethylphosphinimine ($Me_3SiNPEt_3$) with concentrations of 0.0375 M, 0.075 M, 0.15 M, 0.3 M and 0.45 M in toluene. Triphenylphosphine (0.0375 M) was used as an internal standard as this does not interfere in any way with the reaction.[292] Integration of the signal intensities relative to PPh_3 was performed. Using an excess of pinacolborane simplifies the rate law (Equation 3.1) such that it can be written as in Equation 3.2.

$$\text{Rate} = k_{obs}[\text{Me}_3\text{SiNPEt}_3]^y$$

where:

$k_{obs} = k[HBO_2C_2(CH_3)_4]^x$ = the observed rate constant

y = the order of reaction with respect to $Me_3SiNPEt_3$

Equation 3.2: The rate law for the reaction of *N*-trimethylsilyl-triethylphosphinimine with pinacolborane if the concentration of pinacolborane is held constant throughout the reaction.

The formation of PEt_3 and the disappearance of $Me_3SiNPEt_3$ were monitored over time using $^{31}P\{^1H\}$ NMR spectroscopy. The concentrations of $Me_3SiNPEt_3$ and PEt_3 (Appendix B) were determined from spectral integrations. The growth of PEt_3 and the decay of $Me_3SiNPEt_3$ for the reactions of varying phosphinimine concentration with an excess of pinacolborane are shown in Figure 3.7.

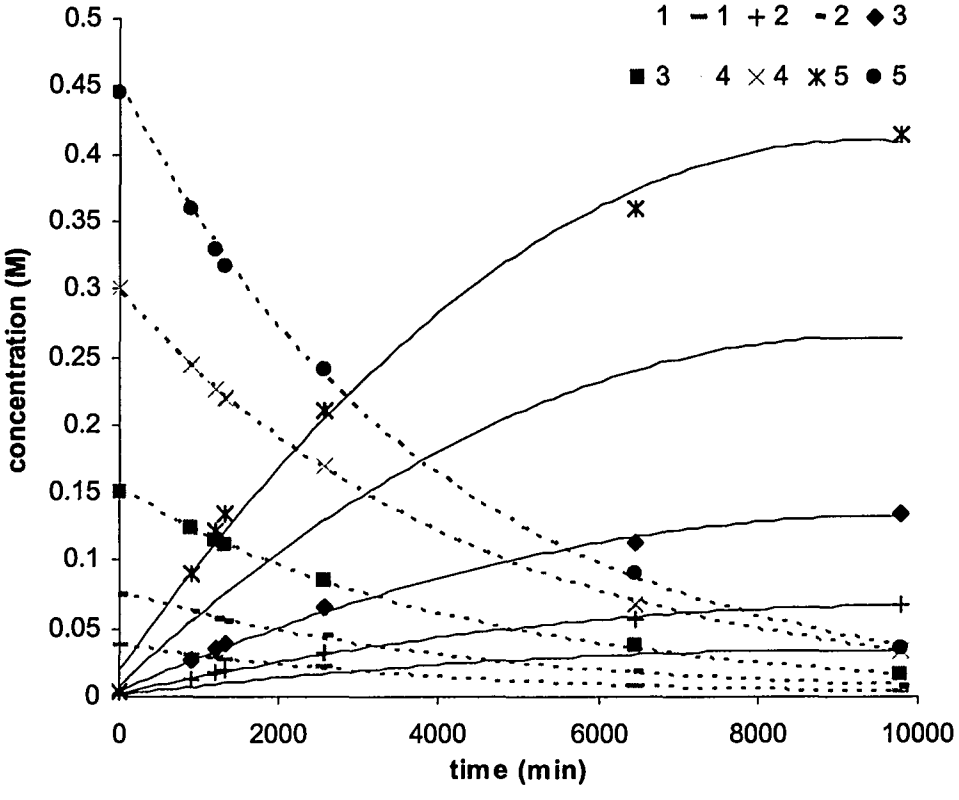

Figure 3.7: A plot of the growth of PEt_3 (—) and the disappearance of $Me_3SiNPEt_3$ (---) for reactions 1-5.

A plot of the natural logarithm of the concentrations of $Me_3SiNPEt_3$ versus time confirmed the reaction as pseudo-first order with respect to $Me_3SiNPEt_3$ (Equation 3.3).

$$\ln[Me_3SiNPEt_3] = k_{obs}t + \ln[Me_3SiNPEt_3]_o$$

Equation 3.3: The integrated rate law for a pseudo-first order reaction.

In Figure 3.8 the linear relationship observed in this plot indicates that the rate determining step in the reaction of HBpin with $Me_3SiNPEt_3$ is first order in phosphinimine.

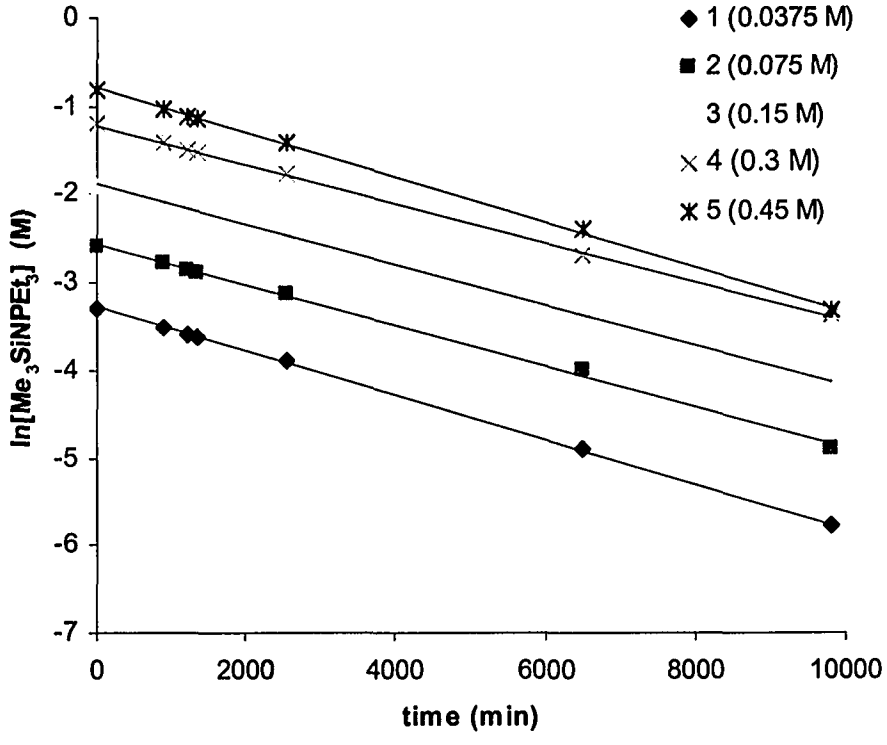

Figure 3.8: A plot of $\ln[Me_3SiNPEt_3]$ *vs.* time for reactions 1-5.

The order of the reaction with respect to $Me_3SiNPEt_3$ was also determined using the differential rate law which employs the method of initial rates. The differential rate law (Equation 3.4(a)) for the reaction of $Me_3SiNPEt_3$ with excess HBpin and the corresponding logarithmic equation (Equation 3.4(b)) are depicted below.

(a) $\boxed{rate_o = k_{obs}([Me_3SiNPEt_3]_o)^y}$

(b) $\boxed{\log(rate_o) = \log(k_{obs}) + y \log[Me_3SiNPEt_3]_o}$

Equation 3.4: (a) The differential rate law and (b) the logarithmic form of the differential rate law.

A plot of the log of the initial rate of reaction ($\log(rate)_o$) versus the log of the initial concentration of $Me_3SiNPEt_3$ ($\log[Me_3SiNPEt_3]_o$) reveals a linear relationship. The slope of the line is approximately equal to 1, confirming the reaction is first order in phosphinimine (Figure 3.9).

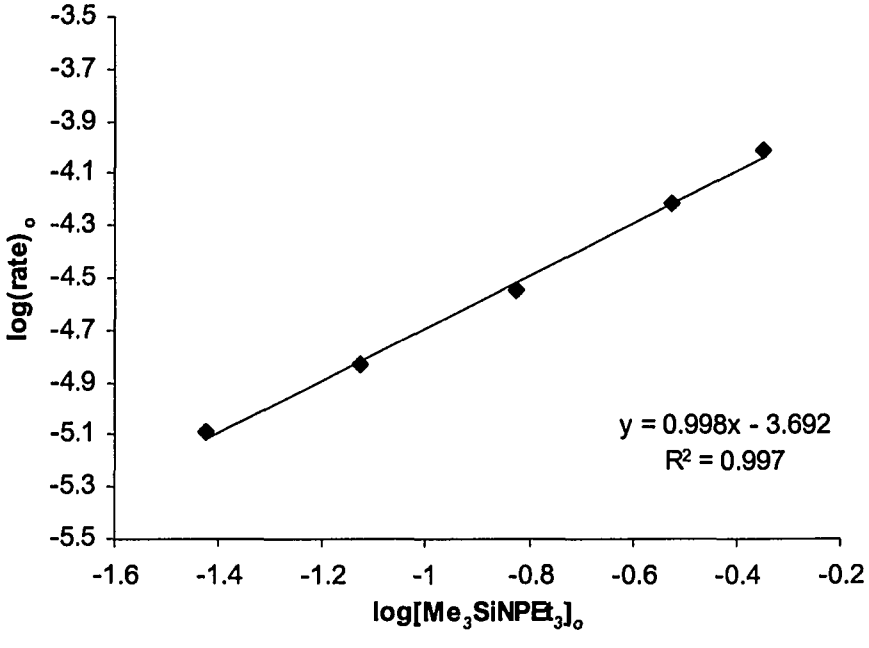

Figure 3.9: A plot of $\log(rate)_o$ versus $\log[Me_3SiNPEt_3]_o$.

To determine the order of reaction in pinacolborane, a second set of experiments was conducted where the concentration of HBpin was instead varied (see Table 3.3) and $Me_3SiNPEt_3$ was used in excess (1.217 M). These reactions were monitored in an identical fashion to the first set of experiments. Since HBpin consumption can not monitored directly by $^{31}P\{^1H\}$ NMR spectroscopy, the concentrations of HBpin were correlated to the growth of PEt_3. When the reaction of pinacolborane and phosphinimine was performed using 1:1 stoichiometric amounts of both reactants, all of the HBpin was consumed whereas half of the phosphinimine starting material remained. Therefore, for every molecule of PEt_3 produced, two equivalents of pinacolborane are consumed. This is illustrated in the plot of the concentrations of PEt_3 and HBpin over time (Figure 3.10). For the raw data see Appendix B.

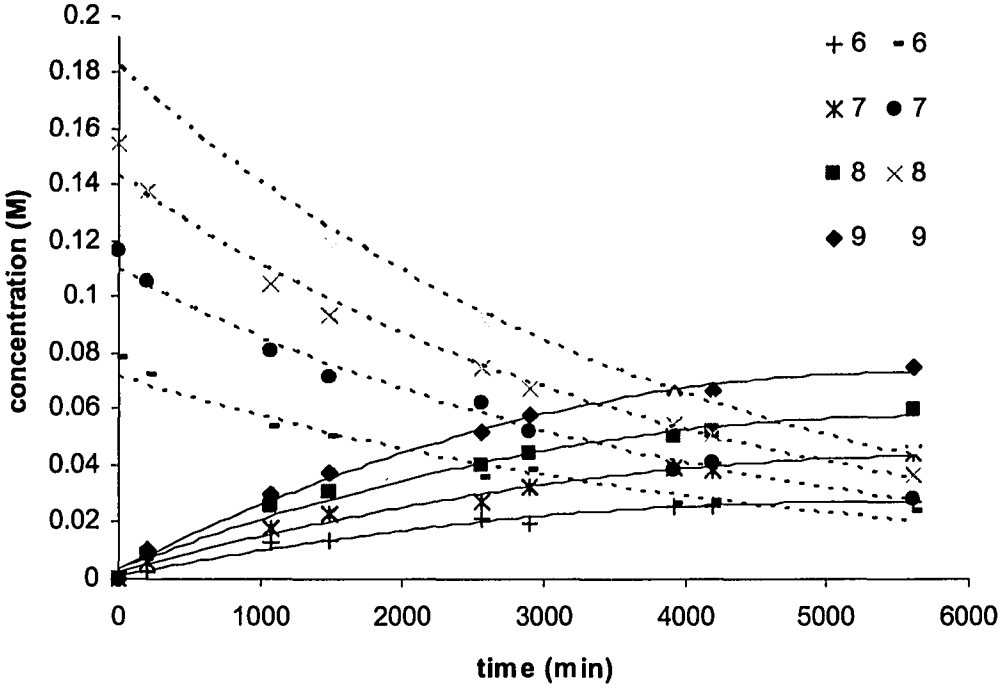

Figure 3.10: The growth of PEt_3 (—) and the consumption of HBpin (----) for reactions 6-9.

The data collected for the reaction of excess $Me_3SiNPEt_3$ with pinacolborane were manipulated in the same fashion for the previous set of experiments and similar results

were determined. The natural logarithmic values of the concentration of HBpin were plotted against time (Figure 3.11) and revealed a linear relationship, indicating that the reaction is first order in pinacolborane (Appendix B).

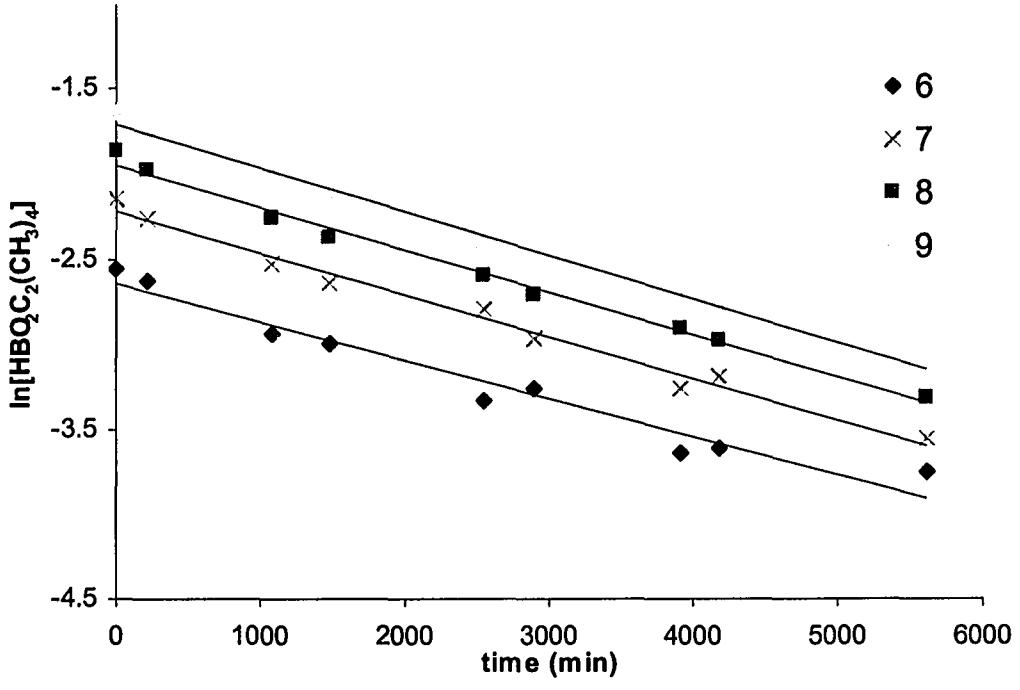

Figure 3.11: A plot of ln[HBpin] versus time for reactions 6-9.

In addition, in a similar fashion to that used above, a plot of the logs of the initial concentration of HBpin versus the initial rate of reaction (Figure 3.12) revealed a slope of approximately 1. This further confirms that the reaction is first order in pinacolborane (Appendix B).

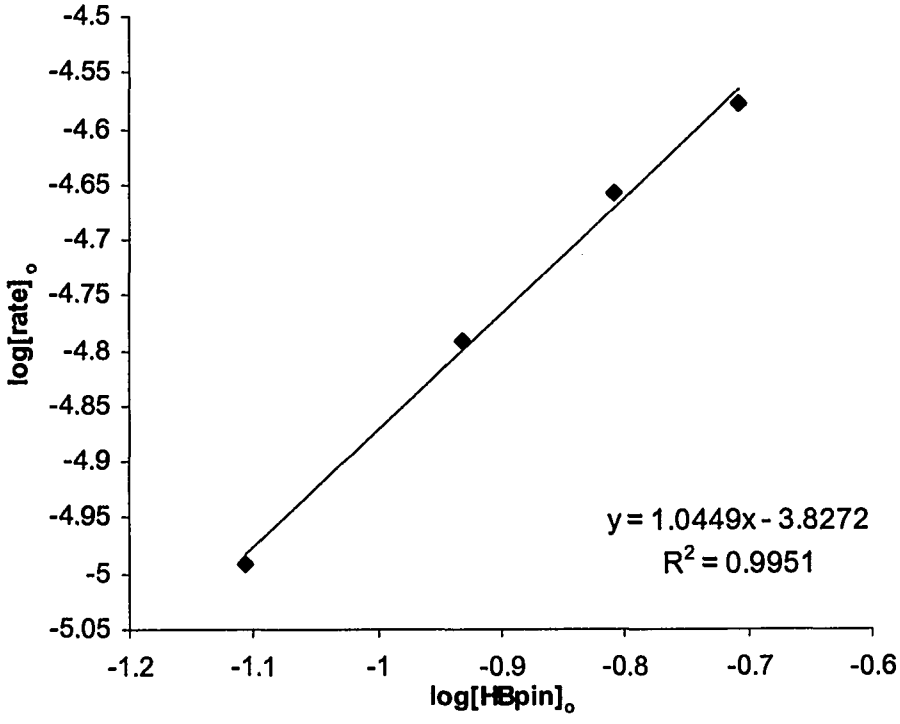

Figure 3.12: A plot of $\log(\text{rate})_o$ versus $\log[\text{HBpin}]_o$.

Since this evidence indicates that the rate-determining step is first order in both pinacolborane and *N*-trimethylsilyl-triethylphosphinimine, a mechanism can be proposed, and is outlined in Figure 3.13.

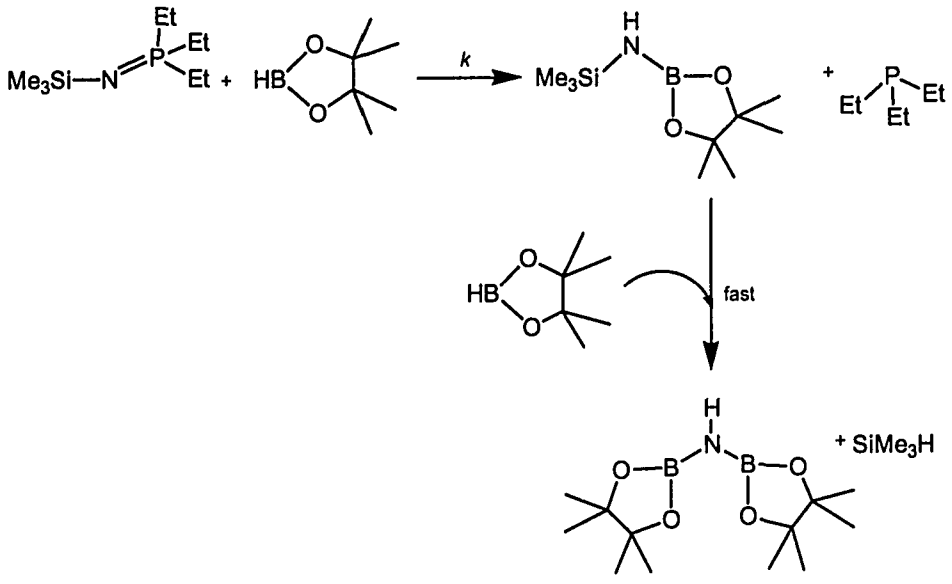

Figure 3.13: The proposed two-step mechanism for the reaction of HBpin with $Me_3SiNPEt_3$.

In the first step, the nitrogen centre of the phosphinimine coordinates to the boron centre of pinacolborane. This is followed by reduction of the phosphorus centre and oxidation of the boron-bound hydrogen atom to give a boryl-amine intermediate and the reaction by-product PEt_3. This is proposed to be the rate-determining step. We propose that the second step involves rapid reaction of the boryl-amine with another equivalent of pinacolborane, resulting in the formation of the diboryl-amine product.

The overall rate constant k derived from the plots above was determined from $k_{obs} = k[\text{HBpin}]$ and $k_{obs} = k[Me_3SiNPEt_3]$. The k_{obs} and k for reactions 1-9 are shown in Table 3.4. The average k value was determined to be $1.3(7) \times 10^{-4}$ $L \cdot mol^{-1} \cdot s^{-1}$.

Table 3.4: The observed rate constant (k_{obs}) and overall rate constant (k) for the reactions in which $Me_3SiNPEt_3$ was combined with excess HBpin (reactions 1-5) and the reactions in which HBpin was combined with excess $Me_3SiNPEt_3$ (reactions 6-9).

Reaction #	k_{obs} (s^{-1})	k ($L \cdot mol^{-1} \cdot s^{-1}$)
1	2.55×10^{-04}	7.36×10^{-05}
2	2.35×10^{-04}	6.78×10^{-05}
3	2.31×10^{-04}	6.70×10^{-05}
4	2.24×10^{-04}	6.49×10^{-05}
5	2.54×10^{-04}	7.36×10^{-05}
6	2.56×10^{-04}	2.11×10^{-04}
7	2.50×10^{-04}	2.05×10^{-04}
8	2.47×10^{-04}	2.03×10^{-04}
9	2.26×10^{-04}	1.86×10^{-04}

The overall rate equation for the reaction of pinacolborane with *N*-trimethylsilyl-triethylphosphinimine is given in Equation 3.5.

$$\text{Rate} = (1.3(7) \times 10^{-4})[\text{HBpin}][Me_3SiNPEt_3]$$

Equation 3.5: The rate law for the reaction of $Me_3SiNPEt_3$ and HBpin.

All experiments performed in this kinetic study were conducted at 55°C. The reaction, when performed at room temperature, took many weeks to reach completion. If the reaction mixtures were heated for long periods of time above 60°C, decomposition of HBpin complicates the kinetic data. Therefore, with respect to time, analogous reactions were not performed at a variety of temperatures and consequently the activation parameters were not determined.

3.3.4 A Computational Investigation of the Reaction of Phosphinimines with Pinacolborane

In order to gain further insight into the apparently counter-intuitive experimental observations that less sterically demanding phosphinimines undergo reduction while, in contrast, bulkier phosphinimines undergo protonolysis to yield *N*-borylphosphinimines, a computational investigation was performed which examined the two proposed mechanisms. The phosphinimine/borane pairs shown in Table 3.5 represent the model systems that were used. The two phosphinimines employed ($HNPH_3$ and $HNPt\text{-}Bu_3$) represent the simplest, prototypical phosphinimine and a sterically encumbered phosphinimine, respectively. The three boranes used ($HBO_2C_2H_4$, HBpin, and $HBO_2C_2(CF_3)_4$) represent a variation in the electropositive nature of the boron atom, with the pinacolate effecting the least electropositive boron centre and the perfluorinated pinacolate effecting the most electropositive boron centre. These calculations were performed as described in the experimental section.

Table 3.5: Optimized phosphinimine/borane pairs and the N-B distances and HNBH angles of the initial phosphinimine-borane adducts.

Pair #	Phosphinimine	Borane	N-B distance (Å)	HNBH angle(°)
1	$HNPH_3$	$HBO_2C_2H_4$	1.556	63.5
2	$HNPH_3$	HBpin	1.603	38.3
3	$HNPH_3$	$HBO_2C_2(CF_3)_4$	1.588	31.6
4	$HNPt\text{-}Bu_3$	$HBO_2C_2H_4$	1.603	4.4
5	$HNPt\text{-}Bu_3$	HBpin	1.611	10.9
6	$HNPt\text{-}Bu_3$	$HBO_2C_2(CF_3)_4$	1.567	17.8

When $HNPH_3$, the simplest phosphinimine considered, is allowed to react with $HBO_2C_2H_4$, HBpin, $HBO_2C_2(CF_3)_4$, the weakly bound adducts $H_3PNH{\cdot}HBO_2C_2H_4$, $H_3PNH{\cdot}HBpin$ and $H_3PNH{\cdot}HBO_2C_2(CF_3)_4$ are formed. These lie lower than the initial reactants by 5.2, 2.5 and 19.2 kcal mol^{-1}, respectively.(see Appendix C) The optimized

structures of the adducts show that they all possess a pseudo tetrahedral geometry at the boron centre, a trigonal planar arrangement at the nitrogen centre and similar N···B distances (Table 3.5). The main difference between the structures is the orientation of the substituents surrounding the N···B interaction; the hydrogen atoms on the nitrogen and boron adopt a staggered conformation, with H-N-B-H angles of 63.5°, 38.3° and 31.6°, respectively. As a result, the H_N-H_B distances are 2.90 Å, 2.70 Å and 2.55 Å, respectively (Figure 3.14). Interestingly, the phosphorus centres in each of the adducts is in close proximity to one of the oxygen atoms of the diolate on boron with P···O distances of 2.13 Å, 2.25 Å and 2.56 Å, respectively. This results in the formation of a pseudo-OBNP four membered ring, reminiscent of the previously proposed phosphetidine intermediate for phosphinimine metathesis.[187] The proximity of the phosphorus and oxygen is further illustrated via Newman projections down the N···B interaction, showing the phosphorus and oxygen atoms to be all but eclipsed, as is shown in Figure 3.14.

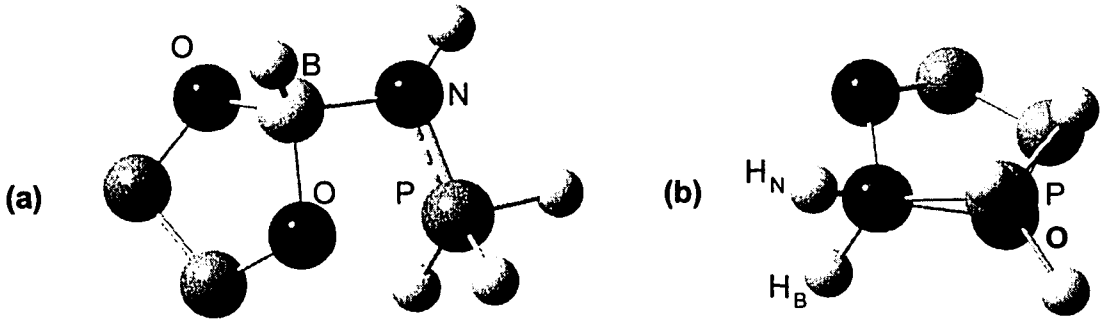

Figure 3.14: Illustrations of (a) the P···O interaction, forming the OBNP pseudo-four-membered ring and (b) Newman projection looking down the N-B bond which illustrates the eclipsed P···O interaction and the staggered H_N-H_B conformation. Substituents on the alkoxide backbone have been eliminated for clarity.

Based on experimental results, it is proposed that these adducts can react via two different mechanisms. It should be noted that it is presumed that, for any given reactants, both proposed mechanisms proceed via the same phosphinimine-borane adduct. It should also be noted that the above adducts represent the lowest energy weakly bound adduct

structures located for each reactant pair. Thus, any alternative conformations will lie slightly higher in energy, but any barriers to interconversion of such conformers can be expected to be small or negligible, and will certainly be considerably less than the barriers to reaction. Hence, they will have no effect on the conclusions of this present study.

For $H_3PNH{\cdot}HBO_2C_2H_4$, $H_3PNH{\cdot}HBpin$ and $H_3PNH{\cdot}HBO_2C_2(CF_3)_4$, the proposed mechanism *pathway 2* (Figure 3.4), in which reduction of the phosphorus atom and formation of the corresponding phosphine and borylamine occurs, is the thermodynamically preferred reaction. Indeed, it is found to proceed with barriers of 37.0, 34.9 and 41.8 kcal mol^{-1} to give weakly bound product complexes $H_3P{\cdot}H_2NBO_2C_2R_4$ (R = H, CH_3 and CF_3), respectively. The transition structures for *pathway 1* and *pathway 2* are depicted in Figure 15.

Figure 3.15: Optimized geometries of the transition structures for (a) *pathway 1* and (b) *pathway 2* for the reaction of $HNPH_3$ and $HBO_2C_2H_4$.

As the potential energy surfaces (PESs) for these mechanisms are quite similar, only the schematic PES for the reaction of $HNPH_3$ and $HBO_2C_2H_4$ proceeding via mechanism 2 is shown here, Figure 3.16(a). The relative energies for the others are given in Appendix C. The alternative mechanism *pathway 1*, formation of the corresponding *N*-borylphosphinimine product, proceeds with activation barriers that are marginally higher by 2.3, 2.7 and 1.1 kcal mol^{-1} than those calculated for *pathway 2*.The schematic

PES for the reaction of $HNPH_3$ with $HBO_2C_2H_4$ proceeding via *pathway 1* is shown in Figure 3.16(b).

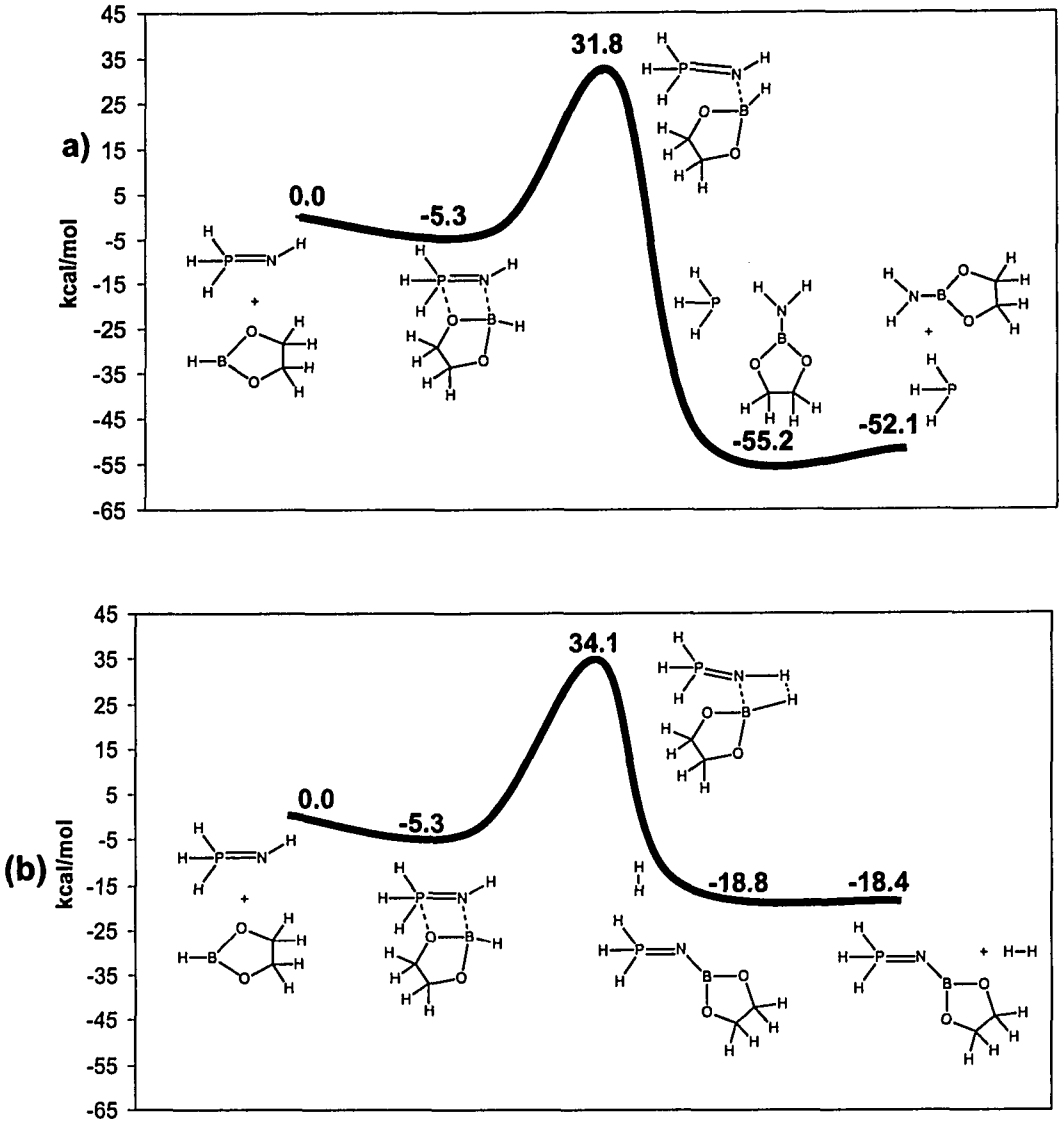

Figure 3.16: Schematic gas phase potential energy surface for the reaction of $HNPH_3$ with $HBO_2C_2H_4$ to yield (a) PH_3 and H_2NBpin (*pathway 2*) and (b) H_2 and $H_3PNBO_2C_2H_4$ (*pathway 1*).

Thus, the preferred orientation of the adducts when a sterically unobtrusive substituent such as hydrogen is employed appears to be dictated by the electrostatic P···O attraction that places the boron- and nitrogen-bound hydrogen atoms in a staggered conformation. In turn, this favours hydride transfer from the boron to nitrogen, resulting in the preferable reduction of the phosphorus atom of the phosphinimine. Such a transfer concomitantly affords the intermediate H_2NBpin. It should be noted that the reduced product is calculated to lie much lower in energy than the *N*-borylphosphinimine product and appears to react readily with a second equivalent of HBpin to give the experimentally observed product $HN(Bpin)_2$ (**3.11**) (Figure 3.13); the intermediate is not observed. This further step was not investigated as a computational study.

We note that the energy difference for the activation barriers for *pathways 1* and *2* are relatively small (≈ 2 kcal/mol). However, it may also help to rationalize why tri-*i*-propylphosphinimine reacts with pinacolborane to afford the products of both reaction pathways (Figure 3.4). In this case the energy difference between the two mechanisms is negligible, however mechanism 2 may be ever so slightly favoured in this case given the ratio of the products formed.

The main difference between the adducts obtained for H and *t*-Bu substituents on phosphorus is the orientation of the atoms about the N-B bond. In the optimized structures of $t\text{-}Bu_3PNH{\cdot}HBO_2C_2H_4$, $t\text{-}Bu_3PNH{\cdot}HBpin$ and $t\text{-}Bu_3PNH{\cdot}HBO_2C_2(CF_3)_4$, the distances separating the phosphorus and closest oxygen were calculated to be 3.47 Å, 3.53 Å, and 3.63 Å, respectively (Figure 3.17). As a result, the corresponding H-N-B-H angles decrease to 4.4°, 10.9°, and 17.8° respectively. Consequently, the H_N-H_B distances also decrease to 2.20 Å, 2.13 Å and 2.13 Å, respectively.

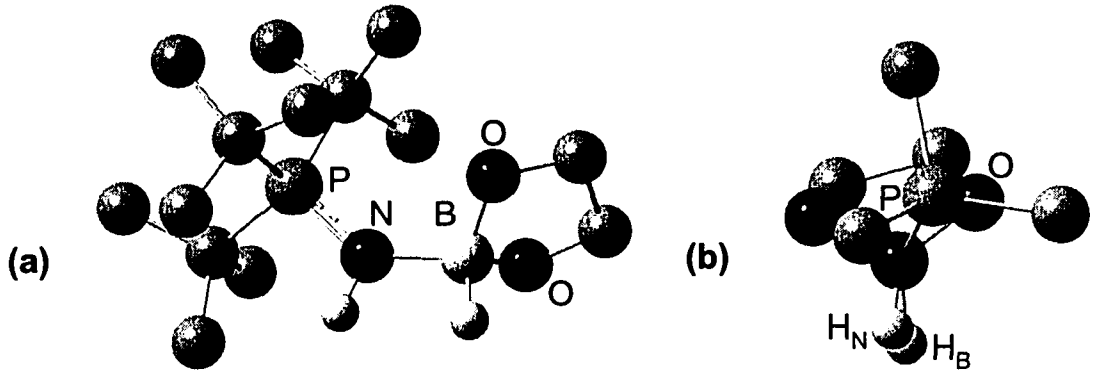

Figure 3.17: Illustrations of *t*-$Bu_3PNH{\cdot}HBO_2C_2H_4$ showing (a) the P···O interaction and (b) the eclipsed H_N and H_B atoms in a Newman projection looking down the N···B bond. The *t*-Bu groups have been omitted for clarity.

Formation of the adducts *t*-$Bu_3PNH{\cdot}HBO_2C_2H_4$, *t*-$Bu_3PNH{\cdot}HBpin$ and *t*-$Bu_3PNH{\cdot}HBO_2C_2(CF_3)_4$ was determined to be less energetically favourable than the formation of $H_3PNH{\cdot}HBO_2C_2H_4$, $H_3PNH{\cdot}HBpin$ and $H_3PNH{\cdot}HBO_2C_2(CF_3)_4$ with binding energies of -1.1, 4.1 and -18.4 kcal mol^{-1}, relative to the energies of the optimized geometries of the uncoordinated phosphinimines and boranes (See Appendix C). In contrast to what is observed in the reactions of $HNPH_3$ with the three different boranes, the lowest energy mechanism for the reactions of HNP*t*-Bu_3 with $HBO_2C_2H_4$, HBpin or $HBO_2C_2(CF_3)_4$ is *pathway 1*; abstraction of hydrogen gas and concomitant formation of the corresponding borylphosphinimine to form the product complex $R_2C_2O_2BNPt\text{-}Bu_3{\cdot}H_2$ (R = H, CH_3 and CF_3). The activation energy barriers for *pathway 1* were determined to be 32.9, 30.3 and 39.4 kcal mol^{-1}, respectively (Appendix C). These barriers are now 11.8, 11.8 and 13.2 kcal mol^{-1}, respectively, lower in energy than those for *pathway 2*; reduction of the phosphinimine. An example of the optimized geometries for the transition structures for *pathway 1* and *pathway 2* in depicted in Figure 3.18.

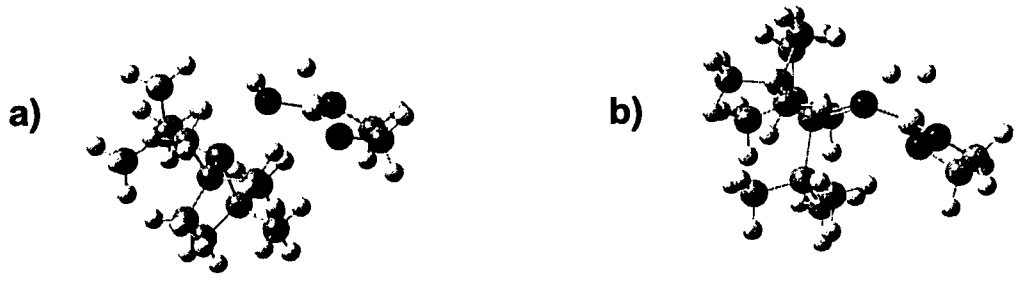

Figure 3.18: Optimized geometries of the transition structures for a) *pathway 1* and b) *pathway 2* for the reaction of HNP*t*-Bu_3 with $HBO_2C_2H_4$.

Figure 3.19 (a) and (b) illustrate the schematic PESs for the reaction of HNP*t*-Bu_3 with $HBO_2C_2H_4$ following *pathway 1* and *pathway 2*, respectively.

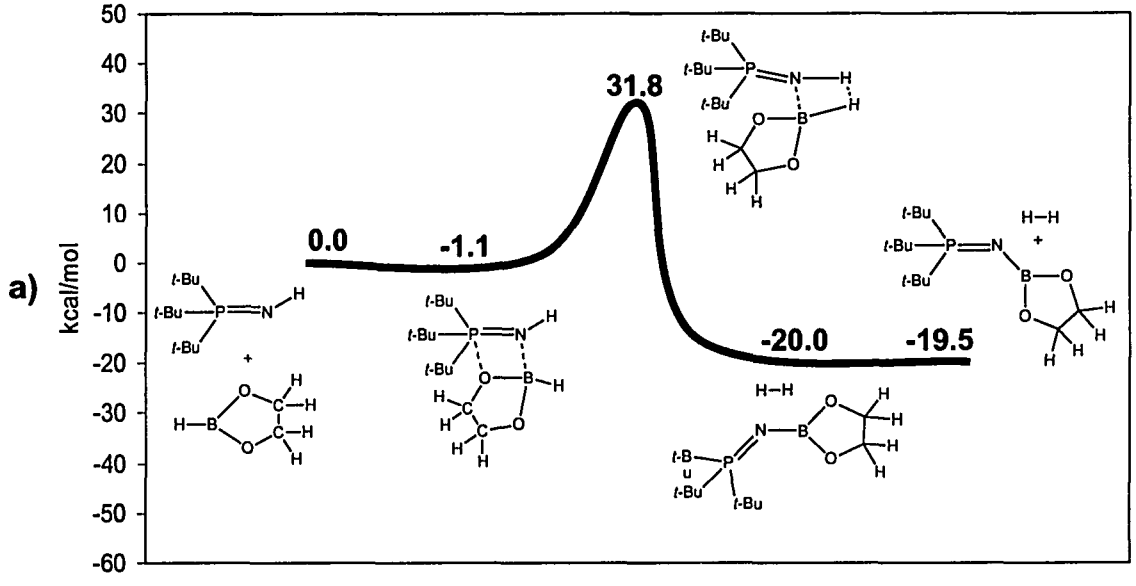

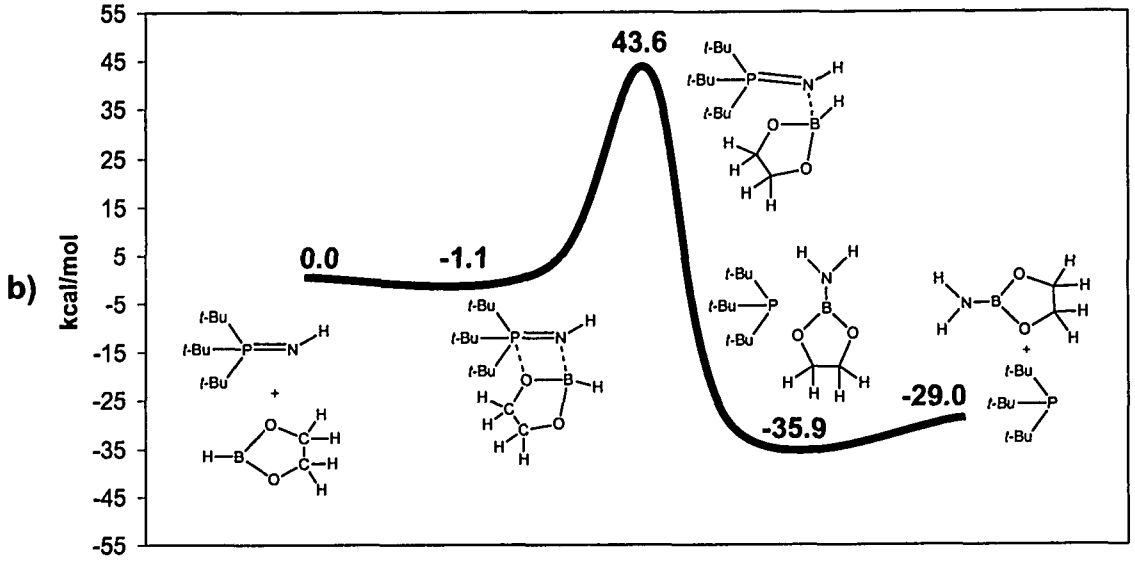

Figure 3.19: Schematic gas phase potential energy surface for the reaction of HNP*t*-Bu_3 with $HBO_2C_2H_4$ to yield (a) *t*-$Bu_3PNBpin$ and H_2 (*pathway 1*) and (b) H_2NBpin and P*t*-Bu_3 (*pathway 2*).

Thus, the present calculations indicate that both reaction pathways are thermodynamically feasible. Interestingly, however, the calculations further suggest that the steric bulk provided by the substituents on the phosphorus atom of the phosphinimine dictates which mechanistic reaction pathway will be energetically more favourable.

A comparison of the relative energy values for the reaction of each phosphinimine with the varying boranes allows a few basic conclusions to be drawn. For the reactions involving X_3PNH (X = H and *t*-Bu) and $HBO_2C_2R_4$ (R = H, CH_3 and CF_3) there are differences in the relative energies of the initial phosphinimine-borane adducts. When R = CH_3 the two molecules are not strongly associated with one another. However, reduction of the steric bulk about the boron center (R =H), or addition of electron-withdrawing groups to the borane backbone (R = CF_3) enables stronger interactions. Due to the increased stabilization of the initial complexes, increased activation barriers are now also observed. This in turn suggests that the reaction between the phosphinimines (X = H, *t*-Bu) and pinacolborane should have the lowest relative activation energy for both *pathway 1* and *pathway 2*, as observed. Lastly, in general, for the reaction of

phosphinimines with pinacolborane, when the substituents on phosphorus are small, *pathway 2* is energetically favourable. In contrast, when the substituents on phosphorus are large *pathway 1* is preferred. The functional group bound to the nitrogen of the phosphinimine also plays a role in whether zero, one, or two equivalents of pinacolborane will react.

As noted above, the second step in *pathway 2* is thought to involve the coordination of a second equivalent of HBpin to the borylamine, followed by loss of hydrogen gas and formation of the diborylamine. This corresponds well with the kinetic data which suggests that the reduction of the phosphorus atom is the rate-determining step and that this second step has a much lower energy barrier and therefore occurs rapidly.

3.3.5 Synthesis of *N*-alkyl and *N*-arylborylamine Complexes

In order to investigate whether *pathway 2* could be halted after the first step, *N*-aryl and *N*-alkyl phosphinimines (PhNP*n*-Bu$_3$ **3.2**, PhNPEt$_3$ **3.3**, and AdNPEt$_3$ **3.4**) were synthesized in high yields (70-96%) via the addition of one equivalent of the tertiary phosphine to one equivalent of phenylazide or adamantylazide. The phosphinimine products were treated with stoichiometric amounts of HBpin at room temperature in *n*-pentane. All of these reactions resulted in the formation of the tertiary phosphine and the corresponding *N*-borylarylamine or borylalkylamine complexes PhNH(Bpin) (**3.12**) or AdNH(Bpin) (**3.13**), depicted in Figure 3.20. Compounds **3.12** and **3.13** were characterized by ^{1}H, ^{13}C{^{1}H}, and ^{11}B{^{1}H} NMR spectroscopy and elemental analysis. The presence of the N-H bond was confirmed by IR spectroscopy.

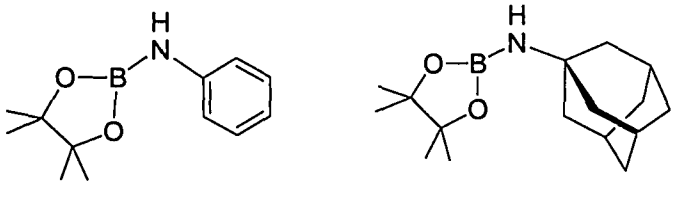

Figure 3.20: Schematic illustrations of PhNH(Bpin) (**3.12**) and AdNH(Bpin) (**3.13**).

X-ray quality crystals of **3.12** were grown from a concentrated *n*-pentane solution stored at -33°C and the X-ray data confirmed the formulation as the borylamine, PhNH(Bpin). The N-B bond distance in **3.12** was determined to be 1.38(1) Å. This bond distance is relatively short when compared to typical N-B bond distances observed in borylamines.[293-298] The B-N-C angle was determined to be 125.8(7)°, comparable with the corresponding angle of 128.7(1)° observed for the borylamine PhNH(B(N(Ph)CH_2)$_2$).[294] Compound **3.12** is portrayed in an ORTEP diagram in Figure 3.21.

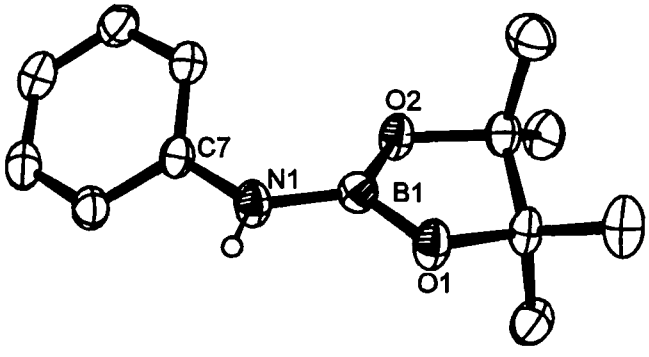

Figure 3.21: ORTEP diagram (30% probability thermal ellipsoids) of PhNH(Bpin) (**3.12**). All hydrogen atoms, except for that on nitrogen, have been omitted for clarity.

3.3.6 Reactions of Borylphosphinimines with Pinacolborane

Since the alkyl and aryl phosphinimines with less bulky substituents on the phosphorus atom also followed the first step in mechanism 2 in which reduction of the phosphorus atom and formation of the borylamine occurred, the reactions of borylphosphinimine complexes with pinacolborane were of interest.

What effect does the substituent bonded to the nitrogen atom of the phosphinimine have on the reactivity of these complexes with pinacolborane?

In order to investigate this further, the complexes HB(NP*t*-Bu$_3$)$_2$ (**3.14**) and ClB(Ph)(NP*n*-Bu$_3$) (**3.16**) were synthesized. Upon repeating the published method for the synthesis of HB(NP*t*-Bu$_3$)$_2$ (**3.14**), only partial conversion of HNP*t*-Bu$_3$ and

$BH_3 \cdot SMe_2$ was observed. Instead, a slightly modified procedure was used, and is included (*vide supra,* **Section 3.2.6**). Compound **3.16** reacted partially but did not reduce the phosphinimine fragment to free phosphine. In the $^{31}P\{^1H\}$ NMR spectrum obtained, several new peaks formed downfield from the starting material, indicating the formation of different phosphorus-containing compounds. Compound **3.14** did not react with pinacolborane (HBpin), as expected.

In order to see if the inert nature of the nitrogen atom in **3.14** was due to the steric encumbrance provided by the *t*-butyl groups, the synthesis of *N*-borylphosphinimine complexes with smaller alkyl groups on phosphorus was attempted. The analogous reaction of $BH_3 \cdot SMe_2$ with 2 equivalents of HNP*n*-Bu*t*-Bu_2, when performed under similar conditions as employed with HNP*t*-Bu_3, yielded the borane-phosphinimine coordination complex *t*-Bu_2*n*-BuPNH·BH_3 (**3.15**) as the major product, and not the *bis*-substituted borane. Instead, based on the $^{31}P\{^1H\}$ NMR data, the *bis*-substituted borane was thought to be produced as a minor product. This reaction could not be forced to completion using refluxing temperatures in toluene or xylene solvents for extended periods of time (> 4 days). X-ray quality crystals of compound **3.15** were grown from hexanes. An ORTEP drawing of compound **3.15** is depicted in Figure 3.22. The P-N-B angle was determined to be 130.6(3)°. The N-P and N-B distances were determined to be 1.592(3) Å and 1.580(5) Å, respectively. These are typical N-P and N-B distances for compounds in which phosphinimines are coordinated to boron.[149, 150, 160, 164]

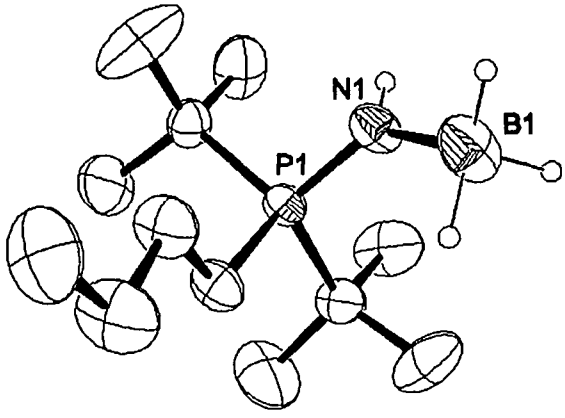

Figure 3.22: An ORTEP drawing (30% probability thermal ellipsoids) of HNP*t*-Bu$_2$*n*-Bu·BH$_3$ (**3.15**). All hydrogen atoms, except for those on nitrogen and boron, have been omitted for clarity.

Further attempts to synthesize *N*-borylphosphinimine complexes that incorporate smaller alkyl groups on phosphorus were unsuccessful. Additional attempts to observe similar reactivity of phosphinimines with a variety of Group 13 complexes including *bis*-*t*-butanolborane, *bis*-4-methyl-2,6-di*t*-butylphenolalane, 9-BBN and pyrazabole proved unsuccessful. This suggests that the clean reactions observed in the work described *vide supra* are specific for pinacolborane.

3.4 Summary

A variety of reactions of phosphinimines with specific boranes have been investigated. The *N*-borylphosphinimine complexes (compounds **3.8**, **3.10**, **3.9**, **3.15** and **3.15**) and borylamines (compounds **3.11**, **3.12**, and **3.13**) have been synthesized and characterized by multi-nuclear NMR spectroscopy and elemental analysis. It was observed that the reaction of phosphinimines with pinacolborane can proceed via two different mechanistic pathways. Mechanism 1 involves the formation of the corresponding *N*-borylphosphinimine complex and the evolution of hydrogen gas. In contrast, mechanism 2 involves the reduction of the phosphorus atom of the

phosphinimine to the corresponding tertiary phosphine with the concomitant formation of pinacolborylamine. The preferred reaction pathway appears to be directly related to the steric bulk of the substituents on the phosphorus atom of the phosphinimine. Bulky phosphinimines, such as HNP*t*-Bu_3 and HNP*t*-Bu_2*n*-Bu, preferentially follow mechanism 1 whereas the smaller phosphinimines, such as $HNPEt_3$ and HNP*n*-Bu_3, prefer mechanism 2. When an intermediate phosphinimine such as HNP*i*-Pr_3 is employed, the products of both mechanistic pathways are observed.

A kinetic study of mechanism 2 was performed using $^{31}P\{^1H\}$ NMR spectroscopy. This study revealed that the rate determining step involves the reduction of the phosphorus atom and formation of tertiary phosphine and pinacolborylamine. This step is presumably followed by the fast reaction of pinacolborane with pinacolborylamine to yield the diboron complex $O(Bpin)_2$. The rate law for the reaction of pinacolborane with *N*-trimethylsilyl-tri-*i*-propylphosphinimine was determined to be: rate = $(1.3(7)x10^{-4})$[HBpin][$Me_3SiNPEt_3$].

A density functional theory study of both reaction pathways was also performed. The optimized geometries of the phosphinimine-borane adducts revealed the formation of an OBNP pseudo-four membered ring for adducts involving the smaller phosphinimines were involved. This interaction forces a large HNBH dihedral angle, orientating the hydrogen atoms on the nitrogen and boron into a staggered conformation. This orientation may suggest why mechanism 2 is preferred over mechanism 1 for the phosphinimine with smaller alkyl groups on the phosphorus atom. The relative energies of the optimized structures for the reaction of HNP*t*-Bu_3 with $HBO_2C_2(R)_4$ (R = H, CH_3, CF_3) indicate that mechanism 1 has lower activation energies than mechanism 2 by 11.8, 11.8 and 13.2 kcal mol^{-1}, respectively. The opposite is observed for the reaction of $HNPH_3$ with $HBO_2C_2R_4$ (R = H, CH_3 and CF_3), but to a lesser degree. The calculations also suggest that the reactions of phosphinimines with HBpin have lower activation barriers than reactions using $HBO_2C_2R_4$ (R = H, CF_3). This may be attributed to the electron-donating methyl groups on the pinacolate moiety which decreases the electropositive nature of the boron centre.

Therefore, depending on the steric bulk of the substituents on the phosphorus of the phosphinimine, the reaction with pinacolborane can proceed through a basic hydrogen

metathesis reaction and/or the reduction of the phosphorus centre and formation of the borylamine.

4 Reactions of Catecholborane with Phosphinimine Derivatives

4.1 Introduction

To the best of our knowledge there are no aryloxyborylphosphinimine complexes of the general formula $(ArO)_2BNPR_3$ (Ar = aryl groups) published in the literature. Related molecules which have a boron atom that is covalently bound to both a phosphinimide ligand and an oxygen atom are depicted in Figure 4.1.[157, 158, 160]

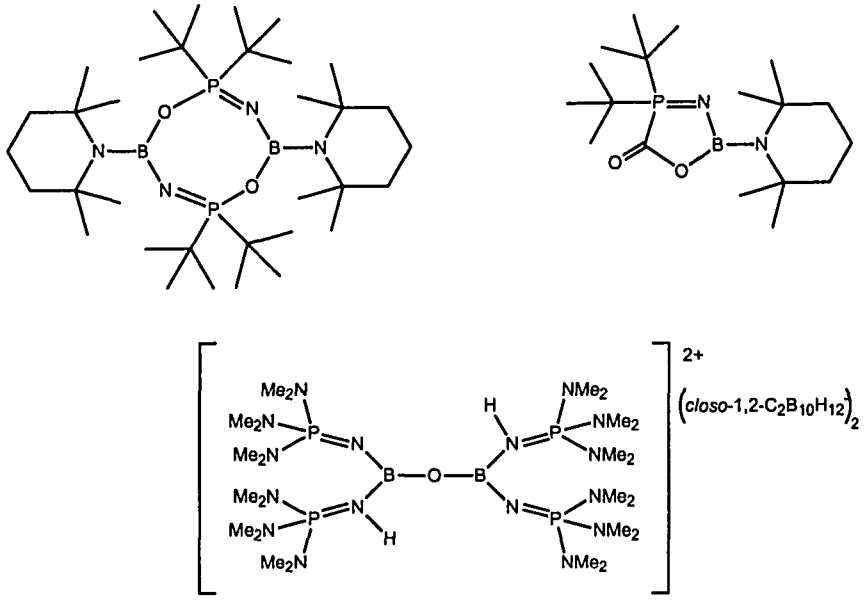

Figure 4.1: Molecules containing an OBNP linkage.[157, 158, 160]

Given the scarcity of this family of compounds, the synthesis of aryloxyborylphosphinimide complexes was proposed. Due to the commercial availability and the extensive use in hydroboration,[299-307] catecholborane ($HBO_2C_6H_4$ or HBcat) and chlorocatecholborane ($ClBO_2C_6H_4$ or ClBcat) were utilized as precursors in the following work. Reactivity of phosphinimide complexes is known to depend on both the steric bulk of the alkyl or aryl groups on the phosphorus atom and the basicity of the nitrogen atom.

Herein, the synthesis of a new class of aryloxyborylphosphinimide complexes and some initial reactivity studies are discussed.

4.2 Experimental

4.2.1 General Considerations

All preparations were performed under an atmosphere of dry O_2-free N_2 either employing Schlenk-line techniques or working in a Vacuum Atmospheres Glovebox. ^1H, $^{13}C\{^1H\}$, $^{31}P\{^1H\}$, $^{11}B\{^1H\}$ and ^{19}F NMR spectra were recorded on a Bruker Avance 300 or 500 spectrometer. For broad peaks the line widths at half height ($\Delta\nu_{1/2}$) are given in Hertz. For ^1H and $^{13}C\{^1H\}$ NMR spectra, trace amounts of protonated solvents were used as internal references, and the chemical shifts are reported in parts per million relative to tetramethylsilane. $^{31}P\{^1H\}$ NMR spectra are referenced to an external standard consisting of an 85% aqueous solution of H_3PO_4. $^{11}B\{^1H\}$ NMR spectra are referenced to $BF_3{\cdot}Et_2O$ or a saturated $NaBH_4$ solution where indicated and ^{19}F NMR spectra are referenced to CCl_3F. All coupling constants are reported as absolute values. Combustion analyses were performed at the University of Windsor Chemical Laboratories employing a Perkin Elmer CHN Series 2400 Analyzer.

4.2.2 Solvents

Anhydrous toluene, hexanes, *n*-pentane, and dichloromethane were purchased from Aldrich Chemical Company and were purified employing Grubbs-type column systems manufactured by Innovative Technologies or in-house by the University of Windsor Physics Machine Shop. Subsequently, the solvents were refluxed and distilled from the appropriate drying agents[272] under a nitrogen atmosphere. Deuterated benzene and deuterated toluene were purchased from Cambridge Isotopes Laboratories and stirred over sodium and benzophenone for 16 h, deoxygenated by three freeze/pump/thaw degas cycles, and collected by vacuum distillation.

4.2.3 Materials

Hyflo Super Cel®, which will be referred to as Celite throughout the text, was purchased from Aldrich Chemical Company and dried in a vacuum oven for 16 h before storing in the glove box. 4 Å molecular sieves were purchased from Aldrich Chemical Company and dried at 100°C under vacuum.

4.2.4 Reagents

Catecholborane, chlorocatecholborane, and azidotrimethylsilane were used as received from Aldrich Chemical Company. Tri-*i*-propylphosphine, tri-*n*-butylphosphine, triethylphosphine, and tri-*t*-butylphosphine were used as received from Strem Chemicals. N-trimethylsilyl-tri-*t*-butylphosphinimine in a 50 wt% solution in toluene, N-trimethylsilyl-di-*t*-butyl-*n*-butylphosphinimine, and *tris*pentafluorophenylborane were generously donated by Nova Chemicals Corporation. *N*-trimethylsilyl-triphenylphosphinimine, *N*-trimethylsilyl-tri-*i*-propylphosphinimine and *N*-H-tri-*t*-butylphosphinimine were prepared via literature methods.[3, 4] *N*-trimethylsilyl-triethylphosphinimine, *N*-trimethylsilyl-tri-*n*-butylphosphinimine were prepared via a modified version of literature methods[2, 3, 274] that are outlined in Chapter 3.

4.2.5 Syntheses of *N*-Catecholborylphosphinimine Complexes

$(Et_3P\mu\text{-}NBcat)_2$ (4.1): A solution of ClBcat (0.270 g, 1.75 mmol) in 20 mL of toluene was added to a solution of $Me_3SiNPEt_3$ (0.360 g, 1.75 mmol) in 2 mL of toluene and was stirred for 1 h at room temperature. Toluene and $SiMe_3Cl$ were removed *in vacuo*. The product was washed with *n*-pentane (3 x 2 mL) and dried *in vacuo*. A white solid was isolated in 82% yield. ^1H NMR (500 MHz, C_6D_6) δ: 7.10 (m, 4H, $BO_2C_6\mathbf{H}_4$ (*o*-H)), 6.89 (m, 4H, $BO_2C_6\mathbf{H}_4$ (*m*-H)), 1.22 (dq, 12H, $P(C\mathbf{H}_2CH_3)_3$, $^2J_{P\text{-}H}$ = 12 Hz, $^3J_{H\text{-}H}$ = 8 Hz), 0.73 (dt, 18H, $P(CH_2C\mathbf{H}_3)_3$, $^3J_{P\text{-}H}$ = 17 Hz, $^3J_{H\text{-}H}$ = 8 Hz); $^{31}P\{^1H\}$ NMR (202.5 MHz, C_6D_6) δ: 40.7; $^{13}C\{^1H\}$ NMR

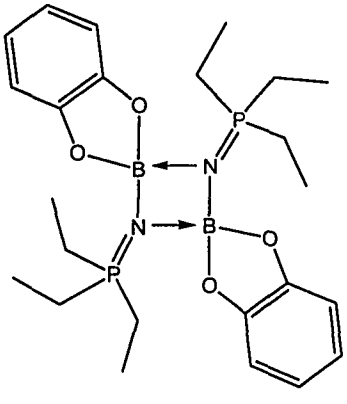

(125.8 MHz, C_6D_6) δ: 153.4 (s, $BO_2C_6H_4$ (*ipso*-C)), 119.0 (s, $BO_2C_6H_4$ (*o*-C)), 109.2 (s, $BO_2C_6H_4$ (*m*-C)), 16.9 (s, $P(CH_2CH_3)_3$) 5.7 (s, $P(CH_2CH_3)_3$); $^{11}B\{^1H\}$ NMR (160.5 MHz, C_6D_6) δ: 8.1. Calculated: H: 7.63%, C: 57.41%, N: 5.58%; Found: H: 7.67%, C: 57.59%, N: 5.55%.

(*n*-Bu_3Pμ-NBcat)$_2$ (4.2): A solution of ClBcat (0.533 g, 3.454 mmol) in 5 mL of toluene was added to a solution of Me_3SiNPn-Bu_3 (1.0 g, 3.454 mmol) in 15 mL of toluene and was stirred for 12 h at room temperature. Toluene and $SiMe_3Cl$ were removed *in vacuo*. The product was dissolved in hexanes, filtered through Celite, dried *in vacuo* and isolated in 97% yield. ^1H NMR (300 MHz, C_6D_6) δ: 7.02 (m, 4H, $BO_2C_6H_4$ (*o*-H)), 6.84 (m, 4H, $BO_2C_6H_4$ (*m*-H)), 1.36 (m, 24H, $P(CH_2CH_2CH_2CH_3)_3$), 1.07 (m, 12H, $P(CH_2CH_2CH_2CH_3)_3$), 0.76 (t, 18H, $P(CH_2CH_2CH_2CH_3)_3$, $^3J_{H\text{-}H}$ = 7.2 Hz); $^{31}P\{^1H\}$ NMR (121.5 MHz, C_6D_6) δ: 35.9; $^{13}C\{^1H\}$ NMR (75.5 MHz, C_6D_6) δ: 153.4 (s, $BO_2C_6H_4$ (*ipso*-C)), 118.9 (s, $BO_2C_6H_4$ (*o*-C)), 109.2 (s, $BO_2C_6H_4$ (*m*-C)), 25.7 (s, $P(CH_2CH_2CH_2CH_3)_3$), 24.8 (s, $P(CH_2CH_2CH_2CH_3)_3$), 24.0 (s, $P(CH_2CH_2CH_2CH_3)_3$), 14.0 (s, $P(CH_2CH_2CH_2CH_3)_3$); $^{11}B\{^1H\}$ NMR (96.3 MHz, C_6D_6) δ: 8.1. Calculated: H: 9.32%, C: 64.49%, N: 4.18%; Found: H: 9.77%, C: 64.25%, N: 4.09%.

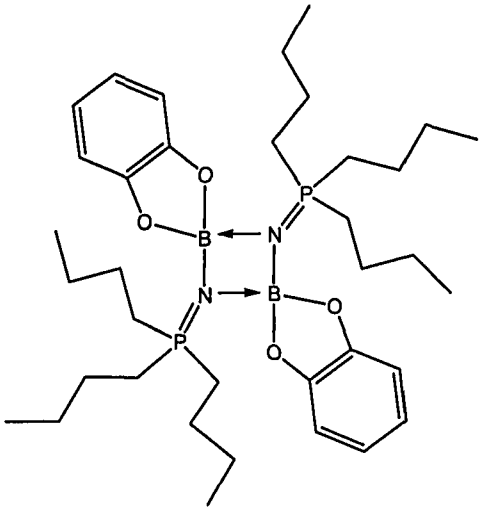

($Ph_3P\mu$-NBcat)$_2$ (4.3): A solution of $Me_3SiNPPh_3$ (0.500 g, 1.43 mmol) in 5 mL of toluene was added to a solution of ClBcat (0.22 g, 1.43 mmol) in 10 mL of toluene. The flask was evacuated and the solution was stirred for 16 h under a static vacuum environment resulting in a cloudy mixture. Subsequent removal of the solvent and $SiMe_3Cl$ resulted in the isolation of a white powder. The powder was dissolved in 5 mL of dichloromethane from which X-ray quality crystals were grown (0.388 g, 69%). ^{1}H NMR (500 MHz, $C_6D_5CD_3$) δ: 7.70 (dd, 12H, $PC_6\mathbf{H}_5$, $^3J_{P\text{-}H}$ =13 Hz, $^3J_{H\text{-}H}$ = 8 Hz), 6.99 (m, 22H, $PC_6\mathbf{H}_5$, $BO_2C_6\mathbf{H}_4$), 6.75 (m, 4H, $BO_2C_6\mathbf{H}_4$); $^{31}P\{^1H\}$ NMR (202.5 MHz, $C_6D_5CD_3$) δ: 34.1; $^{13}C\{^1H\}$ NMR (125.8 MHz, $C_6D_5CD_3$) δ: 132.8 ($P\mathbf{C}_6H_5$), 131.8 ($P\mathbf{C}_6H_5$), 128.8 ($P\mathbf{C}_6H_5$), 121.3 ($BO_2\mathbf{C}_6H_4$), 111.5 ($BO_2\mathbf{C}_6H_4$); $^{11}B\{^1H\}$ NMR (160.5 MHz, $C_6D_5CD_3$) δ: 8.4; Calculated: H: 4.85%, C: 72.94%, N: 3.54%; Found: H: 5.07%, C: 72.61 %, N: 3.58%.

(i-$Pr_3P\mu$-NBcat)$_2$ (4.4): A solution of Me_3SiNP*i*-Pr_3 (0.100 g, 0.40 mmol) in 5 mL of toluene was added to a solution of ClBcat (0.062 g, 0.40 mmol) in 10 mL of toluene. The flask was evacuated and the solution was stirred for 16 h under a static vacuum environment. Subsequent removal of the solvent and $ClSiMe_3$ resulted in the isolation of a white powder. The powder was dissolved in a toluene/*n*-pentane solution from which X-ray quality crystals were grown (0.098 g, 83%). ^{1}H NMR (500 MHz, $C_6D_5CD_3$) δ: 6.95 (m, 4H, $BO_2C_6\mathbf{H}_4$ (*o*-H)), 6.76 (m, 4H, $BO_2C_6\mathbf{H}_4$ (*m*-H)), 1.82 (dseptet, 6H, $PC\mathbf{H}(CH_3)_2$, $^2J_{P\text{-}H}$ = 12 Hz, $^3J_{H\text{-}H}$ = 7 Hz), 0.96 (dd, 36H, $PCH(C\mathbf{H}_3)_2$, $^3J_{P\text{-}H}$ = 15 Hz, $^3J_{H\text{-}H}$ = 7 Hz); $^{31}P\{^1H\}$ NMR (202.5 MHz, $C_6D_5CD_3$) δ: 49.2; $^{13}C\{^1H\}$ NMR (125.8 MHz, $C_6D_5CD_3$) δ: 153.0 ($BO_2\mathbf{C}_6H_4$ (*o*-C)), 121.6 ($BO_2\mathbf{C}_6H_4$ (*o*-C)), 109.1 ($BO_2\mathbf{C}_6H_4$ (*m*-C)), 25.2 (d, $PCH(CH_3)_2$), 17.2 ($PCH(CH_3)_2$); $^{11}B\{^1H\}$ NMR (160.5 MHz, $C_6D_5CD_3$) δ: 7.8. Calculated: H: 8.60%, C: 61.46%, N: 4.78%; Found: H: 8.48%, C: 61.23%, N: 4.65%.

***n*-Bu(*t*-Bu)$_2$PNBcat (4.5):** Solid ClBcat (0.138 g, 0.864 mmol) was added to a solution of Me_3SiNPn-Bu(*t*-Bu)$_2$ (0.250 g, 0.864 mmol) in 10 mL of toluene. The solution was stirred for 16 h, then the toluene and $SiMe_3Cl$ were removed *in vacuo*. The resulting product was washed with 3 mL of *n*-pentane, redissolved in toluene and filtered through Celite. The supernatant was stored at -30°C from which X-ray quality crystals of (*n*-Bu(*t*-Bu)$_2$PNBcat)$_2$ were collected in 60% yield. ^{1}H NMR (500 MHz, C_6D_6) δ: 7.09 (m, 2H, $BO_2C_6\mathbf{H}_4$ (*o*-H)), 6.80 (m, 2H, $BO_2C_6\mathbf{H}_4$ (*m*-H)), 1.67 (m, 2H, $PC\mathbf{H}_2CH_2CH_2CH_3$), 1.49 (m, 2H, $PCH_2C\mathbf{H}_2CH_2CH_3$), 1.26 (m, 2H, $PCH_2CH_2C\mathbf{H}_2CH_3$), 1.03 (d, 18H, $PC(C\mathbf{H}_3)_3$, $^3J_{P\text{-}H}$ = 14 Hz), 0.83 (t, 3H, $P(CH_2CH_2CH_2C\mathbf{H}_3)$, $^3J_{H\text{-}H}$ = 7 Hz); $^{31}P\{^1H\}$ NMR (202.5 MHz, C_6D_6) δ: 38.8; $^{13}C\{^1H\}$ NMR (75.5 MHz, C_6D_6) δ: 151.1 (s, $BO_2\mathbf{C}_6H_4$ (*ipso*-C)), 121.4 (s, $BO_2\mathbf{C}_6H_4$ (*o*-C)), 111.49 (s, $BO_2\mathbf{C}_6H_4$ (*m*-C)), 36.6 (d, $P\mathbf{C}(CH_3)_3$, $^1J_{P\text{-}C}$ = 62 Hz), 27.4 (s, $PC(\mathbf{C}H_3)_3$, 26.5 (d, $PCH_2CH_2CH_2CH_3$, $^3J_{P\text{-}C}$ = 1 Hz), 25.4 (d, $PCH_2CH_2CH_2CH_3$, $^3J_{P\text{-}C}$ = 13 Hz), 22.18 (d, $PCH_2CH_2CH_2CH_3$, $^3J_{P\text{-}C}$ = 57 Hz), 14.7 (s, $PCH_2CH_2CH_2\mathbf{C}H_3$); $^{11}B\{^1H\}$ NMR (160.5 MHz, C_6D_6) δ: 24.4. Calculated: H: 9.32%; C: 64.49%; N: 4.18%; Found: 9.29%, C: 64.71%, N: 4.18%.

***t*-Bu$_3$PNBcat (4.6):** *1*: A solution of ClBcat (0.224 g, 1.45 mmol) in 5 mL of toluene was added to a solution of Me_3SiNPt-Bu$_3$ (0.421 g, 1.454 mmol) in 15 mL of toluene and this solution was stirred for 12 h at room temperature. Toluene and $SiMe_3Cl$ were removed *in vacuo*. The product was dissolved in hexanes, filtered through Celite, dried *in vacuo* and isolated in 73% yield. X-ray quality crystals were obtained from a concentrated toluene solution at -33°C.

2: HBcat (0.049 mL, 0.46 mmol) was added to $HNPt$-Bu$_3$ (0.100 g, 0.46 mmol) in 1 mL of toluene. Gas evolution was observed. The solution was stirred for 16 h, then the solvent was removed *in vacuo*. The resulting white solid was washed with *n*-pentane (3 x 2 mL), dried *in vacuo*, and isolated in 94% yield. ^{1}H NMR (500 MHz, toluene-d_8) δ: 7.09 (m, 2H, $BO_2C_6\mathbf{H}_4$ (*o*-H)), 6.81 (m, 2H, $BO_2C_6\mathbf{H}_4$

(*m*-H)), 1.19 (d, 27H, PC(CH_3)$_3$, $^3J_{P-H}$ = 13 Hz); $^{31}P\{^1H\}$ NMR (202.5 MHz, toluene-d_8) δ: 42.7; $^{13}C\{^1H\}$ NMR (125.8 MHz, toluene-d_8) δ: 151.2 (s, $BO_2C_6H_4$ (*ipso*-C)), 121.2 (s, $BO_2C_6H_4$), 111.4 (s, C_6H_4), 40.4 (d, PC(CH_3)$_3$, $^1J_{P-C}$ = 53 Hz), 29.7 (s, PC(CH_3)$_3$); $^{11}B\{^1H\}$ NMR (125.76 MHz, toluene-d_8) δ: 24.2; Calculated: H: 9.32%, C: 64.49%, N: 4.18%; Found: H: 9.44%, C: 64.10%, N: 4.29 %.

$Et_3PNBcat{\cdot}B(C_6F_5)_3$ (4.7): ($Et_3PNBcat)_2$ (**4.1**) (0.034 g, 0.135 mmol) was dissolved in 3 mL of toluene. To this solution was added solid $B(C_6F_5)_3$ (0.069 g, 0.135 mmol). The resulting solution was stirred at ambient temperature for 10 min. The solvent was removed *in vacuo* and the resulting white solid was isolated in 82% yield. ^1H NMR (500 MHz, C_6D_6) δ: 6.78 (m, 2H, C_6H_4 (*o*-H)), 6.64 (m, 2H, C_6H_4 (*m*-H)), 1.65 (dq, 6H, P(CH_2CH_3)$_3$, $^2J_{P-H}$ = 13 Hz, $^3J_{H-H}$ = 8 Hz), 0.38 (dt, 9H, P(CH_2CH_3)$_3$, $^3J_{P-H}$ = 19 Hz, $^3J_{H-H}$ = 8 Hz); $^{31}P\{^1H\}$ NMR (202.5 MHz, C_6D_6) δ: 68.0; $^{13}C\{^1H\}$ NMR (125.8 MHz, $C_6D_5CD_3$) δ: 147.0 (s, BC_6F_5), 140.0 (s, $BO_2C_6H_4$ (*ipso*-C)), 139.1 (s, BC_6F_5), 135.3 (s, BC_6F_5), 122.7 (s, $BO_2C_6H_4$ (*o*-C)), 111.7 (s, $BO_2C_6H_4$ (*m*-C)), 17.6 (d, PCH_2CH_3 , $^1J_{P-C}$ = 60 Hz), 5.9 (s, PCH_2CH_3); $^{11}B\{^1H\}$ NMR (160.5 MHz, C_6D_6) δ: 28.0 (**B**$O_2C_6H_4$), -6.4 (**B**(C_6F_5)), ^{19}F NMR (282.4 MHz, $C_6D_5CD_3$): -162.4, -156.4, -131.8.

4.2.6 Procedure for Attempted Polymerizations of Methylmethacrylate (MMA)

A sample procedure for the polymerization of MMA is indicated below:

5 mL of a 10 mmol/L solution of *t*-Bu_3PNBcat (**4.6**) in toluene was placed in a 100 mL Schlenk flask equipped with a septum. 50 equivalents (0.54 mL) of MMA were added to the flask via a syringe. The resulting solutions were stirred for one hour. The reaction solution was quenched with 60 mL of ACS grade methanol. No precipitate formed in the reaction, and therefore no polymer was produced.

These reactions were carried out at room temperature and at -78°C and performed in conjunction with a blank run in which MMA was added to toluene and quenched with methanol to rule out the possibility of MMA polymerizing under the conditions attempted in the absence of a catalyst.

4.2.7 Experimental for X-ray Crystallographic Data

4.2.7.1 X-ray Data Collection and Reduction

Refer to Section 2.2.7.1.

4.2.7.2 Structure Solutions and Refinements

Refer to Section 2.2.7.2.

X-ray structural solutions of $(Et_3P\mu\text{-}NBcat)_2$ **(4.1)**, $(n\text{-}Bu_3P\mu\text{-}NBcat)_2$ **(4.2)**, $(Ph_3P\mu\text{-}NBcat)_2$ **(4.3)**, $(i\text{-}Pr_3P\mu\text{-}NBcat)_2$ **(4.4)**, $(n\text{-}Bu(t\text{-}Bu)_2P\mu\text{-}NBcat)_2$ **(4.5)** and *t*-$Bu_3PNBcat$ **(4.6)** were performed as described in Section 2.2.7.2. Cell parameters, R, R_w and GoF values are located in Tables 4.1 and 4.2, while detailed structural parameters have been included as an appendix on CD (Appendix A). No residual electron density remained in any of the solutions that were of any chemical significance. ORTEP drawings of **4.1**, **4.2**, **4.3**, **4.4**, **4.5** and **4.6** are depicted in Figure 4.4. Selected bond distances and bond angles are provided in the text.

Table 4.1: X-ray crystallographic data obtained from crystals of $(Et_3P\mu\text{-}NBcat)_2$ **(4.1)**, $(n\text{-}Bu_3P\mu\text{-}NBcat)_2$ **(4.2)** and $(Ph_3P\mu\text{-}NBcat)_2$ **(4.3)**.

Crystal	4.1	4.2	4.3
Molecular Formula	$H_{38}C_{24}B_2N_2O_4P_2$	$H_{62}C_{36}B_2N_2O_4P_2$	$H_{38}C_{48}B_2N_2O_4P_2 \cdot CH_2Cl_2$
Formula Weight	502.14	770.46	988.32
a (Å)	10.189(2)	10.007(5)	13.7714(6)
b (Å)	11.550(3)	10.283(5)	9.5732(5)
c (Å)	11.881(3)	10.035(5)	17.6408(9)
α°	90	65.115(8)	90
β°	102.538(5)	84.46(1)	96.568(1)
γ°	90	61.646(7)	90
Crystal System	Monoclinic	Triclinic	Monoclinic
Space Group	$P2_1/c$	P-1	$P2_1/n$
Volume ($Å^3$)	1364.9(5)	980.3(8)	2310.4(2)
D_{calc} (gcm^{-3})	1.217	1.136	1.380
Z	4	2	6
Abs coeff, μ, mm^{-1}	0.191	0.148	0.374
θ range (°)	2.05 – 23.32	2.39 – 23.37	1.78 – 23.28
Reflections Collected	6502	4227	11201
Data $F_o^2 > 3\sigma(F_o^2)$	1962	2810	3335
Parameters	154	208	289
R[a]	0.0727	0.0477	0.0618
R_w[b]	0.01202	0.0662	0.0943
Goodness of Fit	1.052	1.000	1.038

This data was collected at 20°C with Mo Kα radiation (λ = 0.71069 Å).

[a] $R=\Sigma(F_o-F_c)/\Sigma F_o$

[b] $R_w=(\Sigma[w(F_o^2-F_c^2)^2] /\Sigma[w(F_o)^2])^{½}$

Table 4.2: X-ray crystallographic data obtained from crystals (*i*-$Pr_3P\mu$-NBcat)$_2$ **(4.4)**, (*n*-Bu(*t*-Bu)$_2P\mu$-NBcat)$_2$ **(4.5)** and *t*-Bu_3PNBcat **(4.6)**.

Crystal	4.4	4.5	4.6
Molecular Formula	$H_{50}C_{30}B_2N_2O_4P_2$	$H_{62}C_{36}B_2N_2O_4P_2$	$H_{62}C_{36}B_2N_2O_4P_2$
Formula Weight	586.28	770.46	770.46
a (Å)	12.298(2)	8.593(2)	14.167(7)
b (Å)	9.093(1)	16.421(3)	10.073(5)
c (Å)	15.410(2)	13.797(3)	15.201(8)
α°	90	90	90
β°	101.719(3)	103.341(5)	113.254(9)
γ°	90	90	90
Crystal System	Monoclinic	Monoclinic	Monoclinic
Space Group	$P2_1/n$	$P2_1/n$	$P2_1/n$
Volume (Å^3)	1687.1(3)	1894.3(6)	1993(2)
D_{calc} (gcm^{-3})	1.154	1.175	1.117
Z	4	4	4
Abs coeff, μ, mm^{-1}	0.163	0.154	0.146
θ range (°)	1.94 – 23.29	1.96 – 23.26	1.67 – 23.24
Reflections Collected	8148	9150	8264
Data $F_o^2 > 3\sigma(F_o^2)$	2423	2722	2830
Parameters	181	208	208
R[a]	0.0559	0.0832	0.0366
R_w[b]	0.1123	0.1601	0.0534
Goodness of Fit	1.019	1.024	1.011

This data was collected at 20°C with Mo Kα radiation (λ = 0.71069 Å).

[a] $R=\Sigma(F_o-F_c)/\Sigma F_o$

[b] $R_w=(\Sigma[w(F_o^2-F_c^2)^2]/\Sigma[w(F_o)^2])^{1/2}$

4.3 Results and Discussion

4.3.1 Synthesis and Characterization of *N*-Catecholborylphosphinimine Complexes

The *N*-catecholborylphosphinimine complexes of the general formula $(R_3PNBcat)_x$ (R = Et, Ph, *n*-Bu, *i*-Pr, x = 2; R_3 = *n*-Bu(*t*-Bu)$_2$, x = 1 (solution) or 2 (solid state); R = *t*-Bu, x = 1; cat = $O_2C_6H_4$) were synthesized via a simple metathetical route in which the corresponding *N*-trimethylsilylphosphinimine and chlorocatecholborane were combined in toluene at room temperature and stirred for varying amounts of time (Figure 4.2).

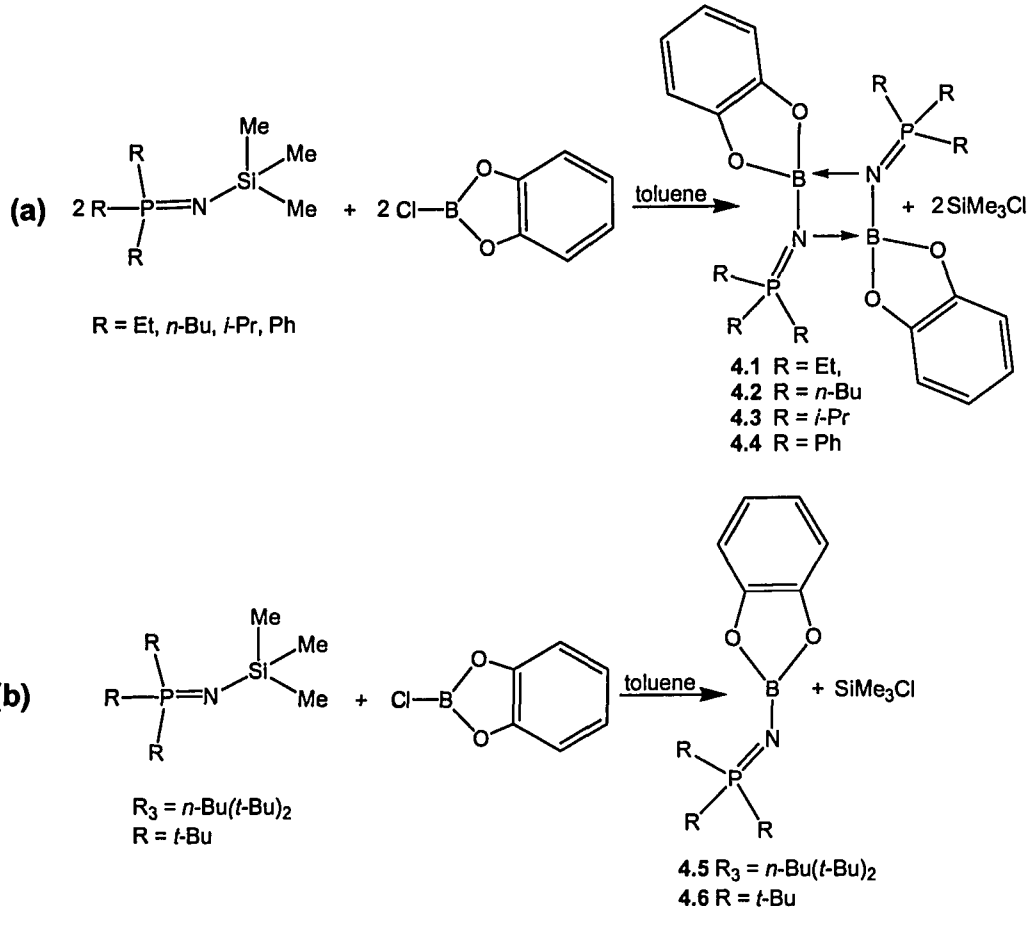

Figure 4.2: Synthesis of *N*-catecholborylphosphinimine complexes containing alkyl or aryl groups (compounds **4.1-4.6**). These complexes are depicted as they occur in solution.

All of the above *N*-catecholborylphosphinimine derivatives have been characterized by ^{1}H, $^{31}P\{^{1}H\}$, $^{13}C\{^{1}H\}$ and $^{11}B\{^{1}H\}$ NMR spectroscopy, elemental analysis and X-ray crystallography. In the solid state, complexes **4.1**, **4.2**, **4.3**, **4.4** and **4.5** were determined to be dimeric. The bridge is composed of a four-atom core with coordination of the nitrogen atoms to the boron atom of the adjacent unit, yielding a tetrahedral geometry about boron and a trigonal planar geometry about nitrogen. Figure 4.3 depicts the four-atom B_2N_2 core.

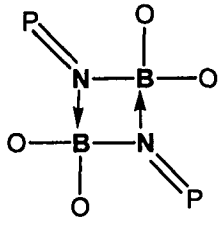

Figure 4.3: Depiction of the four-atom core in the dimeric structures of compounds **4.1**, **4.2**, **4.3**, **4.4** and **4.5**.

The ORTEP drawings of the crystal structures of complexes **4.1** through **4.5** are depicted in Figure 4.4.

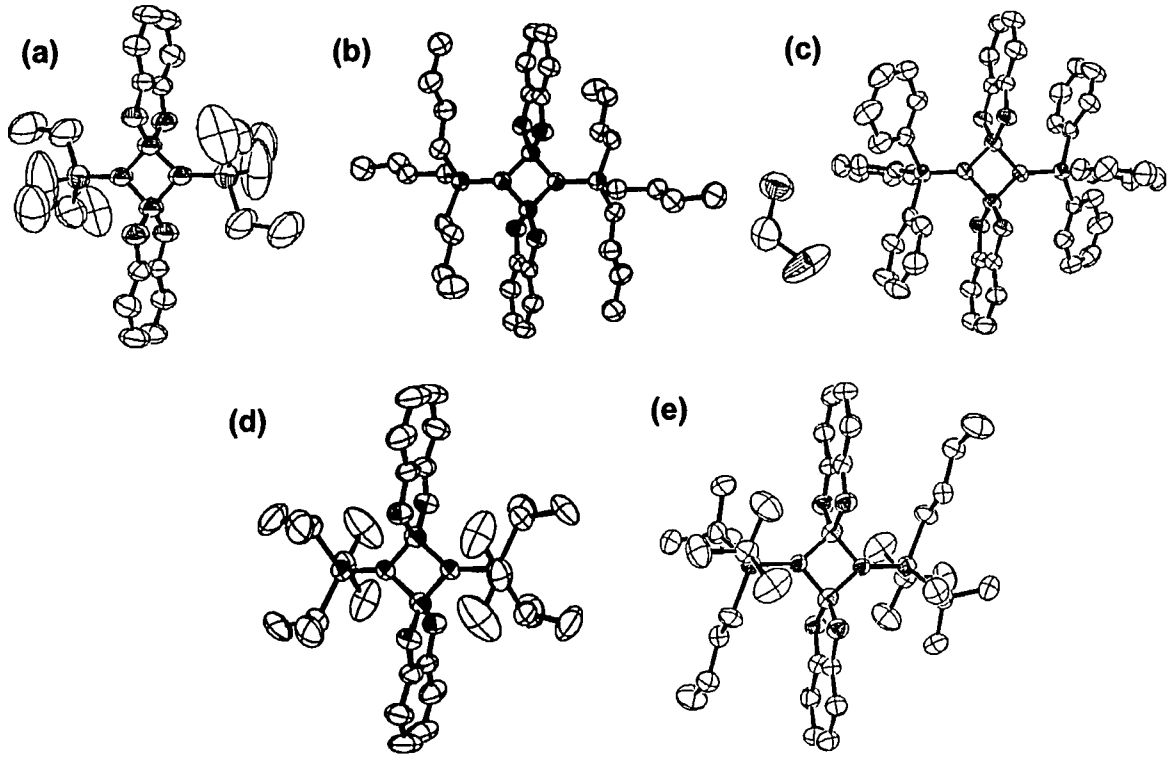

Figure 4.4: ORTEP diagrams (50% probability thermal ellipsoids) of complexes (a) **4.1**, (b) **4.2**, (c) **4.3**, (d) **4.4** and (e) **4.5.** Hydrogen atoms have been omitted for clarity.

The N(1)-P(1) bond distances, N(1)-B(1) bond distances, P(1)-N(1)-B(1) angles and B(1)-N(1)-B(1A) angles for these complexes are given in Table 4.3. The N(1)-B(1) bond distances of these complexes (average N(1)-B(1) distance = 1.548(6) Å) are slightly longer than those observed for the *N*-borylphosphinimine halide complexes $(Me_3P\mu\text{-}NBBr_2)_2$ (1.504(7) Å), $(Ph_3P\mu\text{-}NBCl_2)_2$ (1.527(5) Å) and $(Et_3P\mu\text{-}NBCl_2)_2$ (1.510(5) Å) which also contain a similar four-atom core.[153, 164] These longer bond lengths are attributed to the presence of the catechol group which decreases the electropositive nature of the boron center. With the exception of the ethyl derivative (**4.1**), the P(1)-N(1)-B(1) angles increase as the steric bulk of phosphine increases. The B(1)-N(1)-B(1A)-N(1A) core is planar for compounds **4.1** – **4.5**. The two oxygen atoms and two *ipso*-carbon atoms of the catechol group are planar and are approximately orthogonal to the B(1)-N(1)-B(1A)-N(1A) plane.

Table 4.3: Selected bond distances and angles for $(Et_3P\mu\text{-}NBcat)_2$ (**4.1**), $(n\text{-}Bu_3P\mu\text{-}NBcat)_2$ (**4.2**), $(Ph_3P\mu\text{-}NBcat)_2$ (**4.3**), $(i\text{-}Pr_3P\mu\text{-}NBcat)_2$ (**4.4**) and $(n\text{-}Bu(t\text{-}Bu)_2P\mu\text{-}NBcat)_2$ (**4.5**).

Complex	N(1)-P(1) (Å)	N(1)-B(1) (Å)	P(1)-N(1)-B(1) (°)	B(1)-N(1)-B(1A) (°)
4.1	1.563(4)	1.536(7)	133.2(3)	90.1(4)
4.2	1.603(2)	1.563(3)	127.9(2)	89.8(2)
4.3	1.585(3)	1.573(6)	129.7(3)	90.3(3)
4.4	1.594(3)	1.529(5)	135.4(3)	89.6(3)
4.5	1.607(5)	1.540(9)	138.8(4)	90.2(5)

The formation of a monomeric *N*-catecholborylphosphinimine complex in the solid state was achieved, as evidenced by the X-ray crystallographic data for $t\text{-}Bu_3NPBcat$ (**4.6**). This is most likely due to the large steric bulk provided by the three *t*-Bu groups attached to the phosphorus atom. Indeed, the Tolman cone angles (θ)[308] for the phosphines incorporated in these compounds are as follows: PEt_3: θ = 132°; P*n*-Bu_3: θ = 132°; PPh_3: θ = 145°, P*i*-Pr_3: θ = 160°, P*t*-Bu_3: θ = 182°. The influence of bulk of the *t*-Bu groups on the structure of complex **4.6** becomes apparent when one views the ORTEP drawing of the crystal structure (Figure 4.5)

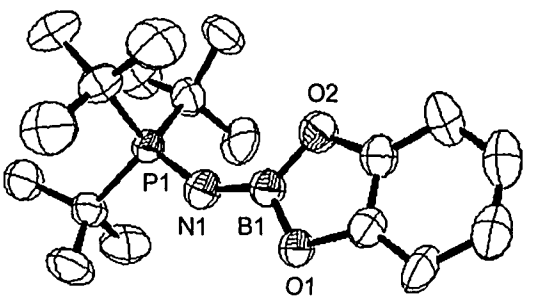

Figure 4.5: ORTEP diagram (50% probability thermal ellipsoids) of $t\text{-}Bu_3PNBcat$ (**4.6**).

The X-ray crystallographic data reveal a trigonal-planar geometry about B and the N-B and N-P bond distances were determined to be 1.369(3) Å and 1.563(2) Å, respectively. The N-P bond length is slightly longer than the average N-P bond lengths of the monomeric borylphosphinimine complexes $B(NPPh_3)_3$ (1.549(5)m Å)[154] and $HB(NPt\text{-}Bu_3)_2$ (1.531(5)Å)[166] and the N-B bond is slightly shorter than the average N-B bond lengths of $B(NPPh_3)_3$ (1.45(1) Å) and $HB(NPt\text{-}Bu_3)_2$ (1.41(5) Å). This may be due to the more electropositive nature of the boron atom due to the catechol group, resulting in a shorter B-N bond and therefore a longer P-N bond. The N-B bond distance is much shorter than those observed for the dimeric *N*-catecholborylphosphinimine complexes (**4.1 - 4.5**), as is expected. The relatively large P-N-B angle of 145.6(2)° is consistent with strong N to B π-donation and the steric demands of the *t*-butyl substituents of the phosphinimine.[166]

Upon comparing the dimeric complex $(Ph_3P\mu\text{-}NBcat)_2$ to the monomeric complex $B(NPPh_3)_3$, the relative difference in steric protection provided by the phosphinimide ligands vs. the chelated catechol ligand is apparent. The triphenylphosphinimide ligands provide more steric bulk than the catechol ligand. However, the Lewis acidity of the boron centre may also play a role in the formation of dimer or monomer since the boron atom is $(Ph_3P\mu\text{-}NBcat)_2$ is more electron deficient than the boron centre in $B(NPPh_3)_3$.

4.3.2 Analysis of Multi-Nuclear NMR Spectra

A relationship between the $^{31}P\{^1H\}$ chemical shifts of all the *N*-trimethylsilylphosphinimine starting materials and the corresponding *N*-catecholborylphosphinimine exists, as demonstrated by a downfield shift that is observed for all of the peaks upon replacement of the trimethylsilyl group with the catecholboryl group at the nitrogen atom of the phosphinimine. This downfield shift is consistent with the deshielding of the phosphorus centre caused by the more electron-withdrawing boron atom. Similarly, in the ^1H NMR spectra for compounds **4.1 - 4.6** the catechol protons are shifted downfield upon exchange of chloride for phosphinimide at boron.

In order to determine if the dimeric nature of complexes **4.1 - 4.5** were strictly a solid state phenomenon or if the dimers existed in solution, the respective $^{11}B\{^1H\}$ NMR

spectra were analyzed. Compounds **4.1** - **4.4** all display $^{11}B\{^1H\}$ chemical shifts between 6.0 – 8.4 ppm, this is typical of 4-coordinate systems of this type and therefore are consistent with dimer formulations in solution.[309, 310] The dimeric nature of compound **4.4** compared to the monomeric nature of analogous *N*-pinacolborylphosphinimine derivative (**3.10**) is not surprising given that the pinacolboryl fragment is bulkier and less Lewis acidic than the catecholboryl fragment. Compound **4.5** which is dimeric in the solid state is clearly monomeric in solution as its $^{11}B\{^1H\}$ chemical shift is 24.4 ppm. Compound **4.6** is also monomeric in solution based on its $^{11}B\{^1H\}$ chemical shift of 24.2 ppm.

Further evidence of the dimeric nature in solution is provided by exchange studies in which complexes **4.1** and **4.4** were combined in solution and monitored by $^{31}P\{^1H\}$ NMR spectroscopy. The exchange of "monomeric" units, in which the dimeric complexes contained two different phosphorus environments, was observed. The resulting NMR spectra indicate the presence of the precursor symmetric dimers and the unsymmetric dimer which was generated upon addition at room temperature. NMR spectra of $(Et_3P\mu\text{-}NBcat)_2$, $(i\text{-}Pr_3P\mu\text{-}NBcat)_2$ and the resulting spectrum upon combining the two reactants are illustrated in Figure 4.6.

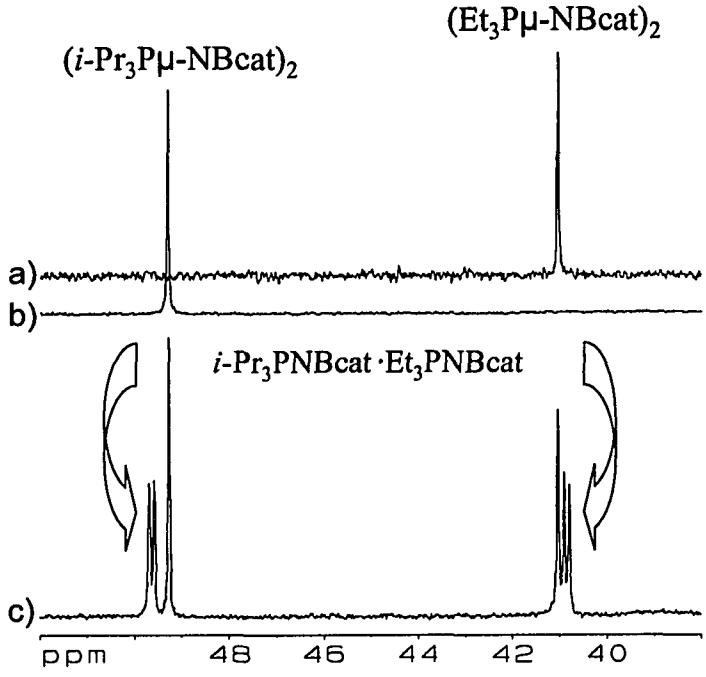

Figure 4.6: $^{31}P\{^{1}H\}$ NMR spectrum of a) $(Et_3P\mu\text{-}NBcat)_2$ **(4.1)**, b) $(i\text{-}Pr_3P\mu\text{-}NBcat)_2$ **(4.4)** and c) $(i\text{-}Pr_3P\mu\text{-}NBcat)_2$ **(4.4)**, $(Et_3P\mu\text{-}NBcat)_2$ **(4.1)** and $i\text{-}Pr_3PNBcat{\cdot}Et_3PNBcat$.

The $^{31}P\{^{1}H\}$ NMR spectrum shown in Figure 4.6 (c) indicates four phosphorus environments, those for the symmetric dimeric complexes $(i\text{-}Pr_3P\mu\text{-}NBcat)_2$ and $(Et_3P\mu\text{-}NBcat)_2$ and for the asymmetrical dimer, $i\text{-}Pr_3PNBcat{\cdot}Et_3PNBcat$. Both observed doublets are a result of the two-bond $^{31}P\text{-}^{31}P$ coupling in $i\text{-}Pr_3PNBcat{\cdot}Et_3PNBcat$. The corresponding coupling constants were determined to be approximately 21 Hz. This shows that exchange is possible since the N-B-N-B four-atom centres of the *N*-catecholborylphosphinimine complexes **4.1** and **4.4** may dissociate in solution to form the corresponding monomeric derivatives. This result is of interest, because it suggests that an equilibrium between monomer and dimer exists in solution. Based on the NMR spectral data the dimeric form is greatly favoured over the monomeric form. In future work, concentration dependent studies or temperature dependent studies would provide valuable information to determine the equilibrium constants of these reactions and hence, data about structure-activity relationships.

Similar exchange experiments were also conducted using the following pairs of compounds: **4.2** and **4.4**, **4.2** and **4.5** and **4.2** and **4.6**. The reaction using the first pair resulted in the formation of two doublets and the presence of both starting material dimers. However, no exchange was observed in the $^{31}P\{^{1}H\}$ NMR spectrum upon addition of (*n*-$Bu_3P\mu$-NBcat)$_2$, (**4.2**) to the monomeric complex *n*-Bu(*t*-Bu)$_2$PNBcat. Similarly, in the reaction of (*n*-$Bu_3P\mu$-NBcat)$_2$, (**4.2**) with *t*-Bu_3PNBcat (**4.6**) no change was observed in the $^{31}P\{^{1}H\}$ NMR spectrum. These results suggest that the dimeric compounds **4.1**, **4.2** and **4.4** can dissociate in solution, therefore facilitating further studies of reactivity. Retention of the monomeric nature of compounds **4.5** and **4.6** in the presence of smaller phosphinimines indicates protected nitrogen atom environments, which may impede any further reactivity for the more bulky derivatives.

The reaction of $(Et_3P\mu\text{-NBcat})_2$ (**4.1**) with two equivalents of *tris*pentafluorophenylborane ($B(C_6F_5)_3$) resulted in quantitative conversion to Et_3PNBcat·$B(C_6F_5)_3$ (**4.7**). This coordination compound is most likely bound through the nitrogen atom of the phosphinimine and the boron atom of the borane (Figure 4.7).

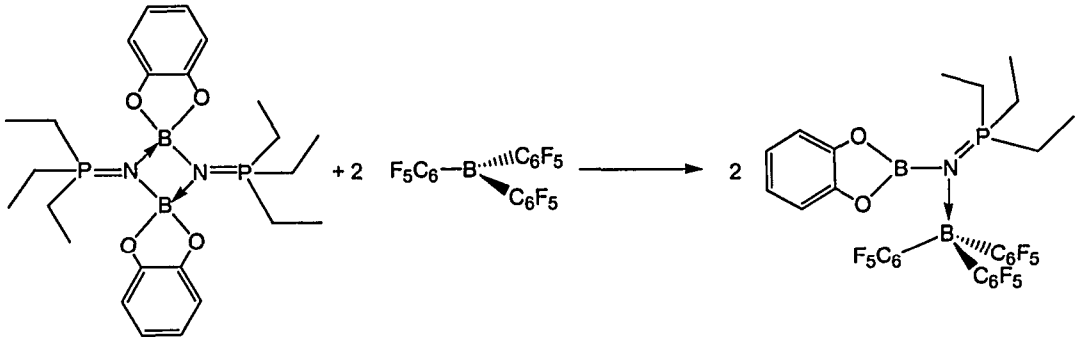

Figure 4.7: Synthesis of the *N*-catecholborylphosphinimine borane adduct (**4.7**).

The formation of complex **4.7** was monitored using $^{31}P\{^{1}H\}$ NMR spectroscopy. A downfield shift from 40.7 ppm to 68.0 ppm was observed upon breaking the *N*-catecholboryl-phosphinimine dimeric species and forming the *N*-catecholborylphosphinimine *tris*pentafluorophenylborane adduct. In the $^{11}B\{^{1}H\}$ NMR spectrum of compound **4.7** the two peaks at 28.0 ppm and -6.4 ppm are consistent with

the chemical shifts of other three coordinate boron centres in catecholboryl derivatives[310] and four-coordinate boron atoms in $B(C_6F_5)_3$ adducts,[149] respectively. Interestingly, similar chemical shifts in the $^{11}B\{^1H\}$ NMR spectrum were observed when compound **4.5** was reacted with an equivalent of $B(C_6F_5)_3$. The two peaks observed at 22.1 ppm and -3.9 ppm suggest that *n*-Bu(*t*-Bu)$_2$PNBcat has coordinated to $B(C_6F_5)_3$ via the nitrogen atom, as does the downfield shift from 38.8 ppm to 72.8 ppm in the $^{31}P\{^1H\}$ NMR spectrum. Additional characterization of this *N*-catecholborylphosphinimine-borane adduct was not completed. Thus far, it has been determined that *n*-Bu(*t*-Bu)$_2$PNBcat is monomeric in solution but that it crystallizes as a dimer. Compound **4.5** remains monomeric in the presence of less sterically hindered *N*-catecholborylphosphinimine complexes, but readily forms a coordination complex with *tris*pentafluorophenylborane. This suggests that the mild Lewis acidity of the boron centre and the steric bulk provided by substituents on phosphorus of another molecule of itself make dimerization unfavourable. However, even given the steric bulk of the substituents on phosphorus, in the presence of a more Lewis acidic boron centre such as $B(C_6F_5)_3$ formation of the *N*-catecholborylphosphinimine-borane adduct is favourable.

Moreover, the addition of $B(C_6F_5)_3$ to the monomeric complex *t*-Bu$_3$PNBcat resulted in no change in the $^{31}P\{^1H\}$, $^{11}B\{^1H\}$ and ^1H NMR spectra. In complex **4.6**, *t*-Bu groups on the phosphorus atom provide steric congestion about the nitrogen atom. This bulk along with that provided by the pentafluorophenyl rings of the borane prevent a strong interaction between the nitrogen atom and the boron atom of $B(C_6F_5)_3$. Therefore the formation of the nitrogen-coordinated species described in this chapter appears to be dictated by both the Lewis acidic nature of the boron centre and the steric impediments of the peripheral groups about the phosphorus and boron atoms.

4.3.3 Attempted MMA Polymerizations

Given the recent literature published on borane reagents acting as initiators to effect methylmethacrylate (MMA) polymerization,[311-313] MMA polymerizations using complexes **4.2** and **4.6** as possible initiators were attempted. Complexes **4.2** and **4.6** did not initiate the polymerization of MMA at room temperature or at -78°C. Therefore

complexes **4.2** and **4.6** do not appear to be radical sources and do not mimic the behavior of the related examples reported in the literature.

4.4 Summary

A series of *N*-catecholborylphosphinimine complexes with the general formula $(R_3PNBcat)_x$ have been synthesized via a facile metathetical route. The straightforward removal of volatile by-products and solvent led to the isolation of the desired products in high yields. These complexes have been characterized by multinuclear NMR spectroscopy, X-ray crystallography and elemental analysis.

The dimeric or monomeric nature of these *N*-catecholborylphosphinimine complexes in solution and in the solid state was determined to be dependent upon the extent to which the R groups of the phosphinimine moiety sterically shield the nitrogen atom. When phosphinimines containing hydrocarbon groups such as Et, *n*-Bu, Ph, and *i*-Pr were used, the nitrogen atom of the resulting *N*-catecholborylphosphinimine complex was able to coordinate to a boron atom of another molecule, thereby producing dimeric *N*-catecholborylphosphinimine complexes both in solution and in the solid state. The corresponding *n*-Bu(*t*-Bu)$_2$ derivative was determined to be monomeric in solution and dimeric in the solid state. Moreover, when *t*-Bu$_3$PNSiMe$_3$ was reacted with ClBcat the monomeric complex *t*-Bu$_3$PNBcat (**4.6**) was formed both in solution and in the solid state. Upon combining two different dimeric species together in solution, the formation of the asymmetrical dimer was apparent in the $^{31}P\{^1H\}$ NMR spectrum due to the additional peaks and the observed ^{31}P-^{31}P coupling. NMR studies also revealed that the monomeric derivatives (**4.5** and **4.6**) did not form asymmetrical dimers with the dimeric derivatives in solution.

The addition of $B(C_6F_5)_3$ to $(Et_3P\mu\text{-}NBcat)_2$ (**4.1**) afforded the coordination complex $Et_3PNBcat{\cdot}B(C_6F_5)_3$ (**4.7**). Compound **4.5** reacted with $B(C_6F_5)_3$ to form the *N*-catecholborylphosphinimine-borane adduct. This suggests that nitrogen coordination to boron is directed by both the steric bulk of the substituents of phosphorus and the Lewis acidity of the boron centre. Compound **4.6** did not react with $B(C_6F_5)_3$. The steric bulk provided by the three *t*-Bu groups sufficiently prevented the nitrogen atom from further

coordination even to a strong Lewis acid. Compounds **4.2** and **4.6** were not useful initiators of MMA polymerization.

5 Reduction of Phosphine Oxides by Pinacolborane and the Chemistry of the Diboron Compound $O(Bpin)_2$

5.1 Introduction

With the exception of the reactions of catecholborane with sulfoxides[190] there are no other examples to the best of our knowledge that utilize borane reagents bound by a chelating diolate group to effect reduction of Group 15 or Group 16 complexes. Given our results in Chapter 3 in which pinacolborane reduced small phosphinimine complexes and the proclivity for borane reagents to reduce Group 15 and Group16 complexes (Chapter 1), the reactions of phosphine oxides with pinacolborane were performed. Herein, the synthesis and characterization of the diboron compound $O(Bpin)_2$ is discussed and its reactivity with a variety of metal complexes and main group complexes is detailed.

5.2 Experimental

5.2.1 General Considerations

All preparations were performed under an atmosphere of dry O_2-free N_2 either employing Schlenk-line techniques or working in a Vacuum Atmospheres glovebox. ^1H, $^{13}C\{^1H\}$, $^{31}P\{^1H\}$, $^{11}B\{^1H\}$ and ^{19}F NMR spectra were recorded on either a Bruker Avance 300 or 500 MHz spectrometer. For broad peaks in the $^{11}B\{^1H\}$ or $^{31}P\{^1H\}$ NMR spectra the line widths at half height ($\Delta\nu_{1/2}$) are given in Hertz. Trace amounts of protonated solvent were used as internal references for ^1H NMR spectra. The solvent was used as an internal reference for $^{13}C\{^1H\}$ NMR spectra. The chemical shifts for both ^1H and $^{13}C\{^1H\}$ are reported in ppm relative to tetramethylsilane. $^{31}P\{^1H\}$ NMR spectra are referenced to an external standard consisting of an 85% aqueous solution of H_3PO_4. $^{11}B\{^1H\}$ NMR spectra are referenced externally to $BF_3{\cdot}Et_2O$ unless otherwise noted. ^{19}F NMR spectra are referenced externally to $CFCl_3$. All coupling constants are reported as

absolute values. Combustion analyses were performed at the University of Windsor Chemical Laboratories employing a Perkin Elmer CHN Series 2400 Analyzer.

5.2.2 Solvents

Anhydrous toluene, *n*-pentane, and tetrahydrofuran were purchased from Aldrich Chemical Company and were purified employing Grubbs-type column systems manufactured by Innovative Technologies or in-house by the University of Windsor Physics Machine Shop. Subsequently, the solvents were dried over the appropriate drying agents[272] under a nitrogen atmosphere and distilled. Methanol was purchased from BDH and was dried over activated magnesium and distilled. Deuterated benzene, toluene and tetrahydrofuran were purchased from Cambridge Isotopes Laboratories and purified by stirring over sodium and benzophenone for 16 h, followed by three freeze/pump/thaw degas cycles, and finally collected by vacuum distillation.

5.2.3 Materials

Hyflo Super Cel®, which will be referred to as Celite throughout the text, was purchased from Aldrich Chemical Company and dried in a vacuum oven at 130°C for 16 h before storing in the glovebox. 4 Å molecular sieves were purchased from Aldrich chemical Company and dried at 100°C under vacuum for 16 h.

5.2.4 Reagents

Pinacolborane, triphenylphosphine oxide, and butyllithium were used as received from Aldrich Chemical Company. Triphenylboron and zirconocene dichloride were used as received from Strem Chemical Company. *N*-trimethylsilyl-*n*-butylphosphinimine (**3.2**) was prepared as outlined in Chapter 3. *N*-H-tri-*t*-butylphosphinimine,[3, 4] *N*-H-tri-*i*-propylphosphinimine,[3, 4] zirconocenedimethyl,[314] methyltri*n*-butylphosphonium iodide,[315] and *bis*pentafluorophenylborane,[316] were all prepared via literature methods. *Tris*pentafluorophenylborane was generously donated by NOVA Chemicals Corporation.

5.2.5 Syntheses of Phosphorus- and Boron-containing Derivatives

$OPEt_3$ (5.1): To neat $Me_3SiNPEt_3$ (4.0 g, 18.8 mmol) was added excess dry methanol (30 mL) via cannula at room temperature. The resulting solution was heated at refluxing temperature for 16 h. The excess methanol, $MeOSiMe_3$ and $NMeH_2$ were removed *in vacuo* over a 6 h period. The product was crystallized from an *n*-pentane solution, dried *in vacuo* and recovered in 82% yield. ^1H NMR (300 MHz, C_6D_6) δ: 1.16 (m, 6H, $P(C\mathbf{H}_2CH_3)_3$), 0.86 (m, 9H, $P(CH_2C\mathbf{H}_3)_3$); $^{31}P\{^1H\}$ NMR (121.5 MHz, C_6D_6) δ: 46.2 (s); $^{13}C\{^1H\}$ NMR (75.5 MHz, C_6D_6) δ: 20.6 (d, $P(\mathbf{C}H_2CH_3)$, $^1J_{P\text{-}C}$ = 65.8 Hz); 6.2 (s, $P(CH_2\mathbf{C}H_3)_3$). Calculated: H: 1.27%, C: 53.72%; Found: H: 1.56%, C: 54.20%.

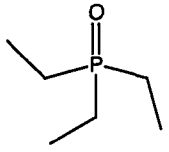

$OPn\text{-}Bu_3$ (5.2): *1*: To neat $Me_3SiNPn\text{-}Bu_3$ (4.2 g, 14.5 mmol) was added excess dry methanol (10 mL, 180 mmol) via cannula at room temperature. The mixture was heated at refluxing temperature for 16 h. Once cooled, $MeOSiMe_3$, $NMeH_2$ and the excess methanol were removed *in vacuo* over a 6 h period. The white solid was recrystallized in minimal amounts of *n*-pentane, dried *in vacuo* and isolated in 85% yield.

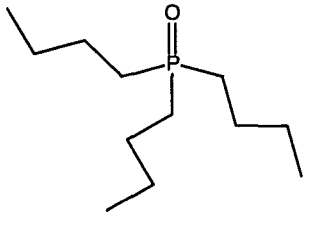

2: To neat $HNPn\text{-}Bu_3$ (0.100 g, 0.46 mmol) was added excess dry methanol (10 mL, 180 mmol) via cannula at room temperature. The resulting solution was stirred at room temperature for 24 h. The excess methanol was removed *in vacuo* over a 2 h period. The white solid was crystallized in minimal amounts of *n*-pentane dried *in vacuo* and isolated in 80% yield. ^1H NMR (300 MHz, C_6D_6) δ: 1.42 (m, 6H, $P(C\mathbf{H}_2CH_2CH_2CH_3)_3$), 1.35 (m, 6H, $P(CH_2C\mathbf{H}_2CH_2CH_3)_3$), 1.23 (m, 6H, $P(CH_2CH_2C\mathbf{H}_2CH_3)_3$), 0.79 (t, 9H, $P(CH_2CH_2CH_2C\mathbf{H}_3)_3$, $^3J_{H\text{-}H}$ = 8 Hz); $^{31}P\{^1H\}$ NMR (121.5 MHz, C_6D_6) δ: 42.0 (s); $^{13}C\{^1H\}$ NMR (75.5 MHz, C_6D_6) δ: 28.9 (d, $P(\mathbf{C}H_2CH_2CH_2CH_3)$, $^1J_{P\text{-}C}$ = 32 Hz), 24.9 (d, $P(CH_2\mathbf{C}H_2CH_2CH_3)_3$, $^2J_{P\text{-}C}$ = 6 Hz); 24.7 (d, $P(CH_2CH_2\mathbf{C}H_2CH_3)_3$, $^3J_{P\text{-}C}$ = 2 Hz), 14.2 (s, $P(CH_2CH_2CH_2\mathbf{C}H_3)_3$). Calculated: H: 12.47%, C: 66.02%; Found: H: 12.49%, C: 65.98%.

O(Bpin)$_2$ (5.3): *1*: HBpin (0.344 mL, 2.73 mmol) was added via syringe to a solution of

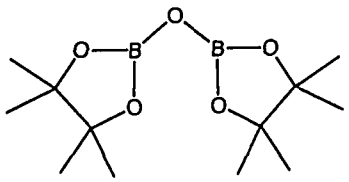

$OPEt_3$ (**5.1**) (0.150 g, 1.13 mmol) in 25 mL of toluene. The solution was heated at refluxing temperature for 72 h. Toluene and PEt_3 were removed *in vacuo* and the product was dissolved in minimal amounts of *n*-pentane. A crystalline product precipitated at -33°C and the supernatant was removed. The crystals were washed with cold *n*-pentane, dried *in vacuo* and isolated in 92 % yield.

2: HBpin (0.291 mL, 2.00 mmol) was added via syringe to a solution of $OPPh_3$ (0.279 g, 1.00 mmol) in 25 mL of toluene. The solution was heated at refluxing temperature for 72 h. After cooling to room temperature, toluene was removed *in vacuo* and a $^{31}P\{^1H\}$ NMR spectrum of the crude solid revealed conversion from the phosphine oxide to the tertiary phosphine. The product was extracted with 10 mL of *n*-pentane and stored at -33°C. White, crystalline solid was isolated from the *n*-pentane solution and dried *in vacuo* to afford the product in 75% yield.

3: HBpin (1.18 mL, 8.06 mmol) was added via syringe to a clear solution of OP*n*-Bu_3 (0.875 g, 4.03 mmol) in 25 mL of toluene. The solution was heated at refluxing temperature for 72 h. Toluene was removed *in vacuo* and the product was dissolved in minimal amount of *n*-pentane. From this solution a crystalline product precipitated at -33°C. The supernatant was removed and the crystals were washed with cold *n*-pentane, dried *in vacuo* and isolated in 65% yield.

4: HBpin (0.4 mL, 0.26 g, 2.0 mmol) was diluted in 40 mL of toluene in a 100 mL Schlenk flask. This solution was heated at refluxing temperature for 144 h, cooled, and the toluene and other unidentified volatile by-products were removed *in vacuo*. The product was collected as a white solid on the sides of the flask in 13% yield. The origin of the oxygen atom is not unambiguous. Possible oxygen sources include pinacolborane, residual water, or oxygen.

5: $ONMe_3$ (0.129 g, 1.72 mmol) was added to a 100 mL Schlenk flask, and then 40 mL of toluene was added. HBpin (0.5 mL, 3.45 mmol) was slowly added to the toluene slurry. The flask was put under static vacuum and stirred for 1 h. The solvent and NMe_3 were removed *in vacuo* and the resulting white solid was dried *in vacuo* for 16 h. The white solid was isolated in 96% yield.

^{1}H NMR (300 MHz, C_6D_6) δ: 1.00 (s, 12H, $BO_2C_2(CH_3)_4$); $^{13}C\{^1H\}$ NMR (75.5 MHz, C_6D_6) δ: 83.3 (s, $BO_2C_2(CH_3)_4$), 25.0 (s, $BO_2C_2(CH_3)_4$); $^{11}B\{^1H\}$ NMR (96.3 MHz, C_6D_6) δ: 21.6 ($(\Delta\nu_{1/2}$ = 750 Hz). Calculated: H: 8.96%; C: 53.39%; Found: H: 8.85%; C: 53.16%.

***n*-Bu$_3$PO·HB(C$_6$F$_5$)$_2$ (5.4)**: To a solution of OP*n*-Bu$_3$ (0.041 g, 0.188 mmol) in 3 mL of toluene, was added a solution of $HB(C_6F_5)_2$ (0.065 g, 0.188 mmol) in 3 mL of toluene. The solution was stirred for 72 h. The solvent was removed *in vacuo* and the product was obtained in 88% yield. ^{1}H NMR (300 MHz, C_6D_6) δ: 1.30 (m, 6H, $P(CH_2CH_2CH_2CH_3)$), 1.00 (m, 12H, $P(CH_2CH_2CH_2CH_3)$), 0.67 (t, 9H, $P(CH_2CH_2CH_2CH_3)$, $^3J_{H-H}$ = 7 Hz); $^{31}P\{^1H\}$ NMR (121.5 MHz, C_6D_6) δ: 76.7; $^{13}C\{^1H\}$ NMR (partial) (75.5 MHz, $C_6D_5CD_3$) δ: 25.1 (d, $P(CH_2CH_2CH_2CH_3)$, $^1J_{P-C}$ = 64 Hz), 24.0 (d, $P(CH_2CH_2CH_2CH_3)$, $^2J_{P-C}$ = 15 Hz), 23.2 ($P(CH_2CH_2CH_2CH_3)$), 13.3 ($P(CH_2CH_2CH_2CH_3)$); ^{11}B NMR (96.3 MHz, C_6D_6, referenced to $NaBH_4$) δ: -11.1; ^{19}F NMR (282.4 MHz, $C_6D_5CD_3$) δ: -136.5, -159.7, -165.3. Calculated: H: 5.00%, C: 51.09%; Found: H: 4.88%, C: 51.01%.

***n*-Bu$_3$PO·B(C$_6$F$_5$)$_3$ (5.5)**: A solution of OP*n*-Bu$_3$ (0.028 g, 0.127 mmol) in 3 mL of toluene was added to $B(C_6F_5)_3$ (0.065 g, 0.127 mmol) in 2 mL of toluene. The resulting solution was stirred for 72 h. The solvent was removed *in vacuo* and the product was obtained in 87% yield. ^{1}H NMR (300 MHz, C_6D_6) δ: 1.28 (m, 6H, $P(CH_2CH_2CH_2CH_3)$), 0.91 (m, 12H, $P(CH_2CH_2CH_2CH_3)$), 0.62 (t, 9H, $P(CH_2CH_2CH_2CH_3)$, $^3J_{H-H}$ = 7 Hz); $^{31}P\{^1H\}$ NMR (121.5 MHz, C_6D_6) δ: 71.8 (s); $^{13}C\{^1H\}$ NMR (75.5 MHz, C_6D_6) δ: 148.8 (d(m), $^1J_{C-F}$ = 242 Hz, C_6F_5 (*o*-C)), 140.7 (d(m), $^1J_{C-F}$ = 249 Hz, C_6F_5 (*p*-C)), 138.0 (d(m), $^1J_{C-F}$ = 249 Hz, C_6F_5 (*m*-C)), 25.3 (d, $P(CH_2CH_2CH_2CH_3)$, $^1J_{P-C}$ = 66 Hz), 24.2 (d, $P(CH_2CH_2CH_2CH_3)$, $^2J_{P-C}$ = 16 Hz), 23.3 (s, 3C, $P(CH_2CH_2CH_2CH_3)$), 13.5 (s, $P(CH_2CH_2CH_2CH_3)$); $^{11}B\{^1H\}$ NMR (96.3 MHz, C_6D_6, referenced to $NaBH_4$) δ: -4.3

(br); ^{19}F NMR (282.4 MHz, C_6D_6, referenced to CCl_3F) δ: -134.0, -157.7, -164.1. Calculated: H: 3.73%, C: 49.34%; Found: H: 3.72%, C: 48.82%.

$SPCy_3$ (5.6): A solution of S_8 (0.086 g, 0.34 mmol) in 15 mL of toluene was added to a solution of PCy_3 (0.727 g, 2.59 mmol) in 15 mL of toluene. The resulting solution was stirred for 36 h at room temperature. The solvent was removed *in vacuo* leaving a white powder in 94% yield. ^1H NMR (500 MHz, C_6D_6) δ: 1.02-1.99 (m, Cy); $^{31}P\{^1H\}$ NMR (121.5 MHz, C_6D_6) δ: 61.7; $^{13}C\{^1H\}$ NMR (75.5 MHz, C_6D_6) δ: 38.0 (d, $^1J_{P\text{-}C}$ = 45 Hz), 27.9 (d, $^2J_{P\text{-}C}$ = 33 Hz), 26.9, 22.0. Calculated: H: 10.64%, C: 69.18%; Found: H: 10.73%, C: 68.65%.

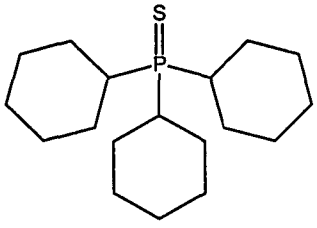

SP*n*-Bu_3 (5.7): A solution of S_8 (0.077 g, 0.30 mmol) in 5 mL of toluene was added to a solution of P*n*-Bu_3 (0.6 mL, 2.41 mmol). The resulting solution was stirred for 36 h at room temperature. The solvent was removed *in vacuo* leaving a colourless liquid in 92% yield. ^1H NMR (500 MHz, C_6D_6) δ: 1.46 (m, 12H, $CH_2CH_2CH_2CH_3$), 1.18 (m, 6H, $CH_2CH_2CH_2CH_3$), 0.79 (t, 9H, $CH_2CH_2CH_2CH_3$, $^3J_{H\text{-}H}$ = 8 Hz); $^{31}P\{^1H\}$ NMR (121.5 MHz, C_6D_6) δ: 47.5.

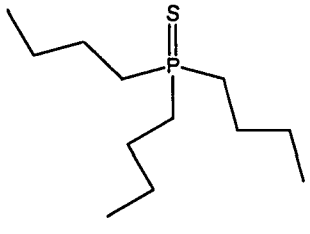

(*n*-Bu_3PCH_2·LiI·THF)$_2$ (5.8): This is a modified literature procedure for the preparation of CH_2Pn-Bu_3.[317] [*n*-Bu_3PCH_3][I] (0.250 g, 0.726 mmol) was dissolved in 25 mL of tetrahydrofuran in a Schlenk flask. *n*-BuLi (0.28 mL of 2.5 M in hexanes, 0.700 mmol) was added to the solution drop wise at room temperature. The resulting orange solution was stirred under static vacuum for 16 h. The solvent was removed *in vacuo*, and the remaining oil was dissolved in 10 mL of *n*-pentane and filtered through Celite. The *n*-pentane was removed *in vacuo* for 16 h.

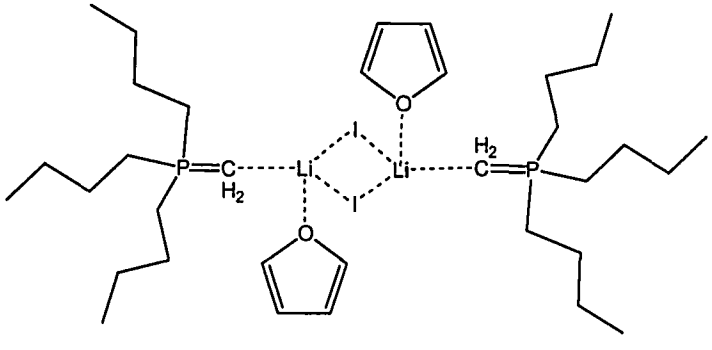

A yellowish-orange oil was isolated in 59% yield. X-ray quality crystals of **5.8** were obtained from a *n*-pentane solution in 30% yield. ^{1}H NMR (300 MHz, C_6D_6) δ: 1.57 (m, 6H, P(C**H**$_2$CH$_2$CH$_2$CH$_3$)$_3$)), 1.35 (m, 12H, P(CH$_2$C**H**$_2$C**H**$_2$CH$_3$)$_3$)), 0.92 (t, 9H, P(CH$_2$CH$_2$CH$_2$C**H**$_3$)$_3$), $^3J_{H\text{-}H}$ = 7 Hz), -0.18 (d, 2H, C**H**$_2$P(CH$_2$CH$_2$CH$_2$CH$_3$)$_3$, $^1J_{P\text{-}H}$ = 10 Hz); ^{31}P{^{1}H} NMR (121.5MHz, C_6D_6) δ: 30.2; ^{13}C{^{1}H} NMR (partial) (75.5MHz, C_6D_6) δ: 26.9 (d, P(**C**H$_2$CH$_2$CH$_2$CH$_3$)$_3$, $^1J_{P\text{-}C}$ = 207 Hz), 25.1 (s, P(CH$_2$**C**H$_2$CH$_2$CH$_3$)$_3$), 24.8 (s, P(CH$_2$CH$_2$**C**H$_2$CH$_3$)$_3$), 14.4 (s, P(CH$_2$CH$_2$CH$_2$**C**H$_3$)$_3$), -8.4 (d, **C**H$_2$P(CH$_2$CH$_2$CH$_2$CH$_3$)$_3$, $^1J_{P\text{-}C}$ = 36.5 Hz). Calculated: H: 8.83%, C: 48.35%; Found: H: 8.86%, C: 47.46%.

Zr(C$_5$H$_5$)$_2$(OBpin)$_2$ (5.9): To a solution of O(Bpin)$_2$ (**5.3**) (0.106 g, 0.398 mmol) in 25 mL of toluene was added solid Zr(C$_5$H$_5$)$_2$Me$_2$ (0.050 g, 0.199 mmol) (the addition vial was rinsed with 1 mL of toluene). The solution was heated at refluxing temperature for 16 h, followed by removal of toluene and MeBpin *in vacuo*. The solid was washed with *n*-pentane, dissolved in a minimal amount of toluene and stored at -33°C. Crystalline material precipitated from the *n*-pentane solution, the supernatant was decanted, and the product was dried *in vacuo*. A white crystalline solid was collected in 82% yield. ^{1}H NMR (500 MHz, C_6D_6) δ: 6.15 (s, 10H, C$_5$**H**$_5$), 1.14 (s, 24H, BO$_2$C$_2$(C**H**$_3$)$_4$)); ^{13}C{^{1}H} NMR (75.5 MHz, C_6D_6) δ: 114.3 (s, **C**$_5$H$_5$), 81.3 (s, BO$_2$**C**$_2$(CH$_3$)$_4$), 25.4 (s, BO$_2$C$_2$(**C**H$_3$)$_4$); ^{11}B{^{1}H} NMR (96.3 MHz, C_6D_6, referenced to $NaBH_4$) δ: 17.6. Calculated: H: 6.75%, C: 52.08%; Found: H: 6.79%, C: 51.85%.

[*t*-Bu$_3$PNH$_2$][pinB(OBpin)$_2$] (5.10): Solid O(Bpin)$_2$ (0.03 g, 0.111 mmol) was added to a solution of HNP*t*-Bu$_3$ (0.024 g, 0.111 mmol) in 2 mL of *n*-pentane. A white solid precipitated from the *n*-pentane solution immediately. The mixture was stirred for 2 h and set aside to allow the solid to settle in the vial. The *n*-pentane and soluble product (*t*-Bu$_3$PNBpin) were decanted off and the solid was washed with 4 mL of *n*-pentane. The product was dried *in vacuo*, resulting in a fine white powder in 80% yield. X-ray quality crystals grew from a toluene solution. ^{1}H NMR (300 MHz, C_6D_6) δ: 1.10 (br d, 63H, P(C(C**H**$_3$)$_3$)$_3$, hidden OBO$_2$C$_2$(C**H**$_3$)$_4$)$_2$BO$_2$C$_2$(C**H**$_3$)$_4$); ^{31}P{^{1}H} NMR (121.5 MHz, C_6D_6) δ: 65.9; ^{13}C{^{1}H} NMR (75.5 MHz, C_6D_6) δ: 39.5 (d, (P(**C**(CH$_3$)$_3$)$_3$, $^1J_{P\text{-}C}$ = 45 Hz), 29.6 (s, P(C(**C**H$_3$)$_3$)$_3$), 26.5 (s, (OBO$_2$C$_2$(CH$_3$)$_4$)$_2$BO$_2$C$_2$(**C**H$_3$)$_4$), 25.3 (s, (OBO$_2$C$_2$(**C**H$_3$)$_4$)$_2$BO$_2$C$_2$(CH$_3$)$_4$)); ^{11}B{^{1}H} NMR (96.3 MHz, C_6D_6, referenced to $NaBH_4$) δ: 23.7, 9.3. Calculated: C: 57.08%, H: 10.39%, N: 2.21%; Found: C: 57.23%, H: 10.40%, N: 2.23%.

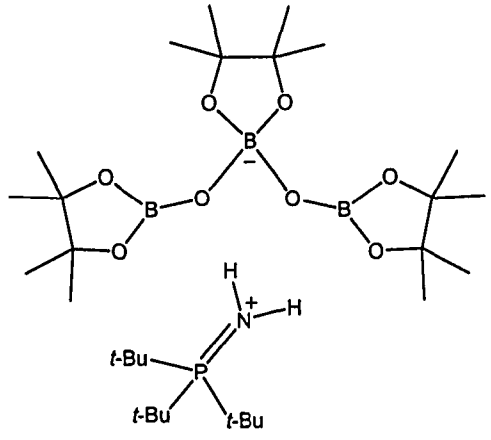

[*t*-Bu$_3$PNH$_2$][Cl] (5.11): From a toluene solution of [*t*-Bu$_3$PNH$_2$][pinB(OBpin)$_2$] (0.050 g, 0.082 mmol) and Ph_3CCl (0.023 g, 0.082 mmol) precipitated colourless crystals of [*t*-Bu$_3$PNH$_2$][Cl] (0.010 g, 0.039 mmol) in 48% yield. The crystals were mounted for characterization by X-ray crystallography and the remaining crystals were dissolved in CD_2Cl_2 and characterized by NMR spectroscopy. ^{1}H NMR (500 MHz, CD_2Cl_2) 0.99 (d, PC(C**H**$_3$)$_3$, $^3J_{P\text{-}H}$ = 13 Hz); ^{31}P{^{1}H} NMR (202.46 MHz, CD_2Cl_2) 70.3; Carbon data and elemental analysis were not collected for this sample.

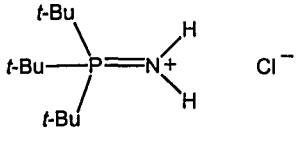

[*i*-Pr$_3$PNH$_2$][HOBPh$_3$] (5.12): To neat HNP*i*-Pr$_3$ (0.050 g, 0.29 mmol) was added a solution of BPh$_3$ (0.069 g, 0.29 mmol) in 5 mL of toluene. The resulting solution was stirred for 12 h and then set aside in the glovebox. A crop of crystals from this solution (0.030 g, 24% yield) were collected and characterized. ^{1}H NMR (300 MHz, C_6D_6) δ: 7.83 (d, 6H, *o*-H, $^3J_{H-H}$ = 7 Hz), 7.38 (t, 6H, *m*-H, $^3J_{H-H}$ = 8 Hz), 7.23 (t, 3H, *p*-H, $^3J_{H-H}$ = 7 Hz), 1.45 (dsept, 3H, C**H**(CH$_3$)$_2$, $^2J_{P-H}$ = 12 Hz, $^3J_{H-H}$ = 7 Hz), 0.57 (dd, 18H, CH(C**H**$_3$)$_2$, $^3J_{P-H}$ = 15 Hz, $^3J_{H-H}$ = 7 Hz); ^{31}P{^{1}H} NMR (121.5 MHz, C_6D_6) δ: 61.0 (s); ^{11}B{^{1}H} NMR (96.3 MHz, C_6D_6, referenced to NaBH$_4$) δ: -7.0; Calculated: H: 9.03%, C: 74.48%, N: 3.22%; Found: H: 9.09%, C: 74.50%, N: 3.18%.

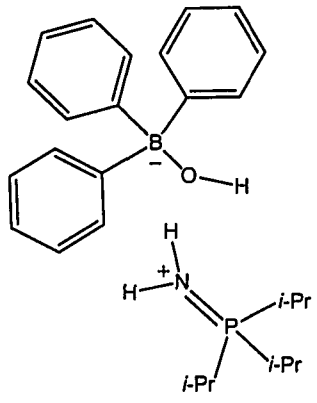

[pinBN(H)P*t*-Bu$_3$][Bcat$_2$] (5.13): From a crude reaction mixture of (catBNP*n*-Bu$_3$)$_2$ (0.050 g, 0.075 mmol) and HBpin (0.022 mL, 0.150 mmol) in toluene, a few X-ray quality crystals were isolated and the solid state structure was determined by X-ray crystallography. Full characterization of this material was not completed.

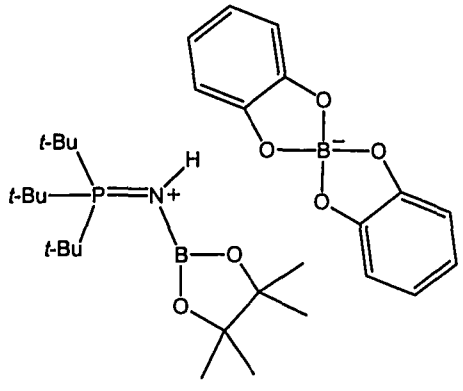

AdNH$_2$·B(OBpin)$_3$ (5.14): From a solution of AdN(H)(Bpin) in *n*-pentane grew a few X-ray quality crystals that were determined to be the coordination compound AdNH$_2$·B(OBpin)$_3$. The *n*-pentane was removed and the remaining bulk sample was characterized using NMR spectroscopy, however, a comparison in the ^{1}H NMR spectra showed the major product to be AdN(H)(Bpin). Therefore, characterization by NMR spectroscopy was not completed. The few crystals that precipitated were collected and

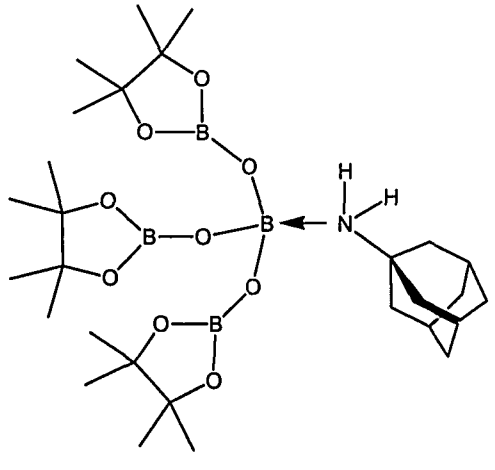

characterized using X-ray crystallography and elemental analysis. Calculated: H: 9.04%, C: 56.91%, N: 2.37%; Found: H: 8.32%, C: 57.63%, N: 2.99%.

5.2.6 X-ray Data Collection and Reduction

Refer to Section 2.2.7.1.

5.2.7 Structure Solutions and Refinements

Refer to Section 2.2.7.2.

X-ray structural solutions of $O(Bpin)_2$ **(5.3)**, (n-Bu_3PCH_2·LiI·THF)$_2$ **(5.8)**, $Zr(C_5H_5)_2(OBpin)_2$ **(5.9)**, [t-Bu_3PNH_2][pinB(OBpin)$_2$] **(5.10)**, [t-Bu_3PNH_2][Cl] **(5.11)**, [i-Pr_3PNH_2][$HOBPh_3$] **(5.12)**, [pinBN(H)Pt-Bu_3][$Bcat_2$] **(5.13)**, and $AdNH_2$·B(OBpin)$_3$ **(5.14)**. Cell parameters, R, R_w and GoF values are located Table 5.1, Table 5.2 and Table 5.3 while detailed structural parameters have been included as an appendix on CD (Appendix A). No residual electron density remained in any of the solutions that were of any chemical significance. ORTEP drawings of are depicted in Figures 5.8, 5.10, 5.13, 5.16, 5.17 and 5.18 respectively. Select bond distances and bond angles are provided in the text.

Table 5.1: X-ray crystallographic data obtained from crystals of $O(Bpin)_2$ **(5.3)**, $(n\text{-}Bu_3PCH_2{\cdot}LiI{\cdot}THF)_2$ **(5.8)**, and $Zr(C_5H_5)_2(OBpin)_2$ **(5.9)**.

Crystal	5.3	5.8	5.9
Molecular Formula	$C_{12}H_{24}B_2O$	$C_{34}H_{74}I_2Li_2O_2P_2$	$C_{22}H_{34}B_2O_6Zr$
Formula Weight (g/mol)	269.93	844.56	507.33
a (Å)	6.544(4)	10.193(7)	20.28(1)
b (Å)	21.29(1)	14.293(9)	13.162(8)
c (Å)	11.767(7)	16.50(1)	19.54(1)
α°	90	90	90
β°	95.60(1)	102.41(1)	100.69(1)
γ°	90	90	90
Crystal System	Monoclinic	Monoclinic	Monoclinic
Space Group	$P2_1/n$	$P2_1/c$	C2/c
Volume ($Å^3$)	1631(2)	2348(3)	5124(5)
D_{calc} (gcm^{-3})	1.099	1.194	1.315
Z	4	2	8
Abs coeff, μ, mm^{-1}	0.081	1.430	0.461
θ range (°)	1.91 – 23.27	1.90 – 23.40	1.85 – 23.29
Reflections Collected	6727	9855	10474
Data $F_o^2 > 3\sigma(F_o^2)$	2340	3359	3687
Parameters	253	190	260
R^a	0.0974	0.0453	0.0942
$R_w{}^b$	0.2677	0.1229	0.2410
Goodness of Fit	0.879	0.910	1.033

This data was collected at 20°C with Mo Kα radiation (λ = 0.71069 Å).

[a] $R=\Sigma(F_o-F_c)/\Sigma F_o$

[b] $R_w=(\Sigma[w(F_o^2-F_c^2)^2]/\Sigma[w(F_o)^2])^{1/2}$

Table 5.2: X-ray crystallographic data of [*t*-Bu_3PNH_2][pinB(OBpin)$_2$] (**5.10**), [*t*-Bu_3PNH_2][Cl] (**5.11**) and [*i*-Pr_3PNH_2][$HOBPh_3$] (**5.12**).

Crystal	5.10	5.11	5.12
Molecular Formula	$C_{30}H_{65}B_3NO_8P$	$C_{12}H_{29}NPCl$	$C_{27}H_{39}BNOP$
Formula Weight	631.23	253.78	435.37
a (Å)	10.752(3)	22.45(1)	10.978(5)
b (Å)	13.737(4)	12.492(6)	11.175(6)
c (Å)	14.181(4)	11.903(6)	11.466(6)
α°	94.422(6)	90	102.242(9)
β°	104.550(6)	113.49(1)	104.788(9)
γ°	106.244(6)	90	91.878(9)
Crystal System	Triclinic	Monoclinic	Triclinic
Space Group	P-1	C2/c	P-1
Volume (Å^3)	1921.9(9)	3061(3)	1323.5(11)
D_{calc} (gcm^{-3})	1.091	1.101	1.093
Z	2	8	2
Abs coeff, μ, mm^{-1}	0.114	0.33	0.121
θ range (°)	1.50 – 23.32	1.91-23.24	2.34 – 23.32
Reflections Collected	8994	7014	5669
Data $F_o^2 > 3\sigma(F_o^2)$	5469	2172	3770
Parameters	394	153	280
R[a]	0.0854	0.0315	0.0660
R_w[b]	0.1554	0.0854	0.1931
Goodness of Fit	0.843	0.962	1.115

This data was collected at 20°C with Mo Kα radiation (λ = 0.71069 Å).

[a] $R=\Sigma(F_o-F_c)/\Sigma F_o$

[b] $R_w=(\Sigma[w(F_o^2-F_c^2)^2] /\Sigma[w(F_o)^2])^{1/2}$

Table 5.3: X-ray crystallographic data obtained from crystals of [pinBN(H)P*t*-Bu_3][$Bcat_2$] (**5.13**) and $AdNH_2$·$B(OBpin)_3$ (**5.14**).

Crystal	5.13	5.14
Molecular Formula	$C_{30}H_{47}B_2NO_6P$	$H_{53}B_4C_{28}NO_9$
Formula Weight	570.28	590.96
a (Å)	8.332(4)	12.7543(8)
b (Å)	35.97(2)	12.7874(9)
c (Å)	11.638(6)	12.9926(9)
α°	90	62.589(1)
β°	103.51(1)	75.084(2)
γ°	90	65.107(1)
Crystal System	Monoclinic	Triclinic
Space Group	$P2_1/n$	P-1
Volume ($Å^3$)	3391(3)	1701.0(2)
D_{calc} (gcm^{-3})	1.117	1.154
Z	4	2
Abs coeff, μ, mm^{-1}	0.119	0.082
θ range (°)	2.13 – 23.29	1.77 – 23.28
Reflections Collected	14433	8489
Data $F_o^2 > 3\sigma(F_o^2)$	4831	4851
Parameters	361	379
R^a	0.0524	0.0724
$R_w{}^b$	0.1185	0.0985
Goodness of Fit	0.917	1.095

This data was collected at 20°C with Mo Kα radiation (λ = 0.71069 Å).

[a] $R=\Sigma(F_o-F_c)/\Sigma F_o$

[b] $R_w=(\Sigma[w(F_o^2-F_c^2)^2]/\Sigma[w(F_o)^2])^{1/2}$

5.3 Results and Discussion:

5.3.1 Synthesis of Phosphine Oxides

The protonolysis of *N*-trimethylsilylphosphinimines produces *N*-H-phosphinimines. It is in this form ($HNPR_3$) that phosphinimines have been used to synthesize a variety of transition metal and main group complexes.[8, 16, 21, 45, 147, 149, 166, 211] *N*-H-phosphinimines are usually prepared by heating *N*-trimethylsilylphosphinimines in an excess amount of methanol, which serves as both the solvent and the reagent in this reaction, for a period of time.[4] This method has served our research group well, as interest in sterically encumbered alkyl and aryl groups on the phosphorus atom of the phosphinimine has been a major focus. However, for the protonolysis of less bulky alkyl *N*-trimethylsilylphosphinimines to *N*-H-phosphinimines, the reaction must be conducted at low temperatures (-30°C) (Section 3.25).[3] If these reactions are performed at temperatures higher than -30°C the conversion of *N*-H-phosphinimines to the corresponding phosphine oxides occurs, as shown in Figure 5.1.[3] This is a clean, yet costly, method to prepare the phosphine oxides, $OPEt_3$ (**5.1**) and $OPn\text{-}Bu_3$ (**5.2**).

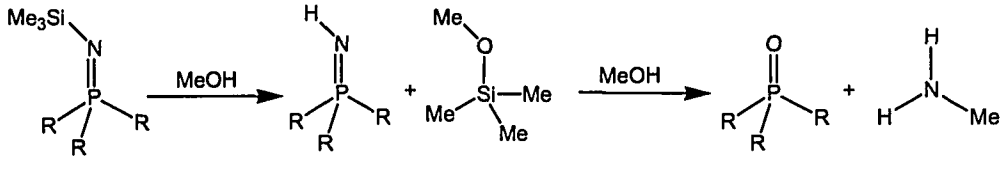

R = Et, *n*-Bu

Figure 5.1: Methanolysis of *N*-trimethylsilylphosphinimine to *N*-H-phosphinimines and subsequent reaction to the corresponding phosphine oxides.

The reactivity observed for the reactions of methanol with phosphinimines with either large or small substituents on phosphorus is reminiscent of that observed for the reactions of phosphinimines with pinacolborane. The steric bulk of the substituents on phosphorus or the lack there of, dictates the reaction mechanism. In order for the synthesis of phosphine oxides from phosphinimines to occur, the substituents on phosphorus must not hinder the approach of a molecule of methanol to phosphinimine to

form a pseudo four-membered P-N-H-O ring (Figure **5.2**). This helps in rationalizing the stability of phosphinimines with larger substituents on phosphorus such as *t*-Bu, *i*-Pr and Ph.

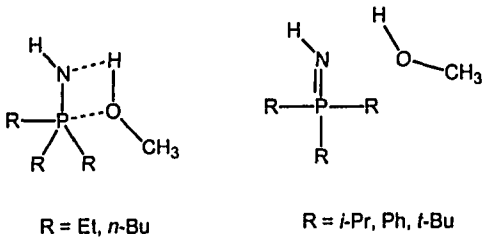

Figure 5.2: The (a) unhindered approach and (b) hindered approach of a molecule of methanol to phosphinimine.

5.3.2 Reduction of Phosphine Oxides using Pinacolborane

Köster and Morita reported that the reactions of trialkylboranes, alkyldiboranes and trialkylamineboranes with phosphine oxides at high temperatures reduce triphenylphosphine oxide to triphenylphosphine.[191] These reactions yielded the tertiary phosphine and a variety of boron-containing compounds. Other groups have reported on the conversion of cyclic phosphine oxides and dimeric phosphine oxides with $BH_3{\cdot}SMe_2$ to produce phosphine-borane adducts[193-195], and the conversion of sec-phosphine oxides with $BH_3{\cdot}SMe_2$ to phosphine-borane complexes.[318, 319] Given that phosphinimines may be reduced with pinacolborane (Chapter 3), the reactions of pinacolborane with the tertiary phosphine oxides ($OPEt_3$, $OPn\text{-}Bu_3$ and $OPPh_3$) were performed to determine if this would generate the respective phosphine derivatives. These reactions were conducted in toluene that was heated at refluxing temperature for a duration of 72 h. Complete conversion to the corresponding tertiary phosphine and the formation of a single boron-containing complex were indicated by the $^{31}P\{^1H\}$ and $^{11}B\{^1H\}$ NMR spectroscopic data. The boron-containing compound was determined to be $O(Bpin)_2$ (**5.3**) from ^1H, $^{11}B\{^1H\}$, and $^{13}C\{^1H\}$ NMR spectroscopy, X-ray crystallography and elemental analysis. The general reaction of pinacolborane and phosphine oxides is depicted in Figure 5.3.

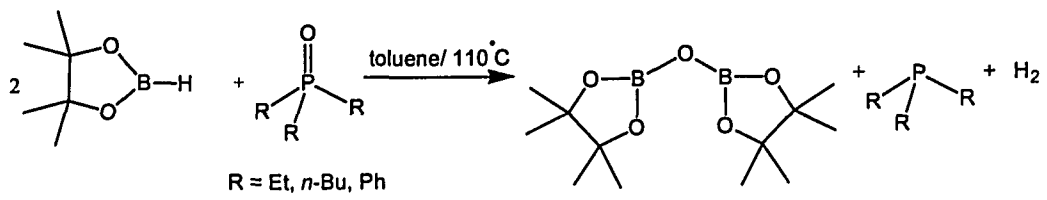

Figure 5.3: Synthesis of $O(Bpin)_2$ and tertiary phosphines.

It is proposed that the initial step in the reaction is the reduction of the phosphorus centre with concomitant generation of pinacolboric acid (HOBpin). The boric acid is an intermediate and not observed because it reacts readily with another equivalent of pinacolborane to yield $O(Bpin)_2$ and hydrogen gas, as depicted in Figure 5.4.[191] This is an analogous mechanism to mechanism 2 proposed in Chapter 3.

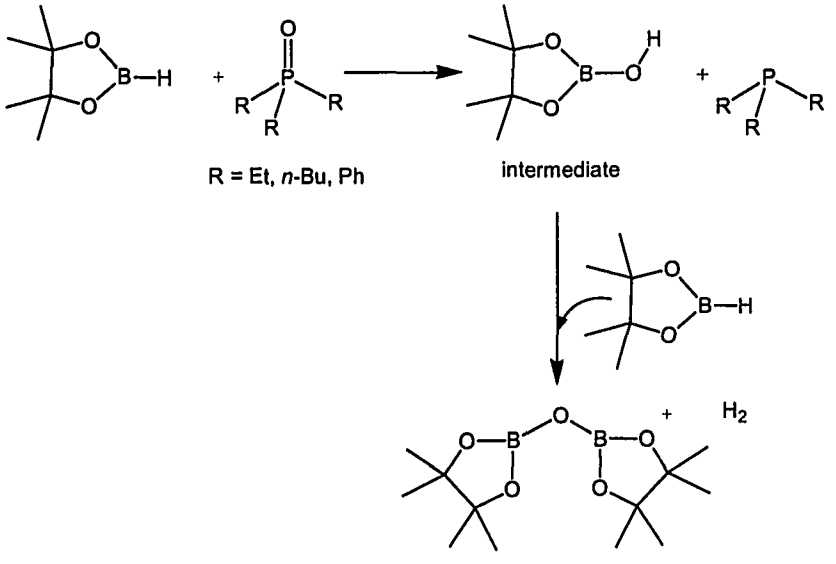

Figure 5.4: Reaction scheme for the synthesis of $O(Bpin)_2$.

Given the volatility of PEt_3, the removal of toluene and PEt_3 *in vacuo* produced $O(Bpin)_2$ cleanly in 92% yield. However, in the reaction where $Pn\text{-}Bu_3$ was produced, $O(Bpin)_2$ was precipitated from a saturated *n*-pentane solution at -33°C in 65% yield.

Moreover, for the reaction yielding triphenylphosphine, the removal of toluene and subsequent addition of *n*-pentane effected the separation of the tertiary phosphine from $O(Bpin)_2$. The *n*-pentane mixture was filtered through Celite and the removal of solvent yielded compound **5.3** in 75% yield. Interestingly, but not surprisingly, the reaction of tri(*t*-butyl)phosphine oxide with pinacolborane did not result in reduction of phosphorus atom. Based on these data, it appears as though pinacolborane is an effective reagent for the reduction of phosphine oxides with sterically less bulky substituents.

Alternative syntheses yielding compound **5.3** have been tested. For example, heating pinacolborane in toluene at refluxing temperature in the absence of any reagent for 144 h, followed by subsequent removal of solvent and volatile by-products produced $O(Bpin)_2$ in 13% yield. However, the most efficient route involves the reaction of trimethylamine-*N*-oxide with pinacolborane at room temperature. This reaction results in the complete conversion of HBpin and $ONMe_3$ to $O(Bpin)_2$, NMe_3 and H_2 at room temperature in 96% yield. This synthetic method is attractive since all the by-products generated are volatile, resulting in straightforward isolation of the product. A similar type of oxidation was reported by Köster and Morita, who observed conversion of B-C groups of trialkyl or triaryl boranes to B-O-C groups, and B-H groups of organoboranes to B-O-H groups using anhydrous tertiary amine-*N*-oxides in 97% yield.[192]

X-ray quality crystals of $O(Bpin)_2$ were grown from a cold *n*-pentane solution. The ORTEP drawing of compound **5.3** is shown in Figure 5.5. X-ray crystallographic data for $O(Bpin)_2$ reveals B(1)-O(5) and B(2)-O(5) bond distances of 1.347(7) Å and 1.333(8) Å. These bond distances are comparable to those observed in the similar complexes such as $O(B(terphenyl)_2)_2$ (1.34(2) Å and 1.35(3) Å)[320], $O(B(Cl(N\textit{i}\text{-}Pr_2)_2)_2$ (1.367(3) Å and 1.367(3) Å)[201], $O(B(N_3(Ph)_2C))_2$ (1.365(4) Å and 1.370(4) Å)[203], and $O(B(C_6H_2\text{-}2,4,6\text{-}Me_3)_2)_2$ (avg. 1.36(2) Å)[321]. The B1-O5-B2 angle was determined to be 133.9(6)° which is similar to but slightly shorter than the angles of the aforementioned related complexes.[201, 203, 291]

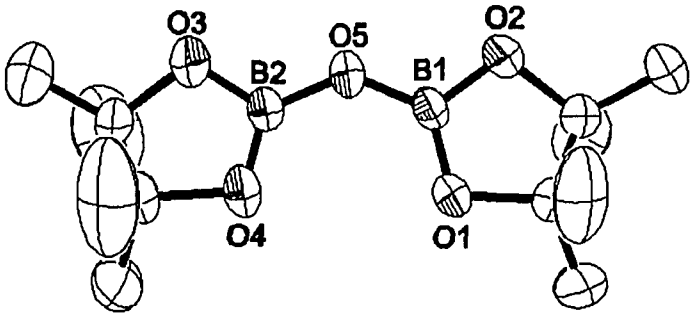

Figure 5.5: ORTEP drawing (50% probability thermal ellipsoids) of $O(Bpin)_2$. Hydrogen atoms have been omitted for clarity.

The first direct comparison of analogous diborylamines and diboryloxides was reported by Paciorek and coworkers who synthesized and crystallized the diboron compounds, $HN(B(HNSiMe_3)_2)_2$ and $O(B(HNSiMe_3)_2)_2$.[291] A comparison of spectroscopic and structural data of $O(Bpin)_2$ (**5.3**) and $HN(Bpin)_2$ (**3.16**) is shown in Table 5.4. to indicate that the two derivatives are distinguishable using several common characterization techniques.

Table 5.4: Characterization data of $HN(Bpin)_2$ (**3.16**) and $O(Bpin)_2$ (**5.3**).

Characterization Data	$HN(Bpin)_2$	$O(Bpin)_2$
^1H NMR (C_6D_6): CH_3 (ppm)	1.04	1.00
$^{13}C\{^1H\}$ NMR (C_6D_6): CH_3 (ppm)	25.1	25.0
$^{13}C\{^1H\}$ NMR (C_6D_6): $C_2(CH_3)_4$ (ppm)	82.8	83.3
$^{11}B\{^1H\}$ NMR (C_6D_6): **B**pin (ppm)	25.2	21.6
X-ray: avg. B-X bond distance (Å) (X = N,O)	1.419(6)	1.340(8)
X-ray: B-X-B bond angle (°) (X = N or O)	132.9(3)	133.9(6)
IR (nujol mull): N-H stretch (cm^{-1})	3334	NA
Elemental Analysis: Found: %H (%H_{calcd})	9.58% (9.37%)	8.85% (8.96%)
Found: %C (%C_{calcd})	54.09% (53.59%)	53.16% (53.39%)
Found: %N (%N_{calcd})	5.22% (5.21%)	0.02% (0%)

Compound **5.3** and compound **3.16** exhibit similar spectral characteristics in the NMR spectral data. As shown in Table 5.4 above, the ^{1}H and $^{13}C\{^{1}H\}$ NMR chemical shifts for both the amine (**3.16**) and oxide (**5.3**) are essentially the same. The IR spectrum of $HN(Bpin)_2$ revealed a band at 3334 cm^{-1} which can be assigned to the N-H stretching vibration. As expected, a band in this region was not observed in the IR spectrum of $O(Bpin)_2$ (**5.3**). Analogous bond lengths and angles in compounds **3.5** and **5.3**, except for the B-X (X = N, O) bond distance and the B-X-B bond angle, are indistinguishable. The difference in the average N-B and O-B bond distances is similar to that observed by Paciorek and coworkers, with the N-B distances being longer than the B-O distances.[291]

5.3.3 Attempted Synthesis of $O(B(C_6F_5)_2)_2$

Considering the recurrent use of *tris*pentafluorophenylborane and related Lewis acids as activators in olefin polymerization,[128, 322] $O(B(C_6F_5)_2)_2$ was an appealing synthetic target. Therefore, $HB(C_6F_5)_2$[316] and OP*n*-Bu_3 were heated together at refluxing temperature in toluene. A variety of boron-containing products were produced, however no tertiary phosphine was observed in the $^{31}P\{^{1}H\}$ NMR spectrum. By performing this reaction at room temperature the coordination compound *n*-$Bu_3PO{\cdot}HB(C_6F_5)_2$ (**5.4**) was isolated and characterized by ^{1}H, $^{13}C\{^{1}H\}$, $^{31}P\{^{1}H\}$, ^{19}F, and $^{11}B\{^{1}H\}$ NMR spectroscopy (Figure 5.6). A variety of complexes with the general formula $R_3PO{\cdot}B(C_6F_5)_3$ have been reported in the literature.[323, 324] To the best of our knowledge, the *tris*pentafluorophenylborane adduct of tri*n*-butylphosphine oxide, *n*-$Bu_3PO{\cdot}B(C_6F_5)_3$ (**5.5**) has not been reported and was synthesized to compare the chemical shifts and further establish evidence for the synthesis of **5.4**.

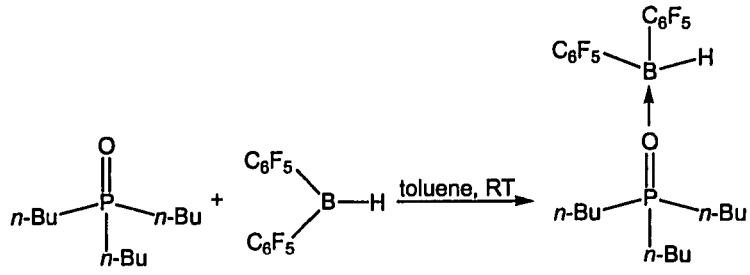

Figure 5.6: The synthesis of *n*-$Bu_3PO{\cdot}HB(C_6F_5)_2$ (**5.4**).

The $^{11}B\{^1H\}$ and $^{31}P\{^1H\}$ NMR spectra for compounds **5.4** and **5.5** are similar. The upfield shifts in the $^{11}B\{^1H\}$ NMR spectra are consistent with the conversion of a three-coordinate boron centre to a four-coordinate boron centre.[325] The downfield shifts in the $^{31}P\{^1H\}$ NMR spectra of these complexes are typical for coordination complexes of phosphine oxides.[323] In the ^1H NMR spectrum the peaks for the B-H interaction are not observed, this is most likely due to the P-H coupling by splitting the initial four peaks into eight unobservable peaks.

5.3.4 Reactions of Pinacolborane with XPR_3 (X =S, CH_2; R = *n*-Bu, Cy)

Thus far, it has been shown that pinacolborane reduces the phosphorus centre in both phosphinimines (Chapter 3) and phosphine oxides (*vide supra*). The next logical extension was to treat thiophosphines (SPR_3) and phosphaylides (CH_2PR_3) with pinacolborane to determine if this methodology could produce the analogues $S(Bpin)_2$ and $H_2C(Bpin)_2$. The thiophosphines ($SPCy_3$ (**5.6**) and $SPn\text{-}Bu_3$ (**5.7**)) were synthesized by adding S_8 to eight equivalents of the corresponding tertiary phosphine in toluene and stirring at room temperature. From the reaction of tri*n*-butylphosphinimonium iodide with methyl lithium crystallized the other precursor of interest, namely the tetrahydrofuran lithium iodide adduct of tri*n*-butylphosphaylide (**5.8**). The ORTEP diagram of this complex is depicted in Figure 5.7.

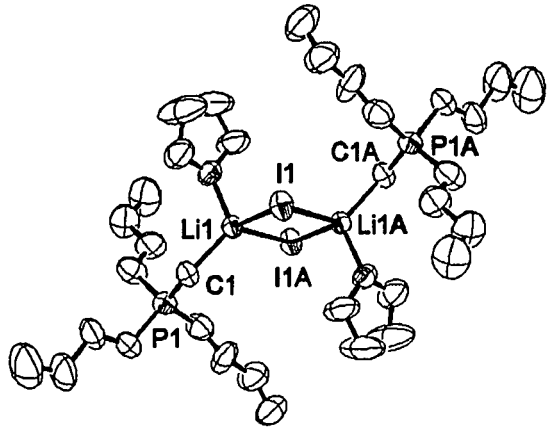

Figure 5.7: ORTEP drawing (30% probability thermal ellipsoids) of *n*-Bu_3PCH_2·LiI·THF (**5.8**). Hydrogen atoms have been omitted for clarity.

The crystallographic data of **5.8** revealed a C(1)-P(1) bond distance of 1.688(6) Å which is slightly longer than phosphaylides that are not interacting with a metal atom such as $CH_2P(NMe_2)_3$ (1.655(6) Å),[326] and CH_2PPh_3 (1.662(6) Å)[327]. However, the C(1)-P(1) bond distance is shorter than phosphaylides coordinated to a transition metal such as $YCp^*_2(o\text{-}C_6H_4PPh_2CH_2)$ (1.737(3) Å).[328] The P(1)-C(1)-Li(1) bond angle was determined to be 122.7(4)°, indicating a pseudo tetrahedral environment about C(1).

Both thiophosphines and the phosphaylide THF salt did not react with pinacolborane to yield tertiary phosphine and the corresponding borylthiol or borylmethane. In a similar vein, Bestmann and Arenz prepared boron-bridged diylides by adding four equivalents of phosphaylides to alkyldichloroboranes; no reduction was observed (Figure 5.8).[329]

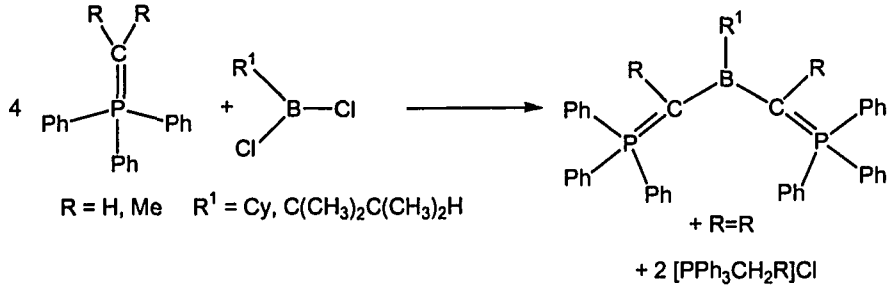

Figure 5.8: The reaction of phosphaylides with alkyldichloroboranes.[329]

Moreover, Shapiro and coworkers found that combining $PhBCl_2$ with CH_2PPh_3 resulted only in adduct formation.[330] The reactions of the thiophosphines and the phosphaylide THF salt with pinacolborane were attempted in the presence of 5 mol% Wilkinson's catalyst;[190] however, no reduction of phosphorus was observed. Therefore, pinacolborane does react with phosphinimines and phosphine oxides to produce free trialkylphosphine and $HN(Bpin)_2$ or $O(Bpin)_2$, respectively, but this is not a universal reagent to reduce any P(V) derivative to P(III).

5.3.5 Synthesis of Zirconocene *Bis*(pinacolboryl)oxide

The reactivity of $O(Bpin)_2$ (**5.3**) with dimethylzirconocene was probed. At ambient temperatures no reaction occurred between the metal complex and the diboryl oxide. However, upon heating the reaction mixture at refluxing temperature in toluene, two equivalents of (**5.3**) reacted with $Zr(C_5H_5)_2Me_2$ to yield $Zr(C_5H_5)_2(OBpin)_2$ (**5.9**) and (presumably) two equivalents of methyl pinacolborane (Figure 5.9). Coles and coworkers have reported zirconium complexes of the general formula $[Zr(C_5H_5)_2(\mu\text{-}O_2BAr)]_2$ which were synthesized via protonolysis of $Zr(C_5H_5)_2Me_2$ with $PhB(OH)_2$ which was in turn generated *in situ* from $(PhBO)_3$ with 3 equivalents of water.[209] More recently, Tilley and coworkers have published the structure of $Zr(C_5H_5)_2(Me)OB(OSi(O\textit{t}\text{-}Bu)_3)_2$ which was also synthesized via the appropriate boronic acid.[210] To the best of our

knowledge, zirconium boryloxide complexes synthesized via the diboryloxide have not been reported as of yet.

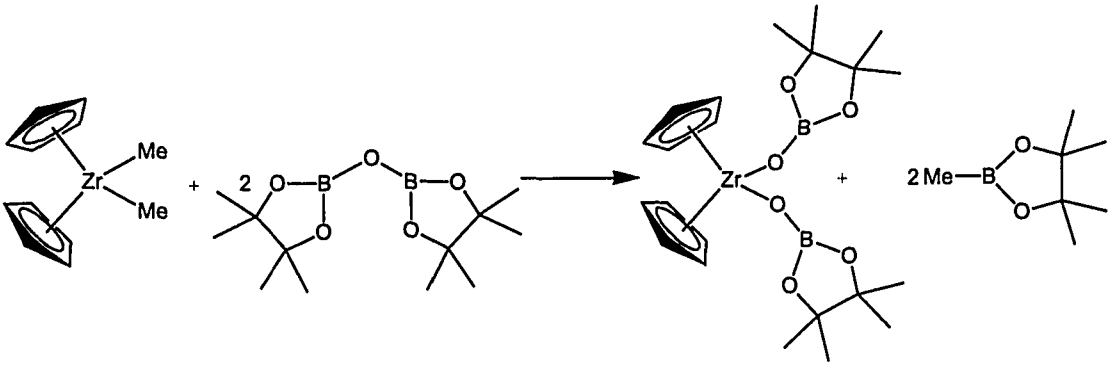

Figure 5.9: The synthesis of $Zr(C_5H_5)_2(OBpin)_2$ (**5.9**).

$Zr(C_5H_5)_2(OBpin)_2$ (**5.9**) was characterized by ^1H, $^{13}C\{^1H\}$ and $^{11}B\{^1H\}$ NMR spectroscopy, elemental analysis and X-ray crystallography. X-ray quality crystals were grown from an *n*-pentane solution. The average Zr-O and O-B bond distances were determined to be 2.02(1) Å and 1.29(2) Å, respectively. These bond lengths are similar to the known zirconium boryloxide complexes.[209, 210] The Zr-O-B bond angles were determined to be 153.0(8)° and 156.3(8)° which are similar to the average Zr-O-B bond angle (160(2)°) determined from the 18 unique molecules of $Zr(C_5H_5)_2(Me)OB(OSi(Ot\text{-}Bu)_3)_2$ in the asymmetric unit. An ORTEP drawing of (**5.9**) is shown in Figure 5.10.

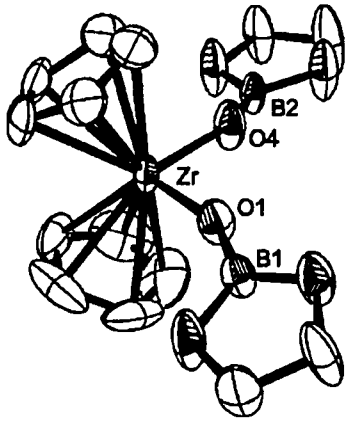

Figure 5.10: ORTEP drawing (30% probability thermal ellipsoids) of $Zr(C_5H_5)_2(OBpin)_2$ (**5.9**). Hydrogen atoms and the methyl groups on the pinacolyl moiety have been omitted for clarity.

The search for new catalytic complexes that polymerize α-olefins has been the focus of much research in the past decade. For this reason, much time, energy and funding has been spent in the search of new cocatalysts for α-olefin polymerization. Enhanced activities upon incorporating boron-oxygen complexes into metallocene/MAO polymerization systems has been reported in the recent patent literature.[331-333] In the reaction of $Zr(C_5H_5)_2Me_2$ with two equivalents of $O(Bpin)_2$, cleavage of boron-oxygen bonds led to the synthesis of the *bis*borylcomplex $Zr(C_5H_5)_2(OBpin)_2$, and presumably, two equivalents of MeBpin. Given this reactivity and the precedent set from published literature,[139, 140, 142, 334] it was proposed that the reaction of trimethylaluminum (TMA) with $O(Bpin)_2$ would lead to an aluminum-boryloxide species that could potentially act as a cocatalyst. A polymerization test mimmicking the polymerization procedure outlined in a US patent,[335] was conducted in which ten equvialents of TMA/$O(Bpin)_2$ was injected into the Büchi reactor (**Section 2.2.8.4**) containing one equivalent of $ZrCp_2Me_2$ in 500 mL of toluene. No polymer product was collected. Due to these results, no further inquiry into this system was performed.

5.3.6 Reactivity of *Bis*(pinacolboryl)oxide with Phosphinimines

Given the propensity for which diboryloxide complexes (also called borylanhydrides) undergo hydrolysis to form boronic acids,[209, 210, 336, 337] the reactions of $O(Bpin)_2$ with *N*-H-phosphinimine complexes were of interest. The *N*-H-phosphinimine complexes have an available proton to form the boronic acid (HOBpin) and the basic nitrogen centre to react with the other pinacolboryl moiety to form the borylphosphinimine complex (*t*-$Bu_3PNBpin$ (**3.13**)). As predicted, a white solid precipitated in 80% yield from a reaction mixture of $O(Bpin)_2$ and $HNPt\text{-}Bu_3$ in *n*-pentane. This solid was dissolved in toluene, and X-ray quality crystals were grown from this solution. The crystallographic data revealed the structure of the phosphinimonium borate salt, [*t*-Bu_3PNH_2][pinB$(OBpin)_2$] (**5.10**). The ORTEP drawing is depicted in Figure 5.11 below.

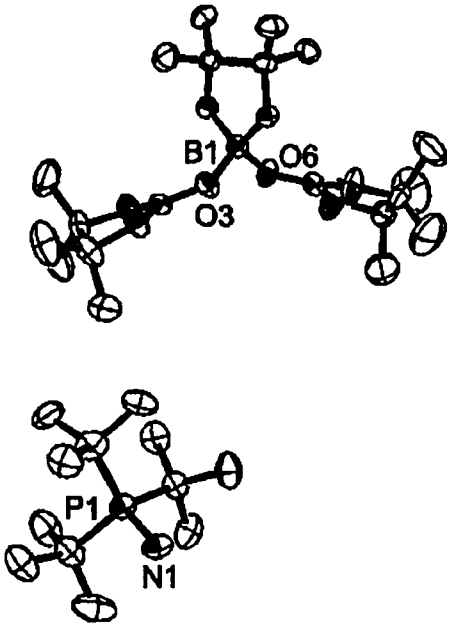

Figure 5.11: ORTEP drawing (30% probability thermal ellipsoids) of [*t*-Bu_3PNH_2][pinB$(OBpin)_2$] (**5.10**). Hydrogen atoms have been omitted for clarity.

The X-ray crystallographic data for [*t*-Bu_3PNH_2][pinB(OBpin)$_2$] (**5.10**) reveals a pseudo tetrahedral environment about the central boron atom. The OBO angle formed from the chelating pinacolate moiety was determined to be 105.0(6)° and is most likely the reason for the small deviation from a true tetrahedral environment. The B(1)-O(3) and B(1)-O(6) bond distances were determined to be 1.466(9) Å and 1.454(9) Å, and the B(2)-O(3)-B(1) and B(3)-O(6)-B(1) angles were determined to be 138.7(6)° and 134.3(6)°, respectively. The N-P bond distance was determined to be 1.648(6) Å; which is a typical bond length for a phosphinimonium cation.[147]

At first glance the formation of the salt [*t*-Bu_3PNH_2][pinB(OBpin)$_2$] (**5.10**) was puzzling. However, a plausible route for the synthesis of [*t*-Bu_3PNH_2][pinB(OBpin)$_2$] is depicted in Figure 5.12 below. The first step (Figure 5.12 a) may involve the formation of the boronic acid and borylphosphinimine intermediate, followed by removal of the proton on the boronic acid to form the phosphinimonium cation and boryl oxide anion (Figure 5.12 b). The boryl oxide anion could then attack another molecule of O(Bpin)$_2$ to form the borate anion [pinB(OBpin)$_2$]$^-$ (Figure 5.12 c). The *n*-pentane solution from which the salt precipitated was collected, the solvent was removed *in vacuo*, and the remaining oil was analyzed by ^{1}H, ^{31}P{^{1}H}, ^{13}C{^{1}H} and ^{11}B{^{1}H} NMR spectroscopy. The oil was determined to be the borylphosphinimine complex *t*-Bu_3PNBpin (**3.13**), supporting the proposed mechanism.

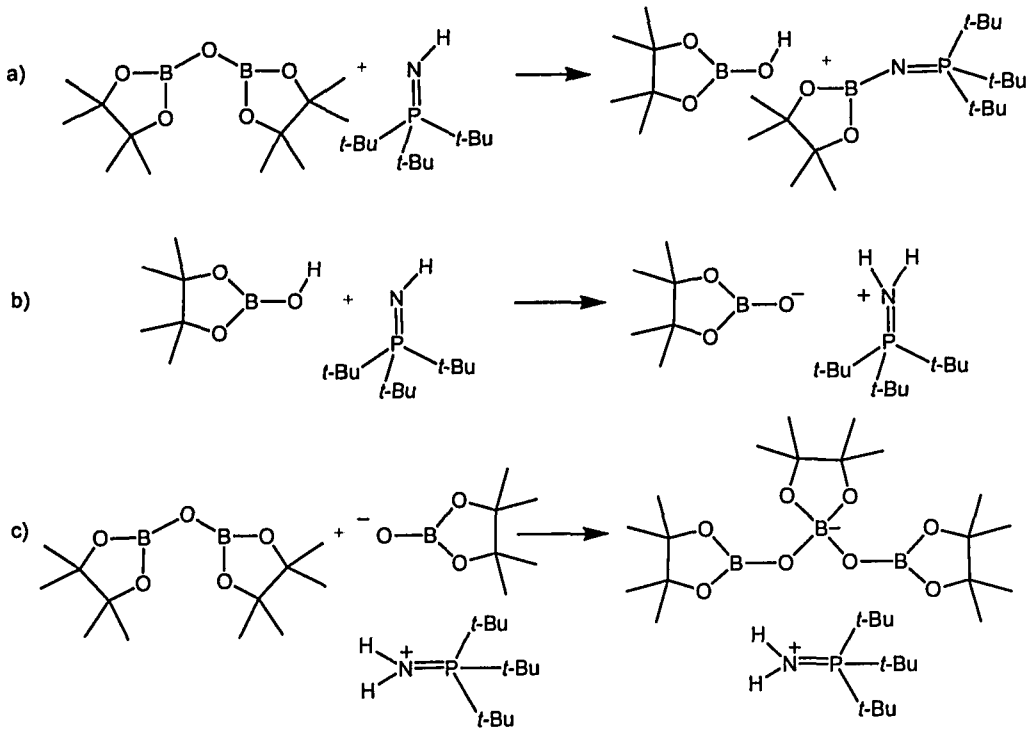

Figure 5.12: A plausible synthetic route for the formation of [*t*-Bu_3PNH_2][pinB(OBpin)$_2$] **(5.10)**.

It was thought that this borate might be useful as a counterion for olefin polymerization. Therefore the exchange reaction of the borate salt **(5.10)** with tritylchloride in toluene was attempted in an effort to synthesize the borate salt [CPh_3][pinB(OBpin)$_2$] and the phosphinimonium salt [*t*-Bu_3PNH_2][Cl]. Given the ease at which **5.10** crystallized out of solution, it was presumed that [CPh_3][pinB(OBpin)$_2$] would crystallize preferentially over the phosphinimonium salt. The isolation of [CPh_3][pinB(OBpin)$_2$] was not successful. Instead, only X-ray quality crystals of the phosphinimonium salt [*t*-Bu_3PNH_2][Cl] **(5.11)** were isolated. This indicates that the trityl borate salt may have formed but this could not unambiguously be determined. In the presence of water or strong acids such as HCl phosphinimonium salts can be synthesized from the parent phosphinimine. For example, the reaction of wet BPh_3 with HNP*i*-Pr_3 yielded the phosphinimonium salt, [*i*-Pr_3PNH_2][$HOBPh_3$] **(5.12)** in 24% yield. The solid state structures of **5.11** and **5.12** are depicted as ORTEP drawings in Figure 5.13 below.

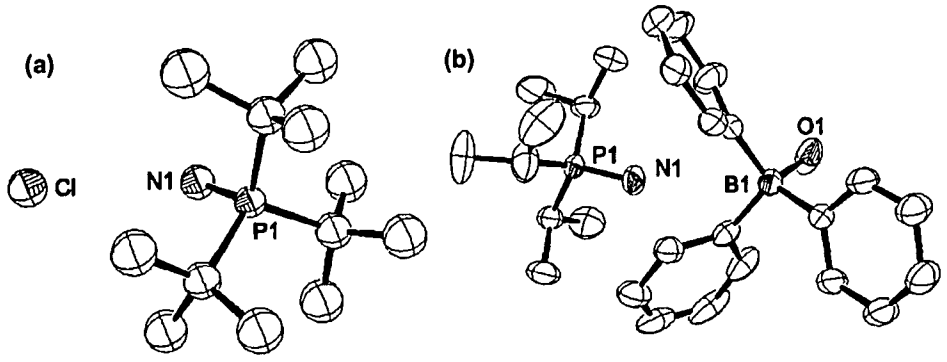

Figure 5.13: ORTEP diagram of (a) [*t*-Bu_3PNH_2][Cl] (**5.11**) and (b) [*i*-Pr_3PNH_2][$HOBPh_3$] (**5.12**) (30% probability thermal ellipsoids).

5.3.7 Decomposition Products Isolated from Reactions Using Pinacolborane

The reactions of catecholborane with phosphine oxides did not proceed cleanly. This may be due the instability of catecholborane in the presence of phosphines. Westcott, Blom and Marder reported that catecholborane (HBcat) decomposes in the presence of tertiary phosphines or phosphinorhodium complexes.[338] Smaller phosphines such as PMe_3, PEt_3 or PMe_2Ph react with HBcat to give [$(PR_3)_2BH_2$][$Bcat_2$], whereas larger phosphines such as PPh_3, P*i*-Pr_3 or PCy_3 react with HBcat to give $BH_3{\cdot}PR_3$ and B_2cat_3. The reactions of catecholborane with the rhodium hydrides $RhH(dppp)_2$ (dppp = 1,3-*bis*(diphenylphosphino)propane) and $RhH(PMe_3)_4$ resulted in the synthesis of [$RhH_2(DPPP)_2$][$Bcat_2$] and [$RhH_2(PMe_3)_4$][$Bcat_2$], respectively.

Even though pinacolborane (HBpin) has been proven to have a higher stability than HBcat in the presence of phosphines[292] similar compounds as those mentioned above have been encountered as byproducts within our own studies. From the reaction mixture of (*n*-$Bu_3PNBcat)_2$ (**4.2**) and HBpin, a few X-ray quality crystals of [pinBN(H)P*n*-Bu_3][$Bcat_2$] (**5.13**) were isolated. These crystals were characterized solely by X-ray crystallography. Anions of this type have been reported previously in the literature.[338, 339] The ORTEP diagram of [pinBN(H)P*t*-Bu_3][$Bcat_2$] is depicted in Figure 5.14 below.

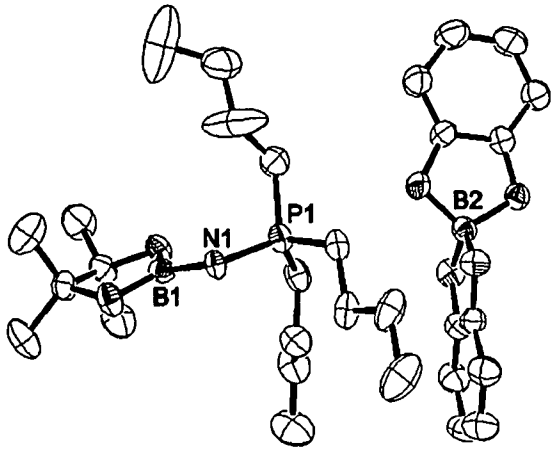

Figure 5.14: ORTEP drawing (30% thermal probability ellipsoids) of [pinBN(H)P*t*-Bu_3][$Bcat_2$] (**5.13**). Hydrogen atoms have been omitted for clarity.

From a crude reaction mixture of $AdNPEt_3$ and excess HBpin yielding AdN(H)Bpin (**3.13**) and PEt_3, the coordination compound $AdNH_2{\cdot}B(OBpin)_3$ (**5.14**) was isolated and characterized by X-ray crystallography and elemental analysis. The cleavage of a pinacol chelate from a boron centre must have occurred in the formation the $B(OBpin)_3$ fragment. The crystal structure of **5.14** is depicted in Figure 5.15.

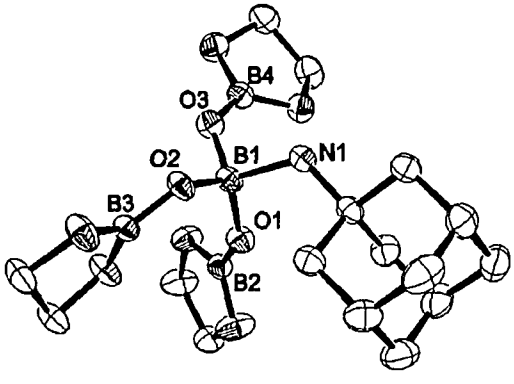

Figure 5.15: ORTEP diagram (30% probability thermal ellipsoids) of $AdNH_2{\cdot}B(OBpin)_3$ (**5.14**). Hydrogen atoms and the methyl groups on the pinacolyl moiety have been omitted for clarity.

The B-O bond distances of the central boron atom B(1) with the three adjacent oxygen atoms average 1.439(8) Å, whereas the B-O bond lengths (B(2)-O(1), B(3)-O(2) and B(4)-O(3)) average 1.334(8) Å. The longer B-O bond distances resemble the B-O bond lengths between the tetracoordinate boron atom and the oxygen atoms in $[Rh(PMe_3)_4][B_5O_6Ar_4]$ (1.46(1) – 1.478(8) Å when Ar = C_6H_4OMe; and 1.46(1) – 1.474(7) Å when Ar = C_6H_3-2,6-Me_2).[340] The nitrogen atom and central boron atom are separated by a distance of 1.643(5) Å, indicating a weak interaction. Borane complexes of this type could have possible application in cocatalyst development for olefin polymerization and investigations of this nature are currently in progress in our research group.

5.4 Summary

The reaction of phosphine oxides with pinacolborane resulted in the reduction of the phosphorus centre to yield the corresponding tertiary phosphine and the *bis*(pinacolboryl)oxide $O(Bpin)_2$ (**5.3**). Compound **5.3** was synthesized via a variety of methods and fully characterized via multi-nuclear NMR spectroscopy, IR spectroscopy, X-ray crystallography and elemental analysis. The reactivity of phosphine oxides and phosphinimines (Chapter 3) with pinacolborane prompted reactions of other high oxidation state phosphorus-containing compounds. However, thiophosphines (**5.6** and **5.7**) and phosphaylides (**5.8**) did not react in a similar manner with pinacolborane, and no obvious reduction of the phosphorus centre was observed by $^{31}P\{^1H\}$ NMR spectroscopy.

The reactivity of $O(Bpin)_2$ with metal complexes and main group compounds was of interest. Two equivalents of compound **5.3** reacted with zirconocene dimethyl to yield the zirconocene diboryloxide complex $Zr(C_5H_5)_2(OBpin)_2$ (**5.9**). Similar reactions using $AlMe_3$ instead of zirconocene dimethyl were conducted and the products of this reaction were tested *in situ* as a potential ethylene polymerization cocatalyst. Although this cocktail was not successful as an activation strategy for olefin polymerization by Group IV catalysts, tweaking of these reactions may prove useful as indicated by literature reports of related systems. The reaction of **5.3** with HNP*t*-Bu_3 yielded the borate-phosphinimonium salt [*t*-Bu_3PNH_2][pinB$(OBpin)_2$] (**5.10**) and *t*-$Bu_3PNBpin$ (**3.13**). With

the synthesis of novel olefin polymerization activators in mind, cation exchange of **5.10** was attempted by addition of one equivalent of tritylchloride; however, the phosphinimonium chloride salt [*t*-Bu_3PNH_2]Cl (**5.11**) was the only product isolated and characterized. With the same intent, efforts to synthesize $O(B(C_6F_5)_2)_2$ yielded instead the coordination compound *n*-$Bu_3PO{\cdot}HB(C_6F_5)_2$ (**5.4**). Several decomposition products from reactions using HBpin were isolated and characterized by X-ray crystallography. There is continued interest in the synthesis of boron-oxygen derivatives given their potential to serve as cocatalysts for ethylene polymerization.

6 Summary

Herein the chemistry of transition metal phosphinimide and main group phosphinimine complexes have been investigated. Specifically, an efficient route to vanadium phosphinimide imide dichloride complexes has been established. Subsequently these precursors were used to synthesize a variety of alkyl, aryl, amido, alkoxide and thiolate derivatives. Moreover, the dichloride derivatives acted as ethylene polymerization catalysts upon activation with MAO. However, the corresponding low to moderate polymerization activities rendered this type of system industrially unfavourable for the polymerization of ethylene under the attempted conditions.

Unlike the Group IV metallocene complexes, when titanium or vanadium phosphinimide/alkoxide complexes were treated with pinacolborane, extraction of the ligand was observed. From these reactions, the corresponding borylphosphinimine and/or borylalkoxide complexes were produced. These reactions inspired the studies of phosphinimines and other phosphorus containing compounds with borane reagents. Upon investigating the reactions of phosphinimines with pinacolborane using experimental evidence, a kinetic study and DFT-based methods, a relationship between the reactivity and the steric influence of the substituents on phosphorus was established. These reactions were progressed via two divergent pathways. The first mechanism involves the formation of hydrogen gas and the corresponding *N*-borylphosphinimine derivative, whereas reduction of the phosphorus centre and formation of the *N*-borylamine occurs in the second mechanism. The steric bulk provided by the substituents on phosphorus dictates the preferred mechanism. Experimentally, it was observed that when the substituents are bulky, such as in HNP*t*Bu$_3$ or HNP*n*-Bu(*t*-Bu)$_2$ the reaction with pinacolborane occurred via the former mechanism. Hence, when the less bulky phosphinimine complexes such as those derived from treatment of HNPEt$_3$ or HNP*n*-Bu$_3$ are treated with pinacolborane, the latter mechanism is preferred. The kinetic data was used to help formulate a reasonable mechanism for the latter pathway. The results of the DFT-based investigation of both mechanisms were in agreement with the experimental results and aided in the elucidation of a plausible explanation for the observed reactivity.

The influence of the steric bulk of the R groups of the phosphinimine fragment (NPR$_3$) was also realized in the bonding modes adopted by *N*-

catecholborylphosphinimine complexes. The smaller derivatives are dimeric whereas, the bulkiest derivative (R = *t*-Bu) is monomeric, in both solution and the solid state. Compound **4.5**, (*n*-Bu(*t*-Bu)$_2$PNBcat)$_2$, was determined to be monomeric in solution and dimeric in the solid state. Upon combining two dimeric species in solution the formation of the corresponding asymmetric dimer was apparent due to the ^{31}P-^{31}P coupling observed by peaks at new chemical shifts in the ^{31}P{^{1}H} NMR spectrum. The monomeric complexes in solution (R = *t*-Bu; R$_3$ = *n*-Bu(*t*-Bu)$_2$) were unaffected by the addition of dimeric complexes. The addition of the Lewis acid B(C$_6$F$_5$)$_3$ to the dimeric complexes resulted in the formation of the *N*-catecholborylphosphinimine-borane coordination complexes. Similarly, addition of B(C$_6$F$_5$)$_3$ to compound **4.5** also resulted in the formation of the *N*-catecholborylphosphinimine-borane coordination complex. This is an indication that the steric bulk and the Lewis acidity of the boron centre affect the reactivity at the nitrogen centre of the phosphinimine.

Finally, given the reactivity observed for the reactions of pinacolborane with phosphinimines, the analogous reactions of pinacolborane with phosphine oxides, phosphaylides and thiophosphines were attempted. The phosphine oxide derivatives with less bulky substituents on phosphorus were reduced in the presence of pinacolborane yielding diboryloxide O(Bpin)$_2$ (**5.3**) and the corresponding tertiary phosphine. Sterically hindered phosphine oxides, thiophosphines and phosphaylides did not undergo reduction to free tertiary phosphine evidenced by ^{31}P{^{1}H} NMR spectroscopy. Treatment of Zr(C$_5$H$_5$)$_2$Me$_2$ with O(Bpin)$_2$ (**5.3**) yielded the zirconium boryl oxide complex Zr(C$_5$H$_5$)$_2$(OBpin)$_2$ (**5.9**) and the phosphinimonium-borate salt (**5.10**). Attempts to synthesize boryloxide compounds and boraluminoxane complexes to aid in the polymerization of olefins by Group IV catalyst systems were unsuccessful thus far. However, continued research of boron-oxygen complexes is ongoing with the intention of synthesizing new activators for olefin polymerization.

Overall, this thesis provides detailed procedures for the synthesis of vanadium phosphinimide complexes and *N*-borylphosphinimine derivatives. Investigations of boron phosphinimine derivatives has aided in understanding the implications that the steric bulk of the substituents has on the reactivity of the phosphinimine moiety.

Bibliography

1. Staudinger, H.; Meyer, J., *Helv. Chim. Acta* **1919,** *2*, 635-46.
2. Buchner, W.; Wolfsberger, W., *Z. Naturforsch., B: Chem. Sci.* **1974,** *29*, (5-6), 328-34.
3. Birkofer, L.; Kim, S. M., *Ber.* **1964,** *97*, (7), 2100-1.
4. Stewart, J. C. Phosphinimide Complexes of Titanium: Synthesis and Reactivity Studies of a New Family of Organometallic Compounds. University of Windsor, Windsor, 2000 and references within.
5. King, A. S., et al., *Inorg. Chem.* **2004,** *43*, (11), 3507-3513.
6. Beddie, C. Titanium Phosphinimide Complexes for Ethylene Polymerization Catalysis: Synthetic, Computational and Polymerization Testing. University of Windsor, Windsor, 2004.
7. Wang, B., et al., *Inorg. Chem.* **2002,** *41*, (7), 1690-1691.
8. Dehnicke, K., et al., *Coord. Chem. Rev.* **1999,** *182*, 19-65.
9. Gibson, V. C., *J. Chem. Soc., Dalton Trans.* **1994,** (11), 1607-18.
10. Britovsek, G. J. P., et al., *Angew. Chem., Int. Ed. Engl.* **1999,** *38*, (4), 428-447.
11. Alt, H. G.; Koppl, A., *Chem. Rev.* **2000,** *100*, (4), 1205-1221.
12. Hlatky, G. G., *Coord. Chem. Rev.* **1999,** *181*, 243-296.
13. Kaminsky, W., *Catal. Today* **2000,** *62*, (1), 23-34.
14. Moehring, P. C.; Coville, N. J., *J. Organomet. Chem.* **1994,** *479*, (1-2), 1-29.
15. Sinn, H., et al., *Angew. Chem.* **1980,** *92*, 396-402.
16. Dehnicke, K.; Straehle, J., *Polyhedron* **1989,** *8*, (6), 707-26.
17. Stephan, D. W., et al., *Organometallics* **1999,** *18*, (11), 2046-2048.
18. Stephan, D. W., et al., *Organometallics* **1999,** *18*, (7), 1116-1118.
19. Stephan, D. W., et al. Supported phosphinimine-cyclopentadienyl catalysts for polymerization of olefins. 890581, 1999.
20. Guerin, F.; Stephan, D. W., *Angew. Chem., Int. Ed. Engl.* **1999,** *38*, (24), 3698-3701.
21. Ong, C. M., et al., *Organometallics* **1999,** *18*, (20), 4197-4204.
22. Guerin, F.; Stephan, D. W., *Angew. Chem., Int. Ed. Engl.***2000,** *39*, (7), 1298-1300.
23. Guerin, F., et al., *Organometallics* **2000,** *19*, (16), 2994-3000.
24. Kickham, J. E., et al., *Angew. Chem., Int. Ed. Engl.* **2000,** *39*, (18), 3263-3266.
25. Kickham, J. E., et al., *Organometallics* **2001,** *20*, (6), 1175-1182.
26. Guerin, F., et al., *Organometallics* **2001,** *20*, (16), 3466-3471.
27. Yue, N., et al., *Organometallics* **2001,** *20*, (21), 4424-4433.
28. Yue, N. L. S.; Stephan, D. W., *Organometallics* **2001,** *20*, (11), 2303-2308.
29. Courtenay, S.; Stephan, D. W., *Organometallics* **2001,** *20*, (7), 1442-1450.
30. Kickham, J. E., et al., *J. Am. Chem. Soc.* **2002,** *124*, (38), 11486-11494.
31. Ong, C., et al., *Organometallics* **2002,** *21*, (8), 1646-1653.
32. LePichon, L., et al., *Organometallics* **2002,** *21*, (7), 1362-1366.
33. Courtenay, S., et al., *Can. J. Chem.* **2003,** *81*, (12), 1471-1476.
34. Hawkeswood, S. B.; Stephan, D. W., *Inorg. Chem.* **2003,** *42*, (17), 5429-5433.
35. Masuda, J. D., et al., *Dalton Transactions* **2003,** (18), 3500-3505.
36. Stephan, D. W., et al., *Organometallics* **2003,** *22*, (9), 1937-1947.
37. Wei, P., et al., *Dalton Transactions* **2003,** (19), 3804-3810.
38. Chan, K. T. K., et al., *Organometallics* **2004,** *23*, (3), 381-390.
39. Graham, T. W., et al., *Organometallics* **2004,** *23*, (13), 3309-3318.
40. Hollink, E.; Stephan, D. W., *Comprehensive Coordination Chemistry II* **2004,** *4*, 105-173.
41. Beddie, C., et al., *Organometallics* **2004,** *23*, 5240-5241.
42. Stephan, D. W., et al. High temperature solution polymerization of olefins in the presence of metallocene catalyst system. 881233, 1998.

43. Shapiro, P. J., et al., *Organometallics* **1990,** *9*, 867.
44. Okuda, J., *Chem. Ber.* **1990,** *123*, 1649-1651.
45. Hollink, E., et al., *Dalton Trans.* **2003**, (20), 3968-3974.
46. Ma, K., et al., *J. Am. Chem. Soc.* **2004,** *126*, 5668-5669.
47. Choukroun, R., et al., *Bull. Soc. Chim.. France* **1979**, (9-10), 373-373.
48. Roesky, H. W., et al., *Z. Naturforsch., B: Chem. Sci.* **1989,** *44*, (1), 35-40.
49. Roesky, H. W., et al., *J. Chem. Soc., Chem. Commun.* **1989**, (6), 366-7.
50. Roesky, H. W., et al., *Inorg. Chem.* **1993,** *32*, (23), 5102-4.
51. Schomber, B. M., et al., *Inorg. Chem.* **1991,** *30*, (24), 4488-90.
52. Olms, P., et al., *Chem. Ber.* **1991,** *124*, (12), 2655-61.
53. Aistars, A., et al., *Inorg. Chem.* **1994,** *33*, (19), 4360-5.
54. Maleczka, R. E., et al., *J. Am. Chem. Soc.* **2003,** *125*, 7792-7793.
55. Hills, A., et al., *J.Chem. Soc., Dalton Trans.* **1993**, (23), 3609-17.
56. Al-Benna, S., et al., *Dalton* **2000**, (23), 4247-4257.
57. Aharonian, G., et al., *Organometallics* **2001,** *20*, (12), 2616-2622.
58. Jimenez-Tenorio, M.; Leigh, G. J., *Polyhedron* **1989,** *8*, (13-14), 1784-5.
59. Cummins, C. C., et al., *J. Am. Chem. Soc.* **1991,** *113*, (8), 2985-94.
60. Cummins, C. C., et al., *J. Am. Chem. Soc.* **1988,** *110*, (26), 8731-3.
61. Glueck, D. S., et al., *J. Am. Chem. Soc.* **1989,** *111*, (7), 2719-21.
62. Walsh, P. J., et al., *J. Am. Chem. Soc.* **1988,** *110*, (26), 8729-31.
63. Preuss, F.; Becker, H., *Z. Naturforsch., B: Chem. Sci.* **1986,** *41B*, (2), 185-90.
64. Preuss, F., et al., *Z. Naturforsch., B: Chem. Sci.* **1987,** *42*, (7), 881-8.
65. Preuss, F., et al., *Z. Naturforsch., B: Chem. Sci.* **1988,** *43*, (9), 1195-200.
66. Preuss, F., et al., *Z. Anorg. Allg. Chem.* **2000,** *626*, (12), 2446-2448.
67. Preuss, F., et al., *Z. Anorg. Allg. Chem.* **2000,** *626*, (12), 2446-2448.
68. Preuss, F., et al., *Z. Naturforsch., B: Chem. Sci.* **2001,** *56*, (3), 255-262.
69. Preuss, F., et al., *Z. Naturforsch., B: Chem. Sci.* **1989,** *44*, (3), 271-7.
70. Preuss, F., et al., *Z. Naturforsch., B: Chem. Sci.* **1984,** *39B*, (1), 61-8.
71. Preuss, F., et al., *Z. Anorg. Allg. Chem.* **1995,** *621*, (10), 1663-71.
72. Preuss, F., et al., *Z. Naturforsch., B: Chem. Sci.* **1986,** *41B*, (9), 1085-92.
73. Preuss, F., et al., *Z. Anorg. Allg. Chem.* **1993,** *619*, (11), 1827-33.
74. Preuss, F., et al., *Z. Naturforsch., B: Chem. Sci.* **1992,** *47*, (10), 1355-62.
75. Preuss, F., et al., *Z. Anorg. Allg. Chem.* **1992,** *609*, 45-50.
76. Preuss, F., et al., *Z. Naturforsch., B: Chem. Sci.* **2001,** *56*, (11), 1100-1108.
77. Preuss, F., et al., *Z. Naturforsch., B: Chem. Sci.* **1984,** *39B*, (11), 1510-17.
78. Preuss, F.; Towae, W., *Z. Naturforsch., B.* **1981,** *36B*, (9), 1130-5.
79. Preuss, F., et al., *Z. Anorg. Allg. Chem.* **2000,** *626*, (7), 1665-1675.
80. Preuss, F.; Tabellion, F., *Z. Naturforsch., B: Chem. Sci.* **2000,** *55*, (8), 735-737.
81. Preuss, F., et al., *Z. Anorg. Allg. Chem.* **1997,** *623*, (8), 1220-1228.
82. Preuss, F., et al., *Z. Naturforsch., B: Chem. Sci.* **1990,** *45*, (12), 1618-24.
83. Preuss, F., et al., *Z. Naturforsch., B: Chem. Sci.* **1999,** *54*, (11), 1396-1404.
84. Preuss, F.; Perner, J., *Z. Naturforsch., B: Chem. Sci.* **2000,** *55*, (1), 1-4.
85. Devore, D. D., et al., *J. Am. Chem. Soc.* **1987,** *109*, (24), 7408-16.
86. Hill, P. L., et al., *J. Chem. Soc., Chem. Commun.* **1995**, (7), 737-8.
87. Maatta, E. A., *Inorg. Chem.* **1984,** *23*, (17), 2560-1.
88. Wheeler, D. E., et al., *Polyhedron* **1998,** *17*, (5-6), 969-976.
89. de With, J., et al., *Organometallics* **1990,** *9*, (8), 2207-9.
90. Buijink, J.-K. F., et al., *J. Organomet. Chem.* **1995,** *497*, (1-2), 161-70.
91. Witte, P. T., et al., *J. Am. Chem. Soc.* **1997,** *119*, (43), 10561-10562.
92. Coles, M. P.; Gibson, V. C., *Polym. Bull. (Berlin)* **1994,** *33*, (5), 529-33.
93. Coles, M. P., et al., *J. Organomet. Chem.* **1999,** *591*, (1-2), 78-87.

94. Scheuer, S., et al., *Organometallics* **1995,** *14*, (6), 2627-9.
95. Arndt-Rosenau, M., et al. Vanadium imidoaryl complexes as catalysts for olefin polymerization. 1284269, 2003.
96. Lorber, C., et al., *Organometallics* **2004,** *23*, (8), 1845-1850.
97. Tabellion, F., et al., *Angew. Chem., Int. Ed. Engl.* **1998,** *37*, (9), 1233-1235.
98. Cloke, F. G. N., et al., *Chem.Comm.* **1999**, (23), 2363-2364.
99. de With, J.; Horton, A. D., *Angew. Chem.* **1993,** *105*, (6), 958-60 (See also Angew. Chem., Int. Ed. Engl., 1993, 32(6), 903-5).
100. de With, J., et al., *Organometallics* **1993,** *12*, (5), 1493-6.
101. Gambarotta, S., *Coord. Chem. Rev.* **2003,** *237*, (1-2), 229-243.
102. Hagen, H., et al., *Chem. Soc. Rev.* **2002,** *31*, (6), 357-364.
103. Gibson, V. C.; Spitzmesser, S. K., *Chem. Rev.* **2003,** *103*, (1), 283-315.
104. Natta, G., et al., *J. Am. Chem. Soc.* **1955,** *77*, 1708-10.
105. Natta, G., et al., *Chimica e l'Industria (Milan, Italy)* **1958,** *40*, 717-24.
106. Reardon, D., et al., *J. Am. Chem. Soc.* **1999,** *121*, (40), 9318-9325.
107. Ma, Y., et al., *Organometallics* **1999,** *18*, (15), 2773-2781.
108. Ma, Y., et al., *Organometallics* **2000,** *19*, (4), 718.
109. Chan, M. C. W., et al., *Chem. Comm.***1997**, (24), 2345-2346.
110. Motevalli, M., et al., *Organometallics* **1994,** *13*, (10), 4109-12.
111. Razavi, A. Production of syndiotactic polyolefins by fluorenyl-containing metallocene catalysts. 1179553, 2002.
112. Zambelli, A., et al., *Macromolecular Rapid Communications* **2001,** *22*, (5), 297-310.
113. Zambelli, A., et al., *Journal of Molecular Catalysis A: Chemical* **2000,** *152*, (1-2), 25-31.
114. De Rosa, C., et al., *Macromolecules* **1998,** *31*, (21), 7430-7435.
115. Doi, Y., et al., *Macromolecules* **1986,** *19*, (12), 2896-900.
116. Zambelli, A., et al., *Makromol. Chem.* **1968,** *112*, 160-82.
117. Natta, G., et al., *J. Am. Chem. Soc.* **1962,** *84*, 1488-90.
118. Feher, F. J.; Blanski, R. L., *J. Am. Chem. Soc.* **1992,** *114*, (14), 5886-7.
119. Feher, F. J.; Blanski, R. L., *Organometallics* **1993,** *12*, (3), 958-63.
120. Feher, F. J.; Walzer, J. F., *Inorg. Chem.* **1991,** *30*, (8), 1689-94.
121. Feher, F. J., et al., *J. Am. Chem. Soc.* **1991,** *113*, (9), 3618-19.
122. Carrick, W. L., *J. Am. Chem. Soc.* **1958,** *80*, 6455-6.
123. Murphy, V. J.; Turner, H., *Organometallics* **1997,** *16*, (12), 2495-2497.
124. Chan, M. C. W., et al., *Chem. Comm.* **1998**, (16), 1673-1674.
125. Nomura, K., et al., *Chem. Lett.* **2001**, 36-37.
126. Casagrande, A. C. A., et al., *Journal of Molecular Catalysis A: Chemical* **2004,** *212*, (1-2), 267-275.
127. Gibson, V. C. Metal imido complexes of Group V or VI metals as polymerization catalysts for olefins. 641804, 1995.
128. Chen, E. Y.-X.; Marks, T. J., *Chem. Comm.***2000,** *100*, (4), 1391-1434.
129. Sinn, H.; Kaminsky, W., *Adv. Organomet. Chem.* **1980,** *18*, 99-149.
130. Sinn, H., et al., *Angew. Chem., Int. Ed. Engl.* **1980,** *19*, 390-392.
131. Babushkin, D. E.; Britzinger, H., *J. Am. Chem. Soc.* **2002,** *124*, 12869-12873.
132. Pedetour, J. N., et al., *Macromol. Rapid Commun.* **2001,** *22*, 1095-1123.
133. Roesky, H. W., et al., *Acc. Chem. Res.* **2001,** *34*, 201-211.
134. Ystenes, M., et al., *J. Polym. Sci., A. Poly. Chem.* **2000,** *38*, 3106-3127.
135. Zurek, E.; Ziegler, T., *Organometallics* **2002,** *21*, 83-92.
136. Li, L.; Marks, T. J., *Organometallics* **1998,** *17*, (18), 3996-4003.
137. Sun, Y., et al., *Organometallics* **2000,** *19*, (9), 1625-1627.
138. Chen, Y.-X., et al., *J. Am. Chem. Soc.* **1997,** *119*, (10), 2582-2583.
139. Richter, B., et al., *Chem. Comm.* **2001**, 1286-1287.

140. Gibson, V. C., et al., *Inorg. Chem.* **2001,** *40*, 826-827.
141. Anulewicz-Ostrowska, R., et al., *Inorg. Chem.* **1999,** *38*, 3796-3800.
142. Anulewicz-Ostrowska, R., et al., *Inorg. Chem.* **2000,** *39*, (25), 5763-5767.
143. Harlan, C. J., et al., *J. Am. Chem. Soc.* **1995,** *117*, 6465.
144. Harlan, C. J., et al., *Organometallics* **1994,** *13*, 2957.
145. Landry, C. C., et al., *Angew. Chem., Int. Ed. Engl.* **1995,** *34*, 1201.
146. Wantanabi, M., et al., *Organometallics* **2001,** *20*, 460.
147. Dehnicke, K.; Weller, F., *Coord. Chem. Rev.* **1997,** *158*, 103-169.
148. Moehlen, M., et al., *Z. Anorg. Allg. Chem.* **1999,** *625*, (10), 1631-1637.
149. Courtenay, S., et al., *Organometallics* **2003,** *22*, (4), 818-825.
150. Holley, W. K., et al., *Inorg. Chim. Acta* **1995,** *239*, (1-2), 171-5.
151. Heshmatpour, F., et al., *Z. Anorg. Allg. Chem.* **1995,** *621*, (3), 443-50.
152. Courtenay, S., et al., *Z. Naturforsch., B: Chem. Sci.* **2002,** *57*, (10), 1184-1188.
153. Moehlen, M., et al., *Z. Anorg. Allg. Chem.* **1997,** *623*, (10), 1567-1576.
154. Moehlen, M., et al., *Z. Anorg. Allg. Chem.* **1998,** *624*, (2), 177-178.
155. Moehlen, M., et al., *Z. Anorg. Allg. Chem.* **2001,** *627*, (7), 1508-1512.
156. Azimi, K.; Neilson, R. H., *Journal of Cluster Science* **2002,** *13*, (4), 553-568.
157. Kroner, J., et al., *Chem. Ber.* **1993,** *126*, (9), 1995-2002.
158. Koelle, P., et al., *Chem. Ber.* **1995,** *128*, (3), 205-12.
159. Noth, H., et al., *Chem. Ber.* **1994,** *127*, (1), 81-85.
160. Davidson, M. G., et al., *Chem. Comm.* **1999,** (17), 1649-1650.
161. Li, B. L., et al., *Inorg. Chem.* **1989,** *28*, (3), 605-7.
162. Moehlen, M., et al., *Z. Anorg. Allg. Chem.* **1998,** *624*, (7), 1105-1110.
163. McWilliams, A. R., et al., *Chem. Comm.* **2002,** (10), 1102-1103.
164. Moehlen, M., et al., *Z. Anorg. Allg. Chem.* **1996,** *622*, (10), 1692-1700.
165. Walsh, D.; Stephan, D. W. Unpublished Results, Unpublished Results.
166. Courtenay, S., et al., *Angew. Chem., Int. Ed. Engl.* **2002,** *41*, (3), 498-501.
167. Sakai, T., et al., *J. Org. Chem.* **1994,** *59*, 7144-7147.
168. Boezio, A., et al., *J. Org. Chem.* **2003,** *68*, 3241-3245.
169. Hoesl, C. E., et al., *J. Comb. Chem.* **2003,** *5*, 155-160.
170. Fernandez, I.; Khiar, N., *Chem. Rev.* **2003,** *103*, 3651-3705.
171. Alvarez-Sarandes, R., et al., *Tetrahedron* **2001,** *57*, 5413.
172. Dhar, M. T. G., et al., *Ogr. Lett.* **2002,** *4*, (12), 2091-2093.
173. Shi, C., et al., *J. Org. Chem.* **1999,** *64*, 925.
174. Bonini, C., et al., *Tetrahedron* **2002,** *58*, 3507-3512.
175. Hinchley, S. L., et al., *Inorg. Chem.* **2004,** *43*, 5522-5528.
176. Lu, W.-C., *Jiegou Huaxue* **2000,** *19*, (6), 444-448.
177. Lu, W. C.; Sun, C. C., *THEOCHEM* **2002,** *593*, 1-7.
178. Magnusson, E., *J. Am. Chem. Soc.* **1993,** *115*, (3), 1051-61.
179. Reed, A. E.; Schleyer, P. v. R., *J. Am. Chem. Soc.* **1990,** *112*, (4), 1434-45.
180. Sundermann, A.; Schoeller, W. W., *J. Am. Chem. Soc.* **2000,** *122*, (19), 4729-4734.
181. Koketsu, J., et al., *Inorg. Chem.* **1997,** *36*, (4), 694-702.
182. Lu, W. C., et al., *J. Phys. Chem. A.* **1999,** *103*, (8), 1078-1083.
183. Lu, W. C., et al., *Chem. Phys. Lett.* **1999,** *311*, (6), 491-498.
184. Xue, Y.; Kim, C. K., *J. Phys. Chem. A* **2003,** *107*, (39), 7945-7951.
185. Bell, S. A., et al., *Chem. Comm.* **2000,** (15), 1375-1376.
186. Bell, S. A., et al., *J. Am. Chem. Soc.* **2002,** *124*, (36), 10698-10705.
187. Burland, M. C.; Meyer, T. Y., *Inorg. Chem.* **2003,** *42*, (11), 3438-3444.
188. Burland, M. C., et al., *J. Org. Chem.* **2004,** *69*, (19), 6173-6184.
189. Rivard, E., et al., *J. Am. Chem. Soc.* **2004,** *126*, (8), 2286-2287.
190. Harrison, D. J., et al., *Tetrahedron Lett.* **2004,** *45*, (46), 8493-8496.

191. Koester, R.; Morita, Y., *Angew. Chem.* **1965,** *77*, (13), 589-90.
192. Koester, R.; Morita, Y., *Angew. Chem., Intern. Ed. Engl.* **1966,** *5*, (6), 580.
193. Keglevich, G., et al., *Tetrahedron* **2000,** *56*, (1), 1-6.
194. Keglevich, G., et al., *Synth. Commun.* **2000,** *30*, (23), 4221-4231.
195. Keglevich, G., et al., *Perkin 1* **2000**, (24), 4451-4455.
196. Veige, A. S., et al., *Inorg. Chem.* **2003,** *42*, (20), 6204-6224.
197. Boezio, A., et al., *J. Am. Chem. Soc.* **2003,** *125*, 14260-14261.
198. Gamble, M. P., et al., *J. Org. Chem.* **1998,** *63*, 6068-6071.
199. Goubeau, J.; Keller, H., *Z.Anorg. Allg. Chem.* **1951,** *267*, 1.
200. Noth, H.; Schweizer, P., *Chem. Ber.* **1964,** *94*, 1464.
201. Maringgele, W., et al., *Organometallics* **1997,** *16*, (11), 2276-2284.
202. Komorowska, M., et al., *Inorg. Chem.* **1990,** *29*, (2), 289-94.
203. Weber, L., et al., *Eur. J. of Inorg. Chem.* **1999**, (7), 1193-1198.
204. Weese, K. J., et al., *Inorg. Chem.* **1987,** *26*, 2409.
205. Chen, H., et al., *Inorg. Chem.* **1990,** *30*, 2884.
206. Chisholm, M. H., et al., *Inorg. Chim. Acta* **1993,** *213*, 17.
207. Gibson, V. C., et al., *Polyhedron* **1997,** *16*, 2637.
208. Lulinski, S., et al., *Inorg. Chem.* **1999,** *38*, 4937.
209. Balkwill, J., E., et al., *Inorg. Chem.* **2002,** *41*, (13), 3548-52.
210. Fujdala, K. L., et al., *Inorg. Chem.* **2003,** *42*, (4), 1140-1150.
211. Hollink, E., et al., *Organometallics* **2004,** *23*, (7), 1562-1569.
212. Anfang, S., et al., *Z. Anorg. Allg. Chem.* **1998,** *624*, (1), 159-166.
213. Huber, S. R., et al., *Organometallics* **1993,** *12*, (1), 91-7.
214. Gibson, V. C., et al., *J. Organomet. Chem.* **1993,** *462*, (1-2), C12-C14.
215. Antonelli, D. M., et al., *Organometallics* **1997,** *16*, (12), 2500-2502.
216. Williams, D. N., et al., *J.Chem. Soc., Dalton Trans.* **1992**, (5), 739-51.
217. Poole, A. D., et al., *J. Chem. Soc., Chem. Commun.* **1992**, (3), 237-9.
218. Siemeling, U.; Gibson, V. C., *J. Organomet. Chem.* **1992,** *426*, (2), C25-C27.
219. Gibson, V. C.; Poole, A. D., *J. Chem. Soc., Chem. Commun.* **1995**, (22), 2261-2.
220. Antonelli, D. M., et al., *J. Organomet. Chem.* **1992,** *438*, (1-2), C4-8.
221. Buijink, J.-K. F., et al., *Organometallics* **1994,** *13*, (8), 2922-4.
222. Cromer, D. T.; Mann, J. B., *Acta Crystallogr., Sect. A: Found. Crystallogr.* **1968,** *24*, (Pt. 2), 321-4.
223. Choukroun, R., et al., *Trans. Metal Chem.* **1979,** *4*, (4), 249-51.
224. Schweda, E., et al., *Z. Anorg. Allg. Chem.* **1985,** *528*, 117-24.
225. Gambarotta, S., et al., *Inorg. Chem.* **1984,** *23*, (12), 1739-47.
226. Haddad, T. S., et al., *Organometallics* **1993,** *12*, (7), 2420-2.
227. Coles, M. P., et al., *J. Chem. Soc., Chem. Commun.* **1995**, (16), 1709-11.
228. Solan, G. A., et al., *Organometallics* **1994,** *13*, (7), 2572-4.
229. Nugent, W. A., *Inorg. Chem.* **1983,** *22*, (6), 965-9.
230. Nugent, W. A.; Haymore, B. L., *Coord. Chem. Rev.* **1980,** *31*, (2), 123-75.
231. Bradley, D. C., et al., *Polyhedron* **1983,** *2*, (8), 849-52.
232. Slawisch, A., *Z. Anorg. Allg. Chem.* **1970,** *374*, (3), 291-6.
233. Shihada, A. F., *Z. Anorg. Allg. Chem.* **1974,** *408*, (1), 9-14.
234. Rehder, D., *Bull. Mag. Res.* **1982,** *4*, (1-2), 33-83.
235. http://mutuslab.cs.uwindsor.ca/schurko/nmrcourse/notes.htm.
236. Hollink, E. Group IV Phosphinimide Complexes in Catalysis. University of Windsor, Windsor, 2003.
237. Smith, P. D., et al., *Inorg. Chem.* **1985,** *24*, (19), 2997-3002.
238. Budzelaar, P. H. M., et al., *Eur. J. Inorg. Chem.* **1998**, (10), 1485-1494.
239. Feghali, K., et al., *Organometallics* **2002,** *21*, (5), 968-976.

240. Bouma, R. J., et al., *Inorg. Chem.* **1984,** *23*, (17), 2715-18.
241. Lorber, C., et al., *Inorg. Chem.* **2002,** *41*, (16), 4217-4226.
242. Koehler, F. H.; Proessdorf, W., *Z. Naturforsch., B: Chem. Sci.* **1977,** *32B*, (9), 1026-9.
243. Hall, V. M., et al., *J. Organomet. Chem.* **1981,** *209*, (1), 69-76.
244. Cotton, F. A., et al., *J. Chem. Soc., Chem. Commun.* **1983**, (23), 1377-8.
245. Jacob, K., et al., *Z. Anorg. Allg. Chem.* **1976,** *427*, (1), 75-84.
246. Pavia, D. L., et al., *Introduction to Spectroscopy: A Guide for Students of Organic Chemistry*. Saunders College Publishing: 1979.
247. Wong, T.-W., et al., *Inorg. Chem.* **1999,** *38*, (26), 6181-6186.
248. Berno, P., et al., *Organometallics*, 1994; 'Vol.' 13, pp 1052-4.
249. Berno, P., et al., *Organometallics* **1994,** *13*, (4), 1052-4.
250. Berno, P.; Gambarotta, S., *Organometallics* **1994,** *13*, (7), 2569-71.
251. Song, J.-I., et al., *J. Am. Chem. Soc.* **1994,** *116*, (15), 6927-8.
252. Montilla, F., et al., *J. Chem. Soc., Dalton Trans. Inorg. Chem.* **1999**, (16), 2893-2896.
253. Montilla, F., et al., *Inorg. Chem.* **1999,** *38*, (20), 4462-4466.
254. Schumann, H., *Inorg. Chem.* **1996,** *35*, (7), 1808-13.
255. Hagen, H., et al., *Inorg. Chem.* **2000,** *39*, (18), 3970-3977.
256. Carofiglio, T., et al., *Inorg. Chem.* **1989,** *28*, (24), 4417-19.
257. Weber, K., et al., *Z. Anorg. Allg. Chem.* **2003,** *629*, (5), 744-754.
258. Kanamori, K., *Coord. Chem. Rev.* **2003,** *237*, (1-2), 147-161.
259. Heater, S. J., et al., *Inorg. Chem.* **2000,** *39*, (17), 3881-3889.
260. Dutta, S. K., et al., *Inorg. Chem.* **1999,** *38*, (9), 1982-1988.
261. Holwerda, R. A., et al., *Inorg. Chem.* **1998,** *37*, (1), 64-68.
262. Fukuda, I., et al., *Chem. Lett.* **1997**, (5), 463-464.
263. Czernuszewicz, R. S., et al., *Inorg. Chem.* **1994,** *33*, (26), 6116-19.
264. Fujdala, K. L.; Tilley, T. D., *Chem. Mater.* **2002,** *14*, (3), 1376-1384.
265. Carrano, C. J., et al., *Inorg. Chem.* **1994,** *33*, (4), 646-55.
266. Kempe, R.; Spannenberg, A., *Z. fuer Kristall. - New Cryst. Struct.* **1997,** *212*, (3), 485-486.
267. Priebsch, W.; Rehder, D., *Inorg. Chem.* **1990,** *29*, (16), 3013-19.
268. Wolff, F., et al., *Eur. J. .Inorg. Chem.***2003**, (4), 628-632.
269. Spandl, J., et al., *Z. Anorg. Allg. Chem.* **2000,** *626*, (10), 2125-2132.
270. Rosenthal, E. C. E.; Girgsdies, F., *Z. Anorg. Allg. Chem.* **2002,** *628*, (8), 1917-1920.
271. Maringgele, W., et al., *Z. Naturforsch., B: Chem. Sci.* **1978,** *33B*, (6), 673-5.
272. Perrin, D. D.; Armarego, W. L. F., *Purification of Laboratory Chemicals*. Butterworth-Heinemann Ltd.: Linacre House, Jordan Hill, Oxford, 1994.
273. Lindsay, R. O.; Allen, C. F. H., *Org. Synth.* **1942,** *22*, 96-8.
274. Wolfsberger, W., *Z. Naturforsch., B: Chem. Sci.* **1975,** *30B*, (11-12), 907-13.
275. Brainard, R. L., et al., *Organometallics* **1986,** *5*, 1481-1490.
276. Engle, T. W., et al., *J. Med. Chem.* **1982,** *25*, 1347-1357.
277. Krolski, M. E., et al., *J. Agric. Food Chem.* **1992,** *40*, 458.
278. *GAUSSIAN 98*, version 1998; Pittsburgh, PA, 1998.
279. *Gaussian 03, Revision C.02*, Gaussian, Inc.: Wallingford, CT, 2004.
280. Becke, A. D., *J. Chem. Phys.* **1993,** *98*, 1372.
281. Becke, A. D., *J. Chem. Phys.* **1993,** *98*, 5648.
282. Stephens, P. J. D., F. J.; Chabalowski, C. F.; Frisch, M. J., *J. Chem. Phys.* **1994,** *98*, 11623.
283. Lee, C. Y., W.; Parr, R. G., *Phys. Rev. B.* **1988,** *37*, 785.
284. Harrison, K.; Marks, T. J., *J. Am. Chem. Soc.* **1992,** *114*, 9220-9221.
285. Pereira, S.; Srebnik, M., *J. Am. Chem. Soc.* **1995,** *14*, 3127-3128.
286. Fieselmann, B. F., et al., *Inorg. Chem.* **1978,** *17*, (7), 1841-1848.
287. Hartwig, J. F., et al., *J. Am. Chem. Soc.* **1996,** *118*, (44), 10936-10937.
288. Al-Juaid, S. S., et al., *J. Organomet. Chem.* **1990,** *385*, (1), 13-21.

289. Bartlett, R. A., et al., *J. Am. Chem. Soc.* **1988,** *110*, (2), 446-9.
290. Maennig, D., et al., *J. Organomet. Chem.* **1986,** *310*, (1), 1-20.
291. Paciorek, K. J. L., et al., *Inorg. Chem.* **1988,** *27*, (14), 2432-6.
292. Crudden, C. M., et al., *J. Am. Chem. Soc.* **2004,** *126*, (30), 9200-9201.
293. Allaoud, S., et al., *J. Organomet. Chem.* **1994,** *469*, (1), 59-68.
294. Braun, U., et al., *Eur. J. .Inorg. Chem.* **2002,** (5), 1132-1145.
295. Chen, H., et al., *J. Am. Chem. Soc.* **1990,** *112*, (3), 1048-55.
296. Erker, G., et al., *Chem. Ber.* **1994,** *127*, (7), 1331-2.
297. Hommer, H., et al., *Eur. J. .Inorg. Chem.* **1998,** (10), 1519-1527.
298. Weber, L., et al., *Z. Naturforsch., B: Chem. Sci.* **1999,** *54*, (3), 363-371.
299. Baker, R. T., et al., *J. Organomet. Chem.* **1995,** *498*, (2), 109-17.
300. Hamilton, M. G., et al., *J. Organomet. Chem.* **2003,** *680*, (1-2), 143-147.
301. Burgess, K., et al., *J. Am. Chem. Soc.* **1992,** *114*, (24), 9350-9.
302. Harrison, K. N.; Marks, T. J., *J. Am. Chem. Soc.* **1992,** *114*, (23), 9220-1.
303. Evans, D. A.; Fu, G. C., *J. Am. Chem. Soc.* **1991,** *113*, (10), 4042-3.
304. Yamamoto, Y., *Yuki Gosei Kagaku Kyokaishi* **1974,** *32*, (7), 544-51.
305. Lane, C. F.; Kabalka, G. W., *Tetrahedron* **1976,** *32*, (9), 981-90.
306. Maennig, D.; Noeth, H. Hydroboration of alkenes and alkynes with catecholborane. 3528320, 1987.
307. Burgess, K.; van der Donk, W. A., *Organometallics* **1994,** *13*, (9), 3616-20.
308. Tolman, C. A., *Chem. Rev.***1977,** *77*, (3), 313-48.
309. Clegg, W., et al., *J. Chem. Soc. Dalton Trans.* **1997**, 839-846.
310. Coapes, R. B., et al., *J. Chem. Soc., Dalton Trans.* **2001**, 1201-1209.
311. Han, H., et al., *Polym. Prepr. (Am. Chem. Soc., Div. Polym. Chem.)* **2002,** *43*, (2), 82-83.
312. Nakabayashi, N.; Masuhara, E., *J. Biomed. Mat. Res.* **1978,** *12*, (2), 149-65.
313. Sonnenschein, M. F., et al. Organoborane amine complex polymerization initiators and polymerizable compositions. 2003076485, 2003.
314. Samuel, E.; Rausch, M. D., *J. Am. Chem. Soc.* **1973,** *95*, (19), 6263-7.
315. Smith, M. B.; March, J., *March's Advanced Organic Chemistry: Reactions, Mechanisms, and Structure*. 5th ed.; Jonh Wiley and Sons, Inc.: 2001; p 1231.
316. Parks, D. J., et al., *Angew. Chem., Int. Ed. Engl.* **1995,** *34*, (7), 809-11.
317. Leroy, J., et al., *Tetrahedron* **1980,** *36*, (13), 1931-6.
318. Stankevic, M., et al., *Synlett* **2004**, (2), 311-315.
319. Stankevic, M.; Pietrusiewicz, K. M., *Synlett* **2003**, (7), 1012-1016.
320. Cynkier, I.; Furmanova, N., *Crys. Structure Comm.* **1980,** *9*, (2), 307-12.
321. Cardin, C. J., et al., *J. Chem. Res., Synop.* **1983**, (4), 93.
322. Bochmann, M., et al., *Spec. Publ. - R. Soc. Chem.* **2000,** *253*, (Contemporary Boron Chemistry), 10-19.
323. Beckett, M. A., et al., *J. Chem. Soc. Dalton Trans.* **2001**, (11), 1768-1772.
324. Beckett, M. A., et al., *Inorg. Chem. Comm.* **2000,** *3*, (10), 530-533.
325. Hartwig, J. F.; De Gala, S. R., *J. Am. Chem. Soc.* **1994,** *116*, (8), 3661-2.
326. Mitzel, N. W., et al., *J. Am. Chem. Soc.* **1996,** *118*, (50), 12673-12682.
327. Bart, J. C. J., *J..Chem. Soc. .B: Phys. Org.* **1969**, (4), 350-65.
328. Booij, M., et al., *Organometallics* **1993,** *12*, (9), 3531-40.
329. Bestmann, H. J.; Arenz, T., *Angew. Chem.* **1986,** *98*, (6), 571-2.
330. Jiang, F., et al., *Angew. Chem., Int. Ed. Engl.* **2003,** *42*, (23), 2651-2653.
331. Welborn, H. C. WO9201005, 1992.
332. Langhauser, F., et al. 1992.
333. Kristen, M. O.; Fischer, D. 1998.
334. Koester, R., et al., *Chem. Ber.* **1986,** *119*, (4), 1174-88.
335. Bohnen, H. 2002.

336. Dunn, H. E., et al., *J. Org. Chem.* **1968,** *33*, (12), 4483-4486.
337. Lang, A., et al., *Chem. Ber.* **1997,** *130*, (3), 363-369.
338. Westcott, S. A., et al., *Inorg. Chem.* **1993,** *32*, (10), 2175-82.
339. Mohr, S., et al., *Z. Naturforsch.* **1990,** *45B*, 308.
340. Nishihara, Y., et al., *Inorg. Chem.* **2002,** *41*, (16), 4090-4092.

7 Appendices

Appendix A: Supplementary X-Ray Data (Chapter 2-5)

Supplementary X-ray data for all structures reported in this thesis are located on the CD attached to the back cover of this thesis.

Appendix B: Kinetic Data (Chapter 3)

Table 7.1: An example of a data set collected for the reaction of varying amounts of $Me_3SiNPEt_3$ with excess HBpin using different delay times (d1). Standard deviation is given by the symbol σ, concentrations ([ ]) are measured in mol L^{-1}.

Initial $[Me_3SiNPEt_3]$ (mol L^{-1})	Delay time (d1) (s)	Integration of $Me_3SiNPEt_3$	Integration of PEt_3	$[Me_3SiNPEt_3]$	Average $[Me_3SiNPEt_3]$ and σ	$[PEt_3]$	Average $[PEt_3]$ and σ
0.0375	60	0.106	0.657	0.005	0.005	0.032	0.032
0.0375	25	0.114	0.662	0.006		0.032	
0.0375	10	0.120	0.763	0.005	± 3.99E-04	0.032	± 3.99E-04
0.0375	5	0.143	0.832	0.005		0.032	
0.0375	1	0.154	0.975	0.005		0.032	
0.075	60	0.247	1.371	0.011	0.012	0.064	0.063
0.075	25	0.262	1.384	0.012		0.063	
0.075	10	0.281	1.509	0.012	± 9.08E-04	0.063	± 9.08E-04
0.075	5	0.317	1.557	0.013		0.062	
0.075	1	0.362	1.923	0.012		0.063	
0.150	60	0.550	2.796	0.025	0.025	0.125	0.125
0.150	25	0.594	2.947	0.025		0.125	
0.150	10	0.595	3.146	0.024	± 9.35E-04	0.126	± 9.35E-04
0.150	5	0.660	3.396	0.024		0.126	
0.150	1	0.693	3.518	0.025		0.125	
0.450	60	1.050	7.491	0.055	0.056	0.395	0.394
0.450	25	1.064	7.504	0.056		0.394	
0.450	10	1.188	8.302	0.056	± 2.64E-03	0.394	± 2.64E-03
0.450	5	1.185	8.467	0.055		0.395	
0.450	1	1.492	9.988	0.058		0.392	

Table 7.2: The concentrations of $Me_3SiNPEt_3$ over time for reactions 1-5 (excess HBpin and varying amounts of $Me_3SiNPEt_3$). The initial concentrations of $Me_3SiNPEt_3$ are given in round brackets.

Time (min)	1 (0.0375 M)	2 (0.075 M)	3 (0.15 M)	4 (0.3 M)	5 (0.45 M)
0	0.0375	0.0750	0.1500	0.3000	0.4500
900	0.0301	0.0619	0.1236	0.2441	0.3592
1220	0.0277	0.0571	0.1153	0.2253	0.3281
1340	0.0265	0.0553	0.1113	0.2191	0.3165
2555	0.0205	0.0435	0.0854	0.1692	0.2404
6480	0.0074	0.0182	0.0365	0.0666	0.0909
9800	0.0031	0.0073	0.0152	0.0340	0.0361

Table 7.3: Summary of the concentrations of HBpin over time for reactions 6-9 (excess amount of $Me_3SiNPEt_3$ and varying amounts of HBpin). The initial concentrations of HBpin are given in round brackets.

Time (min)	6 (0.0782 M)	7 (0.117 M)	8 (0.155 M)	9 (0.196 M)
0	0.078	0.117	0.155	0.196
210	0.073	0.105	0.138	0.176
1075	0.053	0.081	0.104	0.137
1485	0.050	0.071	0.094	0.121
2555	0.036	0.062	0.075	0.092
2900	0.038	0.052	0.067	0.080
3920	0.026	0.038	0.055	0.065
4190	0.027	0.041	0.051	0.062
5610	0.023	0.028	0.036	0.047

Table 7.4: The natural logarithmic value (ln[$Me_3SiNPEt_3$]) of the concentration of $Me_3SiNPEt_3$ in each reaction for the reaction 1 – 5 (excess $HBO_2C_2(CH_3)_4$ (3.45 M) and varying amounts of $Me_3SiNPEt_3$). The initial concentrations of $Me_3SiNPEt_3$ are given in round brackets.

Time (min)	1 (0.0375 M)	2 (0.075 M)	3 (0.15 M)	4 (0.3 M)	5 (0.45 M)
0	-3.283	-2.590	-1.897	-1.204	-4.714
900	-3.502	-2.782	-2.091	-1.410	-1.601
1220	-3.586	-2.862	-2.160	-1.490	-1.306
1340	-3.632	-2.896	-2.196	-1.518	-1.215
2555	-3.887	-3.134	-2.461	-1.777	-0.764
6480	-4.902	-4.007	-3.310	-2.709	-0.226
9800	-5.780	-4.914	-4.189	-3.382	-0.084

Table 7.5: The natural logarithmic value (ln[HBpin]) of the concentration of HBpin in each reaction for reactions 6-9 (excess $Me_3SiNPEt_3$ (1.27 M) and varying amounts HBpin). The initial concentrations of are given in round brackets.

Time (min)	6 (0.0782 M)	7 (0.117 M)	8 (0.155 M)	9 (0.196 M)
0	-2.548	-2.146	-1.864	-1.630
210	-2.623	-2.252	-1.980	-1.739
1075	-2.931	-2.519	-2.259	-1.986
1485	-2.992	-2.642	-2.366	-2.113
2555	-3.323	-2.785	-2.597	-2.383
2900	-3.258	-2.962	-2.704	-2.532
3920	-3.635	-3.264	-2.907	-2.733
4190	-3.613	-3.192	-2.970	-2.773
5610	-3.752	-3.560	-3.318	-3.059

Appendix C: Data from the Computational Study (Chapter 3)

Table 7.6: Optimized (B3LYP/6-311+G(2df,p)//B3LYP-6-31G(d)) energy values for the reaction of $HNPH_3$ and $HBO_2C_2H_4$ in the gas phase for both *pathway 1* and *pathway 2*.

Type of Complex	Complexes	Surface Energy (Hartrees)	Relative Energy (kcal/ mol)
Pathway 1			
Starting Materials	$HNPH_3 + HBO_2C_2H_4$	-653.2113646	0
Initial coordination complex	$H_3PN(H)B(H)O_2C_2H_4$	-653.2197412	-5.3
Transition structure	H_2-$H_3PNBO_2C_2H_4$	-653.1569807	34.1
Second coordination complex	H_2-$H_3PNBO_2C_2H_4$	-653.2413686	-18.8
Products separated infinitely	$H_2 + H_3PNBO_2C_2H_4$	-653.2406922	-18.4
Pathway 2			
Starting Materials	$HNPH_3 + HBO_2C_2H_4$	-653.2113646	0
Initial coordination complex	$H_3PN(H)B(H)O_2C_2H_4$	-653.2197412	-5.3
Transition structure	PH_3-$H_2NBO_2C_2H_4$	-653.1607343	31.8
Second coordination complex	PH_3-$H_2NBO_2C_2H_4$	-653.2993181	-55.2
Products separated infinitely	$PH_3 + H_2NBO_2C_2H_4$	-653.2944313	-52.1

Table 7.7: Optimized (B3LYP/6-311+G(2df,p)//B3LYP-6-31G(d)) energy values for the reaction of HNP*t*-Bu_3 and $HBO_2C_2H_4$ in the gas phase for both *pathway 1* and *pathway 2*.

Type of Complex	Complexes	Surface Energy (Hartrees)	Relative Energy (kcal/ mol)
Pathway 1			
Starting materials	HNP*t*-Bu_3 + $HBO_2C_2H_4$	-1125.119615	0
Initial coordination complex	*t*-$Bu_3PN(H)B(H)O_2C_2H_4$	-1125.12131	-1.1
Transition structure	H_2-*t*-$Bu_3PNBO_2C_2H_4$	-1125.068921	31.8
Second coordination complex	H_2-*t*-$Bu_3PNBO_2C_2H_4$	-1125.151459	-20.0
Products separated infinitely	H_2 + *t*-$Bu_3PNBO_2C_2H_4$	-1125.150653	-19.5
Pathway 2			
Starting materials	HNP*t*-Bu_3 + $HBO_2C_2H_4$	-1125.119615	0
Initial coordination complex	*t*-$Bu_3PN(H)B(H)O_2C_2H_4$	-1125.12131	-1.1
Transition structure	P*t*-Bu_3-$H_2NBO_2C_2H_4$	-1125.050161	43.6
Second coordination complex	P*t*-Bu_3-$H_2NBO_2C_2H_4$	-1125.176776	-35.9
Products separated infinitely	P*t*-Bu_3 + $H_2NBO_2C_2H_4$	-1125.165901	-29.0

Table 7.8: Optimized (B3LYP/6-311+G(2df,p)//B3LYP-6-31G(d)) energy values for the reaction of $HNPH_3$ and HBpin in the gas phase for both *pathway 1* and *pathway 2*.

Type of Complex	Complexes	Surface Energy (Hartrees)	Relative Energy (kcal/ mol)
Pathway 1			
Starting materials	$HNPH_3$ + HBpin	-810.5286784	0
Initial coordination complex	$H_3PN(H)B(H)$pin	-810.5326842	-2.5
Transition structure	H_2-H_3PNBpin	-810.4726974	35.1
Second coordination complex	H_2-H_3PNBpin	-810.6166641	-55.2
Products separated infinitely	H_2 + H_3PNBpin	-810.5577149	-18.2
Pathway 2			
Starting materials	$HNPH_3$ + HBpin	-810.5286784	0
Initial coordination complex	$H_3PN(H)B(H)$pin	-810.5326842	-2.5
Transition structure	PH_3-H_2NBpin	-810.4770511	32.4
Second coordination complex	PH_3-H_2NBpin	-810.6166641	-55.2
Products separated infinitely	PH_3 + H_2NBpin	-810.6147814	-54.0

Table 7.9: Optimized (B3LYP/6-311+G(2df,p)//B3LYP-6-31G(d)) energy values for the reaction of HNP*t*-Bu_3 and HBpin in the gas phase for both *pathway 1* and *pathway 2*.

Type of Complex	Complexes	Surface Energy (Hartrees)	Relative Energy (kcal/ mol)
Pathway 1			
Starting materials	HNP*t*-Bu_3 + HBpin	-1282.436929	0
Initial coordination complex	*t*-Bu_3PN(H)B(H)pin	-1282.430335	4.1
Transition structure	H_2-*t*-Bu_3PNBpin	-1282.382056	34.4
Second coordination complex	H_2-*t*-Bu_3PNBpin	-1282.467549	-19.2
Products separated infinitely	H_2 + *t*-Bu_3PNBpin	-1282.46692	-18.8
Pathway 2			
Starting materials	HNP*t*-Bu_3 + HBpin	-1282.436929	0
Initial coordination complex	*t*-Bu_3PN(H)B(H)pin	-1282.430335	4.14
Transition structure	P*t*-Bu_3-H_2NBpin	-1282.363178	46.3
Second coordination complex	P*t*-Bu_3-H_2NBpin	-1282.498051	-38.4
Products separated infinitely	P*t*-Bu_3 + H_2NBpin	-1282.486251	-30.9

Table 7.10: Optimized (B3LYP/6-311+G(2df,p)//B3LYP-6-31G(d)) energy values for the reaction of $HNPH_3$ and $HBO_2C_2(CF_3)_4$ in the gas phase for both *pathway 1* and *pathway 2*.

Type of Complex	Complexes	Surface Energy (Hartrees)	Relative Energy (kcal/ mol)
Pathway 1			
Starting materials	$HNPH_3$ + $HBO_2C_2(CF_3)_4$	-2001.811033	0
Initial coordination complex	$H_3PN(H)B(H)O_2C_2(CF_3)_4$	-2001.841637	-19.2
Transition structure	H_2-$H_3PNBO_2C_2(CF_3)_4$	-2001.773242	23.7
Second coordination complex	H_2-$H_3PNBO_2C_2(CF_3)_4$	-2001.851825	-25.6
Products separated infinitely	H_2 + $H_3PNBO_2C_2(CF_3)_4$	-2001.852189	-25.8
Pathway 2			
Starting materials	$HNPH_3$ + $HBO_2C_2(CF_3)_4$	-2001.811033	0
Initial coordination complex	$H_3PN(H)B(H)O_2C_2(CF_3)_4$	-2001.841637	-19.2
Transition structure	PH_3-$H_2NBO_2C_2(CF_3)_4$	-2001.77506	22.6
Second coordination complex	PH_3-$H_2NBO_2C_2(CF_3)_4$	-2001.906929	-60.2
Products separated infinitely	PH_3 + $H_2NBO_2C_2(CF_3)_4$	-2001.904338	-58.5

Table 7.11: Optimized (B3LYP/6-311+G(2df,p)//B3LYP-6-31G(d)) energy values for the reaction of HNP*t*-Bu_3 and $HBO_2C_2(CF_3)_4$ in the gas phase for both *pathway 1* and *pathway 2*.

Type of Complex	Complexes	Surface Energy (Hartrees)	Relative Energy (kcal/ mol)
Pathway 1			
Starting materials	HNP*t*-Bu_3 + $HBO_2C_2(CF_3)_4$	-2473.719284	0
Initial coordination complex	*t*-$Bu_3PN(H)B(H)O_2C_2(CF_3)_4$	-2473.744861	-16.0
Transition structure	H_2-*t*-$Bu_3PNBO_2C_2(CF_3)_4$	-2473.685881	21.0
Second coordination complex	H_2-*t*-$Bu_3PNBO_2C_2(CF_3)_4$	-2473.767265	-30.1
Products separated infinitely	H_2 + *t*-$Bu_3PNBO_2C_2(CF_3)_4$	-2473.76784	-30.5
Pathway 2			
Starting materials	HNP*t*-Bu_3 + $HBO_2C_2(CF_3)_4$	-2473.719284	0
Initial coordination complex	*t*-$Bu_3PN(H)B(H)O_2C_2(CF_3)_4$	-2473.744861	-16.0
Transition structure	P*t*-Bu_3-$H_2NBO_2C_2(CF_3)_4$	-2473.664861	34.2
Second coordination complex	P*t*-Bu_3-$H_2NBO_2C_2(CF_3)_4$	-2473.790826	-44.9
Products separated infinitely	P*t*-Bu_3 + $H_2NBO_2C_2(CF_3)_4$	-2473.775807	-35.5

8 Vita Auctoris

Sarah Bess Hawkeswood

Date of Birth: June 15th, 1976

Place of Birth: Vancouver, British Columbia, Canada

EDUCATION

- **Ph.D. Candidate, Inorganic Chemistry**, 1999-Present. University of Windsor, Windsor, Ontario, Canada
- **Honors B.Sc., Chemistry**, 1995-1999. University of Toronto, Toronto, Ontario, Canada

SCHOLARSHIPS AND AWARDS

- Ontario Graduate Scholarship, Ontario Government and University of Windsor (2002-2004)
- University of Windsor Tuition Scholarship, University of Windsor (2001-2004)
- Inorganic Chemistry Poster Prize, 39th IUPAC Congress and 86th Conference of the Canadian Chemical Society, Ottawa, Ontario (2003)
- University of Windsor Travel Scholarship, University of Windsor (2000-2004)
- William Redmond Memorial Bursary, University of Windsor (1999-2000)

PUBLICATIONS

- Hawkeswood, S.B.; Stephan, D.W. Syntheses and Reactions of The *bis*-Boryloxide $O(Bpin)_2$ (pin = $O_2C_2Me_4$). Manuscript Accepted. *Dalton Trans.* **2005.**
- Hawkeswood, S.B.; Wei, P.; Gauld, J.W.; Stephan, D.W. Steric Effects in Metathesis and Reduction Reactions of Phosphinimines with Catechol- and Pinacolboranes. Manuscript accepted, *Inorg. Chem.* **2005.**
- Hawkeswood, S.B.; Wei, P.; Stephan, D.W. *Inorg. Chem.*, **2003**, *42*(17); 5429-5433.

- Smith, S.B.; Stephan, D.W. *Titanium* Comprehensive Coordination Chemistry II, *3*, **2003**.
- Courtenay, S.; Smith, S.; Hollink, E.; Blaschke, U.; Kehr, G.; Fröhlich, R.; Erker, G.; Stephan, D.; *Z. Naturfor, B.: Chem. Sci.* **2002**, *57*, 1184-1188.

CONFERENCE PRESENTATIONS

- Hawkeswood, S.B.; Stephan, D.W. 87th Conference of the Canadian Society for Chemistry. London, Ontario, Canada, June 2004.
- Hawkeswood, S.B.; Stephan, D.W.; Inorganic Discussion Weekend Meeting, McMaster University, Hamilton, Ontario, Canada, October, 2003.
- Hawkeswood, S.B.; Stephan, D.W.; 39th IUPAC Congress and the 86th Conference of the Canadian Society for Chemistry. Ottawa, Ontario, Canada, August 2003.
- Smith, S.B.; Stephan, D.W.; 223rd American Chemical Society National Meeting. Boston, Mass., U.S.A., August 2002.
- Smith, S.B.; Stephan, D.W. 222nd American Chemical Society National Meeting. Chicago, Illinois, U.S.A., August 2001.